Trace elements associated with the coarse and fine aerosol fractions in *Sphagnum* moss within the Athabasca Bituminous Sands region

by

Na Chen

A thesis submitted in partial fulfillment of the requirements for the degree of

Master of Science

in

Land Reclamation & Remediation

Department of Renewable Resources

University of Alberta

ABSTRACT

The Athabasca Bituminous Sands industry in Alberta has dramatic impacts on the economy of the province. Nevertheless, with increasing industrial operations, environmental concerns are also raised regarding the contamination of air and water with trace elements (TEs). To better assess the influence of the industry to the surrounding ecosystems, it is crucial to determine the TEs associated with the coarse and fine aerosols which differ in their size and chemical composition. Here, *Sphagnum* mosses were used as biomonitors of atmospheric deposition, and contributions from bulk deposition and fine aerosols were estimated by determining the abundance of TEs in bulk moss and acid soluble ash (ASA). The ash content of moss clearly increased with decreasing distance towards industry, reflecting increasing mineral dust input. Total concentrations of almost all the elements increased towards industry, while the acid soluble concentrations of the elements varied. Exhibiting high acid soluble proportions, Al, Y, and the elements enriched in bitumen (V and Ni) might be largely contributed by the ultrafine clay minerals such as kaolinite and illite. In contrast, Th, Mo (enriched in bitumen), Pb, Sb, and Tl showed low acid soluble proportions, which could be more influenced by the deposition of larger minerals such as feldspars and heavy minerals (e.g., monazite, zircon) from bituminous sands. Silver and Cd, behaving more like micronutrients such as Cu and Zn, were more impacted by plant uptake than mineral dust deposition. The above results were supported by the calculated enrichments of TEs, particle size distribution, X-ray diffraction, and principal component analysis. The study highlights the importance and necessity to determine the chemical reactivity of TEs in atmospheric dusts when evaluating their associated health risks to living organisms.

PREFACE

This research was supported by the Natural Sciences and Engineering Research Council (NSERC) of Canada and Canada's Oil Sands Innovation Alliance (COSIA).

Chapter 2 was written as a manuscript to be submitted for publication as Na Chen, Fiorella Barraza, René J. Belland, Muhammad B. Javed, Iain Grant-Weaver, Chad W. Cuss, and William Shotyk, "Trace elements in the acid soluble ash fraction of *Sphagnum* moss: Surrogate for atmospheric deposition of sub-micron aerosols within the Athabasca Bituminous Sands region". I was responsible for the sample collection in 2019 and 2020, sample treatment, data analyses and visualization, and manuscript preparation. Iain Grant-Weaver contributed to sample digestion and ICP-MS analysis of pilot experiments. Fiorella Barraza was responsible for ICP-MS analysis of subsequent samples and provided reviews of the manuscript. Muhammad B. Javed provided valuable insights on laboratory work and the manuscript. Chad W. Cuss provided valuable perspectives on laboratory work. William Shotyk and René J. Belland were co-supervisors: they helped to plan and guide the research and thesis, and revised the manuscript.

ACKNOWLEDGEMENTS

I am full of gratitude to my supervisor Dr. William Shotyk (Bill Shotyk), for all the guidance, support, and invaluable perspectives during the course of this research. Your enthusiasm for research and profound knowledge in not only your field but also various others have always inspired me to learn more, discover more, and explore more. You have taught me a lot, in addition to how to do research work.

My very heartfelt thanks to Dr. René J. Belland for leading me into the astonishing world of bryophytes, and all the guidance, insights, and assistance along the way. I am thankful to Dr. Fiorella Barraza for the training on lab instruments, tutorial on ICP-MS data analysis, and reviews on conference abstracts, thesis, and all relevant work. I am grateful to Dr. Muhammad B. Javed for giving me the preliminary knowledge on the project, and valuable suggestions on laboratory work and thesis. Thank you Dr. Tariq Siddique for chairing the final oral exam.

I appreciate Dr. Chad W. Cuss for the indispensable viewpoints, Dr. Yifeng Zhang for the guidance on Chemical Mass Balance (CMB) modelling, Tommy Noernberg for instructions on prep lab instruments, and Tracy Gartner for administrative support. I thank Iain Grant-Weaver for the digestion and ICP-MS analysis for pilot experiments and Judy Schultz for the SEM analysis. Sincere thanks to Lukas Frost for leading the Metals vs. Minerals field trips, and Andrii Oleksandrenko, Dr. Jaqueline Dennett, and Ron Goyhman for helping with the fieldwork. I value the helpful comments Dr. Mandy Krebs, Jinping Xue, Mika Little-Devito, Yu Wang, Iain Grant-Weaver, and Judy Schultz have given on the thesis. Thanks to Sundas Butt, Dr. Lina Du, and Dulani Kandage, for our great memories in Edmonton.

Many thanks go to the other members of the SWAMP Laboratory team and the University of Alberta for various kinds of supports. I sincerely acknowledge the generous financial support from the Natural Sciences and Engineering Research Council (NSERC) of Canada and the Canada's Oil Sands Innovation Alliance (COSIA).

Last but not least, I would like to thank my family for the support of each of my decision, and my relatives and friends for all the encouragement along the way. A big thank you to Dr. Ping Hou who has encouraged me to pursue my aspirations and stiffened my resolution to study abroad. I gratefully acknowledge Dr. Scott X. Chang and Dr. Miles Dyck for all the help and support since my undergraduate. Special thanks to Dr. Christopher Nzediegwu, Dr. Jin-Hyeob Kwak, and Dr. Hua Qin for all of their help. I am also so grateful to all the wonderful people I have met in Edmonton.

My sincere gratitude and appreciation to one and all !

TABLE OF CONTENTS

ABSTRACT ii
PREFACE iii
ACKNOWLEDGEMENTS iv
TABLE OF CONTENTS vi
LIST OF TABLES ix
Chapter 1 ix
Chapter 2 Supporting Information 2 ix
LIST OF FIGURES x
Chapter 1 x
Chapter 2 x
Chapter 2 Supporting Information 1 xi
LIST OF APPENDICES xiv
CHAPTER 1. INTRODUCTION AND OBJECTIVES 1
1. Alberta's Bituminous Sands 2
1.1. Geological settings 2
1.2. Physico-chemical characteristics of Alberta's bituminous sands 3
1.3. Bitumen extraction and processing 5
1.3.1. Bitumen extraction 5
1.3.2. Bitumen upgrading 10
2. Emissions of Aerosols to the Environment 12
3. Use of Mosses as Environmental Biomonitors of Atmospheric Deposition 14
4. Approaches to Determine the Abundance of the Anthropogenic Fraction of Trace Elements in Mosses 17
4.1. Calculating enrichment factors 17
4.2. Determining the natural abundance and anthropogenic concentrations of TEs in samples from impacted sites 18
4.3. Determining the natural abundance and enrichments of TEs in samples from reference sites 19
4.4. Determining trace elements in the acid soluble ash and bulk moss 19
5. Objective 21
6. References 21

CHAPTER 2. TRACE ELEMENTS IN THE ACID SOLUBLE ASH FRACTION OF *SPHAGNUM* MOSS: SURROGATE FOR ATMOSPHERIC DEPOSITION OF SUB-MICRON AEROSOLS WITHIN THE ATHABASCA BITUMINOUS SANDS REGION 31
Abstract 32
Synopsis 33
TOC 33
1. INTRODUCTION 34
2. MATERIALS AND METHODS 37
2.1. Sample Collection 37
2.2. Analytical Methods 38
2.2.1. Sample preparation 38
2.2.2. Acid digestion of dry milled moss and acid leaching of ashed moss 38
2.2.3. Determination of major and trace elements 39
2.2.4. Analysis of particle size, morphology, and mineralogy 39
2.3. Data Analyses and Visualization 40
3. RESULTS AND DISCUSSION 40
3.1. General Description of the Element Concentration Data 40
3.2. Spatial Variation in Trace Element Concentrations 41
a) Lithophile elements 41
b) Elements enriched in bitumen 42
c) Chalcophile elements 42
d) Elements essential to plants 43
3.3. Comparison of Total Concentrations versus ASA 43
3.4. Enrichments of Trace Elements 45
3.5. Mineral Abundance in Moss Ash from Proximal and Distal Locations 45
3.6. Principal Component Analysis 46
3.7. Temporal Trends of Element Accumulation 47
3.8. Dust Deposition in Other Locations in Alberta 47
a) Elk Island National Park 47
b) Wagner Natural Area 48
Acknowledgements 48
References 49
List of Figures 57

Supporting Information 1 64
Presentation of Geochemical Data 64
List of Figures 65
References 91
Supporting Information 2 92
List of Tables 92
CHAPTER 3. SUMMARY AND CONCLUSIONS 100
BIBLIOGRAPHY 103
APPENDIX I 116
APPENDIX II 131
APPENDIX III 140
APPENDIX IV 151

LIST OF TABLES

Chapter 1

Table 1. Comparison of physical-chemical properties of bitumen, conventional crude oil (CCO), and synthetic crude oil (SCO). 5

Table 2. Pros and cons of a lithophile element as the reference element for calculating the enrichment factor. 20

Chapter 2 Supporting Information 2

Table S1. Limit of detection (LOD), limit of quantification (LOQ), standard reference materials (SRMs) recoveries for total concentrations analyzed using ICP-MS……93

Table S2. Limit of detection (LOD), limit of quantification (LOQ), and standard reference materials (SRMs) recoveries for concentrations in acid soluble ash (ASA) analyzed using ICP-MS……..96

Table S3. Limit of detection (LOD), limit of quantification (LOQ), and standard reference materials (SRMs) recoveries for total concentrations analyzed using ICP-OES……98

Table S4. Limit of detection (LOD), limit of quantification (LOQ), and standard reference materials (SRM) recoveries for concentrations in acid soluble ash (ASA) analyzed using ICP-OES……99

LIST OF FIGURES

Chapter 1

Fig. 1. Map of Alberta's Bituminous Sands deposits (Source: Mossop, 1980). 3

Fig. 2. Typical arrangement of bituminous sand particles (Source: Berkowitz and Speight, 1975). 4

Fig. 3. Scheme of mining and extraction of bitumen from Alberta's Bituminous Sands using the open-pit mining method (Source: Gosselin et al., 2010). PSC = particle/primary separation cells. 6

Fig. 4. Scheme of bitumen processing (Source: Masliyah et al., 2004). 8

Fig. 5. Effect of fine solids on bitumen recovery (Source: Wallace et al., 1989). 10

Chapter 2

Fig. 1. Average trace element concentrations (μg kg^{-1} dry moss) at industrial and reference sites out of bulk moss and acid soluble ash (ASA) of *Sphagnum* mosses collected in fall 2015 (a & b) and 2019 (c & d)…….58

Fig. 2. Spatial distribution of total a) Y, b) Pb, c) V, and d) Ni concentrations in *Sphagnum* mosses collected in fall 2015. CMW = Caribou Mountains Wildland, BMW = Birch Mountains Wildland, UTK = Utikuma, WAG = Wagner Natura l Area, EINP = Elk Island National Park……...59

Fig. 3. Total and acid soluble concentrations (mg kg^{-1} dry moss) of Al, Th, Ca, Mn, V, Ni, Mo, Tl, Pb, Sb in *Sphagnum* mosses collected in October 2019 and 2020. ASA = Acid Soluble Ash. McK = Fort Mackay, McM = Fort McMurray, ANZ = Anzac, UTK = Utikuma…….....60

Fig. 4. Enrichments over two of trace elements out of bulk moss (Total) and acid soluble ash (ASA) of *Sphagnum* mosses collected from a) industrial and b) reference sites in fall 2015, 2019, and 2020 relative to the Upper Continental Crust.66 Total and acid soluble concentrations used were out of ash (mg kg^{-1} ash).[75]…….….61

Fig. 5. Mineral abundance (%) from XRD analysis in ash samples of *Sphagnum* mosses collected from JPH4 and UTK in October 2020. UTK = Utikuma…….62

Fig. 6. Principal component analysis of 2015 *Sphagnum* mosses using a) total concentrations and ash content and b) acid soluble concentrations and ash content. The contribution reflects the total contribution of the variables to principal component (PC) 1 and 2. BMW = Birch Mountains Wildland, CMW = Caribou Mountains Wildland, UTK = Utikuma……...63

Chapter 2 Supporting Information 1

Fig. S1. Moss sampling sites within the Athabasca Bituminous Sands Regions in fall 2015 (green points), and 2019 and 2020 (red points except for MIL). 68

Fig. S2. Schematic flow of sample treatments. 69

Fig. S3. Ratios of maximum (Max) to minimum (Min) element concentrations out of bulk moss and acid soluble ash (ASA) of *Sphagnum* mosses collected in fall 2015 (sites EINP and WAG were excluded) and 2019. 70

Fig. S4. a) & b): Average trace element concentrations (µg kg^{-1} dry moss) of industrial and reference sites out of bulk moss and acid soluble ash (ASA) of *Sphagnum* mosses collected in fall **2020**. c) & d): Ratios of maximum (Max) to minimum (Min) element concentrations out of bulk moss and ASA 71

Fig. S5. Ash content (%) of *Sphagnum* mosses collected in fall a) 2015 and b) 2019 and 2020. CMW = Caribou Mountains Wildland, BMW = Birch Mountains Wildland, UTK = Utikuma, WAG = Wagner Natural Area, EINP = Elk Island National Park. McK = Fort Mackay, McM = Fort McMurray, ANZ = Anzac. 72

Fig. S6. Spatial distribution of a) total and b) acid soluble **Al**, and c) total and d) acid soluble **Th** concentrations in *Sphagnum* mosses collected in fall 2015. ASA = Acid Soluble Ash. CMW = Caribou Mountains Wildland, BMW = Birch Mountains Wildland, UTK = Utikuma, WAG = Wagner Natural Area, EINP = Elk Island National Park 73

Fig. S7. Spatial distribution of a) total and b) acid soluble **Fe**, and c) total and d) acid soluble **Mo** concentrations in *Sphagnum* mosses collected in fall 2015. ASA = Acid Soluble Ash. CMW = Caribou Mountains Wildland, BMW = Birch Mountains Wildland, UTK = Utikuma, WAG = Wagner Natural Area, EINP = Elk Island National Park 74

Fig. S8. Correlogram of **total** concentrations and ash content of fall 2015 *Sphagnum* mosses based on the Spearman rank-based correlation test. Sites EINP and WAG were excluded. Corr. Coef. = Correlation coefficient. Significance level = 0.05. Only significant correlations are presented. . 75

Fig. S9. Wind rose diagrams for 2015, 2019, and 2020 at Mildred Station. Historic hourly weather data from May 1 to August 31 of each year was downloaded from the Government of Canada climate station: Mildred Lake (Latitude: 57°02'28.000" N, Longitude: 111°33'32.000" W, Elevation: 310.00 m, Climate Identifier (ID): 3064528, World Meteorological Organization (WMO) ID: 71255, Transport Canada (TC) ID: WMX). Data was processed in R 4.1.1,[2] and visualized using the *openair* package.[3] Wind rose diagram for 2015 was also used in our previous study by Mulland-Boudreau et al.[4] 76

Fig. S10. Total V, Ni, Mo, Pb, Sb, Tl, Ag, and Cd concentration versus total Y concentration (µg kg^{-1} dry moss) in *Sphagnum* mosses collected in fall 2015. CMW = Caribou Mountains Wildland, BMW = Birch Mountains Wildland, UTK = Utikuma, WAG = Wagner Natural Area, EINP = Elk Island National Park 77

Fig. S11. Spatial distribution of a) total and b) acid soluble **Sb**, and c) total and d) acid soluble **Tl** concentrations (μg kg^{-1} dry moss) in *Sphagnum* mosses collected in fall 2015. ASA = Acid Soluble Ash. CMW = Caribou Mountains Wildland, BMW = Birch Mountains Wildland, UTK = Utikuma, WAG = Wagner Natural Area, EINP = Elk Island National Park. 78

Fig. S12. Spatial distribution of a) total and b) acid soluble **Ag**, and c) total and d) acid soluble **Cd** concentrations (μg kg^{-1} dry moss) in *Sphagnum* mosses collected in fall 2015. ASA = Acid Soluble Ash. CMW = Caribou Mountains Wildland, BMW = Birch Mountains Wildland, UTK = Utikuma, WAG = Wagner Natural Area, EINP = Elk Island National Park. 79

Fig. S13. Spatial distribution of a) total and b) acid soluble **Cu**, and c) total and d) acid soluble **Zn** concentrations (mg kg^{-1} dry moss) in *Sphagnum* mosses collected in fall 2015. ASA = Acid Soluble Ash. CMW = Caribou Mountains Wildland, BMW = Birch Mountains Wildland, UTK = Utikuma, WAG = Wagner Natural Area, EINP = Elk Island National Park. 80

Fig. S14. Spatial distribution of acid soluble a) **Y**, b) **Pb**, c) **V**, and d) **Ni** concentrations in *Sphagnum* mosses collected in fall 2015. ASA = Acid Soluble Ash. CMW = Caribou Mountains Wildland, BMW = Birch Mountains Wildland, UTK = Utikuma, WAG = Wagner Natural Area, EINP = Elk Island National Park. 81

Fig. S15. Correlogram of element concentrations in Acid Soluble Ash (**ASA**) and ash content of fall 2015 *Sphagnum* mosses based on the Spearman rank-based correlation test. Sites EINP and WAG were excluded. Corr. Coef. = Correlation coefficient. Significance level = 0.05. Only significant correlations are presented. 82

Fig. S16. Proportion of acid soluble to total concentration of trace elements in *Sphagnum* mosses collected in fall 2019 (a, c, & e) and 2020 (b, d, & f). ASA = Acid Soluble Ash. McK = Fort Mackay, McM = Fort McMurray, ANZ = Anzac, UTK = Utikuma. 83

Fig. S17. Total and acid soluble concentrations (mg kg^{-1} dry moss) of conservative lithophile elements (Y, Cr, La), essential elements (K, Mg, P, S, Fe, Cu, Zn), and potentially toxic elements (Ag, Cd) in *Sphagnum* mosses collected in fall 2019 and 2020. ASA = Acid Soluble Ash. McK = Fort Mackay, McM = Fort McMurray, ANZ = Anzac, UTK = Utikuma. 84

Fig. S18. X-ray diffraction (XRD) analysis of a) JPH4 and b) UTK ash samples. UTK = Utikuma. 85

Fig. S19. Particle size distribution of ash samples of *Sphagnum* mosses by laser diffraction. UTK = Utikuma. 86

Fig. S20. Contributions of variables in accounting for the variability in principal component (PC) 1 and PC 2 from principal component analysis of fall 2015 *Sphagnum* mosses using total concentrations (a, b) and acid soluble concentrations (c, d). The red dashed line indicates the average contribution. 87

Fig. S21. Temporal trends of **total** concentration (μg kg^{-1} dry moss) of selected elements in *Sphagnum* moss collected in fall 2015 (sites EINP and WAG were excluded), 2019, and 2020. Boxplots show the range, 25th and 75th percentiles, and median for each element. 88

Fig. S22. Temporal trends of trace element concentration (μg kg^{-1} dry moss) in the Acid Soluble Ash (**ASA**) fraction of *Sphagnum* moss collected in fall 2015 (sites EINP and WAG were excluded), 2019, and 2020. Boxplots show the range, 25th and 75th percentiles, and median for each element..... 89

Fig. S23. Enrichment factors using **Y** as the reference element with values greater than 2 of a) V, Ni, Mo, Pb, Tl, b) Sb, c) Ag, and d) Cd of *Sphagnum* mosses collected in fall 2015. Enrichment factors of V were all below 2 and are not shown in the plot. CMW = Caribou Mountains Wildland, BMW = Birch Mountains Wildland, UTK = Utikuma, WAG = Wagner Natural Area, EINP = Elk Island National Park..... 90

LIST OF APPENDICES

Appendix I. Tests of filters, filter cleaning, and the optimum amount of ash and acid insoluble ash required……...…….....116

Appendix II. Comparison of total concentrations of elements in *Sphagnum* moss digested with concentrated HNO_3 versus concentrated HNO_3 and HBF_4……...…131

Appendix III. Comparison of Al, Fe, Mn, and Zn concentrations obtained using inductively coupled plasma optical emission spectrometry (ICP-OES) and inductively coupled plasma mass spectrometry (ICP-MS) ……...…140

Appendix IV. Comparison of enrichment factors calculated using different reference elements……...151

CHAPTER 1. INTRODUCTION AND OBJECTIVES

1. Alberta's Bituminous Sands

The bituminous sands deposits in Alberta, covering a surface area of more than 140,000 km^2 contain a huge crude oil reserve of approximately 165.4 billion barrels, being the third-largest oil reserve in the world, after Venezuela and Saudi Arabia (Government of Alberta, 2021). Employing more than 140,000 people as of 2017 and generating $1.48 billion of revenue from 2016 to 2017 (Government of Alberta, 2021), the bituminous sands industry has generated dramatic benefits for the economy of Alberta.

1.1. Geological settings

The bituminous sands deposits in Alberta date from Early Cretaceous geological time (approximately 110 million years ago), being magnitudes larger than the conventional oil fields (Mossop, 1980; Osacky et al., 2013). These deposits are primarily located in Athabasca, Wabasca, Peace River, and Cold Lake regions, with the largest deposit being in the Athabasca region where it covers approximately 42,000 km^2 whilst containing 869 billion barrels of bitumen in place (Fig. 1) (Mossop, 1980; Osacky et al., 2013). The bituminous sands ores are mainly a mixture of four petrologically different kinds of rocks including estuarine sand, estuarine clay, marine sand, and marine clay, deposited in marine and estuarine sedimentary environments (Osacky et al., 2013).

Fig. 1. Map of Alberta's Bituminous Sands deposits (Source: Mossop, 1980).

1.2. Physico-chemical characteristics of Alberta's bituminous sands

The bituminous sands in Alberta are composed of (by weight) 83–88% minerals, 8–14% bitumen, and 3–5% water (Gosselin et al., 2010; Mossop, 1980). Bituminous sands with over 10 wt%, 6–10 wt%, and less than 6 wt% bitumen are considered rich, moderate, and lean bituminous sands, respectively (Takamura, 1985). Bitumen is a heavy petroleum product comprised of highly condensed polycyclic aromatic hydrocarbons (PAHs), with the presence of high levels of sulfur, nitrogen, and metals such as vanadium, nickel, iron, copper, titanium, and zirconium (Table 1) (Cao et al., 2007; Gosselin et al., 2010; Landis et al., 2012; Lévesque, 2014). Bitumen is much heavier (American Petroleum Institute (API) gravity of 8° to 10°) and viscous than the conventional crude oil which has an API gravity of 25° to 40° (Cao et al., 2007; Mossop, 1980). The mineral fraction is composed mainly of light minerals (~99%) including quartz (60–90%) and clay materials dominantly of kaolinite and illite, with minor amounts of feldspar, mica, carbonates,

and chalcedony (Bichard, 1987). It also contains ~1% heavy minerals (density > 2.96 g/cm^3) such as tourmaline and zircon (Bichard, 1987). Elements such as Ag, As, Be, Bi, Cd, Pb, Sb, and Tl are mostly found in the mineral fraction (Bicalho et al., 2017). Each sand grain is wrapped by a roughly 10 nm-thick film of water film which is surrounded by bitumen when in its natural undisturbed state (Fig. 2) (Berkowitz and Speight, 1975; Hepler and Smith, 1994; Mossop, 1980; Takamura, 1985). The hydrophilic property of the bituminous sands makes the hot water extraction process of bitumen possible (Masliyah et al., 2004; Mossop, 1980; Sanford, 1983; Strausz, 1989; Takamura, 1982). The water film is stabilized by the electrical double layer repulsive force between the negatively charged bitumen and sand surfaces (Anderson, 1986; Strausz, 1989; Strausz and Lown, 2003; Takamura, 1982, 1985). High-grade bituminous sands typically have a porosity of 25–35%, resulting from the absence of mineral cement which typically occupies large void space in sandstones (Mossop, 1980; Strausz and Lown, 2003).

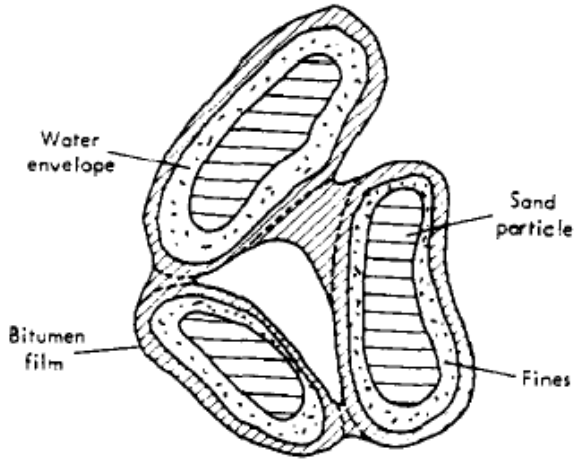

Fig. 2. Typical arrangement of bituminous sand particles (Source: Berkowitz and Speight, 1975).

Table 1. Comparison of physical-chemical properties of bitumen, conventional crude oil (CCO), and synthetic crude oil (SCO).

Property		Bitumen	CCO	SCO
Density at 16 C (kg m^{-3})		1000	860	870
API gravity		10	32	31
Viscosity (mPa s)	15 °C	235,000	14	19
	40 °C	1,050	9	10
Boiling range (C)		250 to >800	30 to 550	50 to 560
Carbon content (wt%)		84	84	85.5
Hydrogen content (wt%)		10.5	13.5	13.5
Sulfur content (wt%)		4.0	1.9	0.3
Nitrogen content (wt%)		0.42	0.09	0.05
Nickel content (ppm)		69	14	<1
Vanadium content (ppm)		190	3.7	<0.6
Hydrocarbon composition (wt%)				
Saturates		30	80	22
Aromatics		70	20	78
Asphaltenes*		10	<1	1

*Measured on the basis of hydrocarbons, but included in aromatics (Source: Gosselin et al. 2010).

1.3. Bitumen extraction and processing

1.3.1. Bitumen extraction

Different technologies are utilized to access the bituminous sands formation, depending on the thickness of the overlay materials (Gosselin et al., 2010). A strip ratio, which is the ratio of overburden to formation volume, of two is considered economic to adopt open-pit mining using trucks and shovels, i.e., when the overburden is less than 70 m (Gosselin et al., 2010). However, only approximately 20% of the total bituminous sands deposits are suitable for surface mining (Cooke et al., 2017; Gosselin et al., 2010; Xing and Du, 2017). When the deposits are over 150 m deep, thermal in-situ methods such as cyclic steam stimulation (CSS) and steam-assisted gravity drainage (SAGD) are employed, of which bitumen recovery is only ~50% (Gosselin et al., 2010; Xing and Du, 2017). The steam is heated by natural gas to over 250 °C to reduce the viscosity of

bitumen, which strongly depends on temperature, to the degree where it can flow as water (Gosselin et al., 2010; Jordaan, 2012; Masliyah et al., 2004; Ramasamy, 2019). Open-pit mining accounts for over 55% of total crude bitumen production in Alberta (Gosselin et al., 2010).

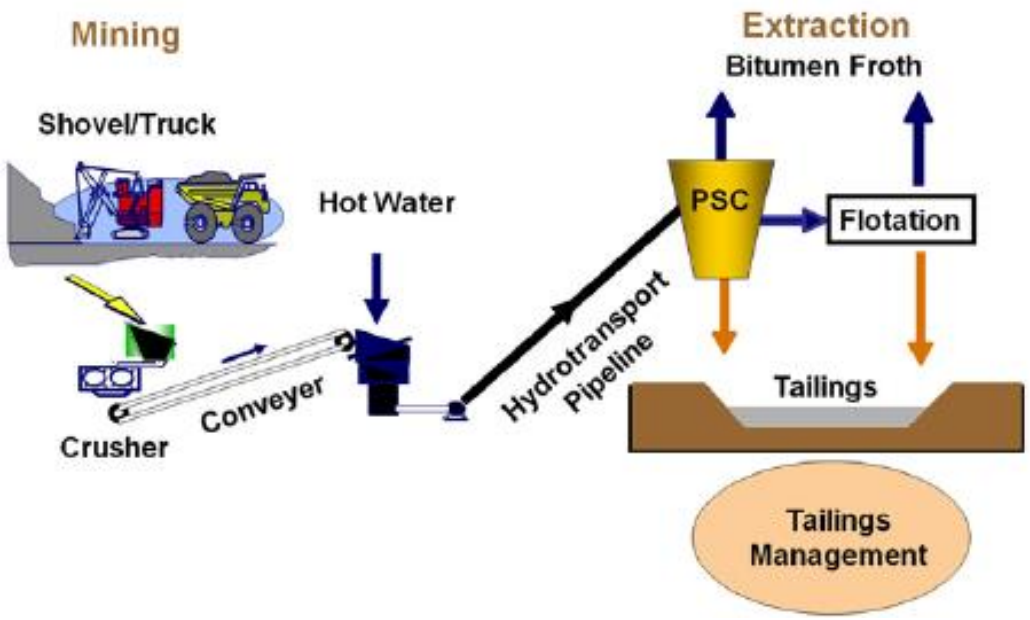

Fig. 3. Scheme of mining and extraction of bitumen from Alberta's Bituminous Sands using the open-pit mining method (Source: Gosselin et al., 2010). PSC = particle/primary separation cells.

The bituminous sands obtained using open-pit mining are crushed and the bitumen is then extracted using the Clarke hot water extraction method, of which bitumen recovery is > 90% (Fig. 3) (Clark and Pasternack, 1932; Gosselin et al., 2010; Jordaan, 2012; Masliyah et al., 2004). Usually, inorganic bases, typically sodium hydroxide (NaOH), are added to hot water (45–60 °C) to maintain a pH of 8.0–8.5 and facilitate bitumen liberation from solids (Gosselin et al., 2010; Takamura, 1982). The increase in slurry pH by the addition of NaOH leads to more negatively charged bitumen and mineral surfaces and hence the increased electrostatic repulsive force between them, which aids bitumen detachment (Liu et al., 2003). In addition, it ionizes the organic acids in bitumen which produce surfactants such as carboxylates and sulfates/sulfonates (Gosselin

et al., 2010; Masliyah et al., 2004; Moschopedis et al., 1980; Sanford, 1983; Sanford and Seyer, 1979).

The crushed and screened bituminous sand lumps (size in 50–150 mm) are conditioned (i.e., lump size reduction, bitumen liberation and aeration) through hydrotransport pipelines and transported to the particle/primary separation cells (PSC) (Gosselin et al., 2010; Masliyah et al., 2004; Ramasamy, 2019). The slurry is then separated into three parts: the primary bitumen froth skimmed from the top of PSC, the middling stream of low-slurry density with fine solids collected from the middle, and settled tailings (i.e., coarse solids in the form of dense slurry) collected from the bottom (Fig. 4) (Gosselin et al., 2010; Masliyah et al., 2004). The bitumen froth contains aerated bitumen, which means the liberated bitumen from sand grains is attached to air bubbles and floated to the top of PSC due to buoyancy effects (Gosselin et al., 2010; Masliyah et al., 2004). Specifically, the collected bitumen froth contains 60 wt% bitumen, 30 wt% water, and 10 wt% solids (Gosselin et al., 2010; Masliyah et al., 2004). It is de-aerated to remove air, and diluted to reduce its viscosity using solvents such as naphtha when an on-site upgrader is available for bitumen upgrading, and paraffin when an on-site upgrader is not available (Gosselin et al., 2010; Lévesque, 2014; Masliyah et al., 2004). The entrained fine solids and water are then removed from the organic phase of diluted bitumen by gravity settling and centrifugation(Gosselin et al., 2010; Masliyah et al., 2004). The obtained bitumen is then ready for upgrading and refining. When paraffin is used as the solvent, the precipitation of asphaltenes leads to the formation of composite aggregates trapping water and solids, thus facilitating gravity separation and providing partial physical upgrading (Gosselin et al., 2010; Masliyah et al., 2004). The middling stream is further treated using flotation technologies where the bitumen-air attachment is facilitated to recover the bitumen remained (Gosselin et al., 2010; Masliyah et al., 2004). The tailings from both bitumen

extraction and froth cleaning are discharged to tailings ponds, where coarse solids settle quickly while fine solids settle slowly and form fluid fine tailings and eventually mature fine tailings (MFT) (Gosselin et al., 2010). Innovative techniques are emerging to treat the fluid fine tailings and MFT to maximum water recycling for bitumen extraction such as the composite/consolidated tailings (CT) process, thickened tailings (TT) process, thin lift drying, and chemical assisted centrifugation/filtration (Gosselin et al., 2010).

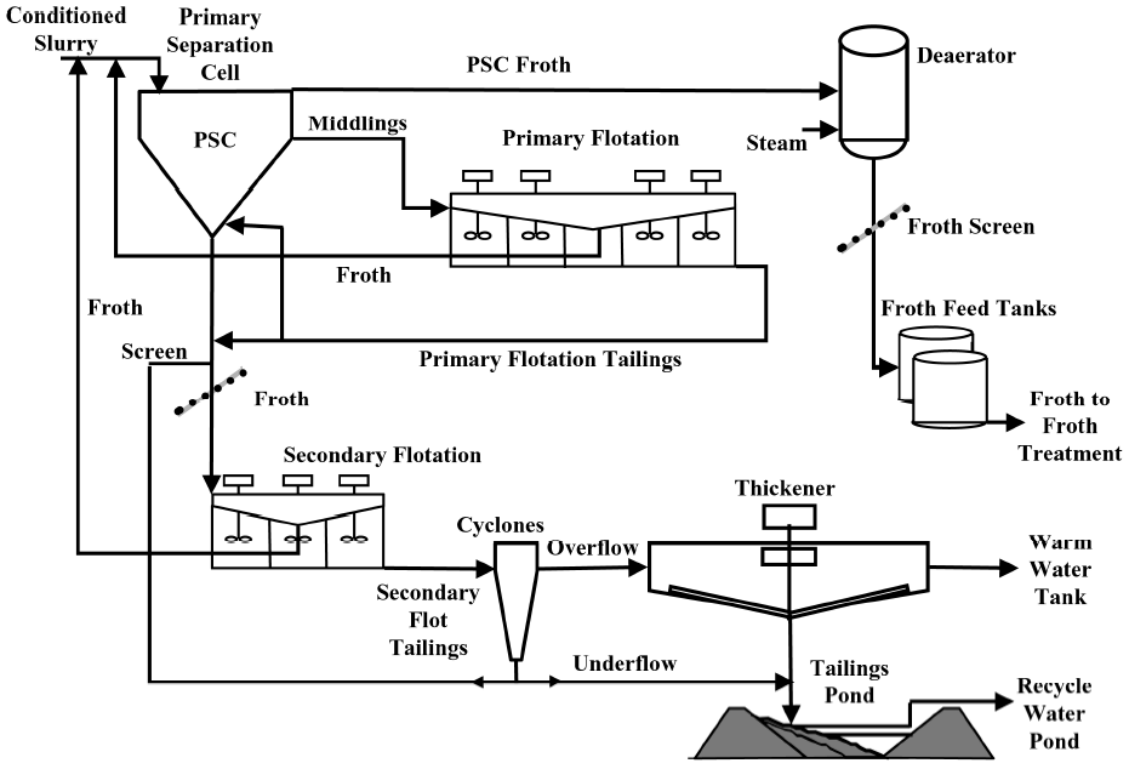

Fig. 4. Scheme of bitumen processing (Source: Masliyah et al., 2004).

The bitumen extraction efficiency could be decreased by high fine solids (< 44 μm) contents of the mineral fraction, and high metal ion concentrations in the process water (Bichard, 1987; Hepler and Smith, 1994; Liu et al., 2004; Liu et al., 2005; Masliyah et al., 2004; Mossop, 1980; Sanford, 1983). Bitumen slime coating, i.e., the coverage of bitumen by fine solids, accounts

in great measure for the poor processability of bituminous sands (Liu et al., 2005). The attachment of large amounts of fine solids to bitumen leads to the inability of bitumen to float (Fig. 5) (Bichard, 1987; Wallace et al., 1989). High fine solids contents would thus require high energy consumption and large amounts of chemical aids to maximize bitumen recovery (Sanford, 1983). In addition, the mineralogy of the clay materials in the mineral fraction also matters. Montmorillonite clays with a synergetic effect of calcium ions (40 mg L^{-1}) can remarkably reduce bitumen recovery by flotation, while such depression was marginal for kaolinite or illite with the presence of calcium ions and for the individual presence of calcium or clays (Kasongo et al., 2000; Liu et al., 2002; Liu et al., 2004; Osacky et al., 2013; Sanford, 1983). This synergetic depression effect is also true for magnesium ions, meaning it is dependent on the valence rather than the type of ions (Masliyah et al., 2004). These divalent ions serve as the bridge for bitumen-clay hetero-coagulation (Masliyah et al., 2011). The strong attachment of montmorillonite to bitumen when calcium is present retards the coagulation of bitumen droplets and contact of bitumen to air bubbles, while kaolinite clays are in a weaker adhesion force to bitumen than montmorillonite clays (Liu et al., 2002; Liu et al., 2004).

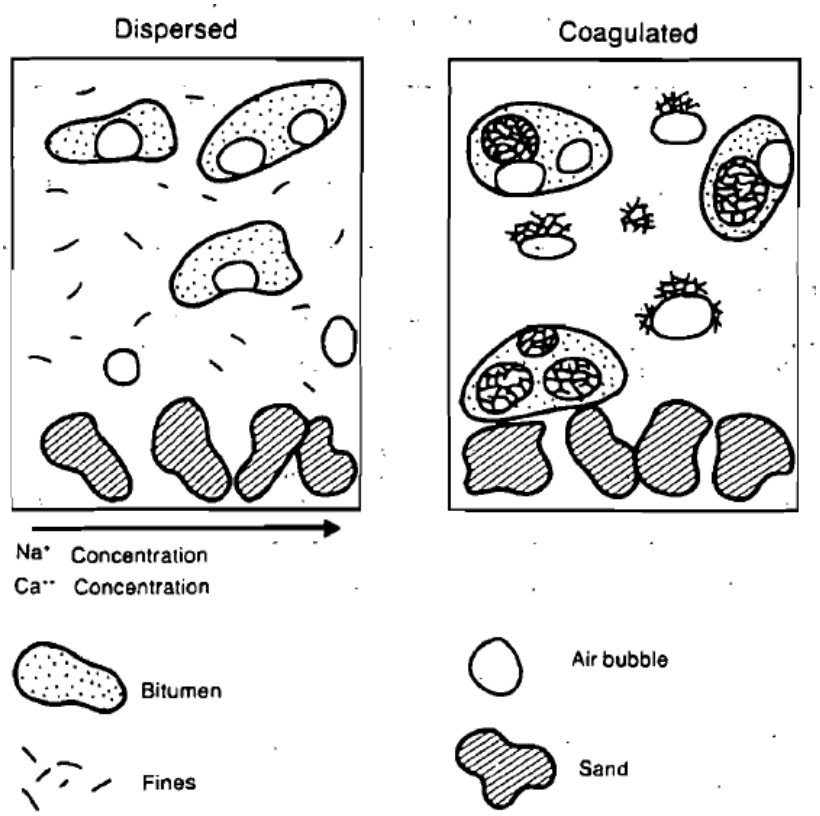

Fig. 5. Effect of fine solids on bitumen recovery (Source: Wallace et al., 1989).

1.3.2. Bitumen upgrading

Bitumen upgrading, including primary and secondary upgrading, aims to reduce bitumen density, viscosity, and molecular weight, increase hydrogen-to-carbon ratio, and remove sulfur, nitrogen, and metals, to increase its market value by producing a high quality synthetic crude oil (SCO) (Gosselin et al., 2010). Approximately 35% of bitumen in Alberta, mainly from mining and hot water extraction, was upgraded to SCO and then sold to downstream refineries (Oil Sands Magazine, 2020).

For bitumen upgrading, vacuum distillation firstly separates overhead light hydrocarbon off gas, liquid gas oils, and heavy vacuum residue in bitumen based on the boiling point (Gosselin et al., 2010). The light hydrocarbon off gas is mostly used as fuels in subsequent upgrading; liquid

gas oils are treated in secondary upgrading; the heavy vacuum residue, with molecular weights over 400, is sent to primary upgrading (Gosselin et al., 2010; Gray, 2015).

Primary upgrading breaks down large molecules and increases the hydrogen content of the liquid product (Gosselin et al., 2010). Coking (delayed and fluid coking) and hydroconversion are the two technologies used in this process (Gosselin et al., 2010; Gray, 2015). During coking, large molecules are cracked at a temperature of 430–550°C and relatively low pressure of ~350 kPa in a coker, into light hydrocarbons such as naphtha, kerosene, and gas oils as a vapour that was removed from the top, leaving a coke (petroleum coke/petcoke) residue (Gosselin et al., 2010; Oil Sands Magazine, 2020). The coke is rich in vanadium and nickel in the form of porphyrin complexes originating from chlorophylls (Barwise, 1990). Fuel gas is used as the heat source for delayed coking and coke for fluid coking (Gosselin et al., 2010). However, despite its high heating value, coke is still largely stockpiled as a waste due to its high sulfur content and low volatile matter (Gosselin et al., 2010). Regarding hydroconversion, large molecules are cracked and hydrogen is added; hot bitumen is reacted with hydrogen at a temperature < 460°C and high pressure up to 200 atm with the presence of catalysts such as platinum, which partially converts aromatics to cycloparaffins (Gosselin et al., 2010; Oil Sands Magazine, 2020). The metallic elements in bitumen are captured in the coke by-product during coking or on the surface of catalysts during hydroconversion and hence do not enter the secondary upgrading units (Gosselin et al., 2010).

The condensed overhead hot gas from primary upgrading is sent to secondary upgrading, which takes place in a catalytic hydrotreater with a temperature < 400°C; hydrogen gas is added to remove sulfur, nitrogen, and oxygen and to hydrogenate polyaromatic and olefin molecules (Gosselin et al., 2010; Gray, 2015). Organic sulfur is converted to H_2S with a conversion rate of >

90% and nitrogen is converted to ammonia with a conversion rate > 70% (Gosselin et al., 2010). The treated gas oils and naphtha products from this process comprise the SCO (Gosselin et al., 2010). The SCO is lower in sulfur, nitrogen, and metal content compared to conventional crude oil (Table 1).

2. Emissions of Aerosols to the Environment

The atmosphere has become a key medium in terms of the transport of potentially toxic trace elements (TEs) to remote aquatic ecosystems (Amodio et al., 2014; Nriagu, 1990). Aerosols emitted into the atmosphere can be divided into coarse and fine aerosols (Whitby et al., 1972; Willeke and Whitby, 1975). Mechanical processes such as open-pit mining, quarrying, road construction, and wind erosion generate non-respirable coarse aerosols with diameters typically between 10–100 μm and short residence time (Graney et al., 2012; Landis et al., 2012; Landis et al., 2017; Phillips-Smith et al., 2017; Swift and Proctor, 1982; Wang et al., 2015; Watson et al., 2014; Willeke and Whitby, 1975; Xing and Du, 2017; Zufall and Davidson, 1998). These particles settle out of the air by sedimentation in minutes to hours and hence have limited transport distances (Schuetz, 1989; Schütz, 1980). They are insoluble and rich in lithophile elements such as Al, Ti, and Sc in the form of silicates and aluminosilicates (Schütz and Rahn, 1982).

In contrast, the combustion of fossil fuels, industrial processes at elevated temperatures such as smelting and refining of metallic ores, and waste incineration yield respirable fine aerosols with diameters mainly of 0.1–1 μm and long atmospheric residence time, which make them capable of transport for thousands of kilometres (Corrin and Natusch, 1979; Natusch et al., 1974; Nriagu, 1990; Schütz, 1980; Swift and Proctor, 1982; Willeke and Whitby, 1975; Xing and Du, 2017; Xu et al., 2011; Zufall and Davidson, 1998). Such long-range transport can lead to the

enrichment of TEs contained in the fine aerosols in regions far away from the source (Pacyna and Pacyna, 2001). For example, the contamination of southern Norway by TEs emitted and transported from other parts of Europe (Berg and Steinnes, 1997a; Steinnes et al., 1989; Steinnes, 1997; Steinnes et al., 2011). These fine particles are enriched in chalcophile elements such as Pb, As, and Cd that are potentially toxic to living organisms, and are mostly in the forms of acid soluble oxides and hydroxides, which enables the TEs to be easily released (Dauvalter et al., 2009; Natusch et al., 1974; Nriagu, 1990). Once released into the environment, the potentially toxic elements can exert large impacts on living organisms. For example, metals like Pb, which is non-biodegradable while bioaccessible, can inhibit root elongation, impair enzyme functions such as during the formation of chlorophyll, and reduce photosynthetic rate of plants (Choudhury and Panda, 2004; Hampp and Lendzian, 1974; Lane and Martin, 1980). It can also cause severe and chronic health problems such as damages to the central nervous system and reproductive system, cardiovascular disease, and mental retardation in animals and humans (Goel et al., 2005; Padmavathiamma and Li, 2007). The concentrations of these potentially toxic elements are found to increase with decreasing particle size, due probably to the preferential condensation/adsorption of the volatilized element from combustion to small particles which have large specific surface areas (Corrin and Natusch, 1979; Davison et al., 1974; Natusch et al., 1974; Xu et al., 2011). Mining, smelting, and refining of metallic ores, burning of fossil fuels, and production and utilization of metallic commercial products have been the three main industrial sources of atmospheric metal pollution (Nriagu, 1990). Industrial emissions have become the dominant atmospheric source for most chalcophile TEs (Nriagu, 1990).

The bituminous sands industry in Alberta thus is expected to emit a significant quantity of coarse aerosols (mineral dust particles) from mechanical processes. However, emissions of fine

aerosols would be limited by the temperatures involved in upgrading (maximum of 550 °C), combined with the use of electrostatic precipitators in the upgrader stacks.

3. Use of Mosses as Environmental Biomonitors of Atmospheric Deposition

The surface layers of ombrotrophic peat bogs are hydrologically isolated from the influences of local groundwaters and surface waters (Damman, 1986; Shotyk, 1996b). As a consequence, bogs receive water and nutrient inputs solely from the atmosphere (Berg and Steinnes, 1997b; Castello, 2007; Čeburnis and Valiulis, 1999; Cloy et al., 2005; Damman, 1986; Malmer, 1988). This condition also applies to TEs, whether beneficial or potentially toxic, which can be retained by mosses from the atmosphere by wet and dry deposition (Amodio et al., 2014; Harmens et al., 2004; Tyler, 1990).

Mosses, especially the carpet-forming species, obtain most of their nutrients directly from the atmosphere, with little uptake from the soil/substrate (Harmens et al., 2004; Tyler, 1990). The new biomass proceeding from the top of the current biomass makes it impossible for any direct interaction with the soil/substrate (Tyler, 1990). The growth of mosses such as *Sphagna* on an organic substrate, or peat, also makes contamination by the substrate less problematic compared to forest mosses that are on a mineral substrate (Kempter et al., 2017). They can retain atmospheric TEs either physically while firmly on moss leaf surfaces (non-bioconcentrated), or chemically to the leaf cells by simple ion exchange or chelation with functional groups (bioconcentrated) (Castello, 2007; Rao et al., 1977; Rao, 1982; Spagnuolo et al., 2013). Such distribution of TEs is variable and hinges on the characteristics of moss and the environment, for example, the amount and type of the element, the solubility of particulates retained, and meteorological conditions (Castello, 2007; Spagnuolo et al., 2013). An experiment on the trapping of fly-ash particles by

Sphagnum mosses showed that the majority of particles were retained firmly on *Sphagnum* surface or in the pores of hyalocysts in the upper 1–3 cm, with only 0.8% of particles washed out (Punning and Alliksaar, 1997). The relative accumulation of major elements in live *Sphagnum* showed an order of K > P > N > Mg > Ca > S (Pakarinen, 1978, 1981). The degree of retention and sorption of TEs generally follows the order of Cu, Pb > Ni > Co > Zn, Mn in *Hylocomium* (Rühling et al., 1970). The concentration ratio of major elements between the living and dead portion of *Sphagnum* moss showed a decreasing order of K > N > P > Mg > Ca (Pakarinen, 1978). In addition, mosses are more resistant to high levels of potentially toxic elements and can accumulate more ions than vascular plants (Ceburnis, 2000; Jiang et al., 2018; Salemaa et al., 2004). For instance, 5–10 times higher concentrations of Fe and 2–3 times of Mn, Zn and Cu are found in *Aulacomnium palustre* (Hedw.) Schwägr., *Climacium dendroides* (Hedw.) F. Weber & D. Mohr, and *Atrichum undulatum* (Hedw.) P. Beauv. than in vascular plants (Ceburnis, 2000; Czarnowska and Rejement-Grochowska, 1974). Metal concentrations in conifer needles were found to be 10% of those in moss growing on the forest floor (Ceburnis, 2000).

Mosses are almost unable to avoid the retention and uptake of atmospheric aerosols (Tyler, 1990) and to exclude the excessive accumulation of toxic substances (Rao, 1982). Nevertheless, mosses possess some self-adjusting mechanisms, which enable them to survive under polluted conditions. For example, *Dicranella varia* (Hedw.) Schimp. can excrete Pb and Zn external to the cell wall, forming a white crust on leaf surfaces (Shimwell and Laurie, 1972); *Grimmia donniana* Sm. also binds Pb extracellularly to the cell wall, preventing Pb from penetrating to the cytoplasm (Brown and Bates, 1972); *Rhytidiadelphus squarrosus* (Hedw.) Warnst retains Pb within the nuclear membrane, making the Pb concentration in the cytoplasm lower than a level that would otherwise impair Pb-sensitive functions (Skaar et al., 1973); *Funaria hygrometrica* (Hedw.)

develops “capsule cells” and “brood cells” to tolerate high levels of Cu and Zn, respectively (Coombes and Lepp, 1974).

The outstanding capacity of *Sphagnum* mosses to retain atmospheric TEs is due to their unique properties. They have large surface areas with their leaves making up to two-thirds of their biomass (Kempter et al., 2017; Maevskaya et al., 2001; Tyler, 1990). The absence of cuticles on their leaves enables ions retained on leaf surfaces to have direct access to the free exchange sites on the cell wall (Kempter et al., 2017; Poikolainen et al., 2004; Shotyk et al., 2015). Shimwell and Laurie (1972) have also reported higher metal accumulation in ‘ectohydric’ moss *Dicranella varia* which lacks cuticles than in 'myxohydric' moss *Philonotis fontana* which has cuticles. Furthermore, the high cation exchange capacity (CEC) of their surfaces, due to the unesterified polyuronic acids, and the large density of negative surface charges give them a significant number of binding sites per unit mass (Clymo, 1963; González and Pokrovsky, 2014; Spearing, 1972; Tyler, 1990; Vile et al., 1999; Watkinson and Watt, 1992).

Using mosses as environmental biomonitors has proven to be an effective means of measuring the spatial and temporal variations of atmospheric TE deposition (Feder, 1978; Harmens et al., 2004; Steinnes et al., 2011). Strong positive linear correlations were observed between metal concentrations in mosses and rates of atmospheric depositions (Berg et al., 1995; Kosior et al., 2020; Pakarinen and Tolonen, 1976; Pilegaard, 1979; Ștefănuț et al., 2019). Moss analysis yields close or identical deposition results compared to those by conventional precipitation collection and analysis, while being much easier and cheaper (Harmens et al., 2004; Tyler, 1990). Thus, mosses have been widely used as biomonitors of atmospheric depositions, for example, in Europe (Berg and Steinnes, 1997a, 1997b; Coşkun et al., 2005; Czarnowska and Gworek, 1992; Davies and White, 1981; Delfanti et al., 1999; Harmens et al., 2004; Kempter et

al., 2017; Sakalys et al., 2009; Sardans and Peñuelas, 2005; Schröder and Pesch, 2007; Steinnes et al., 1989; Steinnes, 1997; Steinnes et al., 2011), North America (Glooschenko and Capobianco, 1978; Pakarinen and Tolonen, 1976; Santelmann and Gorham, 1988; Schilling and Lehman, 2002; Schintu et al., 2005), and Asia (Aboal et al., 2006; Lee et al., 2005; Saxena et al., 2008; Sun et al., 2009), by either passive (Kempter et al., 2017; Pakarinen and Tolonen, 1976; Rühling et al., 1970; Santelmann and Gorham, 1988; Schintu et al., 2005; Shotyk and Cuss, 2019) or active methods using moss bags (Al-Radady et al., 1993; Anicić et al., 2009; Archibold and Crisp, 1983; Cao et al., 2008; Cao et al., 2009; Castello, 2007; Čeburnis and Valiulis, 1999; Sun et al., 2009).

4. Approaches to Determine the Abundance of the Anthropogenic Fraction of Trace Elements in Mosses

The TEs adsorbed by these plants are derived from both natural as well as anthropogenic sources, with the natural sources being mainly soil-derived mineral dust particles (Shotyk et al., 2019). There are several ways to determine the abundance of the anthropogenic fraction of TEs in the moss samples.

4.1. Calculating enrichment factors

The enrichment factor (EF) can be used to determine whether there are additional sources of TEs, over and above those contributed by wind-borne soil dust. It is calculated as the ratio of the abundance of a given element to a conservative lithophile element (e.g., Al, Y, Th, Sc) in the sample, and this is then normalized to the corresponding ratio in the earth's crust (Rahn, 1976), as shown in the equation:

$$EF = \frac{[TE/CLE]_{sample}}{[TE/CLE]_{UCC}}$$

where TE and CLE refer to the concentrations (mg/kg) of the element of interest and the conservative lithophile element, respectively, in the sample and in the Upper Continental Crust (UCC). The ratio of the abundance of the TE to CLE in the UCC can be obtained from published literature such as the paper by Rudnick and Gao (2014). Generally, if the EF is less than two, there are no significant anthropogenic inputs of the element (Barbieri, 2016), i.e., the concentrations are within the range of natural variation. The disadvantage of using EF alone is that it cannot distinguish between the portions of the element enriched due to anthropogenic inputs versus natural bioaccumulation. The pros and cons of using one or another lithophile element for calculating the EF are summarized in Table 2. High EF values in samples from reference sites sometimes can exist, due to the abundance of the elements in natural soils relative to the crust or other unrecognized natural sources such as volcanoes, forest fires, or vegetation (Rahn, 1976).

4.2. Determining the natural abundance and anthropogenic concentrations of TEs in samples from impacted sites

The natural abundance of a trace element (TE_N) in a given sample can be calculated as:

$$TE_N = [TE/Y]_{UCC} \times Y_N$$

where Y_N refers to the abundance (mg/kg) of this element in the sample. It is assumed that Y in the sample is exclusively from natural sources because 1) Y behaves conservatively during chemical weathering; 2) it is supplied to the samples exclusively from soil-derived dust particles; 3) Y is not taken up by plants because it is unavailable to them (because it is hosted by insoluble minerals) and it is not essential for plants. The ratio of the abundances of the TE of interest to Y in the UCC can be obtained from published literature such as the paper by Rudnick and Gao (2014).

The concentration of the TE of interest from anthropogenic sources, TE_A, can then be calculated as:

$$TE_A = TE_T - TE_N$$

where TE_T refers to the total concentration of the element in the sample.

4.3. Determining the natural abundance and enrichments of TEs in samples from reference sites

The natural abundance of TEs and their natural enrichments should also be determined in samples from reference sites that have minimal anthropogenic influences. This is essential to determine the enrichment of TEs in plant samples due to natural processes such as plant uptake of micronutrients such as Cu and Zn, or oxidation reactions involving redox-sensitive species such as Fe and Mn. The EF and anthropogenic fractions are calculated as shown earlier.

4.4. Determining trace elements in the acid soluble ash and bulk moss

Another approach is to determine TEs in acid soluble ash (ASA) and bulk moss. The ASA of moss is composed of carbonates, phosphates, oxides, hydroxides, and sulfates which are mostly formed during the combustion process from elements such as K, Ca, Mg, S, P, Fe, and Mn in moss and are soluble in diluted acids (Sapkota et al., 2007; Steinmann and Shotyk, 1997). This fraction can also contain fine aerosols which are predominantly acid soluble oxides and hydroxides. Bulk moss receives dry and wet deposition, so would contain both the fine and coarse aerosols, if they are present.

Table 2. Pros and cons of commonly used lithophile elements as the reference element for calculating the crustal enrichment factor.

	Pros	Cons	Sources
Al	High concentrations in rock and soil, and dusts derived from them; Few anthropogenic sources; Ease of determination using various analytical techniques; Freedom from contamination during sampling.	Ever-increasing use in commercial and industrial products in urban and rural areas; Aluminum becomes residually enriched in soils during chemical weathering; aerosols derived from soils may be enriched in Al, relative to crustal abundance	Rahn, 1976; Shotyk et al., 2001
Fe	Same as aluminum.	Cannot be used for this purpose in peat cores because of the reductive dissolution of iron-bearing mineral phases under acidic, anoxic conditions.	Rahn, 1976
Hf	Forms oxides and silicates that are highly resistant to chemical weathering; Tend to be found in specific minerals e.g., “heavy” minerals such as zircon.	Concentrations in peat samples with low ash contents at/below the limit of detection in INAA (0.05 μg/g).	Shotyk, 1996a, 1996b
Sc	No preference for specific mineral phases so widely distributed among rock-forming silicate minerals and phyllosilicate clays No significant anthropogenic sources; Can be readily measured using high mass resolution ICP-MS or INAA.	Cannot be determined using ICP-MS with a single quadrupole mass analyzer.	Cloy et al., 2005; Rahn, 1976; Shotyk, 1996a, 1996b; Shotyk et al., 2016
Si	Same as aluminum.	Determined in very few aerosol samples.	Rahn, 1976
Ti	Forms oxides highly resistant to chemical weathering; Readily measured in soils using conventional XRF spectroscopy; Tend to be found in specific minerals e.g., “heavy” minerals such as ilmenite, rutile, and sphene.	Compounds too refractory and insoluble to be digested in acid; Concentrations in peats often approach/at the limit of detection in XRF spectroscopy.	Rahn, 1976; Shotyk, 1996a, 1996b; Weiss et al., 1997
Y	Forms oxides highly resistant to chemical weathering; Tend to be found in specific minerals e.g., “heavy” minerals such as monazite.	Few published studies.	Shotyk, 1996a
Zr	Forms oxides and silicates highly resistant to chemical weathering; Readily measured in soils using conventional XRF spectroscopy; Tend to be found in specific minerals e.g., “heavy” minerals such as zircon.	Concentrations in peats often below the limit of detection in XRF spectroscopy.	Shotyk, 1996a, 1996b

Abbreviation: INAA = Instrumental neutron activation analysis; ICP-MS = Inductively coupled plasma mass spectrometry; XRF = X-ray fluorescence.

5. Objective

With the increasing extent of the bituminous sands industry in Alberta, environmental concerns have grown regarding TE contamination of the air and water of surrounding ecosystems. Our previous studies have found increases in the total deposition of TEs towards industry within the Athabasca Bituminous Sands (ABS) region (Shotyk et al., 2014). Here we are asking if this increase is due to the coarse or the fine aerosol fraction? Hence, the main objective of this study is to estimate the TEs associated with the coarse and fine aerosol fractions in *Sphagnum* moss within the ABS region, by determining the distribution of TEs in bulk moss and the ASA fraction.

6. References

Aboal, J.R., Couto, J.A., Fernández, J.A., Carballeira, A., 2006. Definition and number of subsamples for using mosses as biomonitors of airborne trace elements. Arch. Environ. Contam. Toxicol. 50 (1), 88–96. doi:10.1007/s00244-005-7006-9.

Al-Radady, A.S., Davies, B.E., French, M.J., 1993. A new design of moss bag to monitor metal deposition both indoors and outdoors. Sci. Total. Environ. 133 (3), 275–283. doi:10.1016/0048-9697(93)90249-6.

Amodio, M., Catino, S., Dambruoso, P.R., Gennaro, G. de, Di Gilio, A., Giungato, P., Laiola, E., Marzocca, A., Mazzone, A., Sardaro, A., Tutino, M., 2014. Atmospheric deposition: Sampling procedures, analytical methods, and main recent findings from the scientific literature. Adv. Meteorol. 2014, 1–27. doi:10.1155/2014/161730.

Anderson, W.G., 1986. Wettability Literature Survey- Part 1: Rock/Oil/Brine Interactions and the Effects of Core Handling on Wettability. J. Pet. Technol. 38 (10), 1125–1144. doi:10.2118/13932-PA.

Anicić, M., Tasić, M., Frontasyeva, M.V., Tomasević, M., Rajsić, S., Mijić, Z., Popović, A., 2009. Active moss biomonitoring of trace elements with *Sphagnum girgensohnii* moss bags in relation to atmospheric bulk deposition in Belgrade, Serbia. Environ. Pollut. 157 (2), 673–679. doi:10.1016/j.envpol.2008.08.003.

Archibold, O.W., Crisp, P.T., 1983. The distribution of airborne metals in the Illawarra region of New South Wales, Australia. Appl. Geogr. 3 (4), 331–344. doi:10.1016/0143-6228(83)90049-8.

Barbieri, M., 2016. The importance of enrichment factor (EF) and geoaccumulation index (Igeo) to evaluate the soil contamination. J. Geol. Geophys. 5 (1). doi:10.4172/2381-8719.1000237.

Barwise, A.J.G., 1990. Role of nickel and vanadium in petroleum classification. Energy Fuels 4 (6), 647–652. doi:10.1021/ef00024a005.

Berg, T., Røyset, O., Steinnes, E., 1995. Moss (*Hylocomium splendens*) used as biomonitor of atmospheric trace element deposition: Estimation of uptake efficiencies. Atmos. Environ. 29 (3), 353–360. doi:10.1016/1352-2310(94)00259-N.

Berg, T., Steinnes, E., 1997a. Recent trends in atmospheric deposition of trace elements in Norway as evident from the 1995 moss survey. Sci. Total Environ. 208 (3), 197–206. doi:10.1016/S0048-9697(97)00253-2.

Berg, T., Steinnes, E., 1997b. Use of mosses (*Hylocomium splendens* and *Pleurozium schreberi*) as biomonitors of heavy metal deposition: From relative to absolute deposition values. Environ. Pollut. 98 (1), 61–71. doi:10.1016/S0269-7491(97)00103-6.

Berkowitz, N., Speight, J.G., 1975. The oil sands of Alberta. Fuel 54 (3), 138–149. doi:10.1016/0016-2361(75)90001-0.

Bicalho, B., Grant-Weaver, I., Sinn, C., Donner, M.W., Woodland, S., Pearson, G., Larter, S., Duke, J., Shotyk, W., 2017. Determination of ultratrace (<0.1 mg/kg) elements in Athabasca Bituminous Sands mineral and bitumen fractions using inductively coupled plasma sector field mass spectrometry (ICP-SFMS). Fuel 206, 248–257. doi:10.1016/j.fuel.2017.05.095.

Bichard, J.A., 1987. Oil sands composition and behaviour research: The research papers of John A. Bichard, 1957-1965. Alberta Oil Sands Technology and Research Authority, Edmonton Alta. Canada, 1 v. (various pagings).

Brown, D.H., Bates, J.W., 1972. Uptake of lead by two populations of *Grimmia doniana*. J. Bryol. 7 (2), 187–193. doi:10.1179/jbr.1972.7.2.187.

Cao, M., Gan, W., Liu, Q., 2007. Effect of hydrolyzable metal cations on the coagulation between hexadecane and mineral particles. J. Colloid Interface Sci. 310 (2), 489–497. doi:10.1016/j.jcis.2007.01.068.

Cao, T., An, L., Wang, M., Lou, Y., Yu, Y., Wu, J., Zhu, Z., Qing, Y., Glime, J., 2008. Spatial and temporal changes of heavy metal concentrations in mosses and its indication to the environments in the past 40 years in the city of Shanghai, China. Atmos. Environ. 42 (21), 5390–5402. doi:10.1016/j.atmosenv.2008.02.052.

Cao, T., Wang, M., An, L., Yu, Y., Lou, Y., Guo, S., Zuo, B., Liu, Y., Wu, J., Cao, Y., Zhu, Z., 2009. Air quality for metals and sulfur in Shanghai, China, determined with moss bags. Environ. Pollut. 157 (4), 1270–1278. doi:10.1016/j.envpol.2008.11.051.

Castello, M., 2007. A comparison between two moss species used as transplants for airborne trace element biomonitoring in NE Italy. Environ. Monit. Assess. 133 (1-3), 267–276. doi:10.1007/s10661-006-9579-9.

Ceburnis, D., 2000. Conifer needles as biomonitors of atmospheric heavy metal deposition: comparison with mosses and precipitation, role of the canopy. Atmos. Environ. 34 (25), 4265–4271. doi:10.1016/S1352-2310(00)00213-2.

Čeburnis, D., Valiulis, D., 1999. Investigation of absolute metal uptake efficiency from precipitation in moss. Sci. Total Environ. 226 (2-3), 247–253. doi:10.1016/S0048-9697(98)00399-4.

Choudhury, S., Panda, S.K., 2004. Induction of oxidative stress and ultrastructural changes in moss *Taxithelium nepalense* (Schwaegr.) Broth. under lead and arsenic phytotoxicity. Curr. Sci. 87 (3), 342–348.

Clark, K.A., Pasternack, D.S., 1932. Hot water seperation of bitumen from Alberta bituminous sand. Ind. Eng. Chem. 24 (12), 1410–1416. doi:10.1021/ie50276a016.

Cloy, J.M., Farmer, J.G., Graham, M.C., MacKenzie, A.B., Cook, G.T., 2005. A comparison of antimony and lead profiles over the past 2500 years in Flanders Moss ombrotrophic peat bog, Scotland. J. Environ. Monit. 7 (12), 1137–1147. doi:10.1039/B510987F.

Clymo, R., 1963. Ion exchange in *Sphagnum* and its relation to bog ecology. Ann. Bot. 27 (2), 309–324. doi:10.1093/oxfordjournals.aob.a083847.

Cooke, C.A., Kirk, J.L., Muir, D.C.G., Wiklund, J.A., Wang, X., Gleason, A., Evans, M.S., 2017. Spatial and temporal patterns in trace element deposition to lakes in the Athabasca oil sands region (Alberta, Canada). Environ. Res. Lett. 12 (12), 124001. doi:10.1088/1748-9326/aa9505.

Coombes, A.J., Lepp, N.W., 1974. The effect of Cu and Zn on the growth of *Marchantia polymorpha* and *Funaria hygrometrica*. Bryologist 77 (3), 447. doi:10.2307/3241616.

Corrin, M.L., Natusch, D.F., 1979. Physical and chemical characteristics of environmental lead, in: Boggess, W.R., Wixson, B.G. (Eds.), Lead in the Environment. Castle House Publications.

Coşkun, M., Frontasyeva, M.V., Steinnes, E., Cotuk, A.Y., Pavlov, S.S., Sazonov, A.S., Cayir, A., Belivermis, M., 2005. Atmospheric deposition of heavy metals in thrace studied by analysis of moss (*Hypnum cupressiforme*). Bull. Environ. Contam. Toxicol. 74 (1), 201–209. doi:10.1007/s00128-004-0569-8.

Czarnowska, K., Gworek, B., 1992. Heavy metal content of moss from Kampinos National Park in Poland. Environ. Geochem. Health 14 (1), 9–14. doi:10.1007/BF01783620.

Czarnowska, K., Rejement-Grochowska, I., 1974. Concentration of heavy metals - iron, manganese, zinc and copper in mosses. Acta Soc. Bot. Pol. 43 (1).

Damman, A.W.H., 1986. Hydrology, development, and biogeochemistry of ombrogenous peat bogs with special reference to nutrient relocation in a western Newfoundland bog. Can. J. Bot. 64 (2), 384–394. doi:10.1139/b86-055.

Dauvalter, V.A., Kashulin, N., Lehto, J., Jernstrom, J., 2009. Chalcophile elements Hg, Cd, Pb, As in Lake Umbozero, Murmansk Region, Russia. Int. J. Environ. Res. Public Health 3 (3), 411–428.

Davies, B.E., White, H.M., 1981. Environmental pollution by wind blown lead mine waste: A case study in wales, U.K. Sci. Total Environ. 20 (1), 57–74. doi:10.1016/0048-9697(81)90036-X.

Davison, R.L., Natusch, D.F.S., Wallace, J.R., Evans, C.A., 1974. Trace elements in fly ash: Dependence of concentration on particle size. Environ. Sci. Technol. 8 (13), 1107–1113. doi:10.1021/es60098a003.

Delfanti, R., Papucci, C., Benco, C., 1999. Mosses as indicators of radioactivity deposition around a coal-fired power station. Sci. Total Environ. 227 (1), 49–56. doi:10.1016/S0048-9697(98)00410-0.

Feder, W.A., 1978. Plants as bioassay systems for monitoring atmospheric pollutants. Environ. Health Perspect. 27, 139–147. doi:10.1289/ehp.7827139.

Glooschenko, W.A., Capobianco, J.A., 1978. Metal content of *Sphagnum* mosses from two Northern Canadian bog ecosystems. Water Air Soil Pollut. 10 (2), 215–220. doi:10.1007/BF00464716.

Goel, J., Kadirvelu, K., Rajagopal, C., Kumar Garg, V., 2005. Removal of lead(II) by adsorption using treated granular activated carbon: batch and column studies. J. Hazard. Mater. 125 (1-3), 211–220. doi:10.1016/j.jhazmat.2005.05.032.

González, A.G., Pokrovsky, O.S., 2014. Metal adsorption on mosses: Toward a universal adsorption model. J. Colloid Interface Sci. 415, 169–178. doi:10.1016/j.jcis.2013.10.028.

Gosselin, P., Hrudey, S., Naeth, M., Plourde, A., Therrien, R., Van Der Kraak, G., Xu, Z., 2010. Environmental and health impacts of Canada's oil sands industry. Royal Society of Canada, Ottawa, Ontario: The Royal Society of Canada (RSC), 440 pp. https://rsc-src.ca/sites/default/files/RSC%20Oil%20Sands%20Panel%20Main%20Report%20Oct%202012.pdf.

Government of Alberta, 2021. Oil Sands Facts and Statistics. https://www.alberta.ca/oil-sands-facts-and-statistics.aspx.

Graney, J.R., Landis, M.S., Krupa, S., 2012. Coupling lead isotopes and element concentrations in epiphytic lichens to track sources of air emissions in the Athabasca Oil Sands Region, in: Percy, K.E. (Ed.), Alberta Oil Sands, vol. 11. Elsevier, pp. 343–372.

Gray, M.R., 2015. Tutorial on Upgrading of Oilsands Bitumen. University of Alberta, 2015.

Hampp, R., Lendzian, K., 1974. Effect of lead ions on chlorophyll synthesis. Naturwissenschaften 61 (5), 218–219. doi:10.1007/BF00599926.

Harmens, H., Buse, A., Buker, P., Norris, D., Mills, G., Williams, B., Reynolds, B., Ashenden, T.W., Ruhling, A., Steinnes, E., 2004. Heavy metal concentrations in European mosses: 2000/2001 survey. J. Atmos. Chem. 49, 425–436.

Hepler, L.G., Smith, R.G., 1994. The Alberta oil sands: Industrial procedures for extraction and some recent fundamental research. AOSTRA Technical Publication Series 14. Alberta Oil Sands Technology and Research Authority.

Jiang, Y., Fan, M., Hu, R., Zhao, J., Wu, Y., 2018. Mosses are better than leaves of vascular plants in monitoring atmospheric heavy metal pollution in urban areas. Int. J. Environ. Res. Public Health 15 (6). doi:10.3390/ijerph15061105.

Jordaan, S.M., 2012. Land and water impacts of oil sands production in Alberta. Environ. Sci. Technol. 46 (7), 3611–3617. doi:10.1021/es203682m.

Kasongo, T., Zhou, Z., Xu, Z., Masliyah, J.H., 2000. Effect of clays and calcium ions on bitumen extraction from Athabasca oil sands using flotation. Can. J. Chem. Eng 78 (4), 674–681. doi:10.1002/cjce.5450780409.

Kempter, H., Krachler, M., Shotyk, W., Zaccone, C., 2017. Major and trace elements in *Sphagnum* moss from four southern German bogs, and comparison with available moss monitoring data. Ecol. Indic. 78, 19–25. doi:10.1016/j.ecolind.2017.02.029.

Kosior, G., Frontasyeva, M.V., Ziembik, Z., Zincovscaia, I., Dołhańczuk-Śródka, A., Godzik, B., 2020. The moss biomonitoring method and neutron activation analysis in assessing pollution by trace elements in selected Polish national parks. Arch. Environ. Contam. Toxicol. 79 (3), 310–320. doi:10.1007/s00244-020-00755-6.

Landis, M.S., Pancras, J.P., Graney, J.R., Stevens, R.K., Percy, K.E., Krupa, S., 2012. Receptor modeling of epiphytic lichens to elucidate the sources and spatial distribution of inorganic air pollution in the Athabasca Oil Sands Region, in: Percy, K.E. (Ed.), Alberta Oil Sands, vol. 11. Elsevier, pp. 427–467.

Landis, M.S., Patrick Pancras, J., Graney, J.R., White, E.M., Edgerton, E.S., Legge, A., Percy, K.E., 2017. Source apportionment of ambient fine and coarse particulate matter at the Fort McKay community site, in the Athabasca Oil Sands Region, Alberta, Canada. Sci. Total. Environ. 584-585, 105–117. doi:10.1016/j.scitotenv.2017.01.110.

Lane, S.D., Martin, E.S., 1980. Further Observations on the Distribution of Lead in Juvenile Roots of Raphanus sativus. Z. Pflanzenphysiol. 97 (2), 145–152. doi:10.1016/S0044-328X(80)80028-6.

Lee, C.S.L., Li, X., Zhang, G., Peng, X., Zhang, L., 2005. Biomonitoring of trace metals in the atmosphere using moss (*Hypnum plumaeforme*) in the Nanling Mountains and the Pearl River Delta, Southern China. Atmos. Environ. 39 (3), 397–407. doi:10.1016/j.atmosenv.2004.09.067.

Lévesque, C.M., 2014. Oil sands process water and tailings pond contaminant transport and fate : Physical, chemical and biological processes.

Liu, J., Xu, Z., Masliyah, J., 2005. Interaction forces in bitumen extraction from oil sands. J. Colloid Interface Sci. 287 (2), 507–520. doi:10.1016/j.jcis.2005.02.037.

Liu, J., Xu, Z., Masliyah, J.H., 2003. Studies on Bitumen−Silica Interaction in Aqueous Solutions by Atomic Force Microscopy. Langmuir 19 (9), 3911–3920. doi:10.1021/la0268092.

Liu, J., Xu, Z., Masliyah, J.H., 2004. Role of fine clays in bitumen extraction from oil sands. AIChE J. 50 (8), 1917–1927. doi:10.1002/aic.10174.

Liu, J., Zhou, Z., Xu, Z., Masliyah, J.H., 2002. Bitumen-clay interactions in aqueous media studied by zeta potential distribution measurement. J. Colloid Interface Sci. 252 (2), 409–418. doi:10.1006/jcis.2002.8471.

Maevskaya, S., Kardash, A., Demkiv, O., 2001. Absorption of cadmium and lead ions by gametophyte of the moss *Plagiomnium undulatum*. Russ. J. Plant Physiol. 48 (6), 820–824.

Malmer, N., 1988. Patterns in the growth and the accumulation of inorganic constituents in the *Sphagnum* cover on ombrotrophic bogs in Scandinavia. Oikos 53 (1), 105. doi:10.2307/3565670.

Masliyah, J.H., Czarnecki, J., Xu, Z., 2011. Handbook on Theory and Practice on Bitumen Recovery from Athabasca Oil Sands: Volume I: Theoretical Basis. University of Alberta Libraries.

Masliyah, J.H., Zhou, Z.J., Xu, Z., Czarnecki, J., Hamza, H., 2004. Understanding water-based bitumen extraction from Athabasca oil sands. Can. J. Chem. Eng 82 (4), 628–654. doi:10.1002/cjce.5450820403.

Moschopedis, S.E., Schulz, K.F., Speight, J.G., Morrison, D.N., 1980. Surface-active materials from Athabasca oil sands. Fuel Process. Technol. 3 (1), 55–61. doi:10.1016/0378-3820(80)90023-5.

Mossop, G.D., 1980. Geology of the Athabasca oil sands. Science 207 (4427), 145–152. doi:10.1126/science.207.4427.145.

Natusch, D.F.S., Wallace, J.R., Evans, C.A., 1974. Toxic trace elements: Preferential concentration in respirable particles. Science 183 (4121), 202–204. doi:10.1126/science.183.4121.202.

Nriagu, J.O., 1990. Global metal pollution: Poisoning the biosphere? Environ.: Sci. Policy Sustainable Dev. 32 (7), 7–33. doi:10.1080/00139157.1990.9929037.

Oil Sands Magazine, 2020. Bitumen Upgrading Explained. https://www.oilsandsmagazine.com/technical/bitumen-upgrading.

Osacky, M., Geramian, M., Ivey, D.G., Liu, Q., Etsell, T.H., 2013. Mineralogical and chemical composition of petrologic end members of Alberta oil sands. Fuel 113, 148–157. doi:10.1016/j.fuel.2013.05.099.

Pacyna, J.M., Pacyna, E.G., 2001. An assessment of global and regional emissions of trace metals to the atmosphere from anthropogenic sources worldwide. Environ. Rev. 9 (4), 269–298. doi:10.1139/a01-012.

Padmavathiamma, P.K., Li, L.Y., 2007. Phytoremediation technology: Hyper-accumulation metals in plants. Water Air Soil Pollut. 184 (1-4), 105–126. doi:10.1007/s11270-007-9401-5.

Pakarinen, P., 1978. Production and nutrient ecology of three *Sphagnum* species in southern Finnish raised bogs. Ann. Botan. Fenn. 15 (1), 15–26.

Pakarinen, P., 1981. Regional variation of sulphur concentrations in *Sphagnum* mosses and *Cladonia* lichens in Finnish bogs. Ann. Botan. Fenn. 18 (4), 275–279.

Pakarinen, P., Tolonen, K., 1976. Regional survey of heavy metals in peat mosses (*Sphagnum*). Ambio 5 (1), 38–40.

Phillips-Smith, C., Jeong, C.-H., Healy, R.M., Dabek-Zlotorzynska, E., Celo, V., Brook, J.R., Evans, G., 2017. Sources of particulate matter components in the Athabasca oil sands region: Investigation through a comparison of trace element measurement methodologies. Atmos. Chem. Phys. 17 (15), 9435–9449. doi:10.5194/acp-17-9435-2017.

Pilegaard, K., 1979. Heavy metals in bulk precipitation and transplanted *Hypogymnia physodes* and *Dicranoweisia cirrata* in the vicinity of a Danish steelworks. Water Air Soil Pollut. 11 (1), 77–91. doi:10.1007/BF00163521.

Poikolainen, J., Kubin, E., Piispanen, J., Karhu, J., 2004. Atmospheric heavy metal deposition in Finland during 1985–2000 using mosses as bioindicators. Sci. Total. Environ. 318 (1-3), 171–185. doi:10.1016/S0048-9697(03)00396-6.

Punning, J.-M., Alliksaar, T., 1997. The trapping of fly-ash particles in the surface layers of *Sphagnum*-dominated peat. Water Air Soil Pollut. 94 (1-2), 59–69. doi:10.1007/BF02407093.

Rahn, K.A., 1976. The Chemical Composition of the Atmospheric Aerosol. Graduate School of Oceanography, University of Rhode Island, Kingston, Rhode Island, USA, 279 pp.

Ramasamy, M.G. (Ed.), 2019. Processing of Heavy Crude Oils - Challenges and Opportunities. IntechOpen, London, United Kingdom, 276 pp.

Rao, D., 1982. Responses of bryophytes to air pollution, in: Smith, A. (Ed.), Bryophyte Ecology. Chapman and Hall Ltd, Holborn, London, UK, pp. 445–471.

Rao, D., Robitaille, G., LeBlanc, F., 1977. Influence of heavy metal pollution on lichens and bryophytes. J. Hattori Bot. Lab; (Japan) 42.

Rudnick, R.L., Gao, S., 2014. Composition of the continental crust, in: Holland, H., Turekian, K. (Eds.), Treatise on Geochemistry, vol. 4, 2nd ed. Elsevier, pp. 1–51.

Rühling, Å., Tyler, G., Ruhling, A., 1970. Sorption and retention of heavy metals in the woodland moss *Hylocomium splendens* (Hedw.) Br. et Sch. Oikos 21 (1), 92. doi:10.2307/3543844.

Sakalys, J., Kvietkus, K., Sucharová, J., Suchara, I., Valiulis, D., 2009. Changes in total concentrations and assessed background concentrations of heavy metals in moss in Lithuania and the Czech Republic between 1995 and 2005. Chemosphere 76 (1), 91–97. doi:10.1016/j.chemosphere.2009.02.009.

Salemaa, M., Derome, J., Helmisaari, H.-S., Nieminen, T., Vanha-Majamaa, I., 2004. Element accumulation in boreal bryophytes, lichens and vascular plants exposed to heavy metal and sulfur deposition in Finland. Sci. Total Environ. 324 (1-3), 141–160. doi:10.1016/j.scitotenv.2003.10.025.

Sanford, E.C., 1983. Processibility of Athabasca oil sand: Interrelationship between oil sand fine solids, process aids, mechanical energy and oil sand age after mining. Can. J. Chem. Eng 61 (4), 554–567. doi:10.1002/cjce.5450610410.

Sanford, E.C., Seyer, F., 1979. Processibility of Athabasca tar sand using batch extraction unit: The role of NaOH. CIM Bulletin. 72, 164–169.

Santelmann, M.V., Gorham, E., 1988. The influence of airborne road dust on the chemistry of *Sphagnum* mosses. J. Ecol. 76 (4), 1219. doi:10.2307/2260644.

Sapkota, A., Chebukin, A.K., Bonani, G., Shotyk, W., 2007. Six millennia of atmospheric dust deposition in southern South America (Isla Navarino, Chile). Holocene 17 (5), 561–572. doi:10.1177/0959683607078981.

Sardans, J., Peñuelas, J., 2005. Trace element accumulation in the moss *Hypnum cupressiforme* Hedw. and the trees *Quercus ilex* L. and *Pinus halepensis* Mill. in Catalonia. Chemosphere 60 (9), 1293–1307. doi:10.1016/j.chemosphere.2005.01.059.

Saxena, D.K., Srivastava, K., Singh, S., 2008. Biomonitoring of metal deposition by using moss transplant method through *Hypnum cupressiforme* (Hedw.) in Mussoorie. J. Environ. Biol. 29 (5), 683–688.

Schilling, J.S., Lehman, M.E., 2002. Bioindication of atmospheric heavy metal deposition in the Southeastern US using the moss *Thuidium delicatulum*. Atmos. Environ. 36 (10), 1611–1618. doi:10.1016/S1352-2310(02)00092-4.

Schintu, M., Cogoni, A., Durante, L., Cantaluppi, C., Contu, A., 2005. Moss (*Bryum radiculosum*) as a bioindicator of trace metal deposition around an industrialised area in Sardinia (Italy). Chemosphere 60 (5), 610–618. doi:10.1016/j.chemosphere.2005.01.050.

Schröder, W., Pesch, R., 2007. Synthesizing bioaccumulation data from the German metals in mosses surveys and relating them to ecoregions. Sci. Total. Environ. 374 (2-3), 311–327. doi:10.1016/j.scitotenv.2006.09.015.

Schuetz, L., 1989. Atmospheric mineral dust - properties and source markers, in: Leinen, M., Sarnthein, M. (Eds.), Paleoclimatology and paleometeorology: Modern and past patterns of global atmospheric transport. Kluwer Academic Publishers, Dordrecht, The Netherlands, pp. 359–384.

Schütz, L., 1980. Long range transport of desert dust with special emphasis on the Sahara. Ann. NY Acad. Sci. 338 (1 Aerosols), 515–532. doi:10.1111/j.1749-6632.1980.tb17144.x.

Schütz, L., Rahn, K.A., 1982. Trace element concentrations in erodible soils. Atmos. Environ. 16 (1), 171–176.

Shimwell, D.W., Laurie, A.E., 1972. Lead and zinc contamination of vegetation in the southern Pennines. Environ. Pollut. 3 (4), 291–301. doi:10.1016/0013-9327(72)90024-9.

Shotyk, W., 1996a. Natural and anthropogenic enrichments of As, Cu, Pb, Sb, and Zn in ombrotrophic versus minerotrophic peat bog profiles, Jura Mountains, Switzerland. Water Air Soil Pollut. 90 (3-4), 375–405. doi:10.1007/BF00282657.

Shotyk, W., 1996b. Peat bog archives of atmospheric metal deposition: Geochemical evaluation of peat profiles, natural variations in metal concentrations, and metal enrichment factors. Environ. Rev. 4 (2), 149–183. doi:10.1139/a96-010.

Shotyk, W., Belland, R., Duke, J., Kempter, H., Krachler, M., Noernberg, T., Pelletier, R., Vile, M.A., Wieder, K., Zaccone, C., Zhang, S., 2014. *Sphagnum* mosses from 21 ombrotrophic bogs in the Athabasca Bituminous Sands region show no significant atmospheric contamination of "heavy metals". Environ. Sci. Technol. 48 (21), 12603–12611. doi:10.1021/es503751v.

Shotyk, W., Bicalho, B., Cuss, C.W., Duke, J., Noernberg, T., Pelletier, R., Steinnes, E., Zaccone, C., 2016. Dust is the dominant source of "heavy metals" to peat moss (*Sphagnum fuscum*) in the bogs of the Athabasca Bituminous Sands region of northern Alberta. Environ. Int. 92-93, 494–506. doi:10.1016/j.envint.2016.03.018.

Shotyk, W., Bicalho, B., Grant-Weaver, I., Stachiw, S., 2019. A geochemical perspective on the natural abundance and predominant sources of trace elements in cranberries (*Vaccinium oxycoccus*) from remote bogs in the Boreal region of northern Alberta, Canada. Sci. Total. Environ. 650 (Pt 1), 1652–1663. doi:10.1016/j.scitotenv.2018.06.248.

Shotyk, W., Cuss, C.W., 2019. Atmospheric Hg accumulation rates determined using *Sphagnum* moss from ombrotrophic (rain-fed) bogs in the Athabasca Bituminous Sands region of northern Alberta, Canada. Ecol. Indic. 107, 105626. doi:10.1016/j.ecolind.2019.105626.

Shotyk, W., Kempter, H., Krachler, M., Zaccone, C., 2015. Stable (206Pb, 207Pb, 208Pb) and radioactive (210Pb) lead isotopes in 1 year of growth of *Sphagnum* moss from four ombrotrophic bogs in southern Germany: Geochemical significance and environmental implications. Geochim. Cosmochim. Acta 163, 101–125. doi:10.1016/j.gca.2015.04.026.

Shotyk, W., Weiss, D., Kramers, J.D., Frei, R., Chebukin, A.K., Gloor, M., Reese, S., 2001. Geochemistry of the peat bog at Etang de la Grue‘re, Jura Mountains, Switzerland, and its record of atmospheric Pb and lithogenic trace metals (Sc, Ti, Y, Zr, and REE) since 12,370 ^{14}C yr BP. Geochim. Cosmochim. Acta 65 (14), 2337–2360. doi:10.1016/S0016-7037(01)00586-5.

Skaar, H., Ophus, E., Gullvag, B., 1973. Lead accumulation within nuclei of moss leaf cells. Nature 241 (5386), 215–216. doi:10.1038/241215a0.

Spagnuolo, V., Giordano, S., Pérez-Llamazares, A., Ares, A., Carballeira, A., Fernández, J.A., Aboal, J.R., 2013. Distinguishing metal bioconcentration from particulate matter in moss tissue: testing methods of removing particles attached to the moss surface. Sci. Total. Environ. 463-464, 727–733. doi:10.1016/j.scitotenv.2013.05.061.

Spearing, A.M., 1972. Cation-exchange capacity and galacturonic acid content of several species of *Sphagnum* in sandy ridge bog, Central New York State. Bryologist. 75 (2), 154. doi:10.2307/3241443.

Ștefănuț, S., Öllerer, K., Manole, A., Ion, M.C., Constantin, M., Banciu, C., Maria, G.M., Florescu, L.I., 2019. National environmental quality assessment and monitoring of atmospheric heavy metal pollution - A moss bag approach. J. Environ. Manage. 248, 109224. doi:10.1016/j.jenvman.2019.06.125.

Steinmann, P., Shotyk, W., 1997. Geochemistry, mineralogy, and geochemical mass balance on major elements in two peat bog profiles (Jura Mountains, Switzerland). Chem. Geol. 138 (1-2), 25–53.

Steinnes, E., 1997. Trace element profiles in ombrogenous peat cores from Norway: Evidence of long range atmospheric transport. Water Air Soil Pollut. 100 (3/4), 405–413. doi:10.1023/A:1018388912711.

Steinnes, E., Berg, T., Uggerud, H.T., 2011. Three decades of atmospheric metal deposition in Norway as evident from analysis of moss samples. Sci. Total Environ. 412-413, 351–358. doi:10.1016/j.scitotenv.2011.09.086.

Steinnes, E., Solberg, W., Petersen, H., Wren, C.D., 1989. Heavy metal pollution by long range atmospheric transport in natural soils of Southern Norway. Water Air Soil Pollut. 45 (3-4), 207–218. doi:10.1007/BF00283452.

Strausz, O.P., 1989. Bitumen and heavy oil chemistry, in: Hepler, L.G., Hsi, C. (Eds.), AOSTRA Technical Handbook on Oil Sands, Bitumens and Heavy Oils. Alberta Oil Sands Technology and Research Authority, Edmonton, Alberta, pp. 33–73.

Strausz, O.P., Lown, E.M., 2003. The Chemistry of Alberta Oil Sands, Bitumens and Heavy oil. Alberta Energy Research Institute, Calgary, Alberta, Canada.

Sun, S.-Q., Wang, D.-Y., He, M., Zhang, C., 2009. Monitoring of atmospheric heavy metal deposition in Chongqing, China—based on moss bag technique. Environ. Monit. Assess. 148 (1-4), 1–9. doi:10.1007/s10661-007-0133-1.

Swift, D.L., Proctor, D.F., 1982. Human respiratory deposition of particles during oronasal breathing. Atmos. Environ. 16 (9), 2279–2282. doi:10.1016/0004-6981(82)90307-9.

Takamura, K., 1982. Microscopic structure of athabasca oil sand. Can. J. Chem. Eng 60 (4), 538–545. doi:10.1002/cjce.5450600416.

Takamura, K., 1985. Physio-chemical characterization of Athabasca oil sand and its significance to bitumen recovery. AOSTRA (Alberta Oil Sands Technology Authority) Journal of Research; (Canada) 2:1.

Tyler, G., 1990. Bryophytes and heavy metals: a literature review. Bot. J. Linn. Soc. 104 (1-3), 231–253. doi:10.1111/j.1095-8339.1990.tb02220.x.

Vile, M.A., Wieder, R.K., Novk, M., 1999. Mobility of Pb in *Sphagnum*-derived peat. Biogeochemistry 45 (1), 35–52. doi:10.1007/BF00992872.

Wallace, D., Henry, D., Takamura, K., 1989. A physical chemical explanation for deterioration in the hot water processability of Athabasca oil sands due to aging. Fuel Sci. Technol. Int. 7 (5-6), 699–725. doi:10.1080/08843758908962265.

Wang, X., Chow, J.C., Kohl, S.D., Yatavelli, L.N.R., Percy, K.E., Legge, A.H., Watson, J.G., 2015. Wind erosion potential for fugitive dust sources in the Athabasca Oil Sands Region. Aeolian Res. 18, 121–134. doi:10.1016/j.aeolia.2015.07.004.

Watkinson, S.C., Watt, F., 1992. The cellular localisation of elements in leaf cells of *Sphagnum* with the scanning proton microprobe. Bryologist. 95 (2), 181. doi:10.2307/3243433.

Watson, J.G., Chow, J.C., Wang, X., Kohl, S.D., 2014. Windblown fugitive dust characterization in the Athabasca Oil Sands Region. WBEA-DRI Agreement Number: T108-13. https://wbea.org/wp-content/uploads/2018/03/watson_j_g_et_al_2014_windblown_fugitive_dust_characterization_in_the_athabasca_oil_sands_region.pdf.

Weiss, D., Shotyk, W., Cheburkin, A.K., Gloor, M., Reese, S., 1997. Atmospheric lead deposition from 12,400 to ca. 2,000 yrs BP in a peat bog profile, Jura Mountains, Switzerland. Water Air Soil Pollut. 100 (3/4), 311–324. doi:10.1023/A:1018341029549.

Whitby, K.T., Husar, R., Liu, B., 1972. The aerosol size distribution of Los Angeles smog. J. Colloid Interface Sci. 39 (1), 177–204.

Willeke, K., Whitby, K.T., 1975. Atmospheric aerosols: size distribution interpretation. J. Air Pollut. Control Assoc. 25 (5), 529–534. doi:10.1080/00022470.1975.10470110.

Xing, Z., Du, K., 2017. Particulate matter emissions over the oil sands regions in Alberta, Canada. Environ. Rev. 25 (4), 432–443. doi:10.1139/er-2016-0112.

Xu, M., Yu, D., Yao, H., Liu, X., Qiao, Y., 2011. Coal combustion-generated aerosols: Formation and properties. Proc. Combust. Inst . 33 (1), 1681–1697. doi:10.1016/j.proci.2010.09.014.

Zufall, M.J., Davidson, C.I., 1998. Dry deposition of particles from the atmosphere, in: Linkov, I., Wilson, R. (Eds.), Air Pollution in the Ural Mountains: Environmental, Health and Policy Aspects. Springer Netherlands, Dordrecht, pp. 55–73.

CHAPTER 2. TRACE ELEMENTS IN THE ACID SOLUBLE ASH FRACTION OF *SPHAGNUM* MOSS: SURROGATE FOR ATMOSPHERIC DEPOSITION OF SUB-MICRON AEROSOLS WITHIN THE ATHABASCA BITUMINOUS SANDS REGION

Abstract

Airborne trace elements (TEs) from the development of the Athabasca Bituminous Sands (ABS) in northern Alberta, occur in coarse and fine aerosols. Here, TEs in *Sphagnum* moss and Acid Soluble Ash (ASA, obtained by leaching ash for 15 min using 2% HNO_3) are used as surrogates of these two aerosol fractions. Total concentrations of all elements increase toward industry, but chemical reactivity of the ash varies. Most of the Al is "soluble", but most of the Th is not, with the former assumed to reflect the reactivity of clays, and the latter the stability of heavy minerals. The trends in Ni and V, predominantly present in bitumen, resemble Al. In contrast, Mo (also enriched in bitumen), plus Pb, Sb and Tl, are more like Th in exhibiting limited reactivity. The elements enriched in moss (total and ASA fractions), relative to crustal abundance, are either plant micronutrients (e.g., Cu, Mn, Mo, Zn), or resemble them (e.g., Ag, Cd, Rb, and Re) due to their similar chemical properties, with the greatest values at the control site. The ash of moss collected nearest industry is dominated by quartz (67%) which explains the low concentrations of TEs, absence of enrichment relative to crustal abundance, and limited chemical reactivity of Pb, Sb and Tl .

Keywords: Acid Soluble Ash; Athabasca Bituminous Sands; Atmospheric deposition; Fine aerosol; *Sphagnum* moss; Trace elements

Synopsis

The acid soluble ash of *Sphagnum* moss estimates the abundance of trace elements in the fine aerosol fraction of atmospheric deposition.

TOC

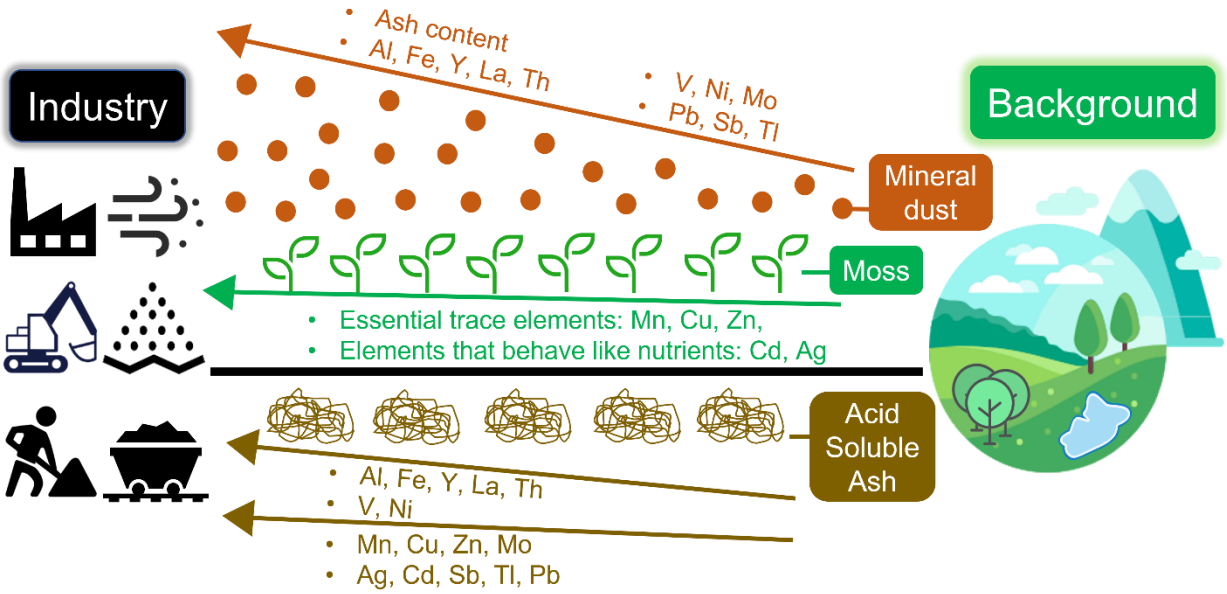

1. INTRODUCTION

Upgrading and refining of hydrocarbons extracted from the Athabasca Bituminous Sands (ABS) in Alberta, Canada has remarkably propelled the economy of the province. Capital investment in oil production has accelerated at a considerable rate from more than $1 billion in 1996, to $16 billion per year from 2006 to 2008.[1] Direct employment of the industry in the Fort McMurray area alone doubled between 1998 and 2008 from 6,000 to 12,000.[1] Total bitumen production was 2981 thousand barrels per day (bbl/d) in 2020, and is forecasted to increase to 4039 thousand bbl/d by 2030.[2] However, with the increasing extent of the industry, environmental concerns regarding trace element (TE) contamination of the surrounding ecosystems are growing.[3–5] Mechanical processing of ABS ores such as open-pit mining, quarrying, and road construction have yielded considerable amounts of dusts that are transported to the surrounding areas.[5–14] Dusts from anthropogenic activities fall generally into one of two classes: coarse and fine aerosols.[15–17]

Coarse aerosols are usually generated during open pit mining activities by mechanical processes such as road construction, blasting operations, rock excavation and crushing activities: these are comparatively large (10–100 μm) and hence non-respirable.[6,7,18] Given their size and density, they are typically removed from the air by sedimentation, giving them short atmospheric residence times (minutes to hours) and limited transport distances[15,17,19–22] On average, the ABS are approximately 85% mineral matter, predominantly dune and beach aeolian sands,[23] with most particles > 100 μm.[24] The mineral composition is dominated by light minerals (99%), mainly quartz (60–90%) and phyllosilicate clays (kaolinite and illite), with minor amounts of feldspars (including orthoclase), mica (biotite and muscovite), carbonates, and chalcedony.[25] Heavy minerals (density > 2.96 g/cm^3) account for 1% of the mineral fraction, and include ilmenite,

tourmaline and zircon.[25] Except for the carbonates, these minerals have limited solubility in dilute acids.[26] Further, they are commonly enriched in conservative, lithophile elements such as Ti, Y, the lanthanides, and Th.

In contrast, fine aerosols are generated by high temperature processes such as the combustion of coal and other fossil fuels, smelting of metallic ores, cement production and waste incineration.[8,27,28] Fine aerosols are typically generated by gas-to-particle conversion reactions, occur in the size range of 0.1–1 μm, and are respirable.[15,17,18,27,29–31] Due to their small size, they remain suspended in the air until they are removed by wet or dry deposition.[17,21,27,31] With long atmospheric residence times (as long as a week), fine aerosols are easily transported for thousands of kilometers.[22,27,30,31] These fine aerosols are mostly in the form of easily acid soluble metal oxides and hydroxides and can be very rich in chalcophile elements such as Pb and Cd.[29,30,32] Particle size and chemical composition have a profound influence on the potential bioaccessibility and bioavailability of TEs in aerosols.[29,33,34] When potentially toxic metals such as these are released to the environment in the form of sub-micron, acid soluble particles, they represent a potential threat to the health of many living organisms.[18,28,35,36] Hence, to gain a better understanding of the associated human and ecosystem health risks of open pit bitumen mining and upgrading, it is important to distinguish between TEs in the coarse versus fine aerosol fractions.

Sphagnum mosses growing in ombrotrophic (rain-fed) bogs are excellent bio-monitors of atmospheric deposition. They receive water and nutrients solely from the atmosphere, and exhibit remarkable capacities to retain atmospheric particles and ionic forms of TEs by either wet or dry deposition, due to their large surface area,[37,38] absence of leaf cuticles,[37,39,40] large density of negative surface charges, and high surface cation exchange capacity.[38,41,42] Further, they are more resistant to higher levels of potentially toxic TEs than vascular plants.[38,43–47] Assessing the spatial

and temporal variations of atmospheric deposition of TEs using mosses has proven to be an efficient, useful, and economic approach for environmental monitoring. Strong positive linear correlations were observed between element concentrations in moss and independently measured atmospheric deposition rates, with results comparable to those obtained by conventional precipitation collection analysis.[38,48–53] Thus, moss techniques for atmospheric deposition analysis have been extensively used around the world.[49,54–56]

Previous studies have found that total concentrations of Ag, Cd, Mo, Ni, Pb, Sb, and Tl in *Sphagnum* within the ABS region were similar to or lower than those in the "cleanest" ancient peat samples from Switzerland, and their increasing concentrations towards the ABS region were attributed to mineral dust deposition.[14] The mineral dust deposition rates within the ABS region were later quantified by distinguishing the acid soluble (ASA) and acid insoluble (AIA) ash fractions of *Sphagnum*.[57] Mass accumulation rates of ash (6.0–27.3 g m^{-2} $year^{-1}$), AIA (1–11.9 g m^{-2} $year^{-1}$), and acid soluble concentrations of individual elements (Ca, Fe, K, Mg, P and S) all showed general increasing trends close to industry.[57] However, in that study, no measurements were made of any TEs in the ASA fraction. Given the concerns regarding potentially toxic TEs, we estimate the chemical reactivity of these dusts by determining the abundance of TEs in the ASA fraction. The ASA fraction is analyzed after filtering the leached ash through a 0.45 μm membrane filter.[57,58] Thus, TEs in the ASA fraction of *Sphagnum* can be used as a surrogate for the fine aerosol fraction, with analyses of bulk moss representing the composition of both coarse and fine aerosols. Comparing the results from these two fractions provides a first assessment of the chemical reactivity of the dusts emitted from bitumen mining and upgrading, with implications for the health of surrounding ecosystems.

2. MATERIALS AND METHODS

2.1. Sample Collection

The *Sphagnum* mosses used in this study were collected in the fall of 2015, 2019, and 2020. In September of 2015, *Sphagnum* moss was collected from 30 bogs within the ABS region, with moss from Utikuma (UTK), Birch Mountains Wildland (BMW), and Caribou Mountains Wildland (CMW) chosen as control sites, as described by Mullan-Boudreau et al. [57] (Supporting Information (SI) 1, Fig. S1). In October of 2019 and 2020, *Sphagnum* moss was collected in the ABS region again, from JPH4, McKay (McK), McMurray (McM), and Anzac (ANZ): these are listed in the order of increasing distance from the centre of industrial activity (SI.1, Fig. S1). Specifically, the four bogs are 12, 25, 49, and 68 km away from the mid-point between the two central bitumen upgraders. UTK, the control site which is 264 km SW from this mid-point, was also included. For comparison and context, samples were also collected from the Wagner Natural Area (WAG) and Elk Island National Park (EINP) which are both near Edmonton.

At each location, samples were collected in triplicate from *Sphagnum* hummocks within relatively open areas, with individual samples taken approximately three meters apart. They were extracted by placing polypropylene (PP) boxes up-side-down on the hummocks, pressing down to have moss fill the container, and then cutting along the edges of the container with a medical-grade stainless steel knife. The mosses were then cut at the base of the box and sealed with the PP lid. Hair nets and polyethylene (PE) gloves were worn during collection. The PP boxes had been washed in the lab using soap and water, rinsed with tap water, and then three times with deionized water before departure to the field. Upon arrival in the lab, the samples were stored at -20 °C to prevent any changes before sample treatment.

2.2. Analytical Methods

2.2.1. Sample preparation

In the lab, the wet *Sphagnum* moss samples were cleaned of all dead and foreign plant materials using surgical stainless steel tweezers while wearing PE gloves and a hair net (SI.1, Fig. S2). The cleaned samples were placed in PP jars and dried at 105 °C in a stainless steel drying oven for two to three days until constant weight.

Subsamples of dried moss were ground by hand using an agate mortar and pestle and reserved for analyses of the bulk plant material. The remainder of each dried sample was ashed at 550 °C for 16 hours in a muffle furnace (MLS Pyro High-Temperature Microwave Muffle Furnace, Leutkirch, Germany) to obtain the ash.

2.2.2. Acid digestion of dry milled moss and acid leaching of ashed moss

Approximately 200 mg of moss was digested in a high-pressure microwave autoclave (Milestone, UltraCLAVE MA 033) as described in detail by Shotyk et al.[14] The concentrated nitric acid (HNO_3, 3 ml) used had been purified twice by sub-boiling distillation in high purity quartz (Duopur, MLS, Leutkirch, Germany). The tetrafluoroboric acid (HBF_4, 0.1 ml) was used as supplied (Certified CAS, Fisher Scientific). For quality control, two standard reference materials (SRMs) were also digested: 1515 Apple Leaves from the National Institute of Standards and Technology (NIST), and Moss-1343 from the Finnish Forest Research Institute (FFRI).

To obtain the ASA fraction of *Sphagnum* moss for TE analyses, the procedure described by Sapkota et al.[58] and Mullan-Boudreau et al.[57] was modified by substituting HNO_3 for HCl in order to minimize interferences (by chloride) in the mass spectra obtained using quadrupole ICP-MS.[59] One hundred to 150 mg of ash was leached with 2% HNO_3 for 15 min at room temperature,

then filtered through 0.45 μm polytetrafluoroethylene (PTFE) filter membranes inside acid-cleaned PP filter holders with silicone gaskets. The filters were cleaned with 15 ml 2% HNO_3 before filtering the extracts. Blanks were obtained by filtering aliquots of 2% HNO_3. The filtrates containing ASA and the filter membranes containing the Acid Insoluble Ash (AIA) were both collected (SI.1, Fig. S2).

2.2.3. Determination of major and trace elements

Digests of bulk *Sphagnum* moss and ASA samples were analyzed for major and TEs. Major elements were determined in the Natural Resources Analytical Laboratory (NRAL) using a Thermo iCAP 6300 Duo ICP-OES, and TEs in the metal-free, ultraclean SWAMP lab using a Thermo iCAP Qc ICP-MS. For quality control, along with the two SRMs noted above, the following water SRMS were analyzed: NIST 1643f Trace Elements in Freshwater, SPS-SW2 Surface Water (Spectrapure Standards), and SLRS-6 River Water (National Research Council of Canada). For both the ICP-MS and ICP-OES results, the limits of detection (LOD), limits of quantification (LOQ), method detection limits (MDL), and recoveries of SRMs were calculated and summarized in Tables S1–S4 (SI.2).

2.2.4. Analysis of particle size, morphology, and mineralogy

Selected ash samples (2019/2020 JPH4, 2020 UTK, and 2015 P6, S3, S16, S20) were analyzed for particle size in the range of 0.4–2000 μm using laser diffraction with a laser particle size analyzer (Beckman Coulter LS 13320, Beckman Coulter) in the NRAL. JPH4 and UTK ash samples from 2020 were also examined using X-ray diffraction (XRD) (Rigaku Ultima IV) in the Department of Earth Sciences at the University of Alberta.

2.3. Data Analyses and Visualization

All data analyses and visualization were conducted in R 4.1.1. [60]

Concentration maps were created using packages *ggmap*[61] and *ggplot2*.[62]

Principal component analysis (PCA) was performed on selected variables to explore the relationships between samples and between variables using the *prcomp* function. To make the variables comparable, the data were scaled (i.e., standardized) by setting "scale = TRUE" in the R code. The PCA was visualized using the *factoextra* package.[63]

Normality of variables was tested using the Shapiro-Wilk's test. With most of the variables being non-normally distributed, Spearman rank-based correlation tests were performed to examine the relationships among variables at a significance level of 0.05 using the *cor* function and visualized using the *ggcorrplot* package.[64]

Simple linear regressions were conducted to explore the specific correlations between certain elements using the *lm* function and visualized with the *ggplot2* package.[62]

3. RESULTS AND DISCUSSION

3.1. General Description of the Element Concentration Data

First, averages and ranges (ratio of maximum to minimum concentration) of the element concentration data were calculated to obtain a general idea of the distribution. The average concentrations of the TEs in both bulk moss (total concentration) and the ASA fraction showed that Al, Fe, and Mn were the three most abundant TEs at either the industrial or reference sites (Fig. 1). In contrast, the potentially toxic TEs, such as Tl, Ag, Sb, Cd, and Pb, exhibited relatively low concentrations. The average TE concentrations in the bulk moss were almost all higher at the industrial sites than at the reference sites, while those in the ASA appeared to be higher at the

reference sites for some elements, including Ag, Cd, Cu, and Zn (Fig. 1). The greatest difference in total concentrations was in the conservative lithophile elements such as Y and Th (~40x, 30x, 20x in 2015, 2019, and 2020, respectively), while the smallest was in the macro- and micronutrients such as S, K, P, Cu, and Zn (1x–4x) (SI.1, Figs. S3, S4). The fact that the greatest differences are seen in the conservative lithophile elements is a reflection of the increases in dust deposition rates with proximity to industry. Similar trends were also seen in the ASA fraction (SI.1, Figs. S3, S4).

The conservative lithophile elements are abundant in the earth's silicate crust and resistant to chemical weathering; their estimated concentrations in the UCC are well known, being relatively consistent among studies.[65,66] Thus, the abundance of these elements can be used as an indicator of the amounts of mineral dust being deposited from the air, and can be used to distinguish the natural background from anthropogenic inputs.[67] In addition, Th and the rare earth elements, including Y and La, are abundant in heavy minerals like monazite and zircon, which are thermodynamically stable.[68–70] These heavy minerals are also found in the mineral fraction of the ABS which is primarily beach and dune sands.[3,23,68,71] Yttrium is not required or taken up by plants and is thus used hereafter to indicate the deposition of the insoluble silicate minerals on the moss.

3.2. Spatial Variation in Trace Element Concentrations

a) Lithophile elements

Spatial variations of total Y, a conservative lithophile element, exhibited an obvious increasing trend towards industry, which resembled the distribution of the ash content (Fig. 2; SI.1, Fig. S5). The other conservative lithophile elements, such as Al, Th, La, and Cr, behaved similarly to Y (SI.1, Fig. S6). Total Fe also showed an obvious increasing trend towards industry and correlated strongly and positively with total Y (Spearman's $\rho = 0.93$, $p < 0.05$; SI.1, Figs. S7, S8).

Although Fe is a lithophile element, its mobility under reducing conditions and strong pollution sources constrain its use as an indicator for dust deposition.[72,73] Moreover, the predominant wind direction from May to August in 2015 was southwest in addition to north and south (SI.1, Fig. S9), which might explain the relatively high concentrations at sites such as S7, S9, S19, and P11.

b) Elements enriched in bitumen

The elements enriched in bitumen, V and Ni,[74] strongly resembled Y in their distribution (Fig. 2). This was also reflected by their strong correlations (SI.1, Fig. S8), which implies the role of mineral dust inputs on their total concentrations.[6,7,9–12,55,57,75,76] In addition, the slope of the regression line of V (4.55) and Ni (2.01) versus Y was similar to their corresponding ratios in the UCC (97/21 = 4.61 and 47/21 = 2.24, respectively) (SI.1., Fig. S10),[66] supporting the influence of mineral dusts.[3,14,68,77–80]

Total Mo, another element enriched in bitumen, also increased near industry, but did not correlate with total Y as strongly as V or Ni (SI.1., Figs. S7, S10). This might be due to the uptake of Mo as a micronutrient,[81,82] and probable leaching from the living (throughfall precipitation) and dead tissues of other plants.[54,83–85]

c) Chalcophile elements

The distribution of the potentially toxic element Pb followed that of Y (Fig. 2). The slope of the regression line of Pb (0.78) to Y was also similar to its corresponding ratios in the UCC (17/21 = 0.81) (SI.1., Fig. S10).[66] The range of total Pb concentration in the ABS region (0.23–1.26 mg kg^{-1}) was comparable to that found in moss collected from a remote Canadian bog (0.65–1.11 mg kg^{-1}) near Great Slave Lake,[50] reflecting its low abundance in the ABS region.

Total Sb and Tl also generally followed the trend of Y (SI.1., Figs. S10, S11). However, total Ag and especially Cd did not (SI.1, Figs. S10, S12). Silver and Cd behave similarly to micronutrients, Cu and Zn, respectively, due to their similar physical and chemical properties resulting from their electronic structure.[86–88] Cadmium uptake in plants has been found to be performed by transporters of essential elements such as Cu, Fe, Mn, and Zn.[89,90] In addition, mosses were also reported to be particularly able to accumulate Ag and Cd.[43,82] Thus, the total concentrations of Ag and Cd were also affected by plant uptake.

d) Elements essential to plants

Total Cu showed a slightly increasing trend towards industry and a moderate positive correlation with total Y (SI.1, Figs. S8, S13). However, total Mn and Zn did not correlate significantly with Y, suggesting the insignificant role of atmospheric dust input on them.[55,68,73,79]

3.3. Comparison of Total Concentrations versus ASA

Total and acid soluble concentrations of selected TEs are shown in Figure 3. The range in behaviours of these elements (Al, Th, Ca, Mn, V, Ni, Mo, Tl, Pb and Sb) is representative and provides a concise description of the TE data obtained. In all cases, the results obtained from sampling in 2019 and 2020 were very reproducible. The general trend is an increase in the acid soluble concentrations of most elements, but proportions vary in important ways. For example, acid soluble Al consistently accounts for the majority of total Al, while acid soluble Th represents only a small fraction of total Th (Fig. 3). Both elements are conservative lithophile elements, but their mineral occurrences differ. We assume that Al concentrations in the moss samples are mainly contributed by the ultrafine clay minerals, whereas Th is from accessory minerals such as monazite

and zircon (which are both comparatively large, dense and stable), with lesser amounts from feldspars. Other conservative lithophile elements (Y, Cr, La) behave like Al (SI.1, Figs. S16, S17) which reflects the broader significance of the phyllosilicate clays. For convenience, ultrafine clay minerals are defined here as mineral particles able to pass through a 0.45 μm membrane filter.[3] Strong positive correlations of lanthanides (Dy, Sm, Eu), Al, and V with the fines content in the ABS are well established.[91] Due to their relatively small size, they can also be transported over a long range. However, the TEs are incorporated within the silicate structures of these minerals and hence are rarely released at ambient conditions.[92] The same is true for the TEs in larger silicate minerals such as quartz, feldspar, mica, and zircon.[70,92] Thus, TEs found in the ASA fraction of *Sphagnum* moss is not necessarily an indicator of the risk they pose to living organisms. Certainly, the ultrafine clay minerals and their ecological significance require further investigation.

For Ca, an important plant macronutrient, the acid soluble concentration correlated significantly with Y and was comparable to the total concentrations (Fig. 3; SI.1, Fig. S15), much like Al. In contrast, Mn, which is also essential to plants, occurs mainly in insoluble form (Fig. 3), resembling the trend in Th. Regarding the elements enriched in bitumen, V and Ni also behaved like Al whereas Mo behaved like Th (Fig. 3) even though Mo too is essential to plants.

In terms of the potentially toxic TEs, Pb, Sb, and Tl behaved like Th (Fig. 3). Of these 3 elements, Tl had the lowest proportion of acid soluble metal. In contrast to these 3 elements, the acid soluble concentrations of Ag and Cd and their acid soluble proportions were both higher at the reference site, UTK (SI.1, Figs. S16, S17).

3.4. Enrichments of Trace Elements

The enrichments of TEs, relative to their corresponding crustal abundance,[66] was determined using both the total and acid soluble concentrations of samples collected from industrial and reference sites.[75] Regarding the total concentrations, very few elements were significantly enriched (i.e. by a factor greater than 2 times, compared to the UCC): Cu, Mn, Mo, and Zn (all plant micronutrients), as well as Ag, Cd, Rb, and Re (Fig. 4). Although this latter group is not required by plants, their enrichments resemble those of the micronutrients, probably because they exhibit similar chemical properties e.g., Cd and Zn, Rb and K, Re and Mo [86,87,93,94]. This was the same for the acid soluble concentrations (Fig. 4). Moreover, the enrichments of two potentially toxic elements, Ag and Cd, were actually higher at the reference sites compared to the industrial sites. Given the long list of TEs investigated here, it is rather remarkable how few elements exhibit significant enrichments in the *Sphagnum* moss collected near industrial development, relative to the corresponding crustal values. The results obtained from samples collected in 2019 and 2020 are very consistent, illustrating the reproducibility of the geochemical data and the approach used to study atmospheric deposition of TEs.

3.5. Mineral Abundance in Moss Ash from Proximal and Distal Locations

X-ray diffraction (XRD) analyses showed that quartz was the predominant mineral in JPH4, followed by hydroxyapatite, arcanite, microcline, muscovite, and CaO (Fig. 5; SI.1, Fig. S18). The abundance of quartz (36.7%) in JPH4 was approximately 6x of that in UTK (6.1%). The minerals found in UTK in decreasing order were fairchildite, arcanite, hydroxyapatite, albite, diopside, quartz, and halite (Fig. 5; SI.1, Fig. S18). Among these minerals, hydroxyapatite, arcanite, CaO, fairchildite, and halite were created during ashing.[95,96] Correcting the mineral abundances for those

created during ashing, quartz accounted for 66.7% of JPH4 ash, but only 15.5% at UTK. The value obtained for JPH4 is within the reported quartz content of 60–90% in the mineral fraction of the ABS.[25] It is well known that quartz is a very poor host for TEs, and most TEs are rare in quartz.[3,91,97] The preponderance of quartz grains in the ash fraction of *Sphagnum* moss collected near industry explains why their ash contents are so high while, at the same time, their TE burdens are so low.

Particle size analyses showed that the volume of particles deposited on moss increased toward industry, with diameters typically ranging from 10 to 100 μm and even to 200 μm, before levelling off (SI.1, Fig. S19). The size of the particles found in the moss samples near industry helps to explain why atmospheric dispersion of the dusts generated by mining have a limited transport distance.[15,21]

3.6. Principal Component Analysis

The results of the PCA of the data were consistent with the observations described above. The PCA for the total concentrations of the 2015 mosses showed that principal component (PC) 1 explained 60.0% of the variation in the dataset (Fig. 6a). The greatest contributors to this PC were the conservative lithophile elements (Y, La, Th, Cr, Al), potentially toxic elements (Pb, Tl, Sb), elements enriched in bitumen (V, Ni, Mo), some other lithophile elements such as Be, Li, and Fe, and the ash content (SI.1, Fig. S20). PC1 is clearly related to the abundance of mineral matter, and separated the reference sites (BMW, CMW, and UTK) from the industrial sites. PC 2 explained 12.3% of the variation in the dataset, which was primarily contributed by plant macro- and micronutrients such as P, Mg, K, Zn, Mn, Ca, and S. The PCA for acid soluble concentrations of

the 2015 mosses showed that PC 1 and 2 explained 52.4 and 15.3% of the variations, respectively (Fig. 6b).

3.7. Temporal Trends of Element Accumulation

The ash contents of the *Sphagnum* moss samples collected in 2019 and 2020 as well as the total concentrations of TEs showed limited variation between the two years (SI.1, Fig. S21). The acid soluble concentrations were also comparable between the two years (SI.1, Fig. S22). *Sphagnum* mosses were collected from the same five sites in October of both years and only the living layer (i.e., top 2 cm of the plants) were processed each time. In all cases, therefore, the samples collected reflect summertime deposition of atmospheric aerosols. Assuming similar rates of *Sphagnum* growth, the comparable concentrations indicate that dust deposition from bitumen mining and upgrading did not vary significantly between the two years. Further, the mosses from 2015 were collected from sites different from those from 2019 and 2020, and yet they all yielded similar concentrations. Taken together, the reproducibility of the findings suggests that the *Sphagnum* moss samples have provided a consistent record of atmospheric deposition of dust particles and their associated TEs.

3.8. Dust Deposition in Other Locations in Alberta

a) Elk Island National Park

Moss collected at EINP was high in both total Ni (3.3 mg kg^{-1}) and acid soluble Ni (2.1 mg kg^{-1}) (Fig. 2). Total Ni is disproportionate to total Y (SI.1, Fig. S10) and the enrichment factor (EF) for Ni (8.3) was the highest among all sites (SI.1, Fig. S23). Clearly, there were additional sources of Ni to these moss samples other than soil dust and windblown soil dust.[14,68,77] The obvious source

of excess Ni in these samples is the nickel refinery in Fort Saskatchewan, Alberta which is only approximately 26 km northwest of EINP.

b) Wagner Natural Area

The moss samples collected at WAG were high in total Sb (63 μg kg^{-1}) and acid soluble Sb (30 μg kg^{-1}) (SI.1, Fig. S11). These samples represent an outlier in the linear regression of Sb with total Y (SI.1, Fig. S10) and yielded the greatest EF value (9.5) among the sites investigated (SI.1, Fig. S23). The high Sb at WAG could be ascribed to road traffic.[98] Antimony sulphide (Sb_2S_3) has been used in brake linings since the late 1990s, and has become a significant source of atmospheric Sb. The high temperatures generated during braking promote the oxidation of Sb_2S_3 to the more easily dissolved antimony trioxide.[99] The particles generated by brake abrasion are respirable, with aerodynamic diameters of 2.8 μm having been found, and particle numbers increasing with increasing temperature.[100,101] Vehicle fuel combustion is also a source of anthropogenic Sb.[83,102] High EF values of Sb in aerosols from automobile traffic have been reported.[83]

Acknowledgements

Sincere thanks to the Natural Sciences and Engineering Research Council (NSERC) of Canada and the Canada's Oil Sands Innovation Alliance (COSIA) for their financial support, and Dr. Mandy Krebs, Mika Little-Devito, Jinping Xue, and Yu Wang for their helpful comments.

References

(1) Gosselin, P.; Hrudey, S.; Naeth, M.; Plourde, A.; Therrien, R.; Van Der Kraak, G.; Xu, Z. *Environmental and health impacts of Canada's oil sands industry*. 2010. https://rsc-src.ca/sites/default/files/RSC%20Oil%20Sands%20Panel%20Main%20Report%20Oct%202012.pdf.

(2) Alberta Energy Regulator. 2021. *Crude Bitumen Production*. https://www.aer.ca/providing-information/data-and-reports/statistical-reports/st98/crude-bitumen/production.

(3) Shotyk, W.; Bicalho, B.; Cuss, C. W.; Donner, M.; Grant-Weaver, I.; Javed, M. B.; Noernberg, T. Trace elements in the Athabasca Bituminous Sands: A geochemical explanation for the paucity of environmental contamination by chalcophile elements. *Chem. Geol.* **2021**, *581*, 120392. DOI: 10.1016/j.chemgeo.2021.120392.

(4) Cooke, C. A.; Kirk, J. L.; Muir, D. C. G.; Wiklund, J. A.; Wang, X.; Gleason, A.; Evans, M. S. Spatial and temporal patterns in trace element deposition to lakes in the Athabasca oil sands region (Alberta, Canada). *Environ. Res. Lett.* **2017**, *12* (12), 124001. DOI: 10.1088/1748-9326/aa9505.

(5) Phillips-Smith, C.; Jeong, C.-H.; Healy, R. M.; Dabek-Zlotorzynska, E.; Celo, V.; Brook, J. R.; Evans, G. Sources of particulate matter components in the Athabasca oil sands region: Investigation through a comparison of trace element measurement methodologies. *Atmos. Chem. Phys.* **2017**, *17* (15), 9435–9449. DOI: 10.5194/acp-17-9435-2017.

(6) Watson, J. G.; Chow, J. C.; Wang, X.; Kohl, S. D. *Windblown fugitive dust characterization in the Athabasca Oil Sands Region*. 2014. WBEA-DRI Agreement Number: T108-13. https://wbea.org/wp-content/uploads/2018/03/watson_j_g_et_al_2014_windblown_fugitive_dust_characterization_in_the_athabasca_oil_sands_region.pdf.

(7) Wang, X.; Chow, J. C.; Kohl, S. D.; Yatavelli, L. N. R.; Percy, K. E.; Legge, A. H.; Watson, J. G. Wind erosion potential for fugitive dust sources in the Athabasca Oil Sands Region. *Aeolian Res.* **2015**, *18*, 121–134. DOI: 10.1016/j.aeolia.2015.07.004.

(8) Xing, Z.; Du, K. Particulate matter emissions over the oil sands regions in Alberta, Canada. *Environ. Rev.* **2017**, *25* (4), 432–443. DOI: 10.1139/er-2016-0112.

(9) Graney, J. R.; Landis, M. S.; Krupa, S. Coupling lead isotopes and element concentrations in epiphytic lichens to track sources of air emissions in the Athabasca Oil Sands Region. In *Alberta Oil Sands*; Percy, K. E., Ed.; Developments in Environmental Science, Vol. 11; Elsevier, 2012; pp 343–372. DOI: 10.1016/B978-0-08-097760-7.00015-9.

(10) Landis, M. S.; Pancras, J. P.; Graney, J. R.; Stevens, R. K.; Percy, K. E.; Krupa, S. Receptor modeling of epiphytic lichens to elucidate the sources and spatial distribution of inorganic air pollution in the Athabasca Oil Sands Region. In *Alberta Oil Sands*; Percy, K. E., Ed.; Developments in Environmental Science, Vol. 11; Elsevier, 2012; pp 427–467. DOI: 10.1016/B978-0-08-097760-7.00018-4.

(11) Landis, M. S.; Patrick Pancras, J.; Graney, J. R.; White, E. M.; Edgerton, E. S.; Legge, A.; Percy, K. E. Source apportionment of ambient fine and coarse particulate matter at the Fort

McKay community site, in the Athabasca Oil Sands Region, Alberta, Canada. *Sci. Total. Environ.* **2017**, *584-585*, 105–117. DOI: 10.1016/j.scitotenv.2017.01.110.

(12) Landis, M. S.; Studabaker, W. B.; Patrick Pancras, J.; Graney, J. R.; Puckett, K.; White, E. M.; Edgerton, E. S. Source apportionment of an epiphytic lichen biomonitor to elucidate the sources and spatial distribution of polycyclic aromatic hydrocarbons in the Athabasca Oil Sands Region, Alberta, Canada. *Sci. Total. Environ.* **2019**, *654*, 1241–1257. DOI: 10.1016/j.scitotenv.2018.11.131.

(13) Jordaan, S. M. Land and water impacts of oil sands production in Alberta. *Environ. Sci. Technol.* **2012**, *46* (7), 3611–3617. DOI: 10.1021/es203682m.

(14) Shotyk, W.; Belland, R.; Duke, J.; Kempter, H.; Krachler, M.; Noernberg, T.; Pelletier, R.; Vile, M. A.; Wieder, K.; Zaccone, C.; Zhang, S. *Sphagnum* mosses from 21 ombrotrophic bogs in the Athabasca Bituminous Sands region show no significant atmospheric contamination of "heavy metals". *Environ. Sci. Technol.* **2014**, *48* (21), 12603–12611. DOI: 10.1021/es503751v.

(15) Willeke, K.; Whitby, K. T. Atmospheric aerosols: size distribution interpretation. *J. Air Pollut. Control Assoc.* **1975**, *25* (5), 529–534. DOI: 10.1080/00022470.1975.10470110.

(16) Whitby, K. T.; Husar, R.; Liu, B. The aerosol size distribution of Los Angeles smog. *J. Colloid Interface Sci.* **1972**, *39* (1), 177–204.

(17) Ramachandran, S. *Atmospheric Aerosols: Characteristics and Radiative Effects*; CRC Press, 2018. DOI: 10.1201/9781315152400.

(18) Swift, D. L.; Proctor, D. F. Human respiratory deposition of particles during oronasal breathing. *Atmos. Environ.* **1982**, *16* (9), 2279–2282. DOI: 10.1016/0004-6981(82)90307-9.

(19) Schuetz, L. Atmospheric mineral dust - properties and source markers. In *Paleoclimatology and paleometeorology: Modern and past patterns of global atmospheric transport*; Leinen, M., Sarnthein, M., Eds.; Mathematical and Physical Sciences, Vol. 282; Kluwer Academic Publishers, 1989; pp 359–384.

(20) Coe, J. M.; Lindberg, S. E. The morphology and size distribution of atmospheric particles deposited on foliage and inert surfaces. *JAPCA* **1987**, *37* (3), 237–243. DOI: 10.1080/08940630.1987.10466218.

(21) Zufall, M. J.; Davidson, C. I. Dry deposition of particles from the atmosphere. In *Air Pollution in the Ural Mountains: Environmental, Health and Policy Aspects*; Linkov, I., Wilson, R., Eds.; Springer Netherlands, 1998; pp 55–73. DOI: 10.1007/978-94-011-5208-2_5.

(22) Schütz, L. Long range transport of desert dust with special emphasis on the Sahara. *Ann. NY Acad. Sci.* **1980**, *338* (1 Aerosols), 515–532. DOI: 10.1111/j.1749-6632.1980.tb17144.x.

(23) Champlin, J. B. F.; Dunning, H. N. A geochemical investigation of the Athabasca bituminous sands. *Econ. Geol.* **1960**, *55* (4), 797–804. DOI: 10.2113/gsecongeo.55.4.797.

(24) Clark, K. Athabasca bituminous sands. *Fuel* **1951** (30), 49–53.

(25) Bichard, J. A. *Oil sands composition and behaviour research*:*The research papers of John A. Bichard, 1957-1965*; AOSTRA Technical Publication Series, #4; Alberta Oil Sands Technology and Research Authority, 1987.

(26) Tomasi, C.; Lupi, A. Primary and secondary sources of atmospheric aerosol. In *Atmospheric Aerosols*:*Life Cycles and Effects on Air Quality and Climate,* 1st; Tomasi, C.,

Fuzzi, S., Kokhanovsky, A. A., Eds.; Wiley Series in Atmospheric Physics and Remote Sensing; Wiley-VCH, 2016; pp 1–86. DOI: 10.1002/9783527336449.ch1.

(27) Corrin, M. L.; Natusch, D. F. Physical and chemical characteristics of environmental lead. In *Lead in the Environment*; Boggess, W. R., Wixson, B. G., Eds.; Castle House Publications, 1979.

(28) Xu, M.; Yu, D.; Yao, H.; Liu, X.; Qiao, Y. Coal combustion-generated aerosols: Formation and properties. *Proc. Combust. Inst* . **2011**, *33* (1), 1681–1697. DOI: 10.1016/j.proci.2010.09.014.

(29) Natusch, D. F. S.; Wallace, J. R.; Evans, C. A. Toxic trace elements: Preferential concentration in respirable particles. *Science* **1974**, *183* (4121), 202–204. DOI: 10.1126/science.183.4121.202.

(30) Nriagu, J. O. Global metal pollution: Poisoning the biosphere? *Environ.: Sci. Policy Sustainable Dev.* **1990**, *32* (7), 7–33. DOI: 10.1080/00139157.1990.9929037.

(31) Amodio, M.; Catino, S.; Dambruoso, P. R.; Gennaro, G. de; Di Gilio, A.; Giungato, P.; Laiola, E.; Marzocca, A.; Mazzone, A.; Sardaro, A.; Tutino, M. Atmospheric deposition: Sampling procedures, analytical methods, and main recent findings from the scientific literature. *Adv. Meteorol.* **2014**, *2014*, 1–27. DOI: 10.1155/2014/161730.

(32) Dauvalter, V. A.; Kashulin, N.; Lehto, J.; Jernstrom, J. Chalcophile elements Hg, Cd, Pb, As in Lake Umbozero, Murmansk Region, Russia. *Int. J. Environ. Res. Public Health* **2009**, *3* (3), 411–428.

(33) Robache, A.; Mathé, F.; Galloo, J. C.; Guillermo, R. Multi-element analysis by inductively coupled plasma optical emission spectrometry of airborne particulate matter collected with a low-pressure cascade impactor. *Analyst* **2000**, *125* (10), 1855–1859. DOI: 10.1039/b003048l.

(34) Davison, R. L.; Natusch, D. F. S.; Wallace, J. R.; Evans, C. A. Trace elements in fly ash:Dependence of concentration on particle size. *Environ. Sci. Technol.* **1974**, *8* (13), 1107–1113. DOI: 10.1021/es60098a003.

(35) Rao, D. Responses of bryophytes to air pollution. In *Bryophyte Ecology*; Smith, A., Ed.; Chapman and Hall Ltd, 1982; pp 445–471.

(36) Rao, D.; Robitaille, G.; LeBlanc, F. Influence of heavy metal pollution on lichens and bryophytes. *J. Hattori Bot. Lab.* **1977**, *42*.

(37) Kempter, H.; Krachler, M.; Shotyk, W.; Zaccone, C. Major and trace elements in *Sphagnum* moss from four southern German bogs, and comparison with available moss monitoring data. *Ecol. Indic.* **2017**, *78*, 19–25. DOI: 10.1016/j.ecolind.2017.02.029.

(38) Tyler, G. Bryophytes and heavy metals: a literature review. *Bot. J. Linn. Soc.* **1990**, *104* (1-3), 231–253. DOI: 10.1111/j.1095-8339.1990.tb02220.x.

(39) Poikolainen, J.; Kubin, E.; Piispanen, J.; Karhu, J. Atmospheric heavy metal deposition in Finland during 1985–2000 using mosses as bioindicators. *Sci. Total. Environ.* **2004**, *318* (1-3), 171–185. DOI: 10.1016/S0048-9697(03)00396-6.

(40) Shotyk, W.; Kempter, H.; Krachler, M.; Zaccone, C. Stable (206Pb, 207Pb, 208Pb) and radioactive (210Pb) lead isotopes in 1 year of growth of *Sphagnum* moss from four ombrotrophic bogs in southern Germany: Geochemical significance and environmental

implications. *Geochim. Cosmochim. Acta* **2015**, *163*, 101–125. DOI: 10.1016/j.gca.2015.04.026.
(41) Clymo, R. Ion exchange in *Sphagnum* and its relation to bog ecology. *Ann. Bot.* **1963**, *27* (2), 309–324. DOI: 10.1093/oxfordjournals.aob.a083847.
(42) González, A. G.; Pokrovsky, O. S. Metal adsorption on mosses: Toward a universal adsorption model. *J. Colloid Interface Sci.* **2014**, *415*, 169–178. DOI: 10.1016/j.jcis.2013.10.028.
(43) Jiang, Y.; Fan, M.; Hu, R.; Zhao, J.; Wu, Y. Mosses are better than leaves of vascular plants in monitoring atmospheric heavy metal pollution in urban areas. *Int. J. Environ. Res. Public Health* **2018**, *15* (6). DOI: 10.3390/ijerph15061105.
(44) Ceburnis, D. Conifer needles as biomonitors of atmospheric heavy metal deposition: comparison with mosses and precipitation, role of the canopy. *Atmos. Environ.* **2000**, *34* (25), 4265–4271. DOI: 10.1016/S1352-2310(00)00213-2.
(45) Shotyk, W. Peat bog archives of atmospheric metal deposition: Geochemical evaluation of peat profiles, natural variations in metal concentrations, and metal enrichment factors. *Environ. Rev.* **1996**, *4* (2), 149–183. DOI: 10.1139/a96-010.
(46) Damman, A. W. H. Hydrology, development, and biogeochemistry of ombrogenous peat bogs with special reference to nutrient relocation in a western Newfoundland bog. *Can. J. Bot.* **1986**, *64* (2), 384–394. DOI: 10.1139/b86-055.
(47) Salemaa, M.; Derome, J.; Helmisaari, H.-S.; Nieminen, T.; Vanha-Majamaa, I. Element accumulation in boreal bryophytes, lichens and vascular plants exposed to heavy metal and sulfur deposition in Finland. *Sci. Total Environ.* **2004**, *324* (1-3), 141–160. DOI: 10.1016/j.scitotenv.2003.10.025.
(48) Harmens, H.; Buse, A.; Buker, P.; Norris, D.; Mills, G.; Williams, B.; Reynolds, B.; Ashenden, T. W.; Ruhling, A.; Steinnes, E. Heavy metal concentrations in European mosses: 2000/2001 survey. *J. Atmos. Chem.* **2004**, *49*, 425–436.
(49) Steinnes, E.; Berg, T.; Uggerud, H. T. Three decades of atmospheric metal deposition in Norway as evident from analysis of moss samples. *Sci. Total Environ.* **2011**, *412-413*, 351–358. DOI: 10.1016/j.scitotenv.2011.09.086.
(50) Pakarinen, P.; Tolonen, K. Regional survey of heavy metals in peat mosses (*Sphagnum*). *Ambio* **1976**, *5* (1), 38–40.
(51) Berg, T.; Røyset, O.; Steinnes, E. Moss (*Hylocomium splendens*) used as biomonitor of atmospheric trace element deposition: Estimation of uptake efficiencies. *Atmos. Environ.* **1995**, *29* (3), 353–360. DOI: 10.1016/1352-2310(94)00259-N.
(52) Pilegaard, K. Heavy metals in bulk precipitation and transplanted *Hypogymnia physodes* and *Dicranoweisia cirrata* in the vicinity of a Danish steelworks. *Water Air Soil Pollut.* **1979**, *11* (1), 77–91. DOI: 10.1007/BF00163521.
(53) Kosior, G.; Frontasyeva, M. V.; Ziembik, Z.; Zincovscaia, I.; Dołhańczuk-Śródka, A.; Godzik, B. The moss biomonitoring method and neutron activation analysis in assessing pollution by trace elements in selected Polish national parks. *Arch. Environ. Contam. Toxicol.* **2020**, *79* (3), 310–320. DOI: 10.1007/s00244-020-00755-6.

(54) Berg, T.; Steinnes, E. Recent trends in atmospheric deposition of trace elements in Norway as evident from the 1995 moss survey. *Sci. Total Environ.* **1997**, *208* (3), 197–206. DOI: 10.1016/S0048-9697(97)00253-2.
(55) Santelmann, M. V.; Gorham, E. The influence of airborne road dust on the chemistry of *Sphagnum* mosses. *J. Ecol.* **1988**, *76* (4), 1219. DOI: 10.2307/2260644.
(56) Rühling, Å.; Tyler, G.; Ruhling, A. Sorption and retention of heavy metals in the woodland moss *Hylocomium splendens* (Hedw.) Br. et Sch. *Oikos* **1970**, *21* (1), 92. DOI: 10.2307/3543844.
(57) Mullan-Boudreau, G.; Belland, R.; Devito, K.; Noernberg, T.; Pelletier, R.; Shotyk, W. *Sphagnum* moss as an indicator of contemporary rates of atmospheric dust deposition in the Athabasca Bituminous Sands Region. *Environ. Sci. Technol.* **2017**, *51* (13), 7422–7431. DOI: 10.1021/acs.est.6b06195.
(58) Sapkota, A.; Chebukin, A. K.; Bonani, G.; Shotyk, W. Six millennia of atmospheric dust deposition in southern South America (Isla Navarino, Chile). *Holocene* **2007**, *17* (5), 561–572. DOI: 10.1177/0959683607078981.
(59) Chen, X.; Houk, R. S. Polyatomic ions as internal standards for matrix corrections in inductively coupled plasma mass spectrometry. *J. Anal. At. Spectrom.* **1995**, *10* (10), 837. DOI: 10.1039/JA9951000837.
(60) R Core Team. *R: A language and environment for statistical computing*; R Foundation for Statistical Computing, 2021. https://www.r-project.org/.
(61) Kahle, D.; Wickham, H. ggmap: Spatial visualization with ggplot2. *R J.* **2013**, *5* (1), 144–161.
(62) Wickham, H. *ggplot2: Elegrant graphics for data analysis*, 2nd ed.; Use R!; Springer, 2016.
(63) Kassambara, A.; Mundt, F. *factoextra: Extract and Visualize the Results of Multivariate Data Analyses]*; Comprehensive R Archive Network (CRAN), 2020. http://www.sthda.com/english/rpkgs/factoextra.
(64) Kassambara, A. *ggcorrplot: Visualization of a Correlation Matrix using 'ggplot2'*; Comprehensive R Archive Network (CRAN), 2019. https://cran.r-project.org/package=ggcorrplot.
(65) Goldschmidt, V. The principles of distribution of chemical elements in minerals and rocks. *J. Chem. Soc.* **1937** (0), 655–673.
(66) Rudnick, R. L.; Gao, S. Composition of the continental crust. In *Treatise on Geochemistry,* 2nd; Holland, H., Turekian, K., Eds.; Elsevier, 2014; pp 1–51. DOI: 10.1016/B978-0-08-095975-7.00301-6.
(67) Shotyk, W.; Weiss, D.; Kramers, J. D.; Frei, R.; Chebukin, A. K.; Gloor, M.; Reese, S. Geochemistry of the peat bog at Etang de la Grue're, Jura Mountains, Switzerland, and its record of atmospheric Pb and lithogenic trace metals (Sc, Ti, Y, Zr, and REE) since 12,370 ^{14}C yr BP. *Geochim. Cosmochim. Acta* **2001**, *65* (14), 2337–2360. DOI: 10.1016/S0016-7037(01)00586-5.
(68) Shotyk, W.; Bicalho, B.; Cuss, C. W.; Duke, J.; Noernberg, T.; Pelletier, R.; Steinnes, E.; Zaccone, C. Dust is the dominant source of "heavy metals" to peat moss (*Sphagnum fuscum*)

in the bogs of the Athabasca Bituminous Sands region of northern Alberta. *Environ. Int.* **2016**, *92-93*, 494–506. DOI: 10.1016/j.envint.2016.03.018.
(69) Wickleder, M. S.; Fourest, B.; Dorhout, P. K. Thorium. In *The Chemistry of the Actinide and Transactinide Elements,* 4th ed.; Morss, L. R., Edelstein, N. M., Fuger, J., Eds.; Springer, Dordrecht, 2010; pp 52–160. DOI: 10.1007/978-94-007-0211-0_3.
(70) Goldich, S. S. A study in rock-weathering. *J. Geol.* **1938**, *46* (1), 17–58. DOI: 10.1086/624619.
(71) Mellon, G. *Geology of the McMurray Formation*:*Part II: Heavy Minerals of the McMurray*. 1956. https://static.ags.aer.ca/files/document/REP/REP_72.pdf.
(72) Rahn, K. A. *The Chemical Composition of the Atmospheric Aerosol*.
(73) Harrison, P. R.; Rahn, K. A.; Dams, R.; Robbins, J. A.; Winchester, J. W.; Brar, S. S.; Nelson, D. M. Areawide trace metal concentrations measured by multielement neutron activation analysis. *J. Air Pollut. Control Assoc.* **1971**, *21* (9), 563–570. DOI: 10.1080/00022470.1971.10469570.
(74) Bicalho, B.; Grant-Weaver, I.; Sinn, C.; Donner, M. W.; Woodland, S.; Pearson, G.; Larter, S.; Duke, J.; Shotyk, W. Determination of ultratrace (<0.1 mg/kg) elements in Athabasca Bituminous Sands mineral and bitumen fractions using inductively coupled plasma sector field mass spectrometry (ICP-SFMS). *Fuel* **2017**, *206*, 248–257. DOI: 10.1016/j.fuel.2017.05.095.
(75) Shotyk, W.; Nesbitt, W. H.; Fyfe, W. S. Natural and anthropogenic enrichments of trace metals in peat profiles. *Int. J. Coal Geol.* **1992**, *20* (1-2), 49–84. DOI: 10.1016/0166-5162(92)90004-G.
(76) Suzuki, K. Characterisation of airborne particulates and associated trace metals deposited on tree bark by ICP-OES, ICP-MS, SEM-EDX and laser ablation ICP-MS. *Atmos. Environ.* **2006**, *40* (14), 2626–2634. DOI: 10.1016/j.atmosenv.2005.12.022.
(77) Shotyk, W.; Cuss, C. W. Atmospheric Hg accumulation rates determined using *Sphagnum* moss from ombrotrophic (rain-fed) bogs in the Athabasca Bituminous Sands region of northern Alberta, Canada. *Ecol. Indic.* **2019**, *107*, 105626. DOI: 10.1016/j.ecolind.2019.105626.
(78) Javed, M. B.; Cuss, C. W.; Grant-Weaver, I.; Shotyk, W. Size-resolved Pb distribution in the Athabasca River shows snowmelt in the bituminous sands region an insignificant source of dissolved Pb. *Sci. Rep.* **2017**, *7* (1), 43622. DOI: 10.1038/srep43622.
(79) Shotyk, W. Trace elements in wild berries from reclaimed lands: Biomonitors of contamination by atmospheric dust. *Ecol. Indic.* **2020**, *110*, 105960. DOI: 10.1016/j.ecolind.2019.105960.
(80) Weiss, D.; Shotyk, W.; Cheburkin, A. K.; Gloor, M.; Reese, S. Atmospheric lead deposition from 12,400 to ca. 2,000 yrs BP in a peat bog profile, Jura Mountains, Switzerland. *Water Air Soil Pollut.* **1997**, *100* (3/4), 311–324. DOI: 10.1023/A:1018341029549.
(81) White, P. J.; Brown, P. H. Plant nutrition for sustainable development and global health. *Ann. Bot.* **2010**, *105* (7), 1073–1080. DOI: 10.1093/aob/mcq085.
(82) Stachiw, S.; Bicalho, B.; Grant-Weaver, I.; Noernberg, T.; Shotyk, W. Trace elements in berries collected near upgraders and open pit mines in the Athabasca Bituminous Sands Region

(ABSR): Distinguishing atmospheric dust deposition from plant uptake. *Sci. Total. Environ.* **2019**, *670*, 849–864. DOI: 10.1016/j.scitotenv.2019.03.238.

(83) Anicić, M.; Frontasyeva, M. V.; Tomasević, M.; Popović, A. Assessment of atmospheric deposition of heavy metals and other elements in Belgrade using the moss biomonitoring technique and neutron activation analysis. *Environ. Monit. Assess.* **2007**, *129* (1-3), 207–219. DOI: 10.1007/s10661-006-9354-y.

(84) Steinnes, E. A critical evaluation of the use of naturally growing moss to monitor the deposition of atmospheric metals. *Sci. Total Environ.* **1995**, *160-161*, 243–249. DOI: 10.1016/0048-9697(95)04360-D.

(85) Dragović, S.; Mihailović, N. Analysis of mosses and topsoils for detecting sources of heavy metal pollution: multivariate and enrichment factor analysis. *Environ. Monit. Assess.* **2009**, *157* (1-4), 383–390. DOI: 10.1007/s10661-008-0543-8.

(86) Brzóska, M.; Moniuszko-Jakoniuk, J. Interactions between cadmium and zinc in the organism. *Food Chem. Toxicol.* **2001**, *39* (10), 967–980. DOI: 10.1016/S0278-6915(01)00048-5.

(87) Hill, C. H.; Matrone, G. Chemical parameters in the study of in vivo and in vitro interactions of transition elements. *Federation* **1970**, *29* (4), 1474–1481.

(88) Vazquez, M. D.; Wappelhorst, O.; Markert, B. Determination of 28 elements in aquatic moss *Fontinalis Antipyretica* Hedw. and water from the upper reaches of the River Nysa (CZ, D), by ICP-MS, ICP-OES and AAS. *Water Air Soil Pollut.* **2004**, *152* (1-4), 153–172. DOI: 10.1023/B:WATE.0000015351.40069.d2.

(89) Huang, X.; Duan, S.; Wu, Q.; Yu, M.; Shabala, S. Reducing cadmium accumulation in plants: Structure-function relations and tissue-specific operation of transporters in the spotlight. *Plants (Basel, Switzerland)* **2020**, *9* (2), 223. DOI: 10.3390/plants9020223.

(90) Thomine, S.; Wang, R.; Ward, J. M.; Crawford, N. M.; Schroeder, J. I. Cadmium and iron transport by members of a plant metal transporter family in Arabidopsis with homology to Nramp genes. *PNAS* **2000**, *97* (9), 4991–4996. DOI: 10.1073/pnas.97.9.4991.

(91) Donkor, K. K.; Kratochvil, B.; Duke, M. J. M. Estimation of the fines content of Athabasca oil sands using instrumental neutron activation analysis. *Can. J. Chem.* **1996**, *74* (4), 583–590. DOI: 10.1139/v96-062.

(92) Essington, M. E. *Soil and Water Chemistry*:*An Integrative Approach*; CRC Press, 2004.

(93) Relman, A. S. The physiological behavior of rubidium and cesium in relation to that of potassium. *Yale J. Biol. Med.* **1956**, *29* (3), 248–262.

(94) Greenwood, N. N.; Earnshaw, A. *Chemistry of the Elements*, 2nd; Butterworth-Heinemann, 1997.

(95) Maschowski, C.; Zangna, M. C.; Trouvé, G.; Gieré, R. Bottom ash of trees from Cameroon as fertilizer. *Appl. Geochem.* **2016**, *72*, 88–96. DOI: 10.1016/j.apgeochem.2016.07.002.

(96) Shaltout, A. A.; Allam, M. A.; Moharram, M. A. FTIR spectroscopic, thermal and XRD characterization of hydroxyapatite from new natural sources. *Spectrochim. Acta A Mol. Biomol. Spectrosc.* **2011**, *83* (1), 56–60. DOI: 10.1016/j.saa.2011.07.036. Published Online: Aug. 3, 2011.

(97) Breiter, K.; Ackerman, L.; Ďurišova, J.; Svojtka, M.; Novák, M. Trace element composition of quartz from different types of pegmatites: A case study from the Moldanubian Zone of the Bohemian Massif (Czech Republic). *Mineral. Mag.* **2014**, *78* (3), 703–722. DOI: 10.1180/minmag.2014.078.3.17.

(98) Dietl, C.; Reifenhäuser, W.; Peichl, L. Association of antimony with traffic — occurrence in airborne dust, deposition and accumulation in standardized grass cultures. *Sci. Total Environ.* **1997**, *205* (2-3), 235–244. DOI: 10.1016/S0048-9697(97)00204-0.

(99) Fort, M.; Grimalt, J. O.; Querol, X.; Casas, M.; Sunyer, J. Evaluation of atmospheric inputs as possible sources of antimony in pregnant women from urban areas. *Sci. Total Environ.* **2016**, *544*, 391–399. DOI: 10.1016/j.scitotenv.2015.11.095.

(100) Garg, B. D.; Cadle, S. H.; Mulawa, P. A.; Groblicki, P. J.; Laroo, C.; Parr, G. A. Brake wear particulate matter emissions. *Environ. Sci. Technol.* **2000**, *34* (21), 4463–4469. DOI: 10.1021/es001108h.

(101) Wåhlin, P.; Berkowicz, R.; Palmgren, F. Characterisation of traffic-generated particulate matter in Copenhagen. *Atmos. Environ.* **2006**, *40* (12), 2151–2159. DOI: 10.1016/j.atmosenv.2005.11.049.

(102) Shotyk, W.; Krachler, M.; Chen, B. Anthropogenic impacts on the biogeochemistry and cycling of antimony. In Metal Ions in Biological Systems:Biogeochemisty, Availability, and Transport of Metals in the Environment; Sigel, A., Sigel, H., Sigel, R. K. O., Eds.; CRC Press, 2005; pp 171–204. DOI: 10.1201/9780849346071-7.

List of Figures

Fig. 1. Average trace element concentrations (µg kg^{-1} dry moss) at industrial and reference sites out of bulk moss and acid soluble ash (ASA) of *Sphagnum* mosses collected in fall 2015 (a & b) and 2019 (c & d)…….58

Fig. 2. Spatial distribution of total a) Y, b) Pb, c) V, and d) Ni concentrations in *Sphagnum* mosses collected in fall 2015. CMW = Caribou Mountains Wildland, BMW = Birch Mountains Wildland, UTK = Utikuma, WAG = Wagner Natura l Area, EINP = Elk Island National Park……...59

Fig. 3. Total and acid soluble concentrations (mg kg^{-1} dry moss) of Al, Th, Ca, Mn, V, Ni, Mo, Tl, Pb, Sb in *Sphagnum* mosses collected in October 2019 and 2020. ASA = Acid Soluble Ash. McK = Fort Mackay, McM = Fort McMurray, ANZ = Anzac, UTK = Utikuma…….....60

Fig. 4. Enrichments over two of trace elements out of bulk moss (Total) and acid soluble ash (ASA) of *Sphagnum* mosses collected from a) industrial and b) reference sites in fall 2015, 2019, and 2020 relative to the Upper Continental Crust.66 Total and acid soluble concentrations used were out of ash (mg kg^{-1} ash).[75]…….….61

Fig. 5. Mineral abundance (%) from XRD analysis in ash samples of *Sphagnum* mosses collected from JPH4 and UTK in October 2020. UTK = Utikuma…….62

Fig. 6. Principal component analysis of 2015 *Sphagnum* mosses using a) total concentrations and ash content and b) acid soluble concentrations and ash content. The contribution reflects the total contribution of the variables to principal component (PC) 1 and 2. BMW = Birch Mountains Wildland, CMW = Caribou Mountains Wildland, UTK = Utikuma……...63

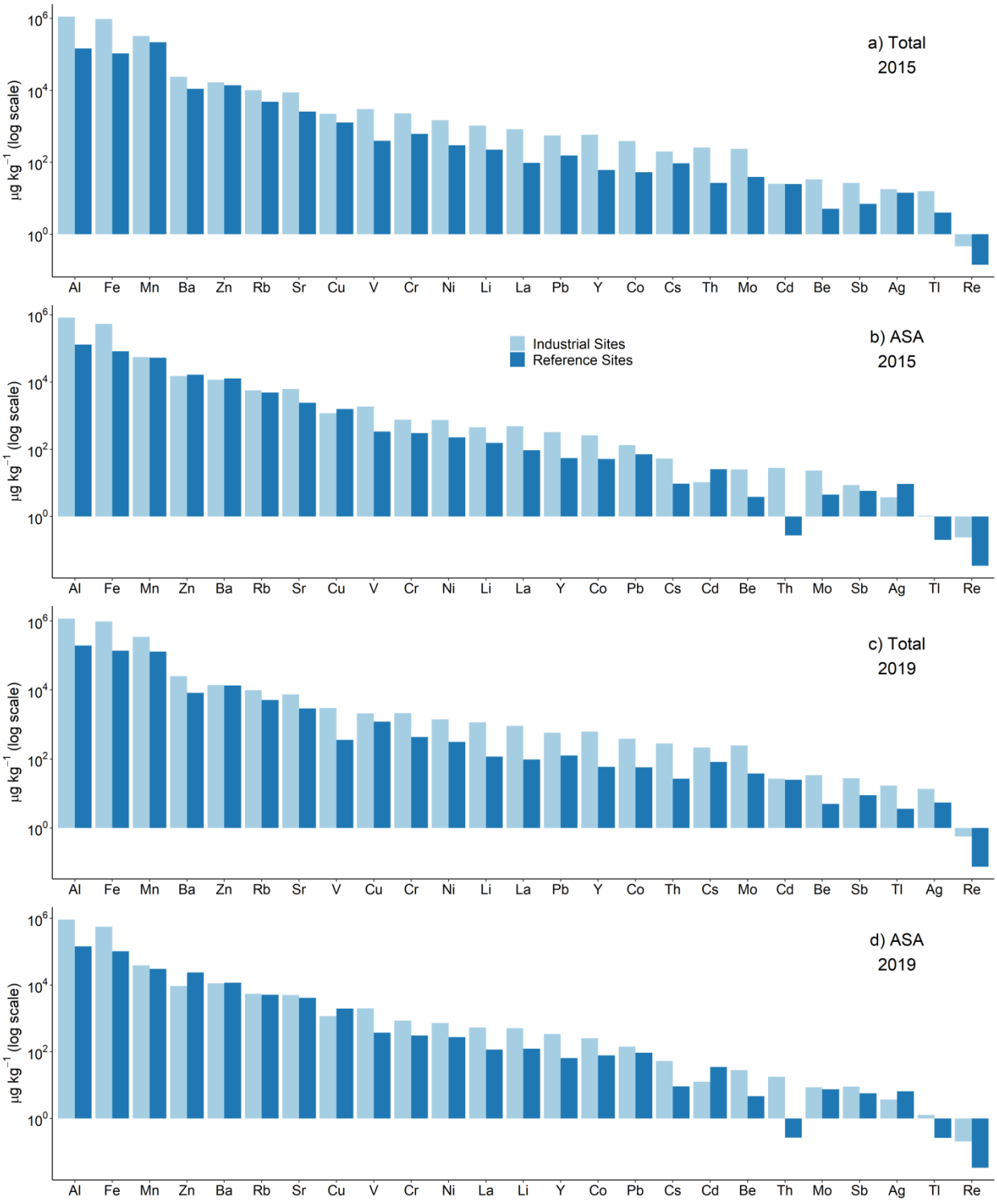

Fig. 1. Average trace element concentrations (µg kg^{-1} dry moss) at industrial and reference sites out of bulk moss and acid soluble ash (ASA) of *Sphagnum* mosses collected in fall 2015 (a & b) and 2019 (c & d).

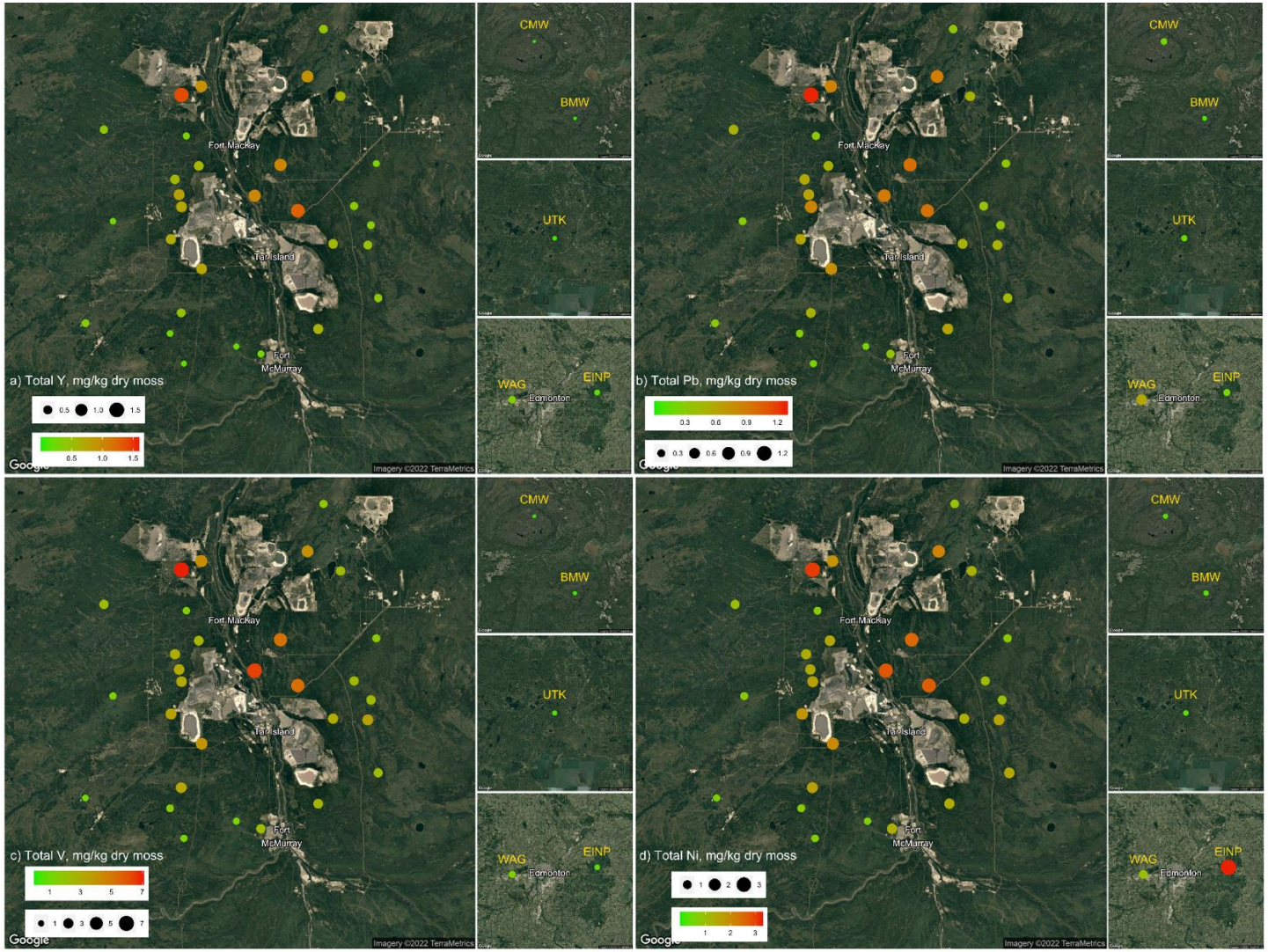

Fig. 2. Spatial distribution of total a) Y, b) Pb, c) V, and d) Ni concentrations in *Sphagnum* mosses collected in fall 2015. CMW = Caribou Mountains Wildland, BMW = Birch Mountains Wildland, UTK = Utikuma, WAG = Wagner Natura l Area, EINP = Elk Island National Park.

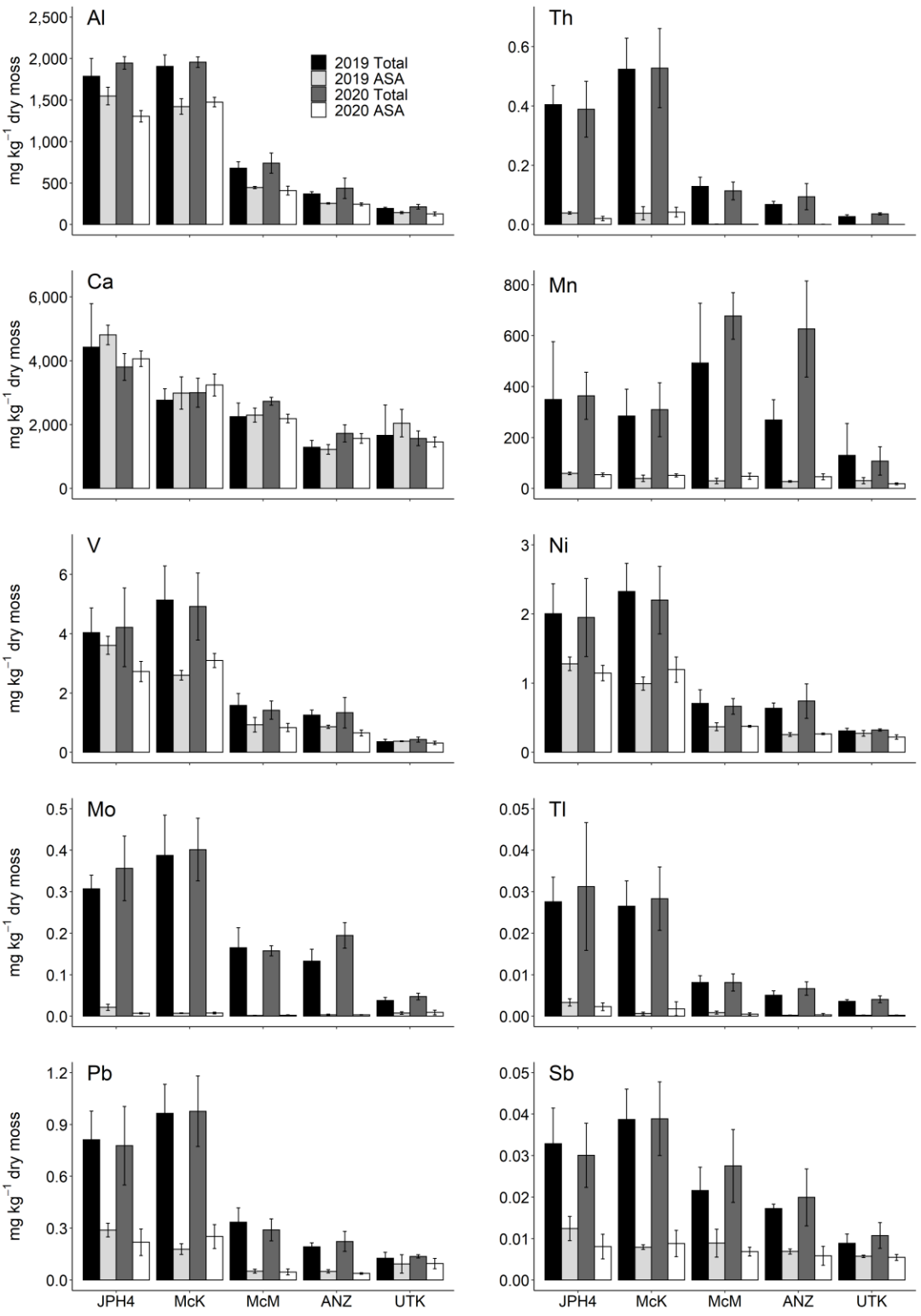

Fig. 3. Total and acid soluble concentrations (mg kg^{-1} dry moss) of Al, Th, Ca, Mn, V, Ni, Mo, Tl, Pb, and Sb in *Sphagnum* mosses collected in October 2019 and 2020. ASA = Acid Soluble Ash. McK = Fort Mackay, McM = Fort McMurray, ANZ = Anzac, UTK = Utikuma.

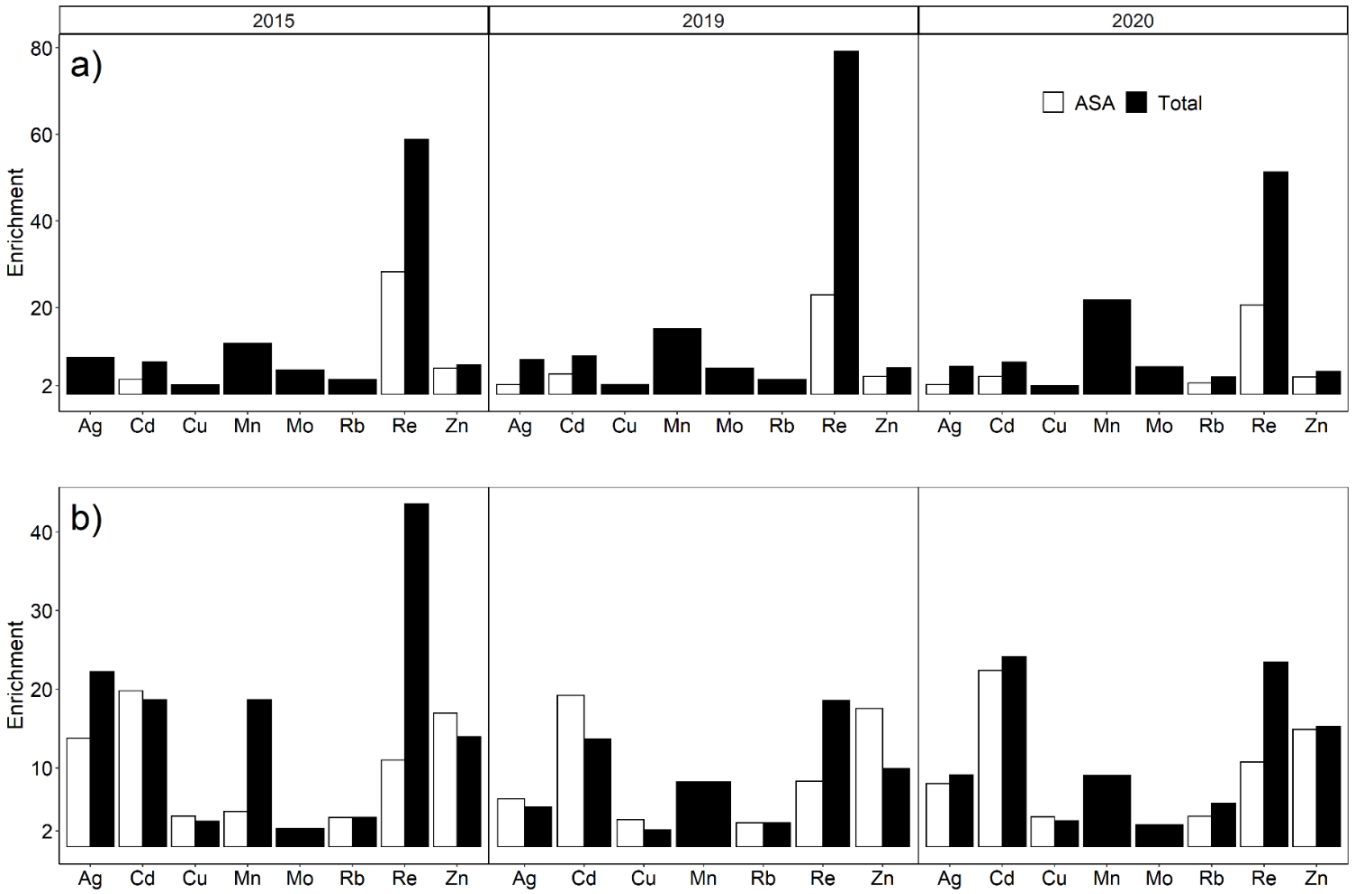

Fig. 4. Enrichments over two of trace elements out of bulk moss (Total) and acid soluble ash (ASA) of *Sphagnum* mosses collected from a) industrial and b) reference sites in fall 2015, 2019, and 2020 relative to the Upper Continental Crust.[66] Total and acid soluble concentrations used were out of ash (mg kg^{-1} ash).[75]

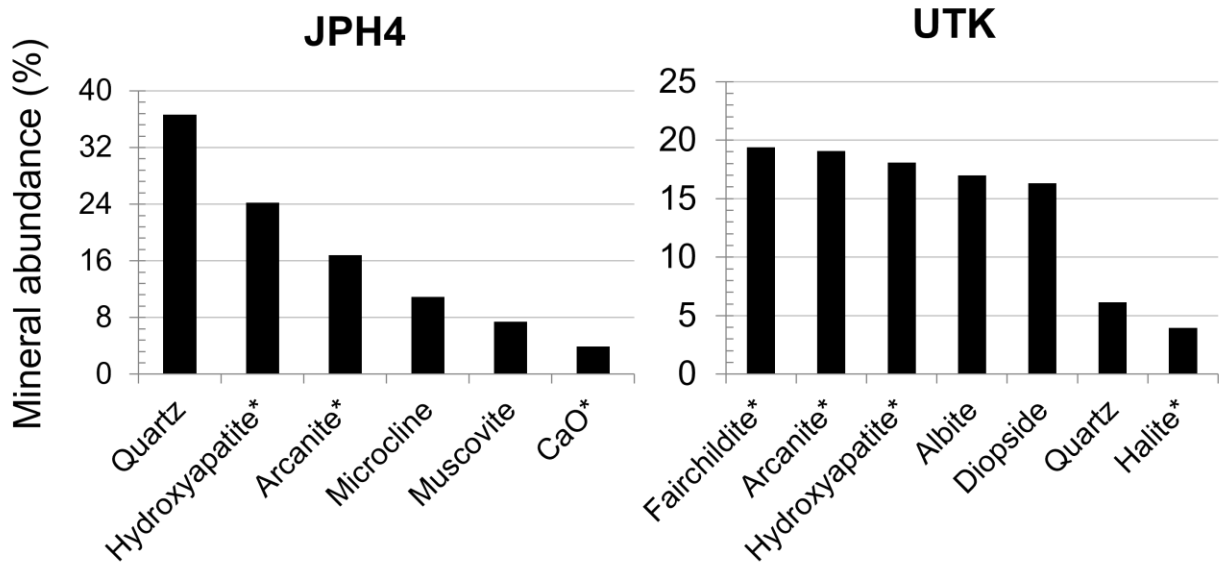

Fig. 5. Mineral abundance (%) from XRD analysis in ash samples of *Sphagnum* mosses collected from JPH4 and UTK in October 2020. UTK = Utikuma.
* Minerals created during ashing.
Note: Ignoring the minerals created during ashing, quartz accounts for 66.7% and 15.5% of JPH4 and UTK ash, respectively.

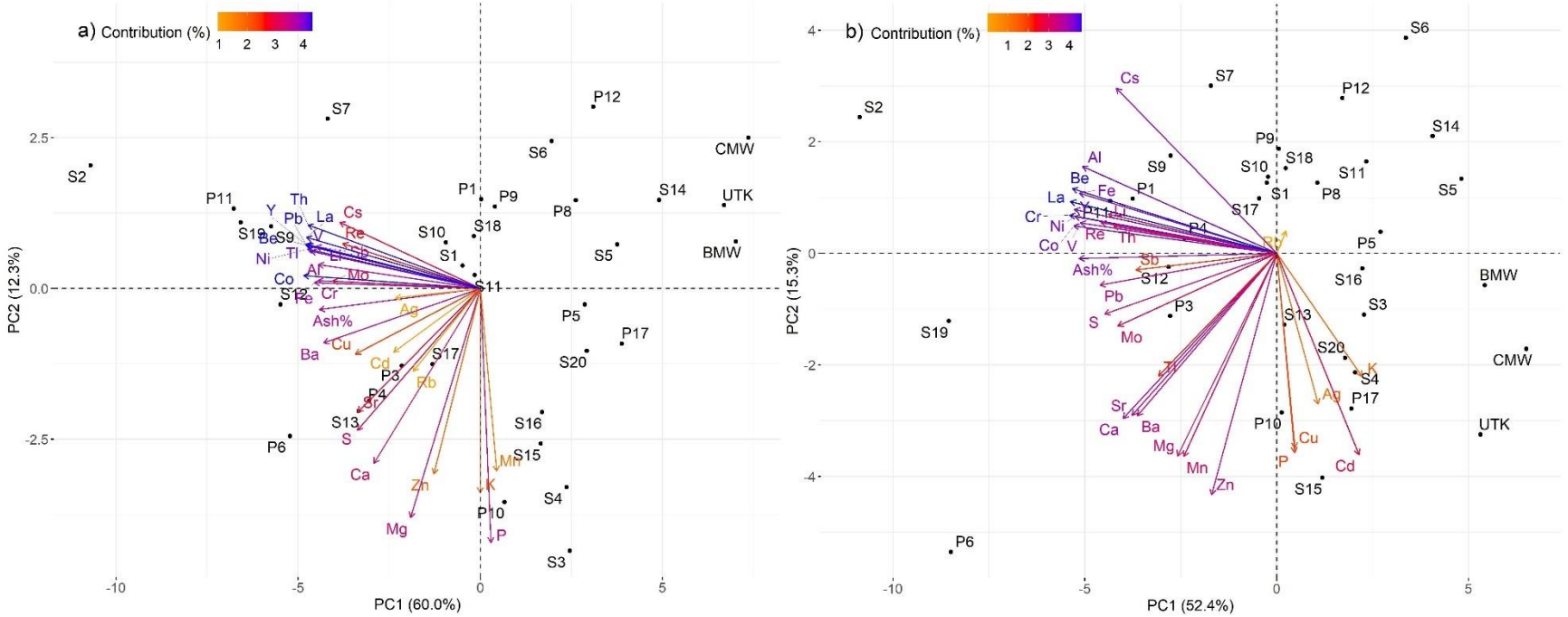

Fig. 6. Principal component analysis of 2015 *Sphagnum* mosses using a) total concentrations and ash content and b) acid soluble concentrations and ash content. The contribution reflects the total contribution of the variables to principal component (PC) 1 and 2. BMW = Birch Mountains Wildland, CMW = Caribou Mountains Wildland, UTK = Utikuma.

Supporting Information 1

Presentation of Geochemical Data

This study generated a considerable volume of geochemical data: mosses were collected in triplicate during 3 seasons from a total of 38 peatlands, and both bulk samples and the acid soluble ash (ASA) fraction were analyzed for 5 major and 36 trace elements (TEs). For the convenience of the reader, the Supporting Information 1 includes: i) a set of maps for the samples collected in 2015, showing the spatial variation in TE concentrations for the bulk moss and ASA fractions; ii) bar graphs summarizing the ranges of concentrations (total and ASA) for industrial and reference sites for 2015, 2019, and 2020, and average TE concentrations for 2020; iii) statistical analyses of the data (i.e. correlograms of all elements and linear regressions of TE concentrations versus Y); iv) box plots to evaluate temporal trends in TE concentrations; and v) enrichment factors.

Enrichment factors were calculated as the ratio of the concentrations of a given TE to that of yttrium (Y), a conservative lithophile element, normalized to the corresponding ratio in the Upper Continental Crust (UCC).[1]

$$EF = \frac{[TE/Y]_{sample}}{[TE/Y]_{UCC}}$$

List of Figures

Fig. S1. Moss sampling sites within the Athabasca Bituminous Sands Regions in fall 2015 (green points), and 2019 and 2020 (red points except for MIL). 68

Fig. S2. Schematic flow of sample treatments. 69

Fig. S3. Ratios of maximum (Max) to minimum (Min) element concentrations out of bulk moss and acid soluble ash (ASA) of *Sphagnum* mosses collected in fall 2015 (sites EINP and WAG were excluded) and 2019. 70

Fig. S4. a) & b): Average trace element concentrations (µg kg^{-1} dry moss) of industrial and reference sites out of bulk moss and acid soluble ash (ASA) of *Sphagnum* mosses collected in fall **2020**. c) & d): Ratios of maximum (Max) to minimum (Min) element concentrations out of bulk moss and ASA 71

Fig. S5. Ash content (%) of *Sphagnum* mosses collected in fall a) 2015 and b) 2019 and 2020. CMW = Caribou Mountains Wildland, BMW = Birch Mountains Wildland, UTK = Utikuma, WAG = Wagner Natural Area, EINP = Elk Island National Park. McK = Fort Mackay, McM = Fort McMurray, ANZ = Anzac. 72

Fig. S6. Spatial distribution of a) total and b) acid soluble **Al**, and c) total and d) acid soluble **Th** concentrations in *Sphagnum* mosses collected in fall 2015. ASA = Acid Soluble Ash. CMW = Caribou Mountains Wildland, BMW = Birch Mountains Wildland, UTK = Utikuma, WAG = Wagner Natural Area, EINP = Elk Island National Park 73

Fig. S7. Spatial distribution of a) total and b) acid soluble **Fe**, and c) total and d) acid soluble **Mo** concentrations in *Sphagnum* mosses collected in fall 2015. ASA = Acid Soluble Ash. CMW = Caribou Mountains Wildland, BMW = Birch Mountains Wildland, UTK = Utikuma, WAG = Wagner Natural Area, EINP = Elk Island National Park 74

Fig. S8. Correlogram of **total** concentrations and ash content of fall 2015 *Sphagnum* mosses based on the Spearman rank-based correlation test. Sites EINP and WAG were excluded. Corr. Coef. = Correlation coefficient. Significance level = 0.05. Only significant correlations are presented. . 75

Fig. S9. Wind rose diagrams for 2015, 2019, and 2020 at Mildred Station. Historic hourly weather data from May 1 to August 31 of each year was downloaded from the Government of Canada climate station: Mildred Lake (Latitude: 57°02'28.000" N, Longitude: 111°33'32.000" W, Elevation: 310.00 m, Climate Identifier (ID): 3064528, World Meteorological Organization (WMO) ID: 71255, Transport Canada (TC) ID: WMX). Data was processed in R 4.1.1,[2] and visualized using the *openair* package.[3] Wind rose diagram for 2015 was also used in our previous study by Mulland-Boudreau et al.[4] 76

Fig. S10. Total V, Ni, Mo, Pb, Sb, Tl, Ag, and Cd concentration versus total Y concentration (µg kg^{-1} dry moss) in *Sphagnum* mosses collected in fall 2015. CMW = Caribou Mountains Wildland, BMW = Birch Mountains Wildland, UTK = Utikuma, WAG = Wagner Natural Area, EINP = Elk Island National Park 77

Fig. S11. Spatial distribution of a) total and b) acid soluble **Sb**, and c) total and d) acid soluble **Tl** concentrations (μg kg^{-1} dry moss) in *Sphagnum* mosses collected in fall 2015. ASA = Acid Soluble Ash. CMW = Caribou Mountains Wildland, BMW = Birch Mountains Wildland, UTK = Utikuma, WAG = Wagner Natural Area, EINP = Elk Island National Park. 78

Fig. S12. Spatial distribution of a) total and b) acid soluble **Ag**, and c) total and d) acid soluble **Cd** concentrations (μg kg^{-1} dry moss) in *Sphagnum* mosses collected in fall 2015. ASA = Acid Soluble Ash. CMW = Caribou Mountains Wildland, BMW = Birch Mountains Wildland, UTK = Utikuma, WAG = Wagner Natural Area, EINP = Elk Island National Park. 79

Fig. S13. Spatial distribution of a) total and b) acid soluble **Cu**, and c) total and d) acid soluble **Zn** concentrations (mg kg^{-1} dry moss) in *Sphagnum* mosses collected in fall 2015. ASA = Acid Soluble Ash. CMW = Caribou Mountains Wildland, BMW = Birch Mountains Wildland, UTK = Utikuma, WAG = Wagner Natural Area, EINP = Elk Island National Park. 80

Fig. S14. Spatial distribution of acid soluble a) **Y**, b) **Pb**, c) **V**, and d) **Ni** concentrations in *Sphagnum* mosses collected in fall 2015. ASA = Acid Soluble Ash. CMW = Caribou Mountains Wildland, BMW = Birch Mountains Wildland, UTK = Utikuma, WAG = Wagner Natural Area, EINP = Elk Island National Park. 81

Fig. S15. Correlogram of element concentrations in Acid Soluble Ash (**ASA**) and ash content of fall 2015 *Sphagnum* mosses based on the Spearman rank-based correlation test. Sites EINP and WAG were excluded. Corr. Coef. = Correlation coefficient. Significance level = 0.05. Only significant correlations are presented. 82

Fig. S16. Proportion of acid soluble to total concentration of trace elements in *Sphagnum* mosses collected in fall 2019 (a, c, & e) and 2020 (b, d, & f). ASA = Acid Soluble Ash. McK = Fort Mackay, McM = Fort McMurray, ANZ = Anzac, UTK = Utikuma. 83

Fig. S17. Total and acid soluble concentrations (mg kg^{-1} dry moss) of conservative lithophile elements (Y, Cr, La), essential elements (K, Mg, P, S, Fe, Cu, Zn), and potentially toxic elements (Ag, Cd) in *Sphagnum* mosses collected in fall 2019 and 2020. ASA = Acid Soluble Ash. McK = Fort Mackay, McM = Fort McMurray, ANZ = Anzac, UTK = Utikuma. 84

Fig. S18. X-ray diffraction (XRD) analysis of a) JPH4 and b) UTK ash samples. UTK = Utikuma. 85

Fig. S19. Particle size distribution of ash samples of *Sphagnum* mosses by laser diffraction. UTK = Utikuma. 86

Fig. S20. Contributions of variables in accounting for the variability in principal component (PC) 1 and PC 2 from principal component analysis of fall 2015 *Sphagnum* mosses using total concentrations (a, b) and acid soluble concentrations (c, d). The red dashed line indicates the average contribution. 87

Fig. S21. Temporal trends of **total** concentration (μg kg^{-1} dry moss) of selected elements in *Sphagnum* moss collected in fall 2015 (sites EINP and WAG were excluded), 2019, and 2020. Boxplots show the range, 25th and 75th percentiles, and median for each element. 88

Fig. S22. Temporal trends of trace element concentration (μg kg^{-1} dry moss) in the Acid Soluble Ash (**ASA**) fraction of *Sphagnum* moss collected in fall 2015 (sites EINP and WAG were excluded), 2019, and 2020. Boxplots show the range, 25th and 75th percentiles, and median for each element..... 89

Fig. S23. Enrichment factors using **Y** as the reference element with values greater than 2 of a) V, Ni, Mo, Pb, Tl, b) Sb, c) Ag, and d) Cd of *Sphagnum* mosses collected in fall 2015. Enrichment factors of V were all below 2 and are not shown in the plot. CMW = Caribou Mountains Wildland, BMW = Birch Mountains Wildland, UTK = Utikuma, WAG = Wagner Natural Area, EINP = Elk Island National Park..... 90

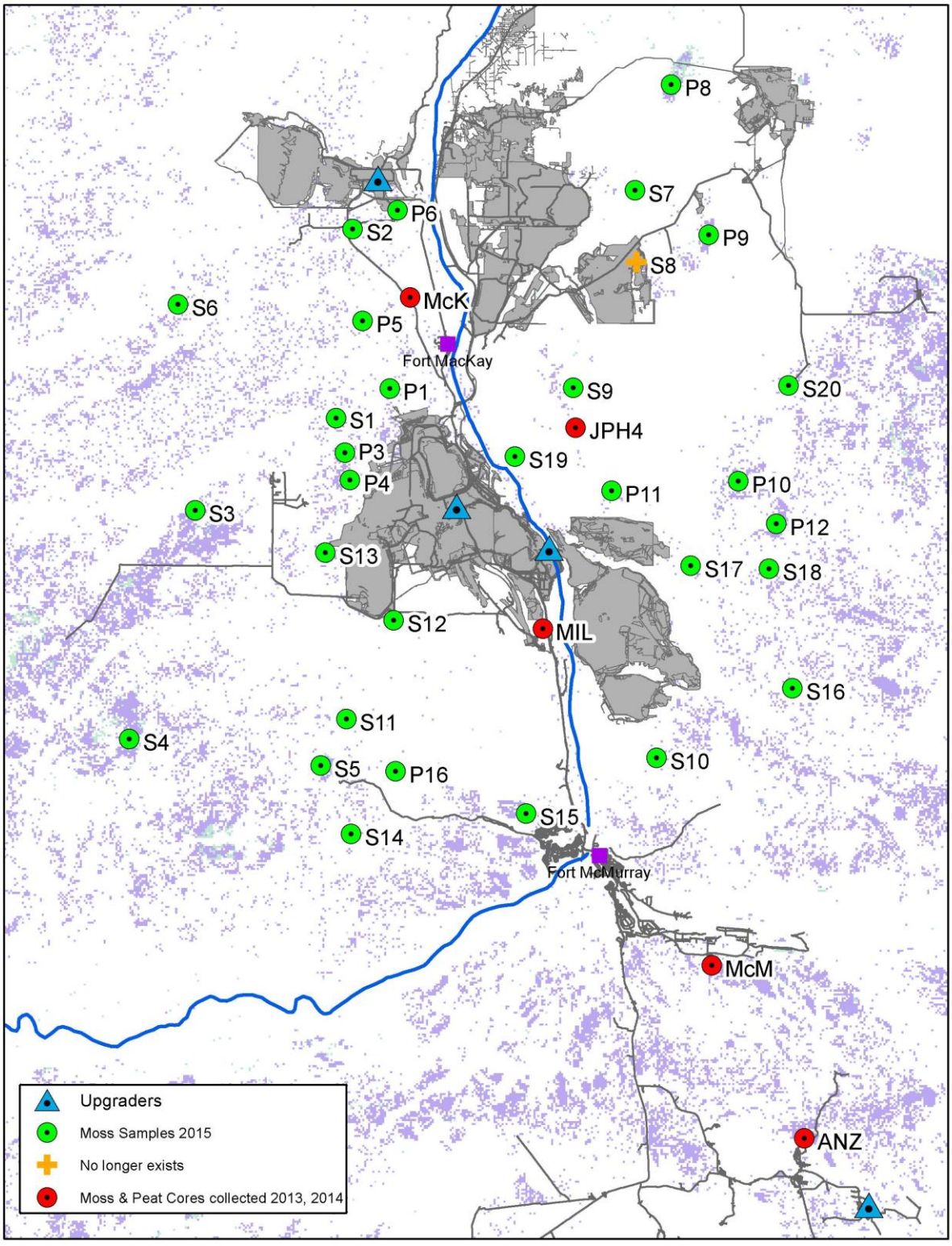

Fig. S1. Moss sampling sites within the Athabasca Bituminous Sands Regions in fall 2015 (green points), and 2019 and 2020 (red points except for MIL).

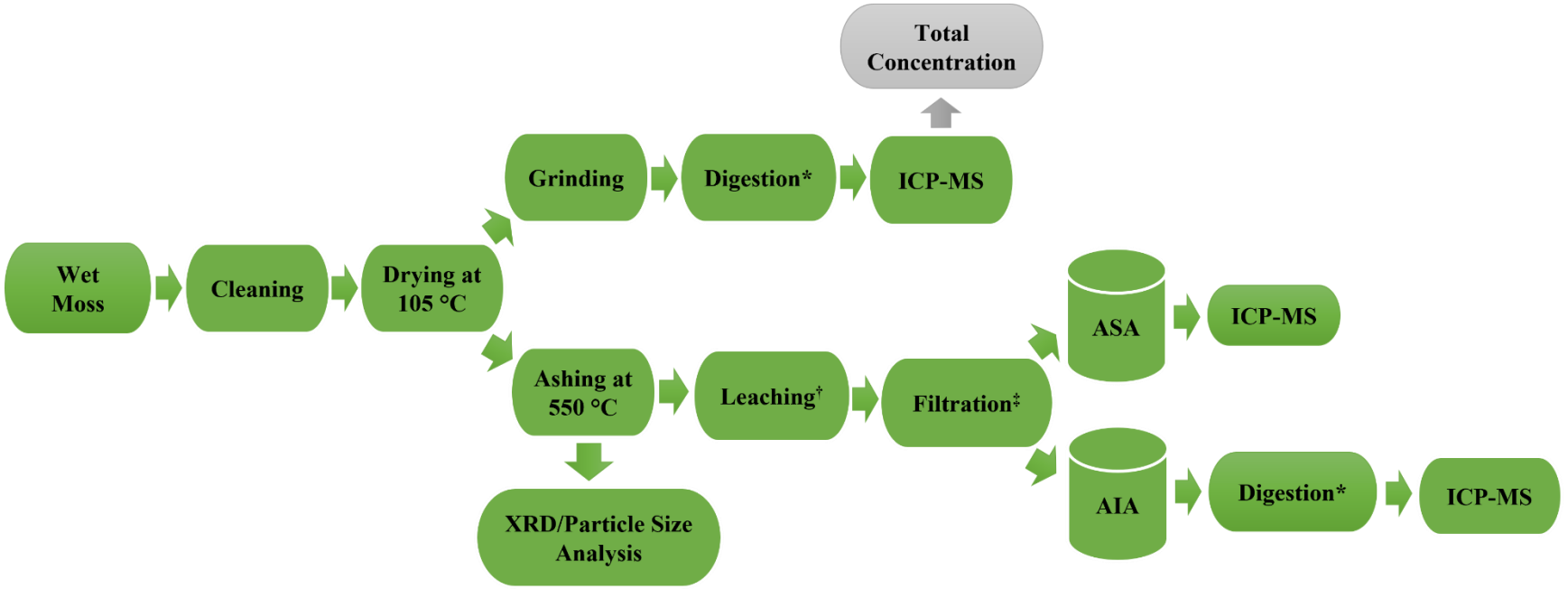

Fig. S2. Schematic flow of sample treatments.
*Digestion: Reaction with concentrated HNO_3 (sub-boiled twice) and HBF_4 for 80 min in a microwave under high temperature and pressure.
†Leaching: Reaction with 2% HNO_3 for 15 min under room temperature and pressure.
‡Filtration: Polypropylene syringes and 0.45 µm polytetrafluoroethylene filter membranes, with polypropylene filter holders and silicone gaskets for sealing. All were acid-cleaned before use.
Note: ASA = Acid Soluble Ash. AIA = Acid Insoluble Ash (not analyzed).

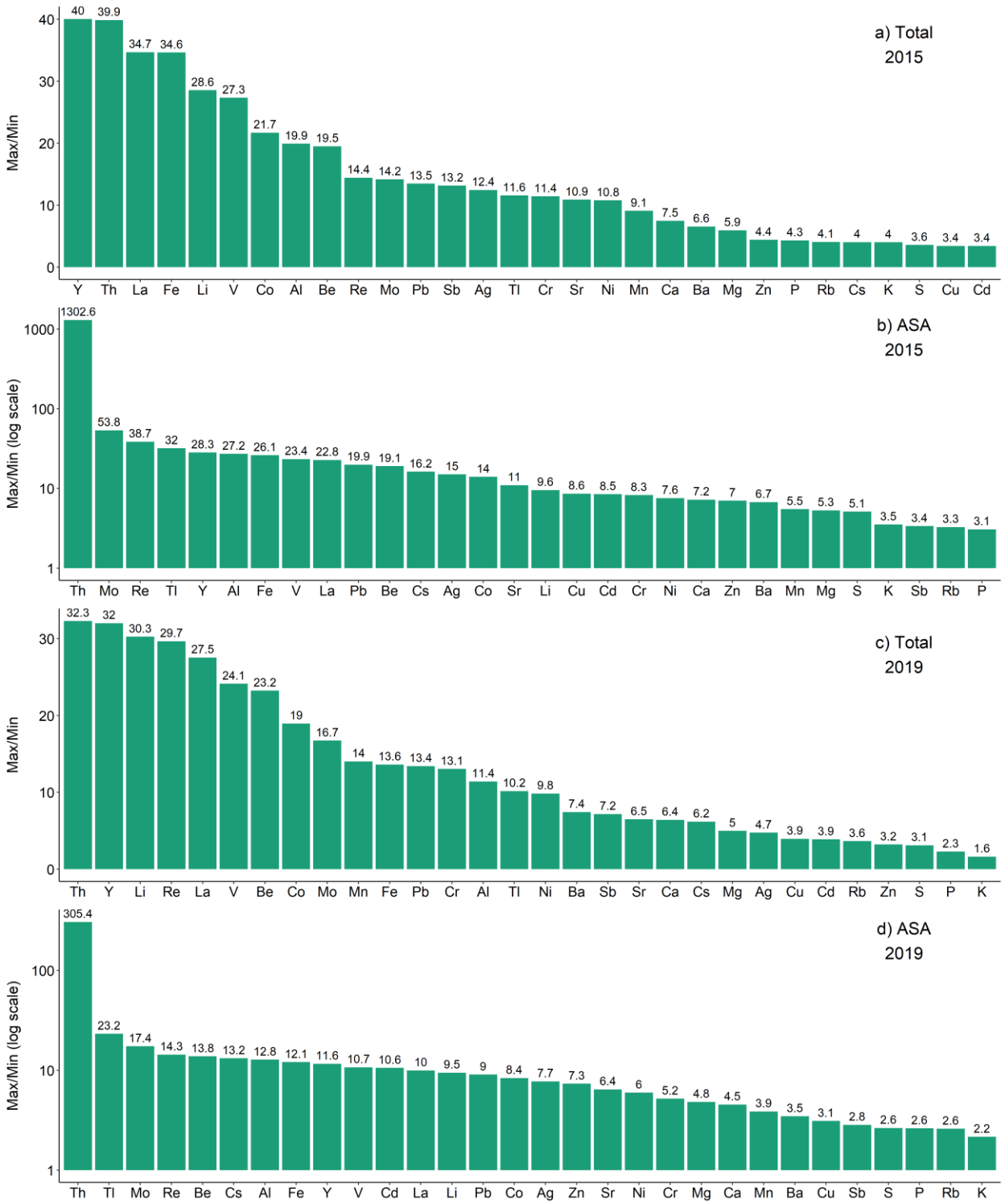

Fig. S3. Ratios of maximum (Max) to minimum (Min) element concentrations out of bulk moss and acid soluble ash (ASA) of *Sphagnum* mosses collected in fall 2015 (sites EINP and WAG were excluded) and 2019.

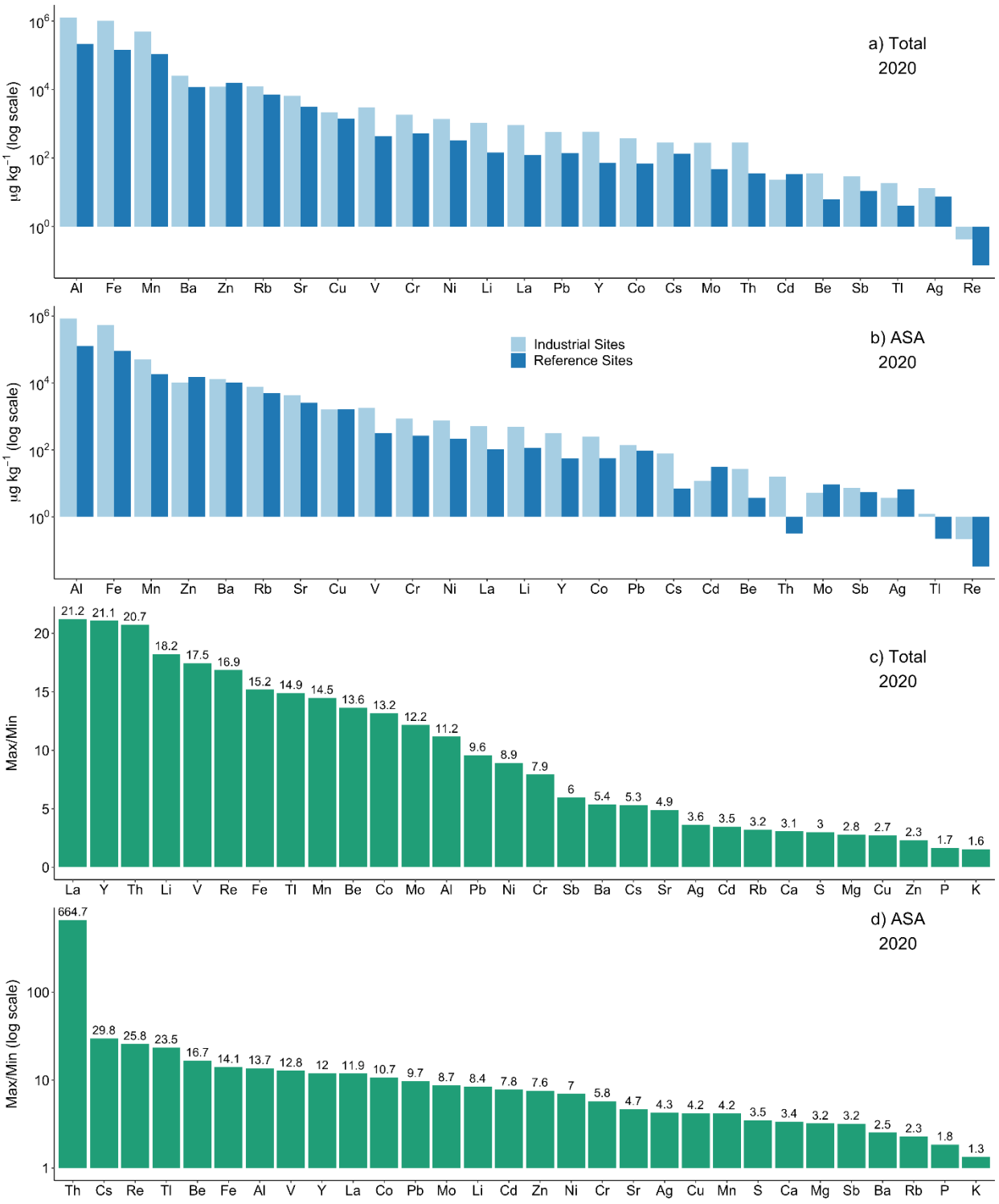

Fig. S4. a) & b): Average trace element concentrations (µg kg^{-1} dry moss) of industrial and reference sites out of bulk moss and acid soluble ash (ASA) of *Sphagnum* mosses collected in fall **2020**. c) & d): Ratios of maximum (Max) to minimum (Min) element concentrations out of bulk moss and ASA.

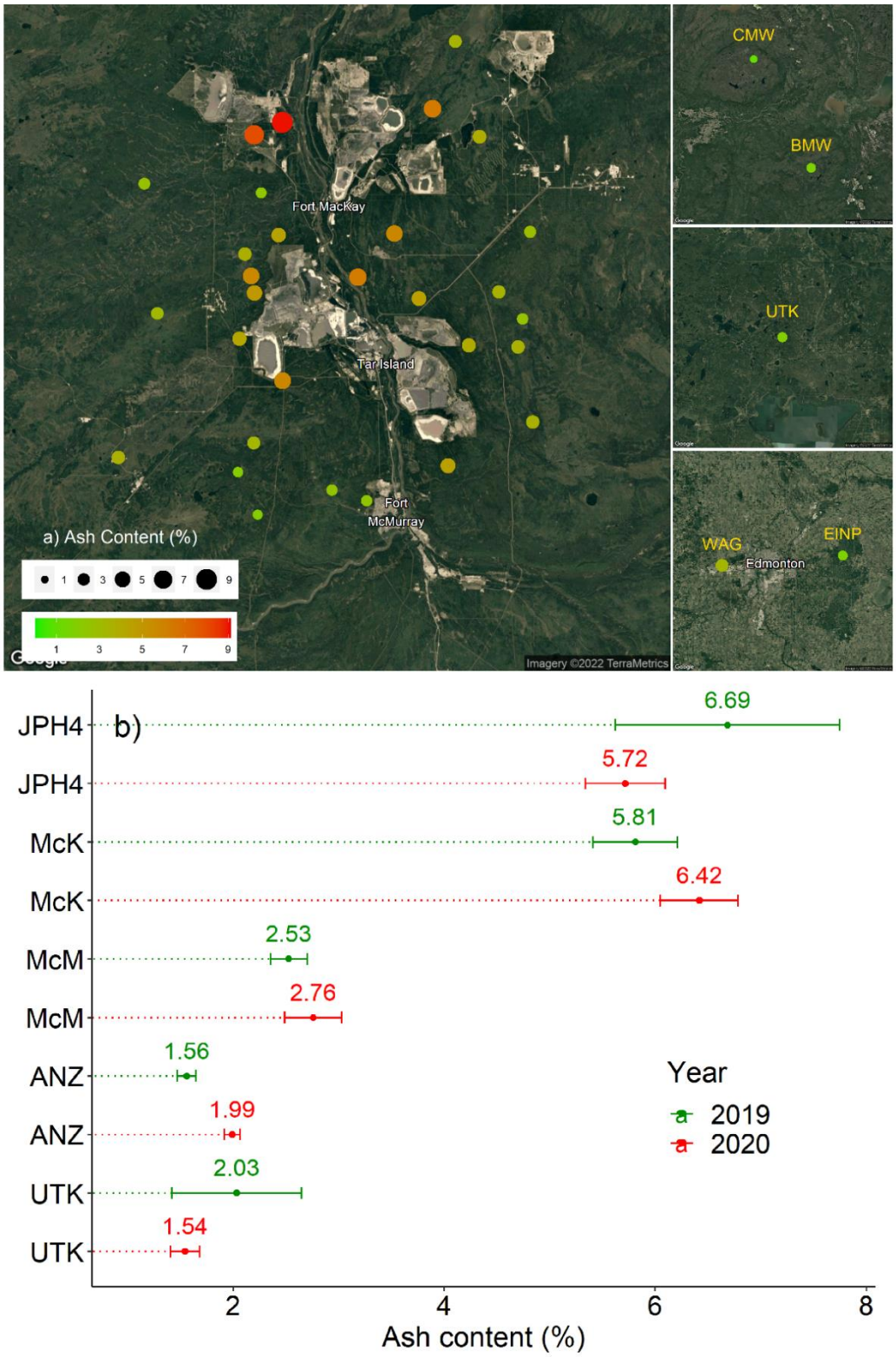

Fig. S5. Ash content (%) of *Sphagnum* mosses collected in fall a) 2015 and b) 2019 and 2020. CMW = Caribou Mountains Wildland, BMW = Birch Mountains Wildland, UTK = Utikuma, WAG = Wagner Natural Area, EINP = Elk Island National Park. McK = Fort Mackay, McM = Fort McMurray, ANZ = Anzac.

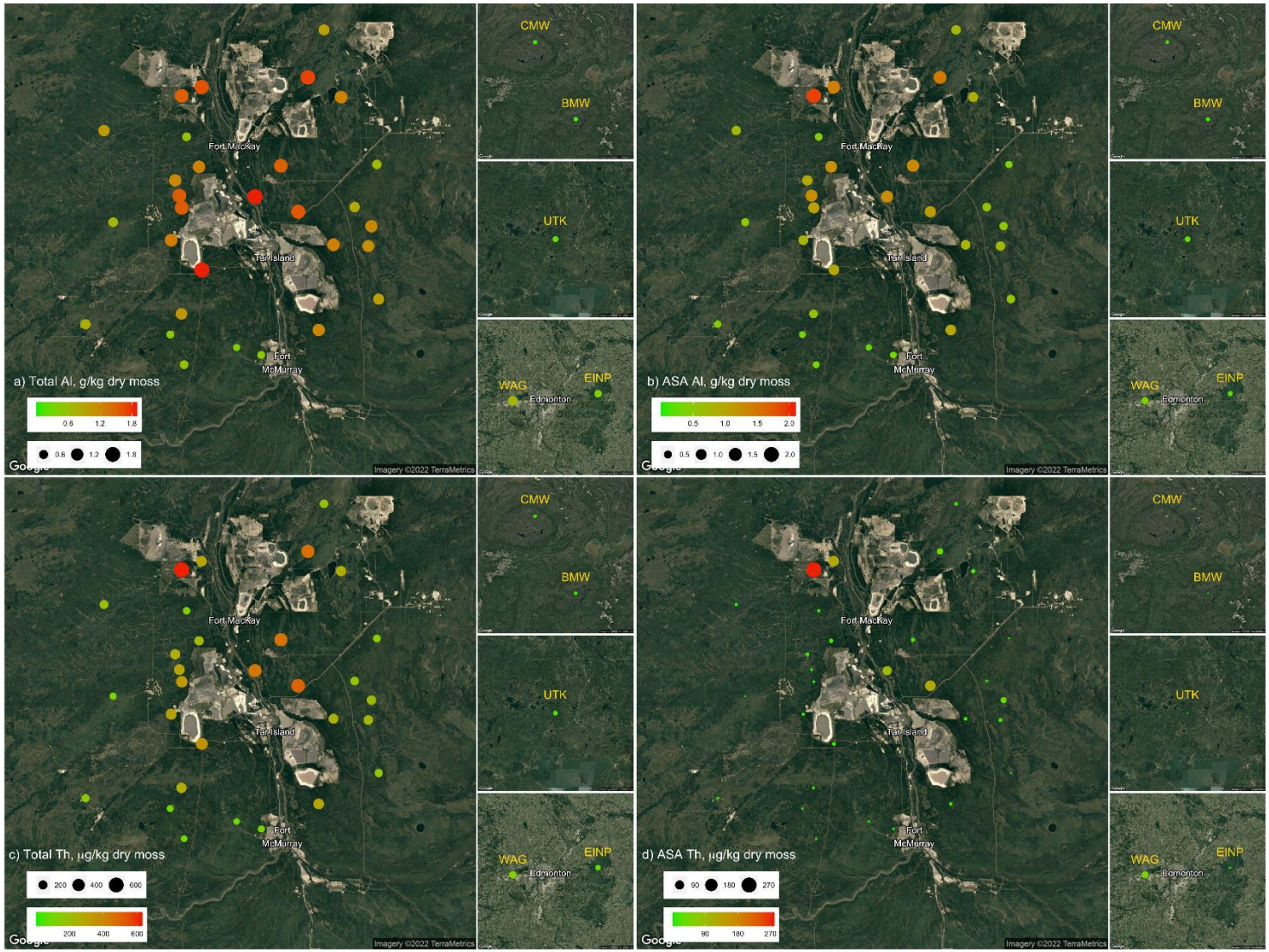

Fig. S6. Spatial distribution of a) total and b) acid soluble **Al**, and c) total and d) acid soluble **Th** concentrations in *Sphagnum* mosses collected in fall 2015. ASA = Acid Soluble Ash. CMW = Caribou Mountains Wildland, BMW = Birch Mountains Wildland, UTK = Utikuma, WAG = Wagner Natural Area, EINP = Elk Island National Park.

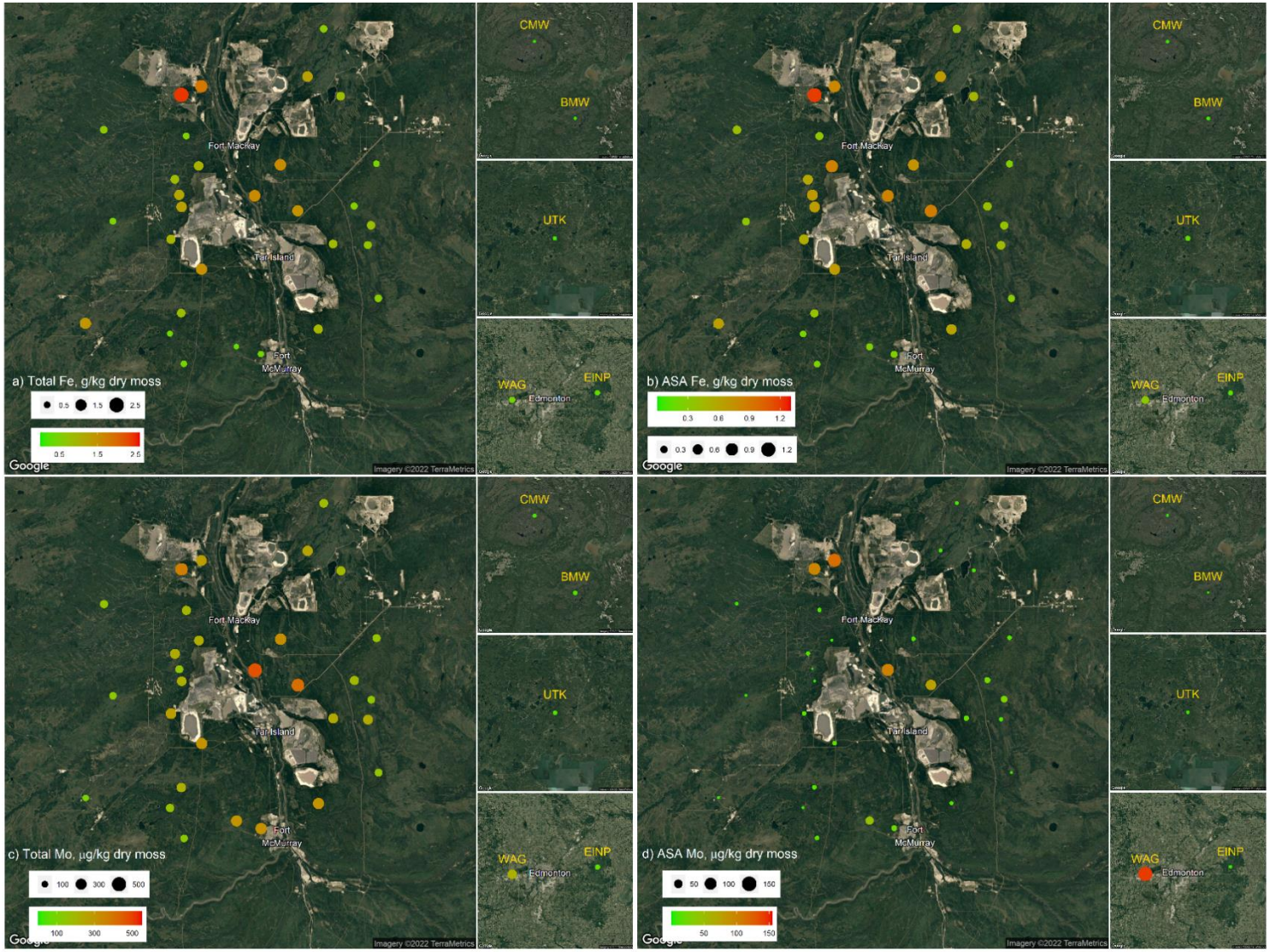

Fig. S7. Spatial distribution of a) total and b) acid soluble **Fe**, and c) total and d) acid soluble **Mo** concentrations in *Sphagnum* mosses collected in fall 2015. ASA = Acid Soluble Ash. CMW = Caribou Mountains Wildland, BMW = Birch Mountains Wildland, UTK = Utikuma, WAG = Wagner Natural Area, EINP = Elk Island National Park.

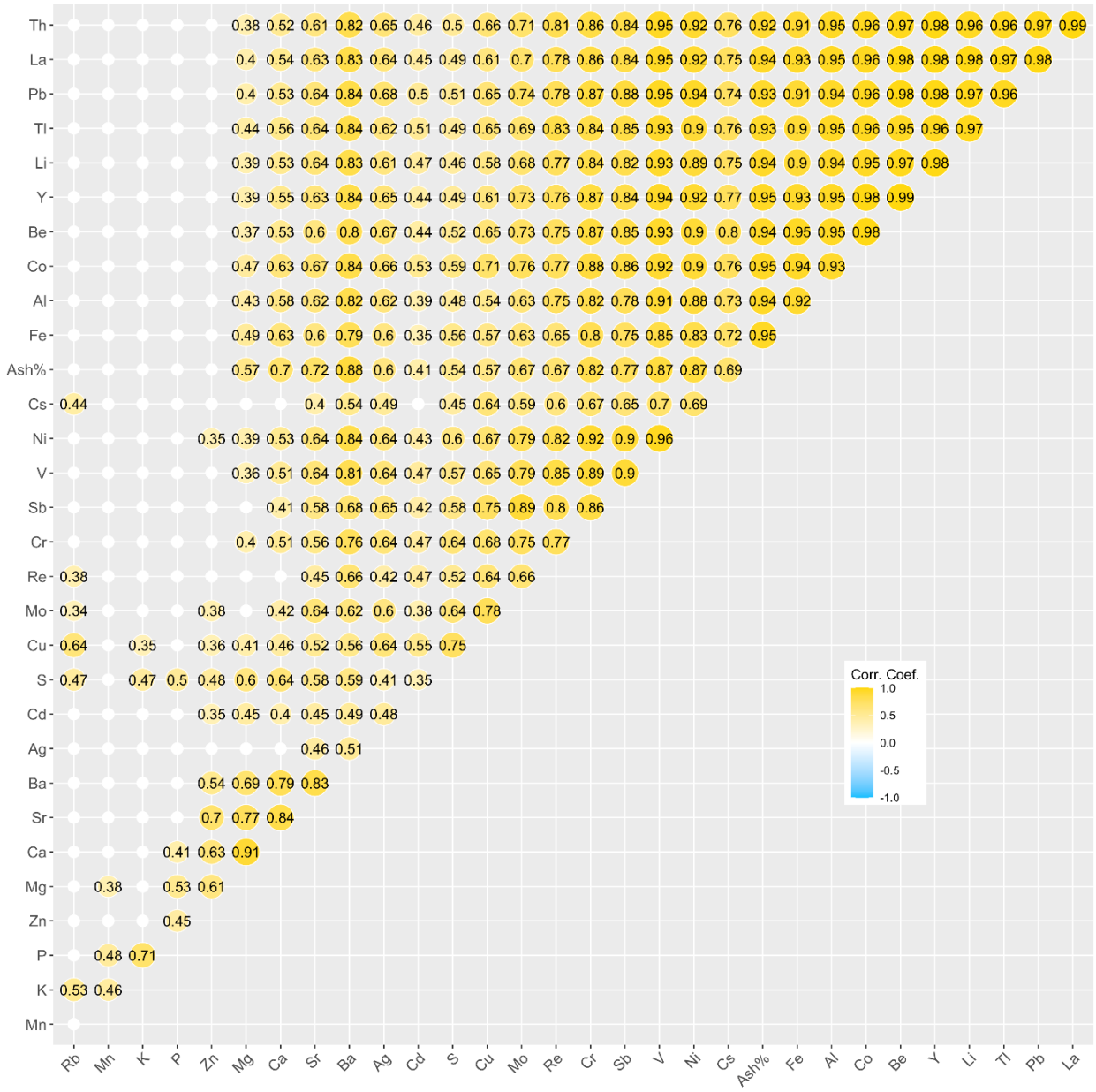

Fig. S8. Correlogram of **total** concentrations and ash content of fall 2015 *Sphagnum* mosses based on the Spearman rank-based correlation test. Sites EINP and WAG were excluded. Corr. Coef. = Correlation coefficient. Significance level = 0.05. Only significant correlations are presented.

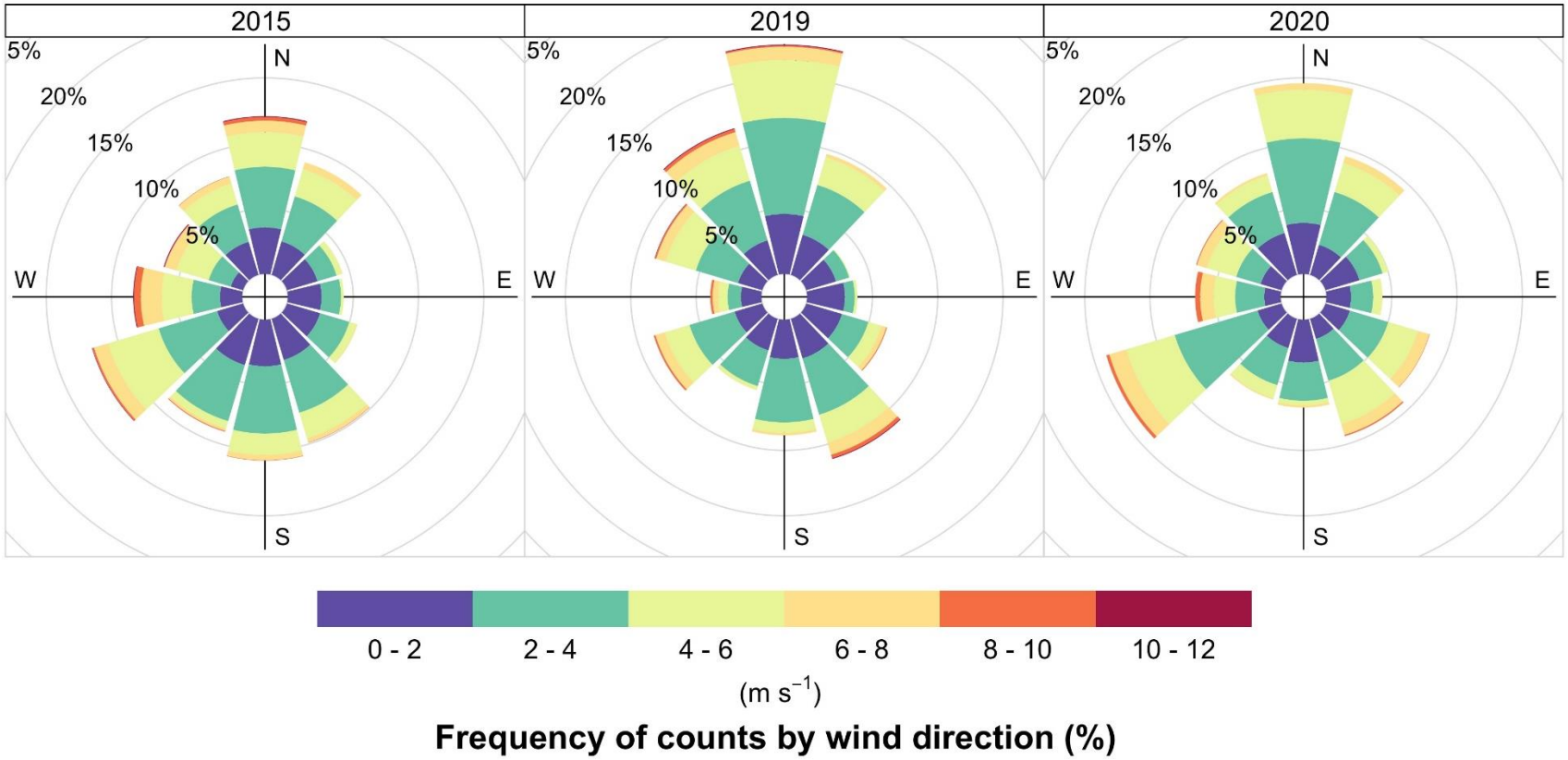

Fig. S9. Wind rose diagrams for 2015, 2019, and 2020 at Mildred Station. Historic hourly weather data from May 1 to August 31 of each year was downloaded from the Government of Canada climate station: Mildred Lake (Latitude: 57°02'28.000" N, Longitude: 111°33'32.000" W, Elevation: 310.00 m, Climate Identifier (ID): 3064528, World Meteorological Organization (WMO) ID: 71255, Transport Canada (TC) ID: WMX). Data was processed in R 4.1.1,[2] and visualized using the *openair* package.[3] Wind rose diagram for 2015 was also used in our previous study by Mulland-Boudreau et al.[4]

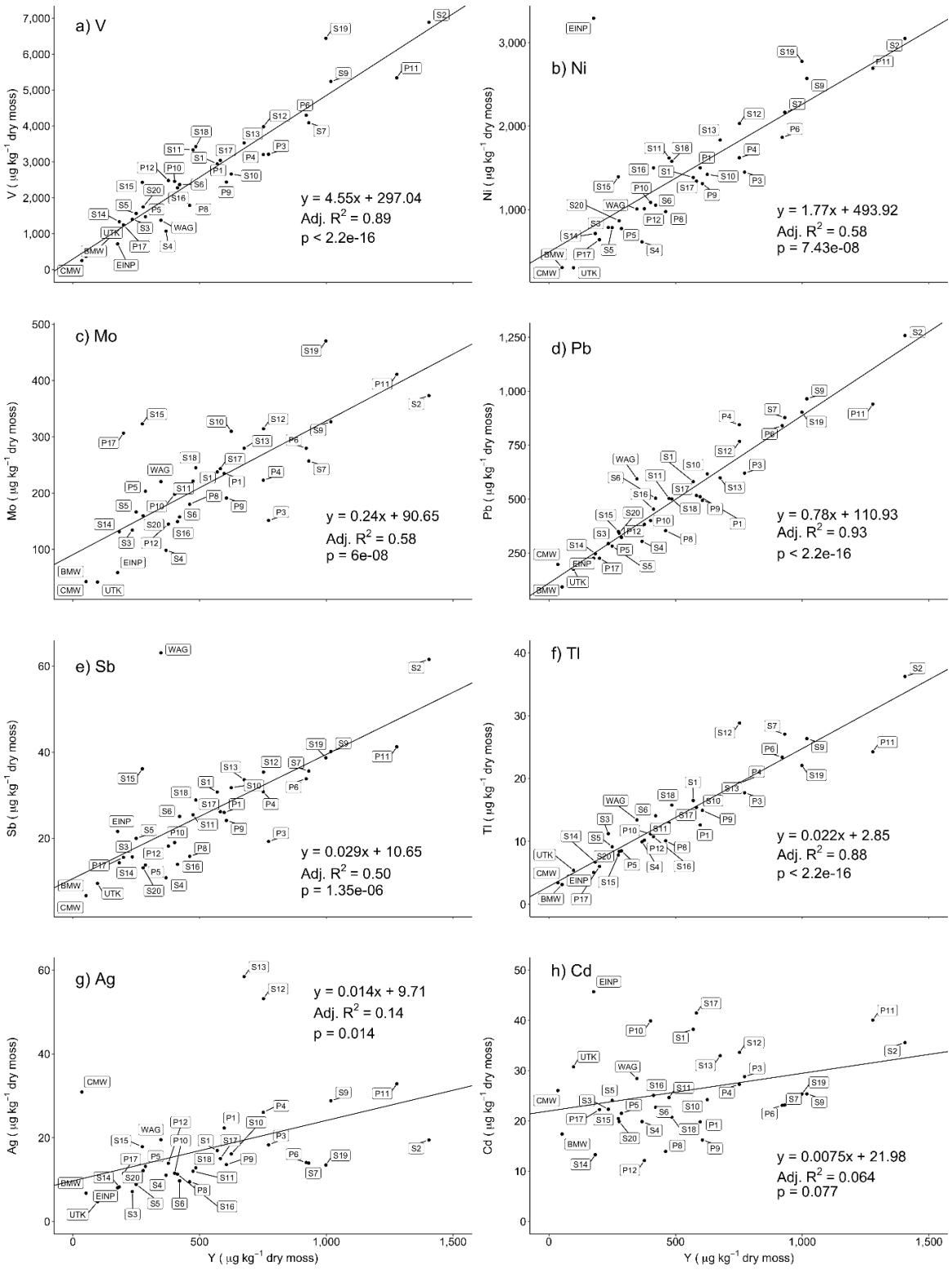

Fig. S10. Total V, Ni, Mo, Pb, Sb, Tl, Ag, and Cd concentration versus total Y concentration (µg kg^{-1} dry moss) in *Sphagnum* mosses collected in fall 2015. CMW = Caribou Mountains Wildland, BMW = Birch Mountains Wildland, UTK = Utikuma, WAG = Wagner Natural Area, EINP = Elk Island National Park.

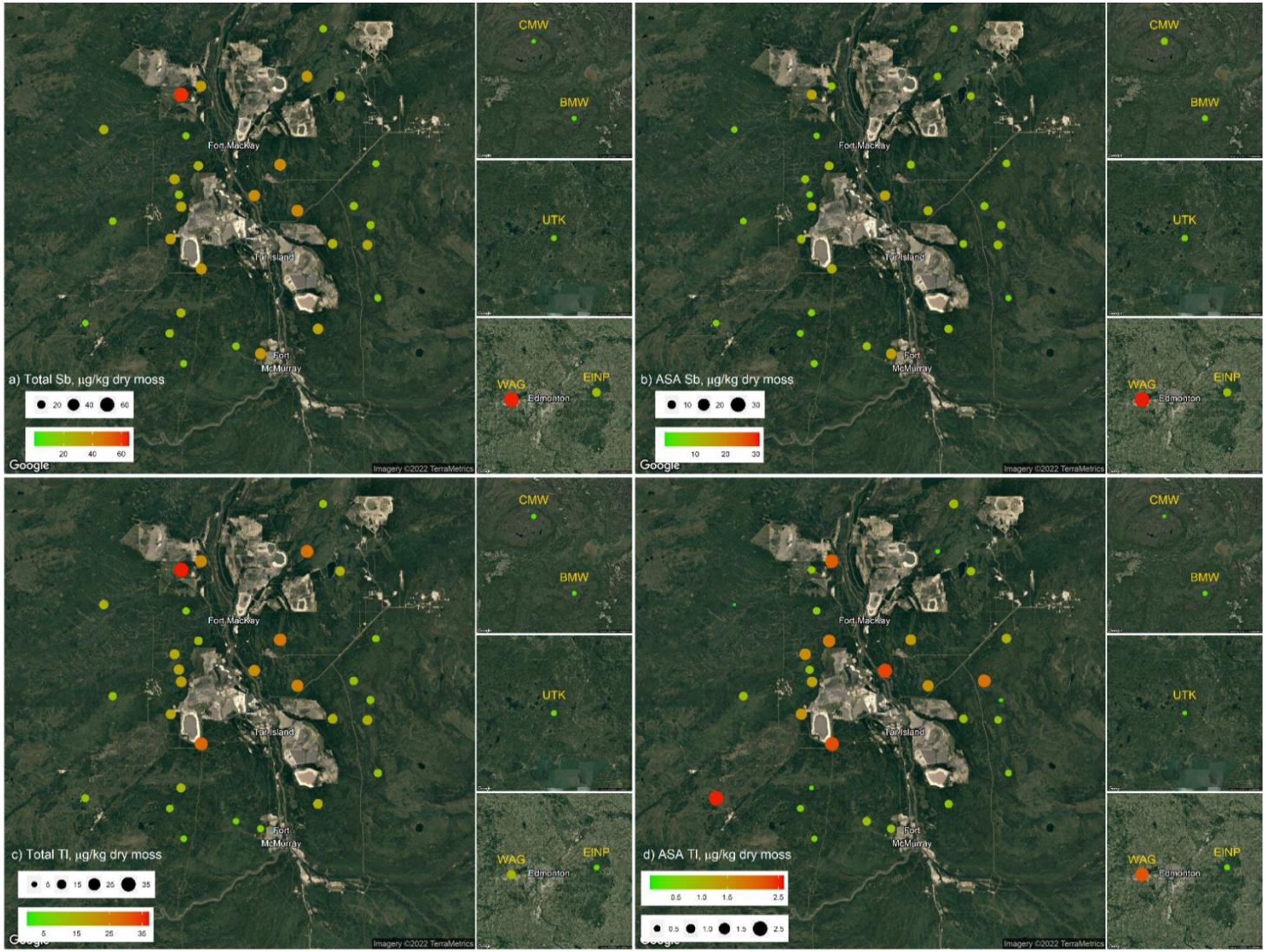

Fig. S11. Spatial distribution of a) total and b) acid soluble **Sb**, and c) total and d) acid soluble **Tl** concentrations (µg kg^{-1} dry moss) in *Sphagnum* mosses collected in fall 2015. ASA = Acid Soluble Ash. CMW = Caribou Mountains Wildland, BMW = Birch Mountains Wildland, UTK = Utikuma, WAG = Wagner Natural Area, EINP = Elk Island National Park.

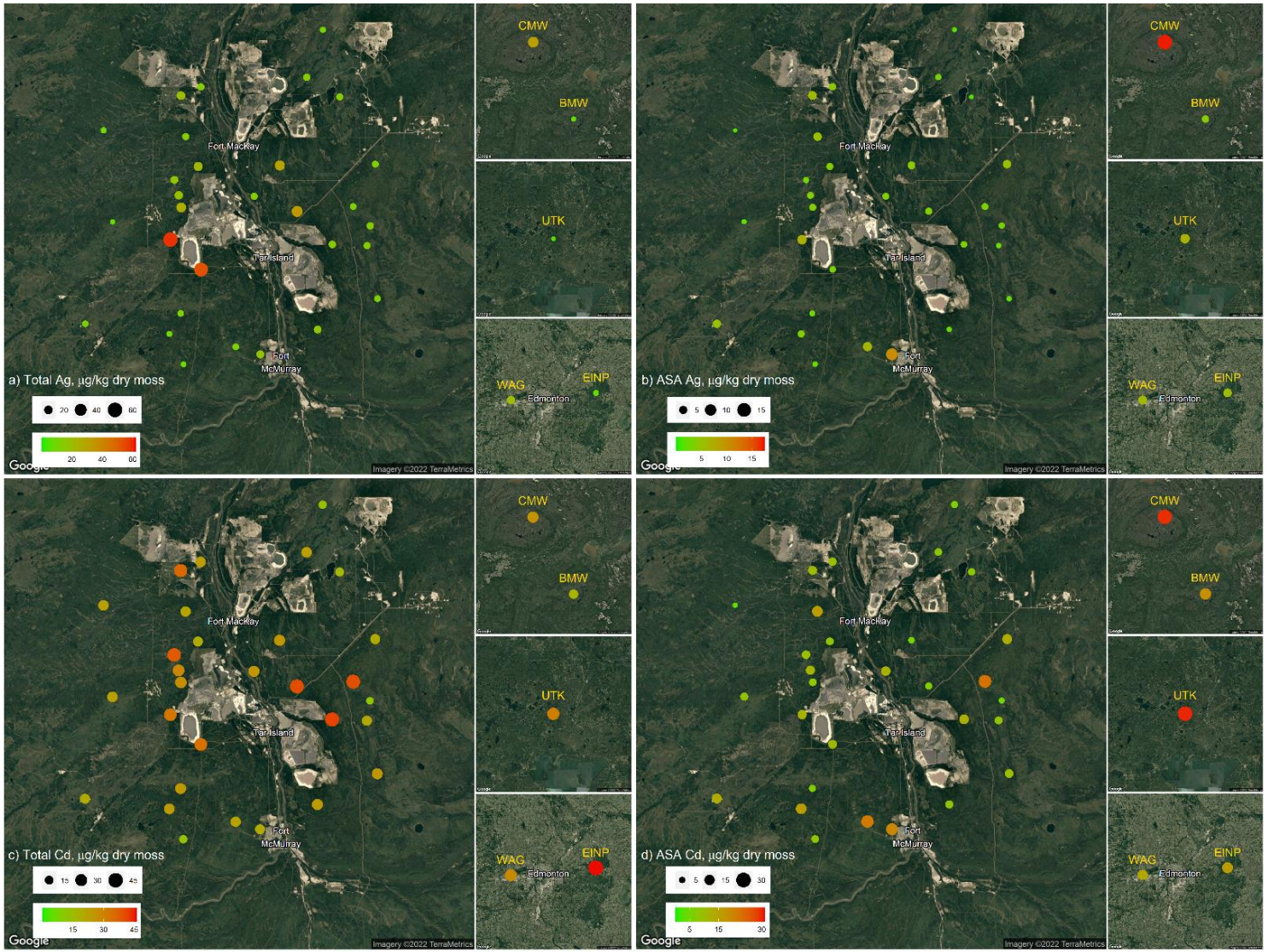

Fig. S12. Spatial distribution of a) total and b) acid soluble **Ag**, and c) total and d) acid soluble **Cd** concentrations (µg kg^{-1} dry moss) in *Sphagnum* mosses collected in fall 2015. ASA = Acid Soluble Ash. CMW = Caribou Mountains Wildland, BMW = Birch Mountains Wildland, UTK = Utikuma, WAG = Wagner Natural Area, EINP = Elk Island National Park.

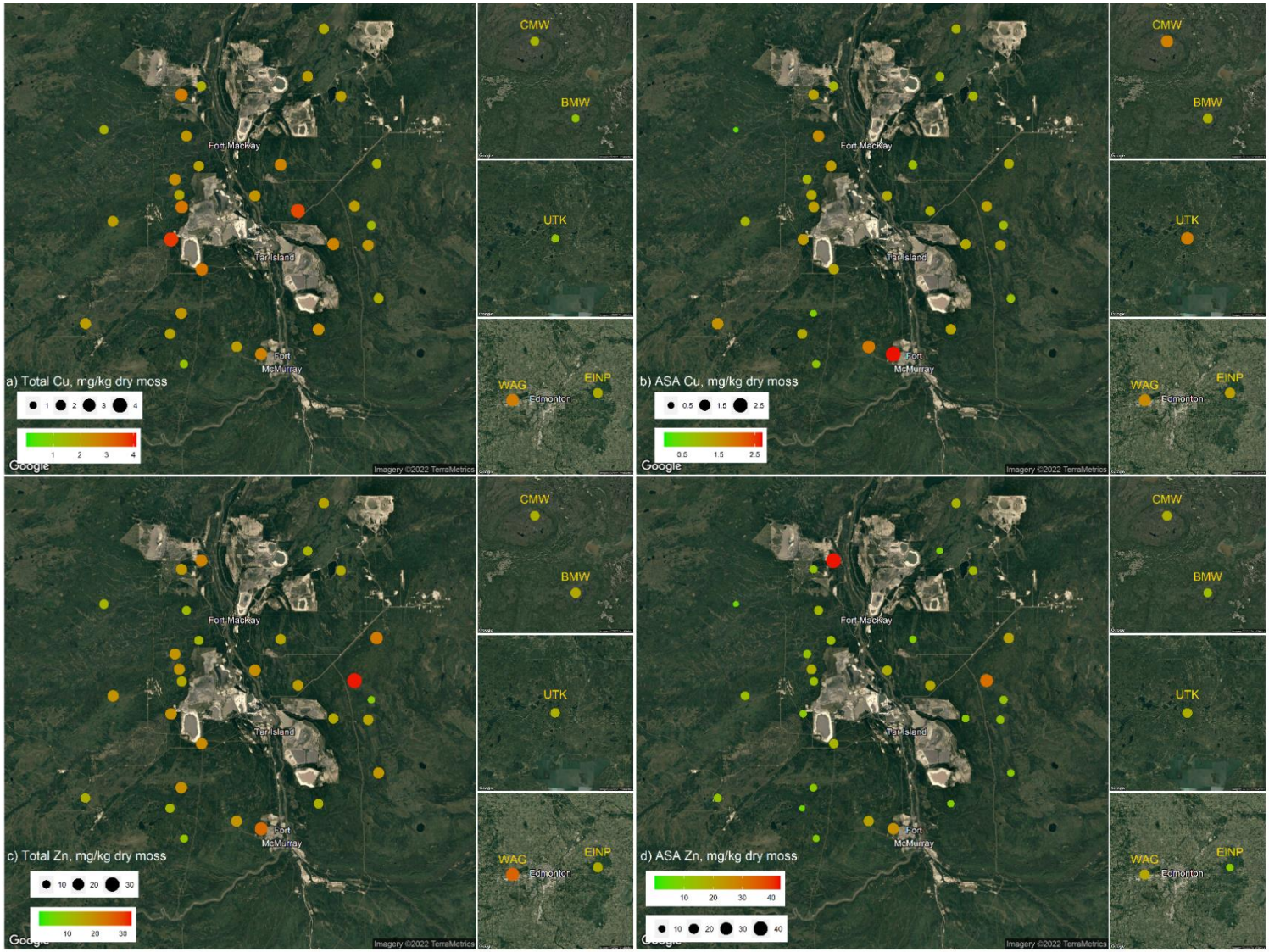

Fig. S13. Spatial distribution of a) total and b) acid soluble **Cu**, and c) total and d) acid soluble **Zn** concentrations (mg kg^{-1} dry moss) in *Sphagnum* mosses collected in fall 2015. ASA = Acid Soluble Ash. CMW = Caribou Mountains Wildland, BMW = Birch Mountains Wildland, UTK = Utikuma, WAG = Wagner Natural Area, EINP = Elk Island National Park.

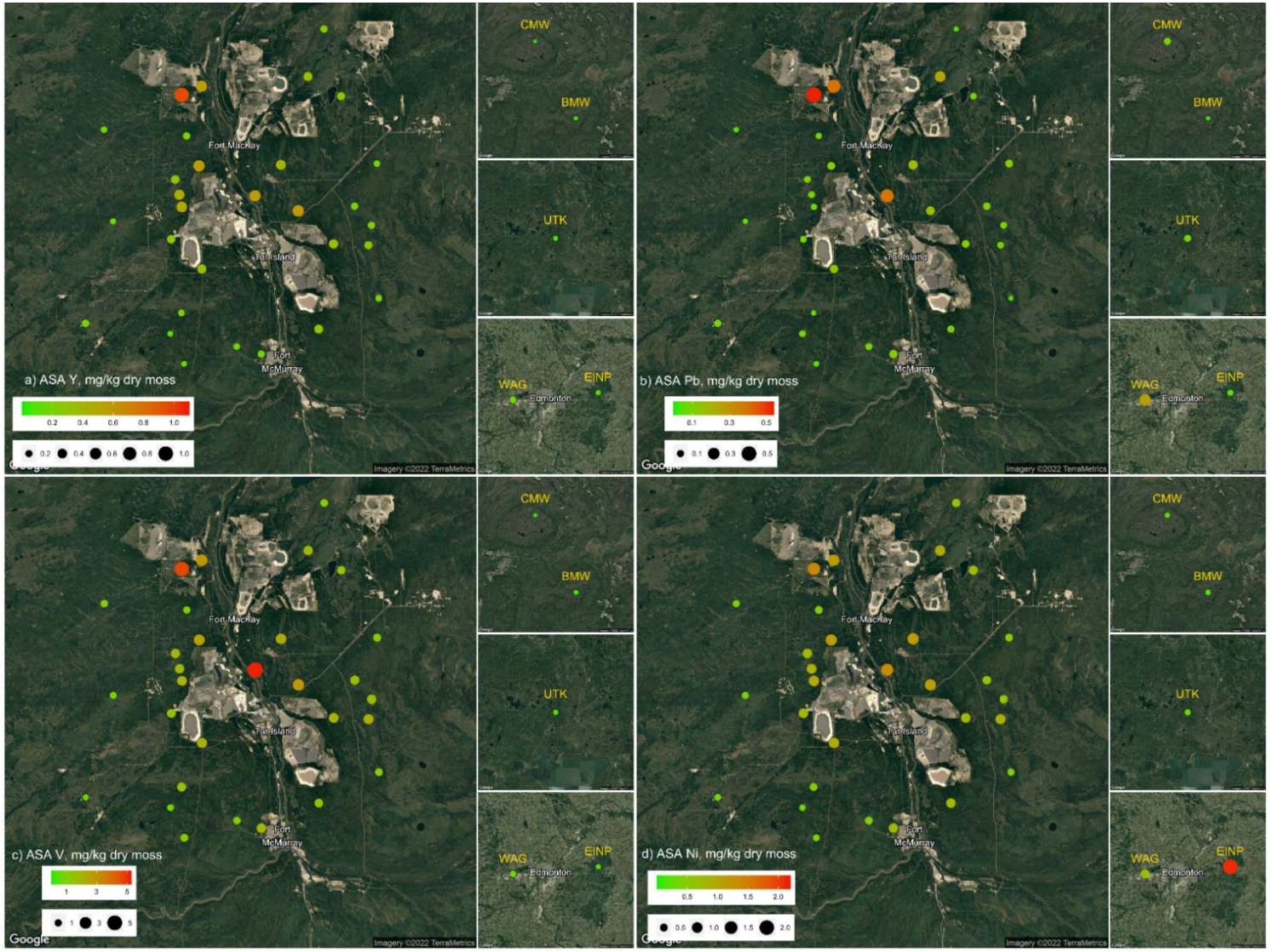

Fig. S14. Spatial distribution of acid soluble a) **Y**, b) **Pb**, c) **V**, and d) **Ni** concentrations in *Sphagnum* mosses collected in fall 2015. ASA = Acid Soluble Ash. CMW = Caribou Mountains Wildland, BMW = Birch Mountains Wildland, UTK = Utikuma, WAG = Wagner Natural Area, EINP = Elk Island National Park.

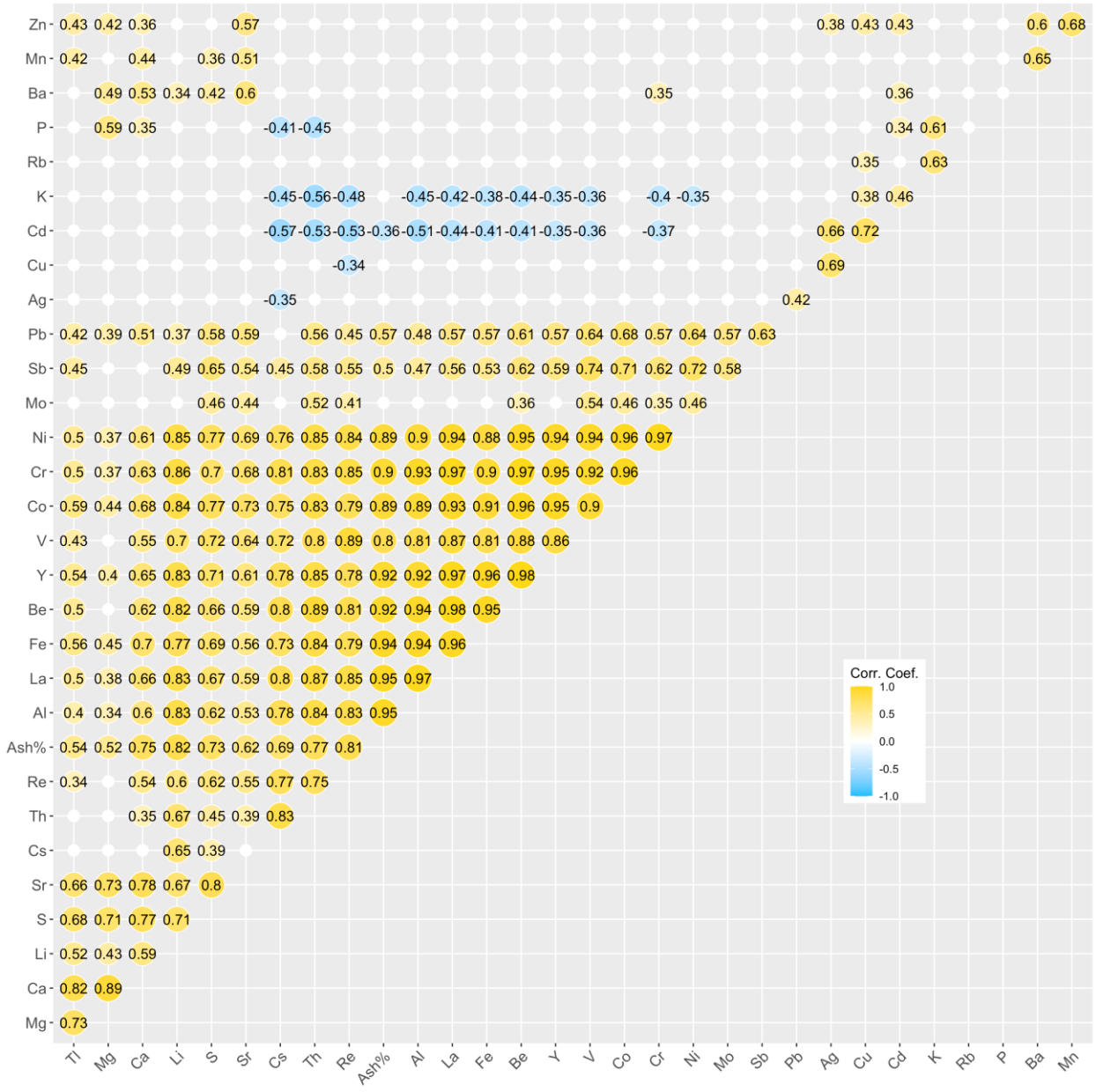

Fig. S15. Correlogram of element concentrations in Acid Soluble Ash (**ASA**) and ash content of fall 2015 *Sphagnum* mosses based on the Spearman rank-based correlation test. Sites EINP and WAG were excluded. Corr. Coef. = Correlation coefficient. Significance level = 0.05. Only significant correlations are presented.

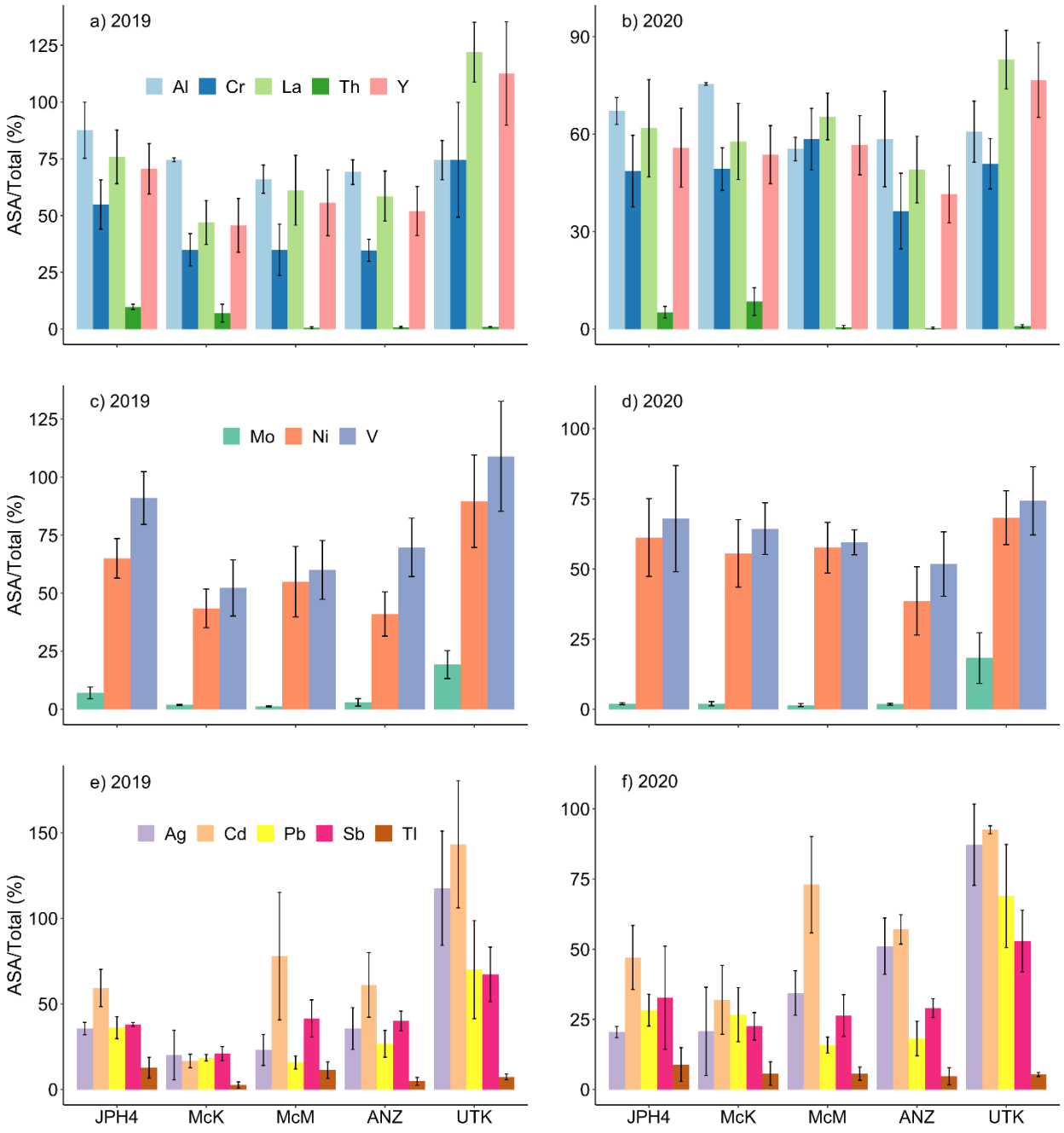

Fig. S16. Proportion of acid soluble to total concentration of trace elements in *Sphagnum* mosses collected in fall 2019 (a, c, & e) and 2020 (b, d, & f). ASA = Acid Soluble Ash. McK = Fort Mackay, McM = Fort McMurray, ANZ = Anzac, UTK = Utikuma.

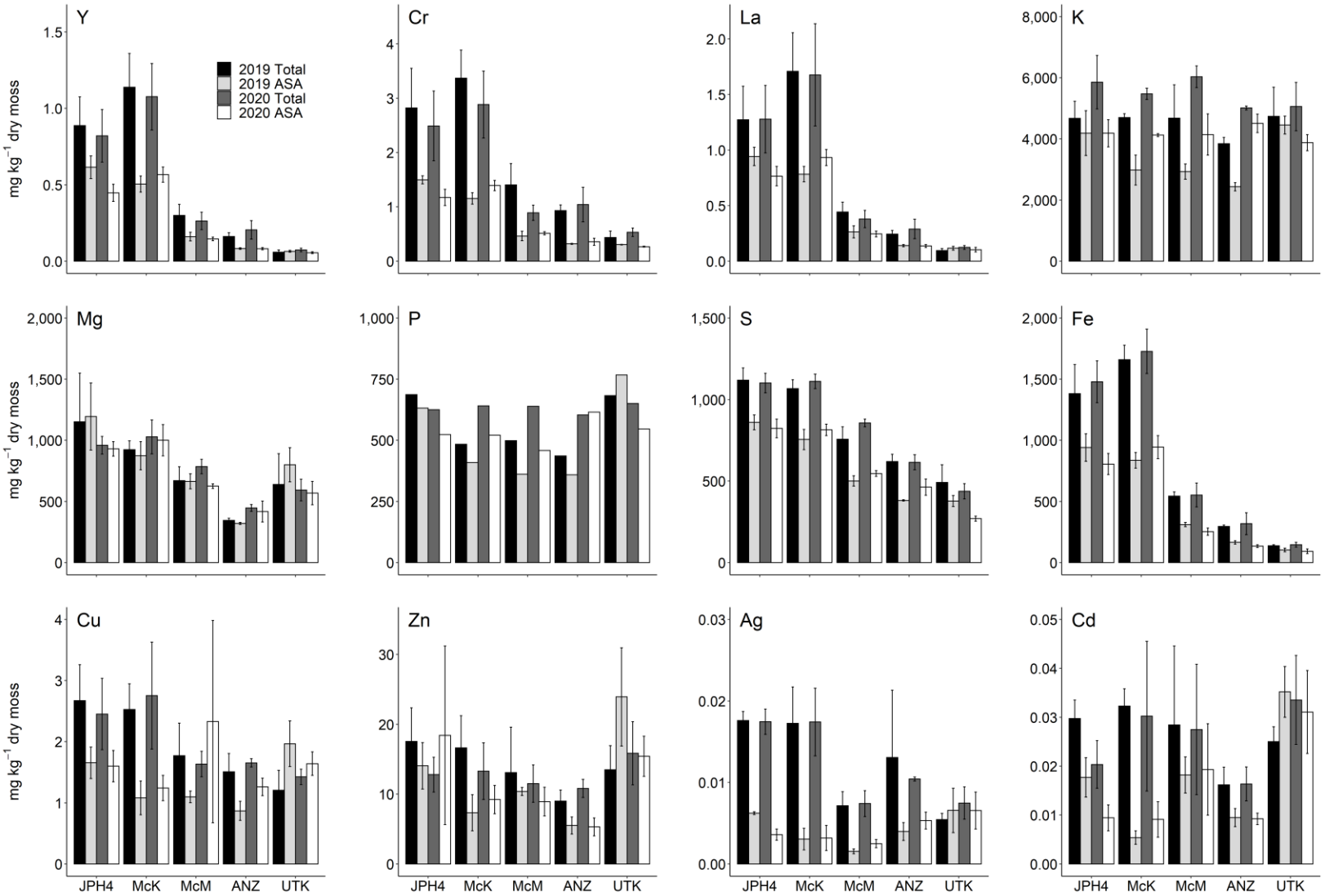

Fig. S17. Total and acid soluble concentrations (mg kg^{-1} dry moss) of conservative lithophile elements (Y, Cr, La), essential elements (K, Mg, P, S, Fe, Cu, Zn), and potentially toxic elements (Ag, Cd) in *Sphagnum* mosses collected in fall 2019 and 2020. ASA = Acid Soluble Ash. McK = Fort Mackay, McM = Fort McMurray, ANZ = Anzac, UTK = Utikuma.

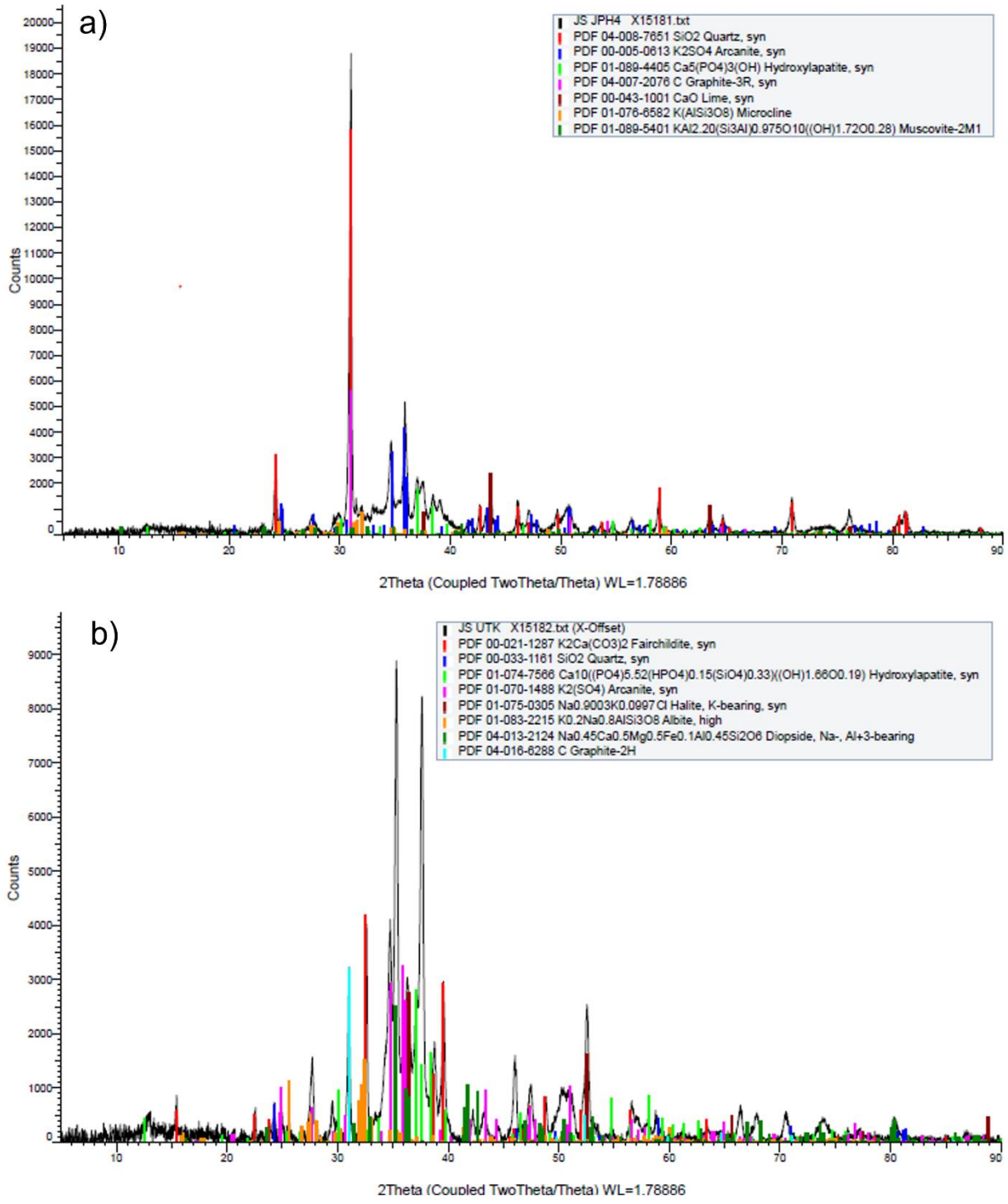

Fig. S18. X-ray diffraction (XRD) analysis of a) JPH4 and b) UTK ash samples. UTK = Utikuma.

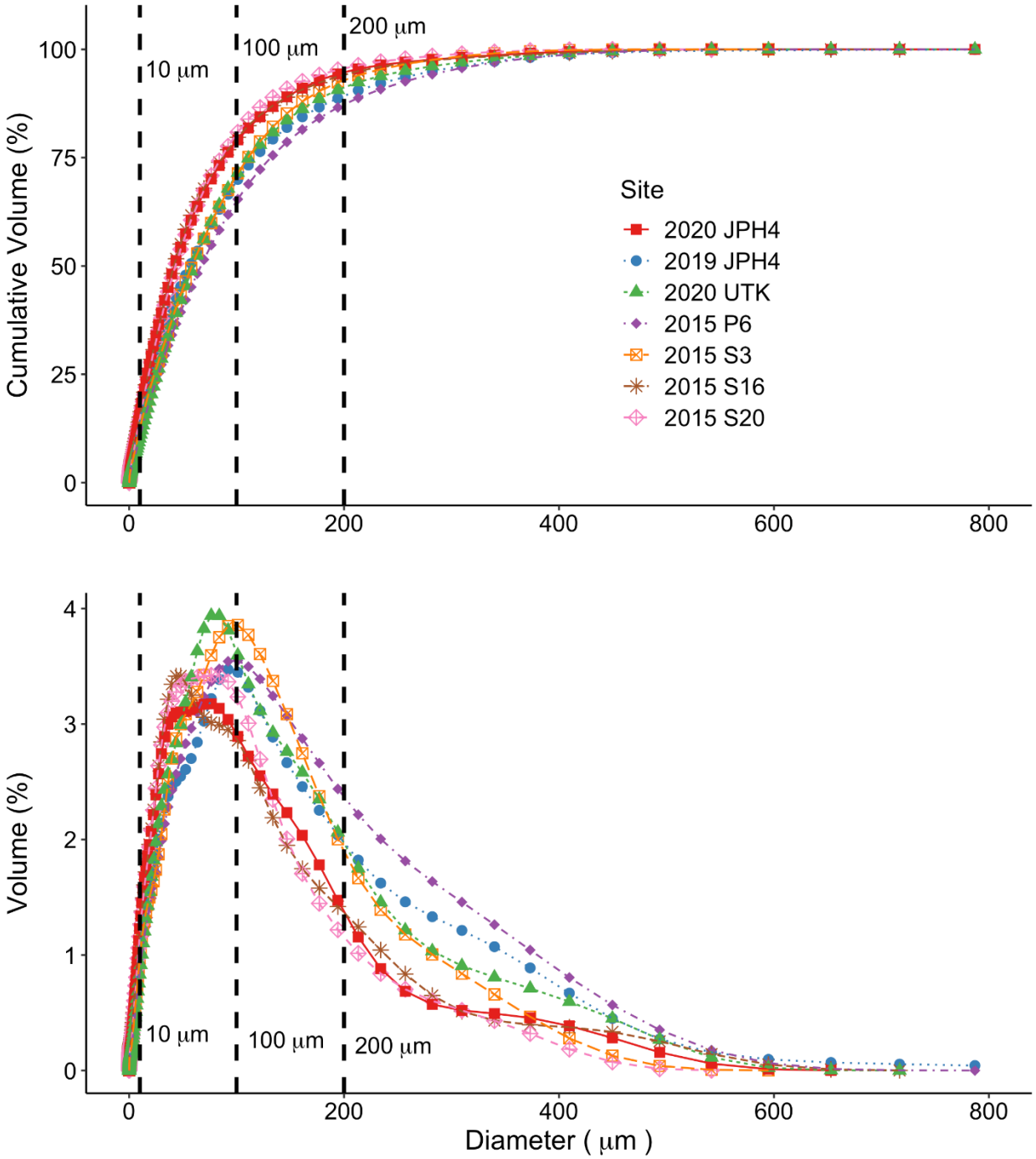

Fig. S19. Particle size distribution of ash samples of *Sphagnum* mosses by laser diffraction. UTK = Utikuma.

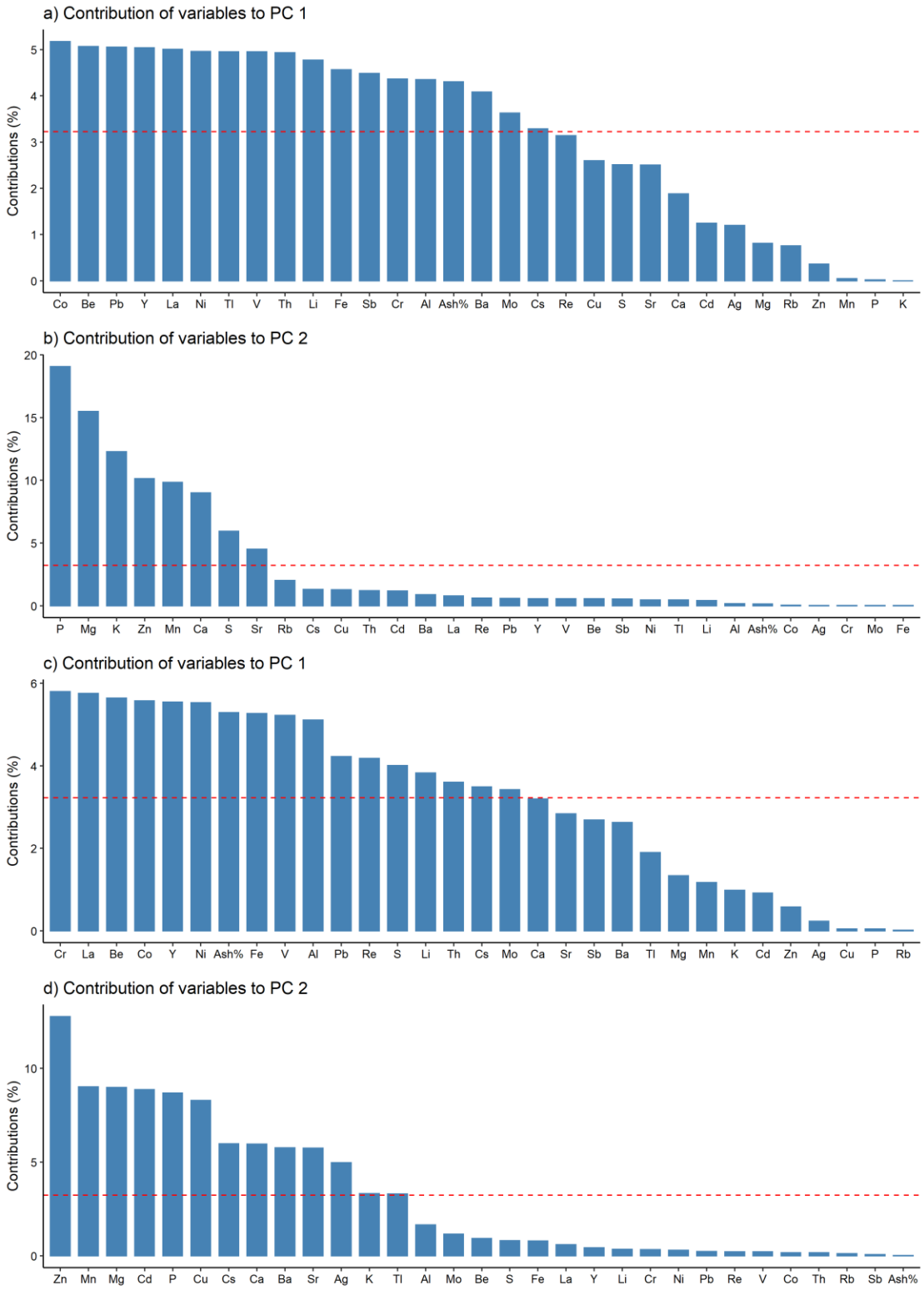

Fig. S20. Contributions of variables in accounting for the variability in principal component (PC) 1 and PC 2 from principal component analysis of fall 2015 *Sphagnum* mosses using total concentrations (a, b) and acid soluble concentrations (c, d). The red dashed line indicates the average contribution.

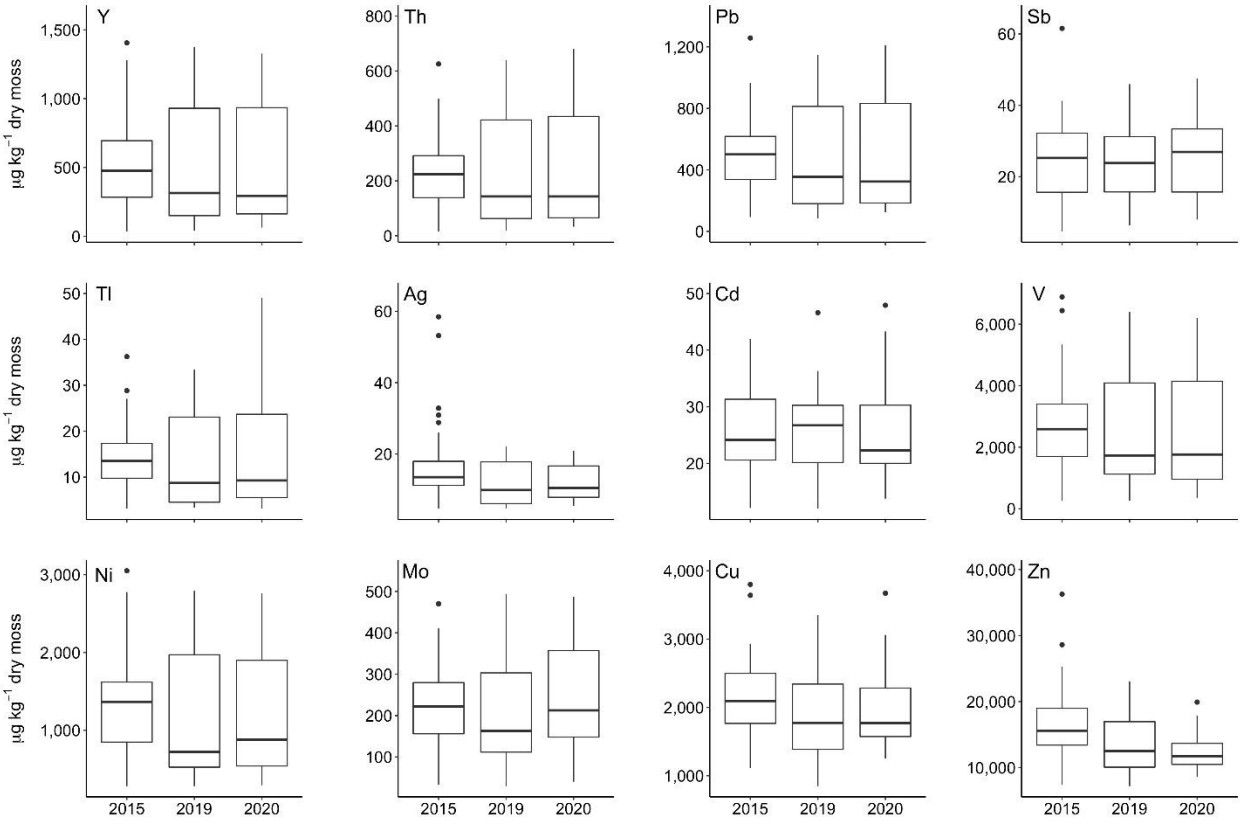

Fig. S21. Temporal trends of **total** concentration (µg kg^{-1} dry moss) of selected elements in *Sphagnum* moss collected in fall 2015 (sites EINP and WAG were excluded), 2019, and 2020. Boxplots show the range, 25th and 75th percentiles, and median for each element.

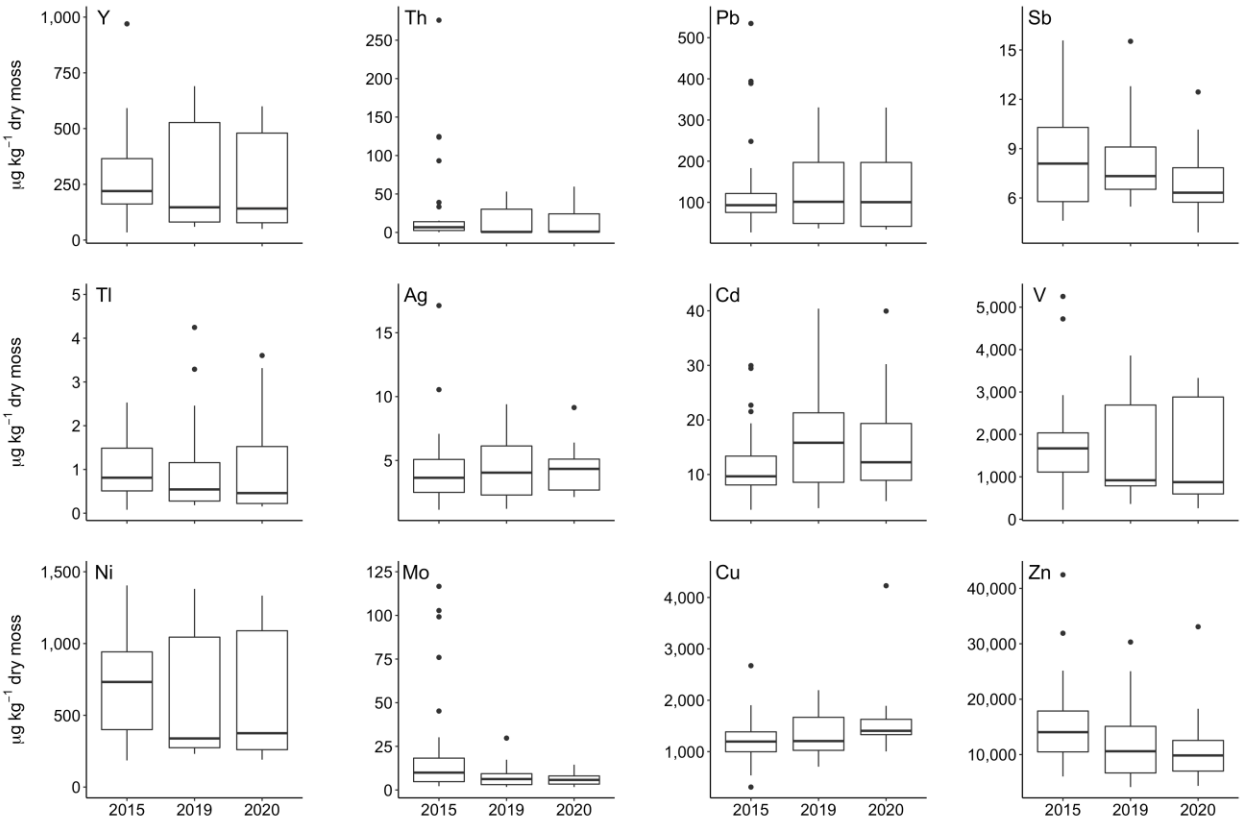

Fig. S22. Temporal trends of trace element concentration (µg kg^{-1} dry moss) in the Acid Soluble Ash (**ASA**) fraction of *Sphagnum* moss collected in fall 2015 (sites EINP and WAG were excluded), 2019, and 2020. Boxplots show the range, 25th and 75th percentiles, and median for each element.

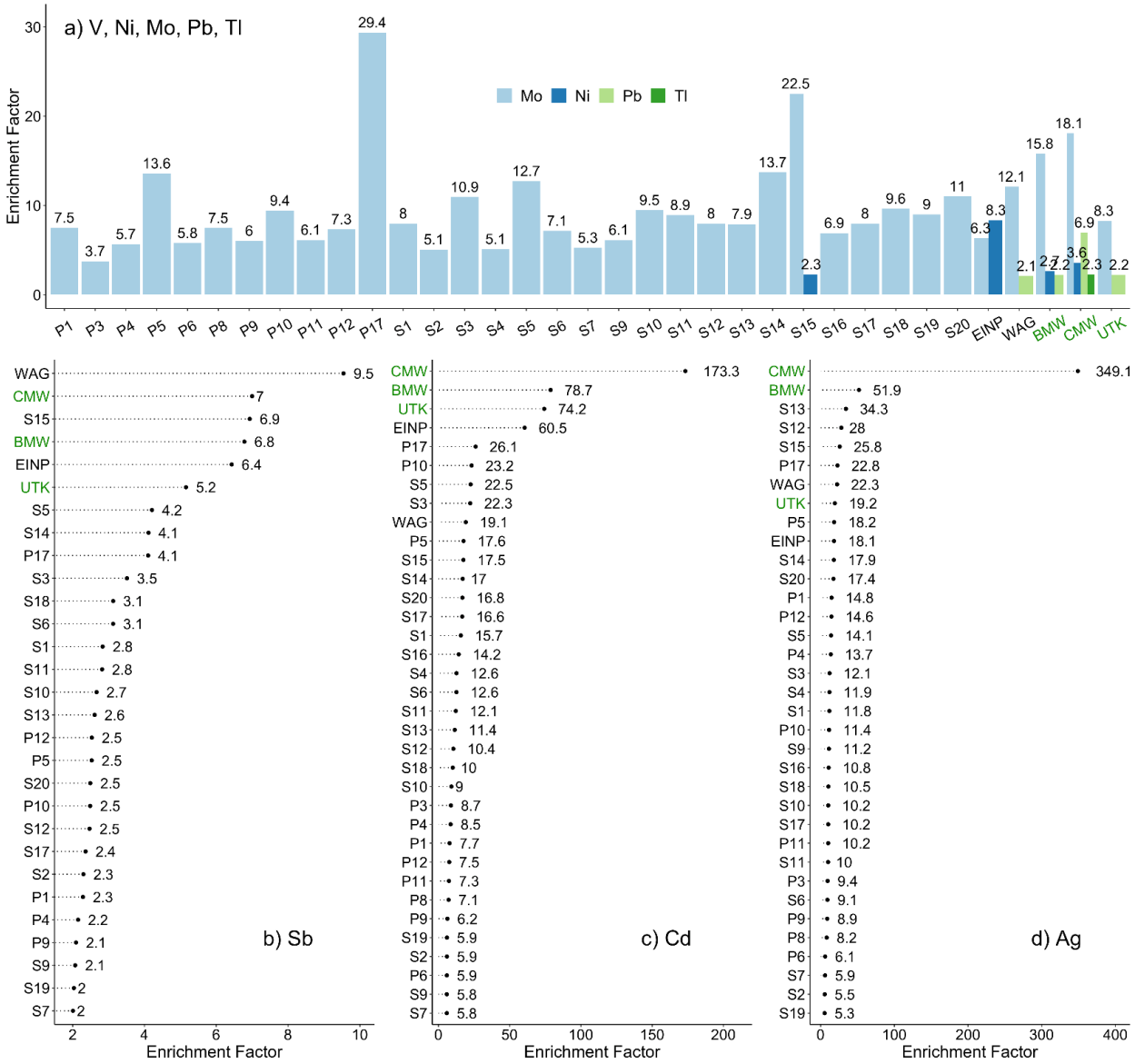

Fig. S23. Enrichment factors using **Y** as the reference element with values greater than 2 of a) V, Ni, Mo, Pb, Tl, b) Sb, c) Ag, and d) Cd of *Sphagnum* mosses collected in fall 2015. Enrichment factors of V were all below 2 and are not shown in the plot. CMW = Caribou Mountains Wildland, BMW = Birch Mountains Wildland, UTK = Utikuma, WAG = Wagner Natural Area, EINP = Elk Island National Park.

References

(1) Rudnick, R. L.; Gao, S. Composition of the continental crust. In *Treatise on Geochemistry,* 2nd ed.; Holland, H., Turekian, K., Eds.; Elsevier, 2014; pp 1–51. DOI: 10.1016/B978-0-08-095975-7.00301-6.

(2) R Core Team. *R: A language and environment for statistical computing*; R Foundation for Statistical Computing, 2021. https://www.r-project.org/.

(3) Carslaw, D. C.; Ropkins, K. openair - An R package for air quality data analysis. *Environ. Model. Softw.* **2012**, *27-28* (0), 52–61. DOI: 10.1016/j.envsoft.2011.09.008.

(4) Mullan-Boudreau, G.; Belland, R.; Devito, K.; Noernberg, T.; Pelletier, R.; Shotyk, W. *Sphagnum* moss as an indicator of contemporary rates of atmospheric dust deposition in the Athabasca Bituminous Sands Region. *Environ. Sci. Technol.* **2017**, *51* (13), 7422–7431. DOI: 10.1021/acs.est.6b06195.

Supporting Information 2

List of Tables

Table S1. Limit of detection (LOD), limit of quantification (LOQ), standard reference materials (SRMs) recoveries for total concentrations analyzed using ICP-MS……93

Table S2. Limit of detection (LOD), limit of quantification (LOQ), and standard reference materials (SRMs) recoveries for concentrations in acid soluble ash (ASA) analyzed using ICP-MS……..96

Table S3. Limit of detection (LOD), limit of quantification (LOQ), and standard reference materials (SRMs) recoveries for total concentrations analyzed using ICP-OES……98

Table S4. Limit of detection (LOD), limit of quantification (LOQ), and standard reference materials (SRM) recoveries for concentrations in acid soluble ash (ASA) analyzed using ICP-OES……99

Table S1. Limit of detection (LOD), limit of quantification (LOQ), standard reference materials (SRMs) recoveries for total concentrations analyzed using ICP-MS.

			NIST 1643f Freshwater				
	LOD	LOQ	Certified value	Measured value*10 (mean, n=7)	Recovery	Measured value*100 (mean, n=7)	Recovery
	µg/L	µg/L	µg/L	µg/L	%	µg/L	%
Ag	0.000	0.001	0.9703	0.90	93	0.94	96
As	0.002	0.008	57.42	54.21	94	54.18	94
Ba	0.001	0.004	518.2	492.39	95	513.15	99
Be	0.000	0.002	13.67	12.35	90	12.85	94
Cd	0.000	0.001	5.89	5.61	95	5.75	98
Ce	0.000	0.000					
Co	0.000	0.000	25.3	23.20	92	23.61	93
Cr	0.000	0.006	18.5	16.52	89	18.18	98
Cs	0.000	0.000					
Cu	0.001	0.010	21.66	19.21	89	21.00	97
Dy	0.000	0.000					
Er	0.000	0.000					
Eu	0.000	0.000					
Fe	0.014	0.066	93.44	88.77	95	94.62	101
Ga	0.000	0.001					
Gd	0.000	0.000					
Ho	0.000	0.000					
La	0.000	0.000					
Li	0.000	0.002	16.59	14.72	89	15.69	95
Lu	0.000	0.000					
Mn	0.001	0.003	37.14	40.98	110	42.96	116
Mo	0.000	0.001	115.3	102.31	89	105.62	92
Nd	0.000	0.000					
Ni	0.002	0.025	59.8	54.50	91	55.71	93
Pb	0.000	0.000	18.488	16.77	91	17.87	97
Pr	0.000	0.000					
Rb	0.000	0.001	12.64	12.01	95	12.26	97
Re	0.000	0.000					
Sb	0.002	0.009	55.45	57.62	104	58.76	106
Se	0.024	0.112	11.7	11.02	94	11.30	97
Sm	0.000	0.000					
Sr	0.001	0.004	314	300.11	96	312.11	99
Tb	0.000	0.000					
Th	0.000	0.000					
Tl	0.000	0.000	6.892	6.16	89	6.52	95
Tm	0.000	0.000					
U	0.000	0.000					
V	0.000	0.001	36.07	33.33	92	34.59	96
Y	0.000	0.000					
Yb	0.000	0.000					
Zn	0.007	0.056	74.4	71.16	96	71.86	97

Note: NIST = National Institute of Standards and Technology; SPS = Spectrapure Standards AS; FFRI = Finnish Forest Research Institute.

Table S1. Limit of detection (LOD), limit of quantification (LOQ), and standard reference materials (SRMs) recoveries for total concentrations analyzed using ICP-MS (continued).

	SPS-SW2 Surface Water				
	Certified value	Measured value*10 (mean, n=7)	Recovery	Measured value*100 (mean, n=7)	Recovery
	µg/L	µg/L	%	µg/L	%
Ag					
As	50	46.33	93	46.98	94
Ba	250	238.97	96	243.74	97
Be					
Cd	2.5	2.44	98	2.37	95
Ce	2.5	2.44	98	2.48	99
Co	10	9.17	92	9.11	91
Cr	10	9.03	90	9.12	91
Cs					
Cu	100	91.80	92	92.87	93
Dy	2.5	2.44	98	2.43	97
Er	2.5	2.42	97	2.43	97
Eu	2.5	2.43	97	2.43	97
Fe	100	93.99	94	92.43	92
Ga					
Gd	2.5	2.44	98	2.40	96
Ho	2.5	2.42	97	2.47	99
La	2.5	2.41	96	2.39	96
Li					
Lu	2.5	2.38	95	2.38	95
Mn	50	56.65	113	57.10	114
Mo	50	44.14	88	45.02	90
Nd	2.5	2.43	97	2.44	98
Ni	50	46.27	93	46.58	93
Pb	25	22.88	92	22.93	92
Pr	2.5	2.43	97	2.44	98
Rb	50	47.26	95	45.91	92
Re					
Sb					
Se	10	12.44	124	13.95	140
Sm	2.5	2.55	102	2.51	101
Sr	250	238.96	96	244.14	98
Tb	2.5	2.49	99	2.47	99
Th	2.5	2.36	94	2.30	92
Tl	2.5	2.28	91	2.30	92
Tm	2.5	2.44	98	2.45	98
U	2.5	2.35	94	2.52	101
V	50	46.44	93	46.91	94
Y	2.5	2.39	96	2.33	93
Yb	2.5	2.37	95	2.37	95
Zn	100	96.22	96	91.59	92

Note: FFRI = Finnish Forest Research Institute; NIST = National Institute of Standards and Technology; SPS = Spectrapure Standards AS.

Table S1. Limit of detection (LOD), limit of quantification (LOQ), and standard reference materials (SRMs) recoveries for total concentrations analyzed using ICP-MS (continued).

	NIST 1515 Apple Leaves			FFRI-Moss-1343		
	Certified value	Measured value/(10*mass) (mean, n=6)	Recovery	Recommended value	Measured value/(10*mass) (mean, n=6)	Recovery
	µg/g	µg/g	%	µg/g	µg/g	%
Ag				0.027	0.02	85
As				0.105	0.77	732
Ba	48.8	49.36	101	13.7	14.06	103
Be						
Cd	0.0132	0.01	113	0.106	0.12	112
Ce	3	3.35	112	0.25	0.27	108
Co	0.09	0.10	114	0.115	0.11	94
Cr	0.3	0.36	120	0.67	0.74	110
Cs				0.189	0.18	94
Cu	5.69	5.77	101	3.76	3.45	92
Dy						
Er						
Eu	0.2	0.26	132			
Fe	82.7	89.40	108	138	166.28	120
Ga				0.084	0.12	140
Gd	3	3.16	105			
Ho						
La	20	21.13	106	0.131	0.14	106
Li						
Lu						
Mn	54.1	62.41	115	535	565.66	106
Mo	0.095	0.10	101	0.1	0.06	56
Nd	17	16.99	100			
Ni	0.936	1.05	112	0.95	1.07	112
Pb	0.47	0.41	87	3.33	3.54	
Pr						
Rb	10.2	9.93	97	19.5	18.80	96
Re						
Sb	0.013	0.02	125	0.052	0.05	102
Se				0.115	0.13	115
Sm	3	3.06	102			
Sr	25.1	26.62	106	4.64	4.70	101
Tb	0.4	0.39	98			
Th	0.03	0.03	93	0.027	0.03	
Tl				0.085	0.05	
Tm						
U	0.006	0.01	141	0.085	0.02	
V	0.254	0.24	93	1.19	1.18	99
Y				0.067	0.08	117
Yb	0.3	0.19	65			
Zn	12.45	14.96	120	25.4	28.01	110

Note: NIST = National Institute of Standards and Technology; SPS = Spectrapure Standards AS; FFRI = Finnish Forest Research Institute.

Table S2. Limit of detection (LOD), limit of quantification (LOQ), and standard reference materials (SRMs) recoveries for concentrations in acid soluble ash (ASA) analyzed using ICP-MS.

			NIST 1643f Freshwater				
	LOD	LOQ	Certified value	Measured value*10 (mean, n=7)	Recovery	Measured value*100 (mean, n=7)	Recovery
	µg/L	µg/L	µg/L	µg/L	%	µg/L	%
Ag	0.000	0.000	0.9703	0.96	99	1.01	104
As	0.003	0.011	57.42	57.15	100	58.50	102
Ba	0.000	0.003	518.2	500.35	97	524.34	101
Be	0.000	0.001	13.67	13.51	99	13.69	100
Cd	0.000	0.000	5.89	5.79	98	6.10	104
Ce	0.000	0.000					
Co	0.000	0.000	25.3	25.70	102	26.50	105
Cr	0.001	0.007	18.5	18.19	98	19.28	104
Cs	0.000	0.000					
Cu	0.003	0.020	21.66	22.55	104	25.10	116
Dy	0.000	0.000					
Er	0.000	0.000					
Eu	0.000	0.000					
Fe	0.004	0.033	93.44	97.76	105	102.02	109
Ga	0.000	0.001					
Gd	0.000	0.000					
Ho	0.000	0.000					
La	0.000	0.000					
Li	0.000	0.002	16.59	16.45	99	16.91	102
Lu	0.000	0.000					
Mn	0.001	0.005	37.14	35.56	96	39.35	106
Mo	0.000	0.001	115.3	118.38	103	122.33	106
Nd	0.000	0.000					
Ni	0.002	0.014	59.8	60.58	101	62.55	105
Pb	0.000	0.001	18.488	17.80	96	19.37	105
Pr	0.000	0.000					
Rb	0.000	0.002	12.64	12.54	99	12.58	100
Re	0.000	0.000					
Sb	0.000	0.001	55.45	53.62	97	56.23	101
Se	0.007	0.043	11.7	12.07	103	12.69	108
Sm	0.000	0.000					
Sr	0.001	0.004	314	314.66	100	326.28	104
Tb	0.000	0.000					
Th	0.000	0.000					
Tl	0.000	0.000	6.892	6.57	95	7.05	102
Tm	0.000	0.000					
U	0.000	0.000					
V	0.000	0.001	36.07	35.18	98	36.98	103
Y	0.000	0.000					
Yb	0.000	0.000					
Zn	0.011	0.102	74.4	79.14	106	88.55	119

Note: NIST = National Institute of Standards and Technology; SPS = Spectrapure Standards AS.

Table S2. Limit of detection (LOD), limit of quantification (LOQ), and standard reference materials (SRMs) recoveries for concentrations in acid soluble ash (ASA) analyzed using ICP-MS (Continued).

	SPS-SW2 Surface Water				
	Certified value	Measured value*10 (mean, n=7)	Recovery	Measured value*100 (mean, n=7)	Recovery
	µg/L	µg/L	%	µg/L	%
Ag					
As	50	49.84	100	52.11	104
Ba	250	241.90	97	245.86	98
Be					
Cd	2.5	2.49	99	2.52	101
Ce	2.5	2.65	106	2.67	107
Co	10	10.16	102	10.13	101
Cr	10	9.93	99	10.42	104
Cs					
Cu	100	107.54	108	129.90	130
Dy	2.5	2.57	103	2.54	102
Er	2.5	2.59	104	2.62	105
Eu	2.5	2.59	104	2.58	103
Fe	100	104.11	104	107.16	107
Ga					
Gd	2.5	2.59	104	2.56	102
Ho	2.5	2.54	101	2.51	100
La	2.5	2.58	103	2.57	103
Li					
Lu	2.5	2.51	100	2.45	98
Mn	50	49.58	99	56.39	113
Mo	50	50.41	101	52.09	104
Nd	2.5	2.60	104	2.56	102
Ni	50	51.54	103	51.46	103
Pb	25	24.27	97	24.14	97
Pr	2.5	2.60	104	2.60	104
Rb	50	47.81	96	46.77	94
Re					
Sb					
Se	10	15.25	152	18.79	188
Sm	2.5	2.70	108	2.65	106
Sr	250	246.44	99	252.29	101
Tb	2.5	2.57	103	2.54	102
Th	2.5	2.59	104	2.51	100
Tl	2.5	2.42	97	2.40	96
Tm	2.5	2.55	102	2.55	102
U	2.5	2.46	98	2.58	103
V	50	48.78	98	48.89	98
Y	2.5	2.70	108	2.66	107
Yb	2.5	2.53	101	2.53	101
Zn	100	120.76	121	133.52	134

Note: NIST = National Institute of Standards and Technology; SPS = Spectrapure Standards AS.

Table S3. Limit of detection (LOD), limit of quantification (LOQ), and standard reference materials (SRMs) recoveries for total concentrations analyzed using ICP-OES.

			NIST 1515 Apple Leaves			**FFRI-Moss-1343**		
	LOD	LOQ	Certified value	Measured value*100/mass (mean, n=6)	Recovery	Recommended value	Measured value*100/mass (mean, n=6)	Recovery
	mg/L	mg/L	mg/kg	mg/kg	%	mg/kg	mg/kg	%
Al	0.004	0.013	284.5	231.77	81	169	223.55	132
Ca	0.004	0.012	15250	12659.43	83	1920	1828.32	95
Cu	0.007	0.012	5.69	<LOD		3.76	<LOD	
Fe	0.001	0.005	82.7	68.84	83	138	150.00	109
K	0.083	0.264	16080	13668.42	85	4510	4705.24	104
Mg	0.005	0.018	2710	2336.76	86	755	719.03	95
Mn	0.001	0.001	54.1	50.66	94	535	466.44	87
P	0.012	0.035	1593	1363.88	86	1050	911.29	87
S	0.009	0.012		1632.74		830	789.60	95
Zn	0.004	0.013	12.45	<LOD		25.4	21.43	84

Note: NIST = National Institute of Standards and Technology; NRCC = National Research Council of Canada.

Table S4. Limit of detection (LOD), limit of quantification (LOQ), and standard reference materials (SRM) recoveries for concentrations in acid soluble ash (ASA) analyzed using ICP-OES.

			NIST 1643f Freshwater			**NRCC SLRS-6 River Water**		
	LOD	LOQ	Certified value	Measured value*10 (mean, n=3)	Recovery	Certified value	Measured value*10 (mean, n=3)	Recovery
	mg/L	mg/L	mg/L	mg/L	%	mg/L	mg/L	%
Al	0.004	0.013	0.1325	0.15	109	0.0338		
Ca	0.004	0.012	29.14	28.48	98	8.76	8.33	95
Cu	0.007	0.012	0.02144			0.0239		
Fe	0.001	0.005	0.09251	0.10	105	0.0843	0.09	101
K	0.083	0.264	1.9133	1.84	96	0.651		
Mg	0.005	0.018	7.38	7.63	103	2.133	2.19	103
Mn	0.001	0.001	0.03677	0.04	109	0.00212		
P	0.012	0.035						
S	0.009	0.012					1.76	
Zn	0.004	0.013	0.0737	0.08	102	0.00176		

Note: NIST = National Institute of Standards and Technology; NRCC = National Research Council of Canada.

CHAPTER 3. SUMMARY AND CONCLUSIONS

Mineral dust inputs, reflected by the ash content of *Sphagnum* moss, increased with decreasing distance towards industry. The elements enriched in bitumen (V, Ni, Mo) and potentially toxic elements (Pb, Sb, Tl) also exhibited obvious increasing trends towards industry, resembling that of the conservative lithophiles (Al, Th, Y, La, Cr) and correlated strongly with them. This reflects the role of mineral dusts (coarse aerosols) in their increasing total concentration. Acid soluble concentrations of these elements (except for Mo) also showed obvious or slight increasing trends and correlated strongly or moderately with acid soluble Y. The ultrafine clay minerals (<0.45 μm, e.g., kaolinite, illite) might largely contribute to the increasing total concentrations of Al, Y, V, and Ni, which leads to their high acid soluble proportions. Larger size minerals (coarse aerosols) such as feldspars and heavy minerals (e.g., monazite, zircon) from bituminous sands might largely contribute to the increasing total concentrations of Th, Mo, Pb, Sb, and Tl which exhibited low acid soluble proportions. Silver and Cd did not exhibit strong positive correlations with the conservative lithophile elements, with their acid soluble fractions behaving more like the micronutrients such as Cu and Zn.

The above results were supported by the calculated enrichments of TEs, particle size distribution, XRD, and PCA. For both the total and acid soluble concentrations, only the essential elements Cu, Mn, Mo, and Zn, as well as Ag, Cd, Rb, and Re which are chemically akin to the micronutrients, were signifciantly enriched (enrichments over 2) compared to the UCC. The particle size analysis of selected ashed moss samples both close to and away from industry showed that the volume of particles deposited on moss increased remarkably from a diameter of 10 to 100 μm, then slightly to 200 μm, before levelling off. This indicates the presence of a large proportion of coarse particles. The XRD analysis demonstrated the predominance of quartz in JPH4 (66.7%),

which was within the reported quartz content of 60–90% in the mineral fraction of the ABS. This also explains the low addition of TEs in moss close to industry. The PCA for total concentrations of 2015 mosses showed that the conservative lithophile elements (Y, La, Th, Cr, Al), potentially toxic elements (Pb, Tl, Sb), elements enriched in bitumen (V, Ni, Mo) were clustered and contributed greatly to principal component 1 (60.0%), while the macro- and micronutrients contributed the most to principal component 2 (12.3%). The PCA for the acid soluble concentrations showed that V and Ni were also closely tied with the conservative lithophile elements (Al, Y, Cr, La), and contributed largely to PC1 (52.4%), while Ag and Cd were associated with the essential elements and contributed the most to PC2 (15.3%).

The study highlights the importance and necessity to determine not only the total concentration but also the chemical reactivity of TEs in atmospheric dusts when evaluating their associated health risks to living organisms.

BIBLIOGRAPHY

Aboal, J.R., Couto, J.A., Fernández, J.A., Carballeira, A., 2006. Definition and number of subsamples for using mosses as biomonitors of airborne trace elements. Arch. Environ. Contam. Toxicol. 50 (1), 88–96. doi:10.1007/s00244-005-7006-9.

Alberta Energy Regulator, 2021. Crude Bitumen Production. https://www.aer.ca/providing-information/data-and-reports/statistical-reports/st98/crude-bitumen/production.

Al-Radady, A.S., Davies, B.E., French, M.J., 1993. A new design of moss bag to monitor metal deposition both indoors and outdoors. Sci. Total. Environ. 133 (3), 275–283. doi:10.1016/0048-9697(93)90249-6.

Amodio, M., Catino, S., Dambruoso, P.R., Gennaro, G. de, Di Gilio, A., Giungato, P., Laiola, E., Marzocca, A., Mazzone, A., Sardaro, A., Tutino, M., 2014. Atmospheric deposition: Sampling procedures, analytical methods, and main recent findings from the scientific literature. Adv. Meteorol. 2014, 1–27. doi:10.1155/2014/161730.

Anderson, W.G., 1986. Wettability Literature Survey- Part 1: Rock/Oil/Brine Interactions and the Effects of Core Handling on Wettability. J. Pet. Technol. 38 (10), 1125–1144. doi:10.2118/13932-PA.

Anić, M., Frontasyeva, M.V., Tomašević, M., Popović, A., 2007. Assessment of atmospheric deposition of heavy metals and other elements in Belgrade using the moss biomonitoring technique and neutron activation analysis. Environ. Monit. Assess. 129 (1-3), 207–219. doi:10.1007/s10661-006-9354-y.

Anić, M., Tasić, M., Frontasyeva, M.V., Tomašević, M., Rajsić, S., Mijić, Z., Popović, A., 2009. Active moss biomonitoring of trace elements with *Sphagnum girgensohnii* moss bags in relation to atmospheric bulk deposition in Belgrade, Serbia. Environ. Pollut. 157 (2), 673–679. doi:10.1016/j.envpol.2008.08.003.

Archibold, O.W., Crisp, P.T., 1983. The distribution of airborne metals in the Illawarra region of New South Wales, Australia. Appl. Geogr. 3 (4), 331–344. doi:10.1016/0143-6228(83)90049-8.

Barbieri, M., 2016. The importance of enrichment factor (EF) and geoaccumulation index (Igeo) to evaluate the soil contamination. J. Geol. Geophys. 5 (1). doi:10.4172/2381-8719.1000237.

Barwise, A.J.G., 1990. Role of nickel and vanadium in petroleum classification. Energy Fuels 4 (6), 647–652. doi:10.1021/ef00024a005.

Berg, T., Røyset, O., Steinnes, E., 1995. Moss (*Hylocomium splendens*) used as biomonitor of atmospheric trace element deposition: Estimation of uptake efficiencies. Atmos. Environ. 29 (3), 353–360. doi:10.1016/1352-2310(94)00259-N.

Berg, T., Steinnes, E., 1997a. Recent trends in atmospheric deposition of trace elements in Norway as evident from the 1995 moss survey. Sci. Total Environ. 208 (3), 197–206. doi:10.1016/S0048-9697(97)00253-2.

Berg, T., Steinnes, E., 1997b. Use of mosses (*Hylocomium splendens* and *Pleurozium schreberi*) as biomonitors of heavy metal deposition: From relative to absolute deposition values. Environ. Pollut. 98 (1), 61–71. doi:10.1016/S0269-7491(97)00103-6.

Berkowitz, N., Speight, J.G., 1975. The oil sands of Alberta. Fuel 54 (3), 138–149. doi:10.1016/0016-2361(75)90001-0.

Bicalho, B., Grant-Weaver, I., Sinn, C., Donner, M.W., Woodland, S., Pearson, G., Larter, S., Duke, J., Shotyk, W., 2017. Determination of ultratrace (<0.1 mg/kg) elements in Athabasca

Bituminous Sands mineral and bitumen fractions using inductively coupled plasma sector field mass spectrometry (ICP-SFMS). Fuel 206, 248–257. doi:10.1016/j.fuel.2017.05.095.

Bichard, J.A., 1987. Oil sands composition and behaviour research: The research papers of John A. Bichard, 1957-1965. Alberta Oil Sands Technology and Research Authority, Edmonton Alta. Canada, 1 v. (various pagings).

Breiter, K., Ackerman, L., Ďurišova, J., Svojtka, M., Novák, M., 2014. Trace element composition of quartz from different types of pegmatites: A case study from the Moldanubian Zone of the Bohemian Massif (Czech Republic). Mineral. Mag. 78 (3), 703–722. doi:10.1180/minmag.2014.078.3.17.

Brown, D.H., Bates, J.W., 1972. Uptake of lead by two populations of *Grimmia doniana*. J. Bryol. 7 (2), 187–193. doi:10.1179/jbr.1972.7.2.187.

Brzóska, M., Moniuszko-Jakoniuk, J., 2001. Interactions between cadmium and zinc in the organism. Food Chem. Toxicol. 39 (10), 967–980. doi:10.1016/S0278-6915(01)00048-5.

Cao, M., Gan, W., Liu, Q., 2007. Effect of hydrolyzable metal cations on the coagulation between hexadecane and mineral particles. J. Colloid Interface Sci. 310 (2), 489–497. doi:10.1016/j.jcis.2007.01.068.

Cao, T., An, L., Wang, M., Lou, Y., Yu, Y., Wu, J., Zhu, Z., Qing, Y., Glime, J., 2008. Spatial and temporal changes of heavy metal concentrations in mosses and its indication to the environments in the past 40 years in the city of Shanghai, China. Atmos. Environ. 42 (21), 5390–5402. doi:10.1016/j.atmosenv.2008.02.052.

Cao, T., Wang, M., An, L., Yu, Y., Lou, Y., Guo, S., Zuo, B., Liu, Y., Wu, J., Cao, Y., Zhu, Z., 2009. Air quality for metals and sulfur in Shanghai, China, determined with moss bags. Environ. Pollut. 157 (4), 1270–1278. doi:10.1016/j.envpol.2008.11.051.

Carslaw, D. C.; Ropkins, K. 2012. openair - An R package for air quality data analysis. *Environ.* Model. Softw., 27-28 (0), 52–61. doi: 10.1016/j.envsoft.2011.09.008.

Castello, M., 2007. A comparison between two moss species used as transplants for airborne trace element biomonitoring in NE Italy. Environ. Monit. Assess. 133 (1-3), 267–276. doi:10.1007/s10661-006-9579-9.

Ceburnis, D., 2000. Conifer needles as biomonitors of atmospheric heavy metal deposition: Comparison with mosses and precipitation, role of the canopy. Atmos. Environ. 34 (25), 4265–4271. doi:10.1016/S1352-2310(00)00213-2.

Čeburnis, D., Valiulis, D., 1999. Investigation of absolute metal uptake efficiency from precipitation in moss. Sci. Total Environ. 226 (2-3), 247–253. doi:10.1016/S0048-9697(98)00399-4.

Champlin, J.B.F., Dunning, H.N., 1960. A geochemical investigation of the Athabasca bituminous sands. Econ. Geol. 55 (4), 797–804. doi:10.2113/gsecongeo.55.4.797.

Chen, X., Houk, R.S., 1995. Polyatomic ions as internal standards for matrix corrections in inductively coupled plasma mass spectrometry. J. Anal. At. Spectrom. 10 (10), 837. doi:10.1039/JA9951000837.

Choudhury, S., Panda, S.K., 2004. Induction of oxidative stress and ultrastructural changes in moss *Taxithelium nepalense* (Schwaegr.) Broth. under lead and arsenic phytotoxicity. Curr. Sci. 87 (3), 342–348.

Clark, K., 1951. Athabasca bituminous sands. Fuel (30), 49–53.

Clark, K.A., Pasternack, D.S., 1932. Hot water seperation of bitumen from Alberta bituminous sand. Ind. Eng. Chem. 24 (12), 1410–1416. doi:10.1021/ie50276a016.

Cloy, J.M., Farmer, J.G., Graham, M.C., MacKenzie, A.B., Cook, G.T., 2005. A comparison of antimony and lead profiles over the past 2500 years in Flanders Moss ombrotrophic peat bog, Scotland. J. Environ. Monit. 7 (12), 1137–1147. doi:10.1039/B510987F.

Clymo, R., 1963. Ion exchange in *Sphagnum* and its relation to bog ecology. Ann. Bot. 27 (2), 309–324. doi:10.1093/oxfordjournals.aob.a083847.

Coe, J.M., Lindberg, S.E., 1987. The morphology and size distribution of atmospheric particles deposited on foliage and inert surfaces. JAPCA 37 (3), 237–243. doi:10.1080/08940630.1987.10466218.

Cooke, C.A., Kirk, J.L., Muir, D.C.G., Wiklund, J.A., Wang, X., Gleason, A., Evans, M.S., 2017. Spatial and temporal patterns in trace element deposition to lakes in the Athabasca oil sands region (Alberta, Canada). Environ. Res. Lett. 12 (12), 124001. doi:10.1088/1748-9326/aa9505.

Coombes, A.J., Lepp, N.W., 1974. The effect of Cu and Zn on the growth of *Marchantia polymorpha* and *Funaria hygrometrica*. Bryologist 77 (3), 447. doi:10.2307/3241616.

Corrin, M.L., Natusch, D.F., 1979. Physical and chemical characteristics of environmental lead, in: Boggess, W.R., Wixson, B.G. (Eds.), Lead in the Environment. Castle House Publications.

Coşkun, M., Frontasyeva, M.V., Steinnes, E., Cotuk, A.Y., Pavlov, S.S., Sazonov, A.S., Cayir, A., Belivermis, M., 2005. Atmospheric deposition of heavy metals in thrace studied by analysis of moss (*Hypnum cupressiforme*). Bull. Environ. Contam. Toxicol. 74 (1), 201–209. doi:10.1007/s00128-004-0569-8.

Czarnowska, K., Gworek, B., 1992. Heavy metal content of moss from Kampinos National Park in Poland. Environ. Geochem. Health 14 (1), 9–14. doi:10.1007/BF01783620.

Czarnowska, K., Rejement-Grochowska, I., 1974. Concentration of heavy metals - iron, manganese, zinc and copper in mosses. Acta Soc. Bot. Pol. 43 (1).

Damman, A.W.H., 1986. Hydrology, development, and biogeochemistry of ombrogenous peat bogs with special reference to nutrient relocation in a western Newfoundland bog. Can. J. Bot. 64 (2), 384–394. doi:10.1139/b86-055.

Dauvalter, V.A., Kashulin, N., Lehto, J., Jernstrom, J., 2009. Chalcophile elements Hg, Cd, Pb, As in Lake Umbozero, Murmansk Region, Russia. Int. J. Environ. Res. Public Health 3 (3), 411–428.

Davies, B.E., White, H.M., 1981. Environmental pollution by wind blown lead mine waste: A case study in wales, U.K. Sci. Total Environ. 20 (1), 57–74. doi:10.1016/0048-9697(81)90036-X.

Davison, R.L., Natusch, D.F.S., Wallace, J.R., Evans, C.A., 1974. Trace elements in fly ash: Dependence of concentration on particle size. Environ. Sci. Technol. 8 (13), 1107–1113. doi:10.1021/es60098a003.

Delfanti, R., Papucci, C., Benco, C., 1999. Mosses as indicators of radioactivity deposition around a coal-fired power station. Sci. Total Environ. 227 (1), 49–56. doi:10.1016/S0048-9697(98)00410-0.

Dietl, C., Reifenhäuser, W., Peichl, L., 1997. Association of antimony with traffic — occurrence in airborne dust, deposition and accumulation in standardized grass cultures. Sci. Total Environ. 205 (2-3), 235–244. doi:10.1016/S0048-9697(97)00204-0.

Donkor, K.K., Kratochvil, B., Duke, M.J.M., 1996. Estimation of the fines content of Athabasca oil sands using instrumental neutron activation analysis. Can. J. Chem. 74 (4), 583–590. doi:10.1139/v96-062.

Dragović, S., Mihailović, N., 2009. Analysis of mosses and topsoils for detecting sources of heavy metal pollution: multivariate and enrichment factor analysis. Environ. Monit. Assess. 157 (1-4), 383–390. doi:10.1007/s10661-008-0543-8.

Essington, M.E., 2004. Soil and Water Chemistry: An Integrative Approach. CRC Press, Boca Raton, 658 pp.

Feder, W.A., 1978. Plants as bioassay systems for monitoring atmospheric pollutants. Environ. Health Perspect. 27, 139–147. doi:10.1289/ehp.7827139.

Fort, M., Grimalt, J.O., Querol, X., Casas, M., Sunyer, J., 2016. Evaluation of atmospheric inputs as possible sources of antimony in pregnant women from urban areas. Sci. Total Environ. 544, 391–399. doi:10.1016/j.scitotenv.2015.11.095.

Garg, B.D., Cadle, S.H., Mulawa, P.A., Groblicki, P.J., Laroo, C., Parr, G.A., 2000. Brake wear particulate matter emissions. Environ. Sci. Technol. 34 (21), 4463–4469. doi:10.1021/es001108h.

Glooschenko, W.A., Capobianco, J.A., 1978. Metal content of *Sphagnum* mosses from two Northern Canadian bog ecosystems. Water Air Soil Pollut. 10 (2), 215–220. doi:10.1007/BF00464716.

Goel, J., Kadirvelu, K., Rajagopal, C., Kumar Garg, V., 2005. Removal of lead(II) by adsorption using treated granular activated carbon: batch and column studies. J. Hazard. Mater. 125 (1-3), 211–220. doi:10.1016/j.jhazmat.2005.05.032.

Goldich, S.S., 1938. A study in rock-weathering. J. Geol. 46 (1), 17–58. doi:10.1086/624619.

Goldschmidt, V., 1937. The principles of distribution of chemical elements in minerals and rocks. J. Chem. Soc. (0), 655–673.

González, A.G., Pokrovsky, O.S., 2014. Metal adsorption on mosses: Toward a universal adsorption model. J. Colloid Interface Sci. 415, 169–178. doi:10.1016/j.jcis.2013.10.028.

Gosselin, P., Hrudey, S., Naeth, M., Plourde, A., Therrien, R., Van Der Kraak, G., Xu, Z., 2010. Environmental and health impacts of Canada's oil sands industry. Royal Society of Canada, Ottawa, Ontario: The Royal Society of Canada (RSC), 440 pp. https://rsc-src.ca/sites/default/files/RSC%20Oil%20Sands%20Panel%20Main%20Report%20Oct%202012.pdf.

Government of Alberta, 2021. Oil Sands Facts and Statistics. https://www.alberta.ca/oil-sands-facts-and-statistics.aspx.

Graney, J.R., Landis, M.S., Krupa, S., 2012. Coupling lead isotopes and element concentrations in epiphytic lichens to track sources of air emissions in the Athabasca Oil Sands Region, in: Percy, K.E. (Ed.), Alberta Oil Sands, vol. 11. Elsevier, pp. 343–372.

Gray, M.R., 2015. Tutorial on Upgrading of Oilsands Bitumen. University of Alberta, 2015.

Greenwood, N.N., Earnshaw, A., 1997. Chemistry of the Elements, 2nd ed. Butterworth-Heinemann, Oxford.

Hampp, R., Lendzian, K., 1974. Effect of lead ions on chlorophyll synthesis. Naturwissenschaften 61 (5), 218–219. doi:10.1007/BF00599926.

Harmens, H., Buse, A., Buker, P., Norris, D., Mills, G., Williams, B., Reynolds, B., Ashenden, T.W., Ruhling, A., Steinnes, E., 2004. Heavy metal concentrations in European mosses: 2000/2001 survey. J. Atmos. Chem. 49, 425–436.

Harrison, P.R., Rahn, K.A., Dams, R., Robbins, J.A., Winchester, J.W., Brar, S.S., Nelson, D.M., 1971. Areawide trace metal concentrations measured by multielement neutron activation analysis. J. Air Pollut. Control Assoc. 21 (9), 563–570. doi:10.1080/00022470.1971.10469570.

Hepler, L.G., Smith, R.G., 1994. The Alberta oil sands: Industrial procedures for extraction and some recent fundamental research. AOSTRA Technical Publication Series 14. Alberta Oil Sands Technology and Research Authority.

Hill, C.H., Matrone, G., 1970. Chemical parameters in the study of in vivo and in vitro interactions of transition elements. Federation 29 (4), 1474–1481.

Huang, X., Duan, S., Wu, Q., Yu, M., Shabala, S., 2020. Reducing cadmium accumulation in plants: Structure-function relations and tissue-specific operation of transporters in the spotlight. Plants (Basel, Switzerland) 9 (2), 223. doi:10.3390/plants9020223.

Javed, M.B., Cuss, C.W., Grant-Weaver, I., Shotyk, W., 2017. Size-resolved Pb distribution in the Athabasca River shows snowmelt in the bituminous sands region an insignificant source of dissolved Pb. Sci. Rep. 7 (1), 43622. doi:10.1038/srep43622.

Jiang, Y., Fan, M., Hu, R., Zhao, J., Wu, Y., 2018. Mosses are better than leaves of vascular plants in monitoring atmospheric heavy metal pollution in urban areas. Int. J. Environ. Res. Public Health 15 (6). doi:10.3390/ijerph15061105.

Jordaan, S.M., 2012. Land and water impacts of oil sands production in Alberta. Environ. Sci. Technol. 46 (7), 3611–3617. doi:10.1021/es203682m.

Kahle, D., Wickham, H., 2013. ggmap: Spatial visualization with ggplot2. R J. 5 (1), 144–161. https://journal.r-project.org/archive/2013-1/kahle-wickham.pdf.

Kasongo, T., Zhou, Z., Xu, Z., Masliyah, J.H., 2000. Effect of clays and calcium ions on bitumen extraction from Athabasca oil sands using flotation. Can. J. Chem. Eng 78 (4), 674–681. doi:10.1002/cjce.5450780409.

Kassambara, A., 2019. ggcorrplot: Visualization of a Correlation Matrix using 'ggplot2'. Comprehensive R Archive Network (CRAN).

Kassambara, A., Mundt, F., 2020. factoextra: Extract and Visualize the Results of Multivariate Data Analyses]. Comprehensive R Archive Network (CRAN).

Kempter, H., Krachler, M., Shotyk, W., Zaccone, C., 2017. Major and trace elements in *Sphagnum* moss from four southern German bogs, and comparison with available moss monitoring data. Ecol. Indic. 78, 19–25. doi:10.1016/j.ecolind.2017.02.029.

Kosior, G., Frontasyeva, M.V., Ziembik, Z., Zincovscaia, I., Dołhańczuk-Śródka, A., Godzik, B., 2020. The moss biomonitoring method and neutron activation analysis in assessing pollution by trace elements in selected Polish national parks. Arch. Environ. Contam. Toxicol. 79 (3), 310–320. doi:10.1007/s00244-020-00755-6.

Landis, M.S., Pancras, J.P., Graney, J.R., Stevens, R.K., Percy, K.E., Krupa, S., 2012. Receptor modeling of epiphytic lichens to elucidate the sources and spatial distribution of inorganic air pollution in the Athabasca Oil Sands Region, in: Percy, K.E. (Ed.), Alberta Oil Sands, vol. 11. Elsevier, pp. 427–467.

Landis, M.S., Patrick Pancras, J., Graney, J.R., White, E.M., Edgerton, E.S., Legge, A., Percy, K.E., 2017. Source apportionment of ambient fine and coarse particulate matter at the Fort McKay community site, in the Athabasca Oil Sands Region, Alberta, Canada. Sci. Total. Environ. 584-585, 105–117. doi:10.1016/j.scitotenv.2017.01.110.

Landis, M.S., Studabaker, W.B., Patrick Pancras, J., Graney, J.R., Puckett, K., White, E.M., Edgerton, E.S., 2019. Source apportionment of an epiphytic lichen biomonitor to elucidate the sources and spatial distribution of polycyclic aromatic hydrocarbons in the Athabasca Oil Sands Region, Alberta, Canada. Sci. Total. Environ. 654, 1241–1257. doi:10.1016/j.scitotenv.2018.11.131.

Lane, S.D., Martin, E.S., 1980. Further Observations on the Distribution of Lead in Juvenile Roots of Raphanus sativus. Z. Pflanzenphysiol. 97 (2), 145–152. doi:10.1016/S0044-328X(80)80028-6.

Lee, C.S.L., Li, X., Zhang, G., Peng, X., Zhang, L., 2005. Biomonitoring of trace metals in the atmosphere using moss (*Hypnum plumaeforme*) in the Nanling Mountains and the Pearl River Delta, Southern China. Atmos. Environ. 39 (3), 397–407. doi:10.1016/j.atmosenv.2004.09.067.

Lévesque, C.M., 2014. Oil sands process water and tailings pond contaminant transport and fate : Physical, chemical and biological processes.

Liu, J., Xu, Z., Masliyah, J., 2005. Interaction forces in bitumen extraction from oil sands. J. Colloid Interface Sci. 287 (2), 507–520. doi:10.1016/j.jcis.2005.02.037.

Liu, J., Xu, Z., Masliyah, J.H., 2003. Studies on Bitumen−Silica Interaction in Aqueous Solutions by Atomic Force Microscopy. Langmuir 19 (9), 3911–3920. doi:10.1021/la0268092.

Liu, J., Xu, Z., Masliyah, J.H., 2004. Role of fine clays in bitumen extraction from oil sands. AIChE J. 50 (8), 1917–1927. doi:10.1002/aic.10174.

Liu, J., Zhou, Z., Xu, Z., Masliyah, J.H., 2002. Bitumen-clay interactions in aqueous media studied by zeta potential distribution measurement. J. Colloid Interface Sci. 252 (2), 409–418. doi:10.1006/jcis.2002.8471.

Maevskaya, S., Kardash, A., Demkiv, O., 2001. Absorption of cadmium and lead ions by gametophyte of the moss *Plagiomnium undulatum*. Russ. J. Plant Physiol. 48 (6), 820–824.

Malmer, N., 1988. Patterns in the growth and the accumulation of inorganic constituents in the *Sphagnum* cover on ombrotrophic bogs in Scandinavia. Oikos 53 (1), 105. doi:10.2307/3565670.

Maschowski, C., Zangna, M.C., Trouvé, G., Gieré, R., 2016. Bottom ash of trees from Cameroon as fertilizer. Appl. Geochem. 72, 88–96. doi:10.1016/j.apgeochem.2016.07.002.

Masliyah, J.H., Czarnecki, J., Xu, Z., 2011. Handbook on Theory and Practice on Bitumen Recovery from Athabasca Oil Sands: Volume I: Theoretical Basis. University of Alberta Libraries.

Masliyah, J.H., Zhou, Z.J., Xu, Z., Czarnecki, J., Hamza, H., 2004. Understanding water-based bitumen extraction from Athabasca oil sands. Can. J. Chem. Eng 82 (4), 628–654. doi:10.1002/cjce.5450820403.

Mellon, G., 1956. Geology of the McMurray Formation: Part II: Heavy Minerals of the McMurray, Edmonton, AB, CA, 50 pp. https://ags.aer.ca/document/REP/REP_72.pdf.

Moschopedis, S.E., Schulz, K.F., Speight, J.G., Morrison, D.N., 1980. Surface-active materials from Athabasca oil sands. Fuel Process. Technol. 3 (1), 55–61. doi:10.1016/0378-3820(80)90023-5.

Mossop, G.D., 1980. Geology of the Athabasca oil sands. Science 207 (4427), 145–152. doi:10.1126/science.207.4427.145.

Mullan-Boudreau, G., Belland, R., Devito, K., Noernberg, T., Pelletier, R., Shotyk, W., 2017. *Sphagnum* moss as an indicator of contemporary rates of atmospheric dust deposition in the Athabasca Bituminous Sands Region. Environ. Sci. Technol. 51 (13), 7422–7431. doi:10.1021/acs.est.6b06195.

Natusch, D.F.S., Wallace, J.R., Evans, C.A., 1974. Toxic trace elements: Preferential concentration in respirable particles. Science 183 (4121), 202–204. doi:10.1126/science.183.4121.202.

Nriagu, J.O., 1990. Global metal pollution: Poisoning the biosphere? Environ.: Sci. Policy Sustainable Dev. 32 (7), 7–33. doi:10.1080/00139157.1990.9929037.

Oil Sands Magazine, 2020. Bitumen Upgrading Explained. https://www.oilsandsmagazine.com/technical/bitumen-upgrading.

Osacky, M., Geramian, M., Ivey, D.G., Liu, Q., Etsell, T.H., 2013. Mineralogical and chemical composition of petrologic end members of Alberta oil sands. Fuel 113, 148–157. doi:10.1016/j.fuel.2013.05.099.

Pacyna, J.M., Pacyna, E.G., 2001. An assessment of global and regional emissions of trace metals to the atmosphere from anthropogenic sources worldwide. Environ. Rev. 9 (4), 269–298. doi:10.1139/a01-012.

Padmavathiamma, P.K., Li, L.Y., 2007. Phytoremediation technology: Hyper-accumulation metals in plants. Water Air Soil Pollut. 184 (1-4), 105–126. doi:10.1007/s11270-007-9401-5.

Pakarinen, P., 1978. Production and nutrient ecology of three *Sphagnum* species in southern Finnish raised bogs. Ann. Botan. Fenn. 15 (1), 15–26.

Pakarinen, P., 1981. Regional variation of sulphur concentrations in *Sphagnum* mosses and *Cladonia* lichens in Finnish bogs. Ann. Botan. Fenn. 18 (4), 275–279.

Pakarinen, P., Tolonen, K., 1976. Regional survey of heavy metals in peat mosses (*Sphagnum*). Ambio 5 (1), 38–40.

Phillips-Smith, C., Jeong, C.-H., Healy, R.M., Dabek-Zlotorzynska, E., Celo, V., Brook, J.R., Evans, G., 2017. Sources of particulate matter components in the Athabasca oil sands region: Investigation through a comparison of trace element measurement methodologies. Atmos. Chem. Phys. 17 (15), 9435–9449. doi:10.5194/acp-17-9435-2017.

Pilegaard, K., 1979. Heavy metals in bulk precipitation and transplanted *Hypogymnia physodes* and *Dicranoweisia cirrata* in the vicinity of a Danish steelworks. Water Air Soil Pollut. 11 (1), 77–91. doi:10.1007/BF00163521.

Poikolainen, J., Kubin, E., Piispanen, J., Karhu, J., 2004. Atmospheric heavy metal deposition in Finland during 1985–2000 using mosses as bioindicators. Sci. Total. Environ. 318 (1-3), 171–185. doi:10.1016/S0048-9697(03)00396-6.

Punning, J.-M., Alliksaar, T., 1997. The trapping of fly-ash particles in the surface layers of *Sphagnum*-dominated peat. Water Air Soil Pollut. 94 (1-2), 59–69. doi:10.1007/BF02407093.

R Core Team, 2021. R: A language and environment for statistical computing. R Foundation for Statistical Computing, Vienna, Austria.

Rahn, K.A., 1976. The Chemical Composition of the Atmospheric Aerosol. Graduate School of Oceanography, University of Rhode Island, Kingston, Rhode Island, USA, 279 pp.

Ramachandran, S., 2018. Atmospheric Aerosols: Characteristics and Radiative Effects. CRC Press, Boca Raton, FL.

Ramasamy, M.G. (Ed.), 2019. Processing of Heavy Crude Oils - Challenges and Opportunities. IntechOpen, London, United Kingdom, 276 pp.

Rao, D., 1982. Responses of bryophytes to air pollution, in: Smith, A. (Ed.), Bryophyte Ecology. Chapman and Hall Ltd, Holborn, London, UK, pp. 445–471.

Rao, D., Robitaille, G., LeBlanc, F., 1977. Influence of heavy metal pollution on lichens and bryophytes. J. Hattori Bot. Lab 42.

Relman, A.S., 1956. The physiological behavior of rubidium and cesium in relation to that of potassium. Yale J. Biol. Med. 29 (3), 248–262.

Robache, A., Mathé, F., Galloo, J.C., Guillermo, R., 2000. Multi-element analysis by inductively coupled plasma optical emission spectrometry of airborne particulate matter collected with a low-pressure cascade impactor. Analyst 125 (10), 1855–1859. doi:10.1039/b0030481.

Rudnick, R.L., Gao, S., 2014. Composition of the continental crust, in: Holland, H., Turekian, K. (Eds.), Treatise on Geochemistry, vol. 4, 2nd ed. Elsevier, pp. 1–51.

Rühling, Å., Tyler, G., Ruhling, A., 1970. Sorption and retention of heavy metals in the woodland moss *Hylocomium splendens* (Hedw.) Br. et Sch. Oikos 21 (1), 92. doi:10.2307/3543844.

Sakalys, J., Kvietkus, K., Sucharová, J., Suchara, I., Valiulis, D., 2009. Changes in total concentrations and assessed background concentrations of heavy metals in moss in Lithuania and the Czech Republic between 1995 and 2005. Chemosphere 76 (1), 91–97. doi:10.1016/j.chemosphere.2009.02.009.

Salemaa, M., Derome, J., Helmisaari, H.-S., Nieminen, T., Vanha-Majamaa, I., 2004. Element accumulation in boreal bryophytes, lichens and vascular plants exposed to heavy metal and sulfur deposition in Finland. Sci. Total Environ. 324 (1-3), 141–160. doi:10.1016/j.scitotenv.2003.10.025.

Sanford, E.C., 1983. Processibility of Athabasca oil sand: Interrelationship between oil sand fine solids, process aids, mechanical energy and oil sand age after mining. Can. J. Chem. Eng 61 (4), 554–567. doi:10.1002/cjce.5450610410.

Sanford, E.C., Seyer, F., 1979. Processibility of Athabasca tar sand using batch extraction unit: The role of NaOH. CIM Bulletin. 72, 164–169.

Santelmann, M.V., Gorham, E., 1988. The influence of airborne road dust on the chemistry of *Sphagnum* mosses. J. Ecol. 76 (4), 1219. doi:10.2307/2260644.

Sapkota, A., Chebukin, A.K., Bonani, G., Shotyk, W., 2007. Six millennia of atmospheric dust deposition in southern South America (Isla Navarino, Chile). Holocene 17 (5), 561–572. doi:10.1177/0959683607078981.

Sardans, J., Peñuelas, J., 2005. Trace element accumulation in the moss *Hypnum cupressiforme* Hedw. and the trees *Quercus ilex* L. and *Pinus halepensis* Mill. in Catalonia. Chemosphere 60 (9), 1293–1307. doi:10.1016/j.chemosphere.2005.01.059.

Saxena, D.K., Srivastava, K., Singh, S., 2008. Biomonitoring of metal deposition by using moss transplant method through *Hypnum cupressiforme* (Hedw.) in Mussoorie. J. Environ. Biol. 29 (5), 683–688.

Schilling, J.S., Lehman, M.E., 2002. Bioindication of atmospheric heavy metal deposition in the Southeastern US using the moss *Thuidium delicatulum*. Atmos. Environ. 36 (10), 1611–1618. doi:10.1016/S1352-2310(02)00092-4.

Schintu, M., Cogoni, A., Durante, L., Cantaluppi, C., Contu, A., 2005. Moss (*Bryum radiculosum*) as a bioindicator of trace metal deposition around an industrialised area in Sardinia (Italy). Chemosphere 60 (5), 610–618. doi:10.1016/j.chemosphere.2005.01.050.

Schröder, W., Pesch, R., 2007. Synthesizing bioaccumulation data from the German metals in mosses surveys and relating them to ecoregions. Sci. Total. Environ. 374 (2-3), 311–327. doi:10.1016/j.scitotenv.2006.09.015.

Schuetz, L., 1989. Atmospheric mineral dust - properties and source markers, in: Leinen, M., Sarnthein, M. (Eds.), Paleoclimatology and paleometeorology: Modern and past patterns of global atmospheric transport. Kluwer Academic Publishers, Dordrecht, The Netherlands, pp. 359–384.

Schütz, L., 1980. Long range transport of desert dust with special emphasis on the Sahara. Ann. NY Acad. Sci. 338 (1 Aerosols), 515–532. doi:10.1111/j.1749-6632.1980.tb17144.x.

Schütz, L., Rahn, K.A., 1982. Trace element concentrations in erodible soils. Atmos. Environ. 16 (1), 171–176.

Shaltout, A.A., Allam, M.A., Moharram, M.A., 2011. FTIR spectroscopic, thermal and XRD characterization of hydroxyapatite from new natural sources. Spectrochim. Acta A Mol. Biomol. Spectrosc. 83 (1), 56–60. doi:10.1016/j.saa.2011.07.036.

Shimwell, D.W., Laurie, A.E., 1972. Lead and zinc contamination of vegetation in the southern Pennines. Environ. Pollut. 3 (4), 291–301. doi:10.1016/0013-9327(72)90024-9.

Shotyk, W., 1996a. Natural and anthropogenic enrichments of As, Cu, Pb, Sb, and Zn in ombrotrophic versus minerotrophic peat bog profiles, Jura Mountains, Switzerland. Water Air Soil Pollut. 90 (3-4), 375–405. doi:10.1007/BF00282657.

Shotyk, W., 1996b. Peat bog archives of atmospheric metal deposition: Geochemical evaluation of peat profiles, natural variations in metal concentrations, and metal enrichment factors. Environ. Rev. 4 (2), 149–183. doi:10.1139/a96-010.

Shotyk, W., 2020. Trace elements in wild berries from reclaimed lands: Biomonitors of contamination by atmospheric dust. Ecol. Indic. 110, 105960. doi:10.1016/j.ecolind.2019.105960.

Shotyk, W., Belland, R., Duke, J., Kempter, H., Krachler, M., Noernberg, T., Pelletier, R., Vile, M.A., Wieder, K., Zaccone, C., Zhang, S., 2014. *Sphagnum* mosses from 21 ombrotrophic bogs in the Athabasca Bituminous Sands region show no significant atmospheric contamination of "heavy metals". Environ. Sci. Technol. 48 (21), 12603–12611. doi:10.1021/es503751v.

Shotyk, W., Bicalho, B., Cuss, C.W., Donner, M., Grant-Weaver, I., Javed, M.B., Noernberg, T., 2021. Trace elements in the Athabasca Bituminous Sands: A geochemical explanation for the paucity of environmental contamination by chalcophile elements. Chem. Geol. 581, 120392. doi:10.1016/j.chemgeo.2021.120392.

Shotyk, W., Bicalho, B., Cuss, C.W., Duke, J., Noernberg, T., Pelletier, R., Steinnes, E., Zaccone, C., 2016. Dust is the dominant source of "heavy metals" to peat moss (*Sphagnum fuscum*) in the bogs of the Athabasca Bituminous Sands region of northern Alberta. Environ. Int. 92-93, 494–506. doi:10.1016/j.envint.2016.03.018.

Shotyk, W., Bicalho, B., Grant-Weaver, I., Stachiw, S., 2019. A geochemical perspective on the natural abundance and predominant sources of trace elements in cranberries (*Vaccinium oxycoccus*) from remote bogs in the Boreal region of northern Alberta, Canada. Sci. Total. Environ. 650 (Pt 1), 1652–1663. doi:10.1016/j.scitotenv.2018.06.248.

Shotyk, W., Cuss, C.W., 2019. Atmospheric Hg accumulation rates determined using *Sphagnum* moss from ombrotrophic (rain-fed) bogs in the Athabasca Bituminous Sands region of northern Alberta, Canada. Ecol. Indic. 107, 105626. doi:10.1016/j.ecolind.2019.105626.

Shotyk, W., Kempter, H., Krachler, M., Zaccone, C., 2015. Stable (206Pb, 207Pb, 208Pb) and radioactive (210Pb) lead isotopes in 1 year of growth of *Sphagnum* moss from four ombrotrophic bogs in southern Germany: Geochemical significance and environmental implications. Geochim. Cosmochim. Acta 163, 101–125. doi:10.1016/j.gca.2015.04.026.

Shotyk, W., Krachler, M., Chen, B., 2005. Anthropogenic impacts on the biogeochemistry and cycling of antimony, in: Sigel, A., Sigel, H., Sigel, R.K.O. (Eds.), Metal Ions in Biological Systems. Biogeochemisty, Availability, and Transport of Metals in the Environment. CRC Press, Boca Raton, pp. 171–204.

Shotyk, W., Nesbitt, W.H., Fyfe, W.S., 1992. Natural and anthropogenic enrichments of trace metals in peat profiles. Int. J. Coal Geol. 20 (1-2), 49–84. doi:10.1016/0166-5162(92)90004-G.

Shotyk, W., Weiss, D., Kramers, J.D., Frei, R., Chebukin, A.K., Gloor, M., Reese, S., 2001. Geochemistry of the peat bog at Etang de la Grue‘re, Jura Mountains, Switzerland, and its record of atmospheric Pb and lithogenic trace metals (Sc, Ti, Y, Zr, and REE) since 12,370 ^{14}C yr BP. Geochim. Cosmochim. Acta 65 (14), 2337–2360. doi:10.1016/S0016-7037(01)00586-5.

Skaar, H., Ophus, E., Gullvag, B., 1973. Lead accumulation within nuclei of moss leaf cells. Nature 241 (5386), 215–216. doi:10.1038/241215a0.

Spagnuolo, V., Giordano, S., Pérez-Llamazares, A., Ares, A., Carballeira, A., Fernández, J.A., Aboal, J.R., 2013. Distinguishing metal bioconcentration from particulate matter in moss tissue: testing methods of removing particles attached to the moss surface. Sci. Total. Environ. 463-464, 727–733. doi:10.1016/j.scitotenv.2013.05.061.

Spearing, A.M., 1972. Cation-exchange capacity and galacturonic acid content of several species of *Sphagnum* in sandy ridge bog, Central New York State. Bryologist. 75 (2), 154. doi:10.2307/3241443.

Stachiw, S., Bicalho, B., Grant-Weaver, I., Noernberg, T., Shotyk, W., 2019. Trace elements in berries collected near upgraders and open pit mines in the Athabasca Bituminous Sands Region (ABSR): Distinguishing atmospheric dust deposition from plant uptake. Sci. Total. Environ. 670, 849–864. doi:10.1016/j.scitotenv.2019.03.238.

Ștefănuț, S., Öllerer, K., Manole, A., Ion, M.C., Constantin, M., Banciu, C., Maria, G.M., Florescu, L.I., 2019. National environmental quality assessment and monitoring of atmospheric heavy

metal pollution - A moss bag approach. J. Environ. Manage. 248, 109224. doi:10.1016/j.jenvman.2019.06.125.

Steinmann, P., Shotyk, W., 1997. Geochemistry, mineralogy, and geochemical mass balance on major elements in two peat bog profiles (Jura Mountains, Switzerland). Chem. Geol. 138 (1-2), 25–53.

Steinnes, E., 1995. A critical evaluation of the use of naturally growing moss to monitor the deposition of atmospheric metals. Sci. Total Environ. 160-161, 243–249. doi:10.1016/0048-9697(95)04360-D.

Steinnes, E., 1997. Trace element profiles in ombrogenous peat cores from Norway: Evidence of long range atmospheric transport. Water Air Soil Pollut. 100 (3/4), 405–413. doi:10.1023/A:1018388912711.

Steinnes, E., Berg, T., Uggerud, H.T., 2011. Three decades of atmospheric metal deposition in Norway as evident from analysis of moss samples. Sci. Total Environ. 412-413, 351–358. doi:10.1016/j.scitotenv.2011.09.086.

Steinnes, E., Solberg, W., Petersen, H., Wren, C.D., 1989. Heavy metal pollution by long range atmospheric transport in natural soils of Southern Norway. Water Air Soil Pollut. 45 (3-4), 207–218. doi:10.1007/BF00283452.

Strausz, O.P., 1989. Bitumen and heavy oil chemistry, in: Hepler, L.G., Hsi, C. (Eds.), AOSTRA Technical Handbook on Oil Sands, Bitumens and Heavy Oils. Alberta Oil Sands Technology and Research Authority, Edmonton, Alberta, pp. 33–73.

Strausz, O.P., Lown, E.M., 2003. The Chemistry of Alberta Oil Sands, Bitumens and Heavy oil. Alberta Energy Research Institute, Calgary, Alberta, Canada.

Sun, S.-Q., Wang, D.-Y., He, M., Zhang, C., 2009. Monitoring of atmospheric heavy metal deposition in Chongqing, China—based on moss bag technique. Environ. Monit. Assess. 148 (1-4), 1–9. doi:10.1007/s10661-007-0133-1.

Suzuki, K., 2006. Characterisation of airborne particulates and associated trace metals deposited on tree bark by ICP-OES, ICP-MS, SEM-EDX and laser ablation ICP-MS. Atmos. Environ. 40 (14), 2626–2634. doi:10.1016/j.atmosenv.2005.12.022.

Swift, D.L., Proctor, D.F., 1982. Human respiratory deposition of particles during oronasal breathing. Atmos. Environ. 16 (9), 2279–2282. doi:10.1016/0004-6981(82)90307-9.

Takamura, K., 1982. Microscopic structure of athabasca oil sand. Can. J. Chem. Eng 60 (4), 538–545. doi:10.1002/cjce.5450600416.

Takamura, K., 1985. Physio-chemical characterization of Athabasca oil sand and its significance to bitumen recovery. AOSTRA (Alberta Oil Sands Technology Authority) Journal of Research; (Canada) 2:1.

Thomine, S., Wang, R., Ward, J.M., Crawford, N.M., Schroeder, J.I., 2000. Cadmium and iron transport by members of a plant metal transporter family in Arabidopsis with homology to Nramp genes. PNAS 97 (9), 4991–4996. doi:10.1073/pnas.97.9.4991.

Tomasi, C., Lupi, A., 2016. Primary and secondary sources of atmospheric aerosol, in: Tomasi, C., Fuzzi, S., Kokhanovsky, A.A. (Eds.), Atmospheric Aerosols. Life Cycles and Effects on Air Quality and Climate, 1st ed. Wiley-VCH, Weinheim, pp. 1–86.

Tyler, G., 1990. Bryophytes and heavy metals: a literature review. Bot. J. Linn. Soc. 104 (1-3), 231–253. doi:10.1111/j.1095-8339.1990.tb02220.x.

Vazquez, M.D., Wappelhorst, O., Markert, B., 2004. Determination of 28 elements in aquatic moss *Fontinalis Antipyretica* Hedw. and water from the upper reaches of the River Nysa (CZ, D), by ICP-MS, ICP-OES and AAS. Water Air Soil Pollut. 152 (1-4), 153–172. doi:10.1023/B:WATE.0000015351.40069.d2.

Vile, M.A., Wieder, R.K., Novk, M., 1999. Mobility of Pb in *Sphagnum*-derived peat. Biogeochemistry 45 (1), 35–52. doi:10.1007/BF00992872.

Wåhlin, P., Berkowicz, R., Palmgren, F., 2006. Characterisation of traffic-generated particulate matter in Copenhagen. Atmos. Environ. 40 (12), 2151–2159. doi:10.1016/j.atmosenv.2005.11.049.

Wallace, D., Henry, D., Takamura, K., 1989. A physical chemical explanation for deterioration in the hot water processability of Athabasca oil sands due to aging. Fuel Sci. Technol. Int. 7 (5-6), 699–725. doi:10.1080/08843758908962265.

Wang, X., Chow, J.C., Kohl, S.D., Yatavelli, L.N.R., Percy, K.E., Legge, A.H., Watson, J.G., 2015. Wind erosion potential for fugitive dust sources in the Athabasca Oil Sands Region. Aeolian Res. 18, 121–134. doi:10.1016/j.aeolia.2015.07.004.

Watkinson, S.C., Watt, F., 1992. The cellular localisation of elements in leaf cells of *Sphagnum* with the scanning proton microprobe. Bryologist. 95 (2), 181. doi:10.2307/3243433.

Watson, J.G., Chow, J.C., Wang, X., Kohl, S.D., 2014. Windblown fugitive dust characterization in the Athabasca Oil Sands Region. 2014. WBEA-DRI Agreement Number: T108-13. https://wbea.org/wp-content/uploads/2018/03/watson_j_g_et_al_2014_windblown_fugitive_dust_characterization_in_the_athabasca_oil_sands_region.pdf.

Weiss, D., Shotyk, W., Cheburkin, A.K., Gloor, M., Reese, S., 1997. Atmospheric lead deposition from 12,400 to ca. 2,000 yrs BP in a peat bog profile, Jura Mountains, Switzerland. Water Air Soil Pollut. 100 (3/4), 311–324. doi:10.1023/A:1018341029549.

Whitby, K.T., Husar, R., Liu, B., 1972. The aerosol size distribution of Los Angeles smog. J. Colloid Interface Sci. 39 (1), 177–204.

White, P.J., Brown, P.H., 2010. Plant nutrition for sustainable development and global health. Ann. Bot. 105 (7), 1073–1080. doi:10.1093/aob/mcq085.

Wickham, H., 2016. ggplot2: Elegrant graphics for data analysis, 2nd ed. Springer, Switzerland.

Wickleder, M.S., Fourest, B., Dorhout, P.K., 2010. Thorium, in: Morss, L.R., Edelstein, N.M., Fuger, J. (Eds.), The Chemistry of the Actinide and Transactinide Elements, 4 ed. Springer, Dordrecht, pp. 52–160.

Willeke, K., Whitby, K.T., 1975. Atmospheric aerosols: size distribution interpretation. J. Air Pollut. Control Assoc. 25 (5), 529–534. doi:10.1080/00022470.1975.10470110.

Xing, Z., Du, K., 2017. Particulate matter emissions over the oil sands regions in Alberta, Canada. Environ. Rev. 25 (4), 432–443. doi:10.1139/er-2016-0112.

Xu, M., Yu, D., Yao, H., Liu, X., Qiao, Y., 2011. Coal combustion-generated aerosols: Formation and properties. Proc. Combust. Inst . 33 (1), 1681–1697. doi:10.1016/j.proci.2010.09.014.

Zufall, M.J., Davidson, C.I., 1998. Dry deposition of particles from the atmosphere, in: Linkov, I., Wilson, R. (Eds.), Air Pollution in the Ural Mountains: Environmental, Health and Policy Aspects. Springer Netherlands, Dordrecht, pp. 55–73.

APPENDIX I

Tests of filters, filter cleaning, and the optimum amount of ash and acid insoluble ash required

1. Introduction

To determine the concentrations of trace elements in the acid soluble ash (ASA) and acid insoluble ash (AIA) of *Sphagnum* moss, it is necessary to separate these two ash fractions. Leaching of ash samples with 2% HNO_3 followed by filtration dissolved the ASA fraction whereas the AIA fraction remained on the filter membrane. As the process of opening regular syringe filters to obtain the AIA on the filter membrane can cause loss of the AIA, reusable membrane filters were considered for filtration.

Due to the low concentrations of most trace elements in moss, filter blanks are of great importance; therefore, these were also tested to determine which amount of 2% HNO_3 for cleaning is adequate for satisfactory filter blanks.

The amount of ash to be leached and AIA to be digested also matters. If the amount is not sufficient, trace element concentrations determined by ICP-MS might not be accurate or below the limit of detection. In addition, as moss cleaning is time-consuming, obtaining too much ash or AIA would be a waste of time. Thus, the optimum amount of ash and AIA required was tested.

2. Materials and methods

Hydrophilic polytetrafluoroethylene (PTFE) filter membranes (Millipore), hydrophilic PTFE syringe filters (Millipore Millex), and hydrophobic PTFE filter membranes (Fluoropore Millipore) were tested to see which one was more efficient. All the filters have a pore size of 0.45 μm and diameter of 25 mm. The filter membranes were used along with acid-cleaned polypropylene (PP) filter holders and silicone gaskets for sealing (Fig. 1). The acid-cleaned syringe

filters are made of PTFE in PP casings (Fig. 1). The syringes used are made of PP and were also acid-cleaned before use.

Hydrophilic PTFE filter membranes used together with filter holders were finally selected for filtration. Cleaning of filter membranes was tested in triplicate by collecting filtrates for the same filter membrane three times; each time the filter membrane was cleaned with 5 ml of 2% HNO_3 (15 ml in total, Table 1). The filter membranes were then left to dry overnight in a clean air cabinet. As the filter membranes shrank after drying, only one could be cleaned again with 10 ml of 2% HNO_3. All filtrates were analyzed using inductively coupled plasma mass spectrometry (ICP-MS) in the ultraclean, metal-free SWAMP Lab at the University of Alberta.

To determine the optimum AIA amount, moss samples were cleaned using tweezers to remove all foreign and dead materials, dried at 105°C in a drying oven, and ashed at 550°C for 16 h in a muffle furnace (MLS Pyro High-Temperature Microwave Muffle Furnace, Leutkirch, Germany). Moss samples were collected in October 2019 from JPH4 and Utikuma (UTK) bogs located 12 and 264 km away from the industrial centre, respectively. This centre is defined as the mid-point between two central upgraders. Two sets of approximately 80 and 150 mg of ash samples from JPH4 and 150 and 300 mg from UTK were leached with 30 ml of 2% HNO_3 for 15 min (Table 2). UTK samples were assumed to contain less AIA, so a larger amount of ash was used. After leaching, samples of set 1 were filtered twice using the PTFE filter membranes, and samples of set 2 were filtered using the PTFE filter membrane first and then the PTFE syringe filter. This double filtration approach was applied because the filter holder was not sealed well the first time, and the filtrate was thus not clear. Another two sets of JPH4 ash samples (approximately 80 mg) were also leached with 2% HNO_3 and filtered once using the PTFE syringe filter or PHLP

filter membrane (Table 2). The filtrates, including blanks for each set, were analyzed using ICP-MS.

Moss cleaning, drying, and ashing were done in the Prep Lab at the University of Alberta, which is of Class 100,000, making it suitable for the preparation work (Details can be found on the SWAMP Lab website). The rest of the work was conducted in the metal-free, ultraclean SWAMP Lab at the University of Alberta.

3. Results and discussion

When the suspensions were filtered solely using hydrophilic PTFE filter membranes (set 1), the element concentrations in the ASA showed minor variations between the two ash masses used from either JPH4 or UTK (Table 3, Fig. 2). The similar concentrations between the two ash masses of each site indicated that approximately 80 mg of ash for JPH4 and 150 mg for UTK might be sufficient to obtain accurate concentrations of trace elements in ASA. Regarding set 2, some element concentrations in the ASA (e.g., Ag, Cd, Li, and Sb in JPH4) had larger variations between the two ash masses used, especially in JPH4, compared to those of set 1. Such a phenomenon indicated that the change in filters might have induced slight variations in element concentrations. Element concentrations in ASA 11 and 13 were generally comparable to those of ASA 1, 2, 6, and 7. However, without pre-treatment of the filter, which might cause contamination of the samples, the hydrophobicity of the filter membrane (set 4) results in difficulty with filtering water suspensions. For example, not all of the leached solution was filtered out and the AIA was not sorbed to the filter membrane after filtration. Hence, a great loss of AIA occurred when opening the filter holder. Considering this, hydrophobic membrane filters were excluded.

The element concentrations in the AIA of set 1 and set 2 showed the same trends as those in the ASA (Table 4, Fig. 3). The comparable concentrations in the AIA from the two ash masses indicated that approximately 80 mg of ash of JPH4 samples and 150 mg of UTK samples might also be sufficient for accurate element analysis in AIA. Given the ease of hydrophilic PTFE filter membranes in filtering acid suspensions and obtaining the membranes from the filter holders, less loss of AIA through this process, and consistent concentrations from the two ash masses, hydrophilic PTFE membrane filters were finally selected.

The filter cleaning test showed that 15 ml of 2% HNO_3 appeared to be sufficient for cleaning. Concentrations of Fe, Mn, Cu, Zn, Ni, and Pb generally decreased after the last filtration for filters 2 and 3, except for Cu of filter 3 (Fig. 4). However, the element concentrations of the filtrates from filter 1 showed increasing trends with the increasing amount of acid used or after the last filtration, which might be caused by experimental errors such as contamination from the syringe and tweezer used. The concentrations of Al of the three filters increased after the last filtration, but the increase was insignificant. Overnight drying and cleaning again with 10 ml of 2% HNO_3 (filtrate 10) decreased Al and Ni concentrations (0.72 and 0.77x, respectively), but increased Fe, Mn, Cu, Zn, and Pb concentrations (1.65, 1.33, 1.78, 2.02, and 3.03x, respectively) compared to filtrate 3. Therefore, and due to the delicacy of the filter membranes, filter cleaning was done right before filtration with 15 ml of 2% HNO_3 for subsequent samples.

Table 1. Filter cleaning test.

Filtrate	Filter	2% HNO_3 used (ml)	Cumulative 2% HNO_3 used (ml)
1	1	5	5
2	1	5	10
3	1	5	15
4	2	5	5
5	2	5	10
6	2	5	15
7	3	5	5
8	3	5	10
9	3	5	15
10	1	10	25

Table 2. Test of filters and the optimum amount of ash and acid insoluble ash (AIA).

Set	Ash (mg)	Site	Filtration	Filtrate	Filter Membrane
1	79.00	JPH4	Double filtration using hydrophilic PTFE membrane filters	ASA1	AIA1
	157.40	JPH4		ASA2	AIA2
	152.20	UTK		ASA3	AIA3
	249.70	UTK		ASA4	AIA4
	0.00	Blank		ASA5	AIA5
2	74.36	JPH4	1st filtration using a hydrophilic PTFE membrane filter, 2nd filtration using a regular hydrophilic PTFE syringe filter	ASA6	AIA6
	161.54	JPH4		ASA7	AIA7
	155.64	UTK		ASA8	AIA8
	308.67	UTK		ASA9	AIA9
	0.00	Blank		ASA10	AIA10
3	80.70	JPH4	Single filtration using a regular hydrophilic PTFE syringe filter	ASA11	AIA11
	0.00	Blank		ASA12	AIA12
4	82.60	JPH4	Single filtration using a hydrophobic PTFE membrane filter	ASA13	AIA13
	0.00	Blank		ASA14	AIA14

Note: ASA = Acid soluble ash. UTK = Utikuma. PTFE = Polytetrafluoroethylene.

Table 3. Element concentrations in acid soluble ash (ASA) after leaching using different ash mass and filtration methods.

Sample		ASA1	ASA2	ASA3	ASA4	ASA6	ASA7	ASA8	ASA9	ASA11	ASA13
Site		JPH4	JPH4	UTK	UTK	JPH4	JPH4	UTK	UTK	JPH4	JPH4
Ash (mg)		79.00	157.40	152.20	249.70	74.36	161.54	155.64	308.67	80.70	82.60
Filtration		Hydrophilic membrane filter*2				Hydrophilic membrane filter*1 + Syringe filter*1				Syringe filter*1	Hydrophobic membrane filter*1
Ag	µg/kg	54.5	67.7	463	368	131	53.3	503	295	50.8	60.0
Al	g/kg	21.0	22.0	8.5	9.s2	20.7	20.4	13.2	12.8	19.8	22.2
Ba	mg/kg	295	290	598	709	293	283	702	568	294	343
Be	µg/kg	665	664	281	312	753	653	473	424	614	716
Cd	µg/kg	163	178	1706	1771	360	201	2141	1996	155	172
Ce	mg/kg	14.4	13.0	1.85	1.78	23.1	15.7	5.85	1.38	11.9	16.1
Co	mg/kg	6.81	6.85	3.42	3.66	8.77	7.39	5.33	5.12	6.58	7.50
Cr	mg/kg	23.8	22.6	17.2	16.4	24.9	22.5	21.6	21.9	22.0	25.8
Cs	mg/kg	1.10	1.04	0.417	0.497	1.87	1.10	0.639	0.638	1.10	1.19
Cu	mg/kg	13.1	13.3	109	102	32.9	15.2	89.5	83.8	10.7	12.9
Dy	mg/kg	1.39	1.36	0.597	0.611	1.66	1.46	0.825	0.784	1.23	1.35
Er	µg/kg	668	654	301	324	830	716	432	399	589	671
Eu	µg/kg	463	448	201	211	537	482	296	268	413	459
Fe	g/kg	11.5	12.4	6.4	6.8	15.4	11.8	10.8	10.2	9.4	11.5
Ga	mg/kg	6.65	6.78	2.71	3.04	7.71	6.58	4.77	4.22	6.17	7.34
Gd	mg/kg	1.93	1.84	0.768	0.818	2.20	1.93	1.14	1.06	1.68	1.89
Ge	mg/kg	4.77	4.43	2.43	2.64	5.08	4.64	3.90	3.39	4.39	5.06
Ho	µg/kg	253	247	112	116	310	266	156	148	219	250
La	mg/kg	14.2	14.1	6.23	6.70	13.9	13.7	9.72	8.77	12.8	14.5
Li	mg/kg	11.2	10.8	8.84	9.53	24.2	12.4	17.4	11.9	8.95	11.0
Lu	µg/kg	74.7	69.6	36.8	37.4	89.3	75.5	52.0	47.6	57.8	67.6

Note: UTK = Utikuma. PTFE = Polytetrafluoroethylene.

Table 3. Element concentrations in acid soluble ash (ASA) after leaching using different ash mass and filtration methods (Continued).

Sample		ASA1	ASA2	ASA3	ASA4	ASA6	ASA7	ASA8	ASA9	ASA11	ASA13
Site		JPH4	JPH4	UTK	UTK	JPH4	JPH4	UTK	UTK	JPH4	JPH4
Ash (mg)		79.00	157.40	152.20	249.70	74.36	161.54	155.64	308.67	80.70	82.60
Filtration		Hydrophilic membrane filter*2				Hydrophilic membrane filter*1 + Syringe filter*1				Syringe filter*1	Hydrophobic membrane filter*1
Mn	mg/kg	800	686	1161	1261	1863	770	738	460	1845	1838
Mo	µg/kg	275	237	434	505	643	258	263	243	748	1367
Nd	mg/kg	11.9	11.7	6.14	6.37	13.0	11.8	9.39	7.92	10.6	11.9
Ni	mg/kg	19.7	20.4	13.3	15.5	24.2	18.4	21.9	18.0	14.8	19.2
Pb	mg/kg	4.12	4.16	6.31	5.65	4.61	3.90	11.8	10.5	3.83	4.67
Pr	mg/kg	3.15	3.05	1.36	1.44	3.28	3.05	2.19	1.90	2.74	3.09
Rb	mg/kg	78.7	73.5	263	279	168	83.5	200	208	74.9	80.6
Re	µg/kg	8.68	8.65	1.59	2.22	3.54	7.02	3.40	3.12	6.48	8.93
Sb	µg/kg	121	114	295	221	240	139	259	224	131	159
Sm	mg/kg	2.17	2.11	0.89	0.92	2.41	2.17	1.36	1.24	1.87	2.12
Sn	µg/kg	102	58.4	22.9	62.4	99.3	42.2	24.2	30.9	69.9	216
Sr	mg/kg	227	219	192	199	224	229	214	204	218	243
Tb	µg/kg	257	242	105	109	299	263	151	142	227	251
Th	µg/kg	1334	984	52.1	38.4	2636	1329	328	237	1191	2684
Tl	µg/kg	24.8	16.7	18.6	26.5	24.9	29.4	22.3	22.4	14.8	14.4
Tm	µg/kg	89.6	83.8	38.4	41.9	111.5	88.6	54.4	52.7	78.3	84.6
U	µg/kg	769	802	581	612	771	733	926	773	703	814
V	mg/kg	57.9	59.4	22.1	24.6	52.2	55.7	40.6	36.7	58.9	67.3
Y	mg/kg	6.83	6.51	3.01	3.30	8.36	7.37	4.38	4.11	6.31	7.01
Yb	µg/kg	512	497	241	256	637	541	351	321	415	495
Zn	mg/kg	332	321	836	828	591	447	869	867	292	308

Note: UTK = Utikuma. PTFE = Polytetrafluoroethylene.

Table 4. Element concentrations in acid insoluble ash (AIA) after leaching using different ash mass and filtration methods.

Sample		AIA1	AIA2	AIA3	AIA4	AIA6	AIA7	AIA8	AIA9	AIA11	AIA13
Site		JPH4	JPH4	UTK	UTK	JPH4	JPH4	UTK	UTK	JPH4	JPH4
Ash (mg)		79.00	157.40	152.20	249.70	74.36	161.54	155.64	308.67	80.70	82.60
Filtration		Hydrophilic membrane filter*2				Hydrophilic membrane filter*1 + Syringe filter*1				Syringe filter*1	Hydrophobic membrane filter*1
Ag	µg/kg	65.5	84.7	178	267	292	148	230	145	68.2	36.6
Al	g/kg	9.84	10.7	4.11	4.24	7.41	12.1	3.78	3.82	12.2	8.08
Ba	mg/kg	83.62	96.70	68.04	96.90	131.30	122.96	60.89	169.41	95.54	73.76
Be	µg/kg	231	232	100	108	182	416	80	99	296	176
Cd	µg/kg	148	188	166	126	360	451	101	112	164	89
Ce	mg/kg	34.6	47.2	36.7	46.1	30.2	49.4	24.8	32.7	42.1	28.3
Co	mg/kg	1.96	2.07	2.32	2.86	3.54	2.59	2.28	2.58	2.70	1.65
Cr	mg/kg	19.3	21.6	55.0	11.8	17.8	23.2	8.55	8.25	22.3	17.0
Cs	mg/kg	1.98	2.39	0.426	0.422	1.09	3.09	0.318	0.525	2.54	1.55
Cu	mg/kg	8.34	9.31	11.5	8.80	18.5	11.8	5.05	5.41	10.8	6.65
Dy	mg/kg	1.08	1.18	0.575	0.620	0.923	1.38	0.467	0.459	1.54	0.971
Er	µg/kg	599	632	350	369	569	727	289	283	866	543
Eu	µg/kg	272	345	148	174	228	391	92	112	386	254
Fe	g/kg	10.4	11.0	5.31	5.39	7.28	12.4	3.74	4.56	13.5	8.27
Ga	mg/kg	6.13	7.17	4.10	4.81	4.65	7.67	3.12	3.73	7.54	5.01
Gd	mg/kg	1.31	1.64	0.679	0.802	1.05	1.89	0.476	0.510	1.85	1.23
Ge	mg/kg	3.48	4.28	1.83	2.08	2.62	4.77	1.10	1.35	4.90	3.32
Ho	µg/kg	215	221	113	122	189	258	113	95	301	186
La	mg/kg	9.53	13.0	4.07	4.77	6.88	14.9	2.63	3.00	13.3	9.50
Li	mg/kg	12.6	13.2	2.85	2.59	5.70	16.7	2.47	3.28	15.4	8.74
Lu	µg/kg	78.7	87.9	48.9	54.0	78.8	101	40.3	49.2	117	78.1

Note: UTK = Utikuma. PTFE = Polytetrafluoroethylene.

Table 4. Element concentrations in acid insoluble ash (AIA) after leaching using different ash mass and filtration methods (Continued).

Sample		AIA1	AIA2	AIA3	AIA4	AIA6	AIA7	AIA8	AIA9	AIA11	AIA13
Site		JPH4	JPH4	UTK	UTK	JPH4	JPH4	UTK	UTK	JPH4	JPH4
Ash (mg)		79.00	157.40	152.20	249.70	74.36	161.54	155.64	308.67	80.70	82.60
Filtration		Hydrophilic membrane filter*2				Hydrophilic membrane filter*1 + Syringe filter*1				Syringe filter*1	Hydrophobic membrane filter*1
Mn	g/kg	2.32	2.59	10.2	14.7	2.27	2.63	6.69	6.28	0.862	0.810
Mo	mg/kg	3.58	3.58	4.01	5.58	1.50	2.79	3.38	4.38	2.27	2.64
Nd	mg/kg	8.73	11.9	4.56	5.29	6.83	13.5	2.61	2.88	12.2	8.53
Ni	mg/kg	11.3	12.5	5.82	4.60	7.20	14.0	2.42	3.63	16.3	9.04
Pb	mg/kg	2.66	3.52	4.53	9.13	4.80	3.99	3.25	3.41	2.53	1.71
Pr	mg/kg	2.42	3.20	1.20	1.43	1.82	3.70	0.691	0.800	3.37	2.36
Rb	mg/kg	36.4	41.1	14.0	17.6	24.5	51.8	10.3	12.8	45.4	30.0
Re	µg/kg	0.568	0.670	0.259	0.310	0.214	0.839	0.292	< LOD	0.768	0.549
Sm	mg/kg	1.58	2.05	0.794	0.971	1.21	2.36	0.475	0.531	2.19	1.51
Sn	µg/kg	110	115	246	423	98.4	96.9	444	516	134	208
Sr	mg/kg	10.9	12.2	11.2	13.6	18.5	16.2	9.54	9.16	13.4	13.3
Tb	µg/kg	199	228	103	117	168	265	81.1	79.6	284	179
Th	mg/kg	4.88	6.69	5.70	6.89	3.99	6.48	4.47	4.71	4.04	3.21
Tl	µg/kg	102	136	34.7	35.3	74.5	310	34.1	50.2	116	74.3
Tm	µg/kg	84.4	88.3	49.6	56.6	80.6	100	40.6	38.1	121	79.3
U	µg/kg	487	582	427	491	566	820	293	315	652	488
V	mg/kg	24.3	28.7	11.6	12.5	17.6	28.5	10.6	12.0	27.0	19.4
Y	mg/kg	5.34	5.34	3.03	3.22	4.83	6.20	2.63	3.01	7.73	4.68
Yb	µg/kg	532	569	330	363	530	650	277	267	759	487
Zn	mg/kg	87.2	69.9	61.8	43.5	49.5	89.3	31.6	28.3	94.3	54.6

Note: UTK = Utikuma. PTFE = Polytetrafluoroethylene.

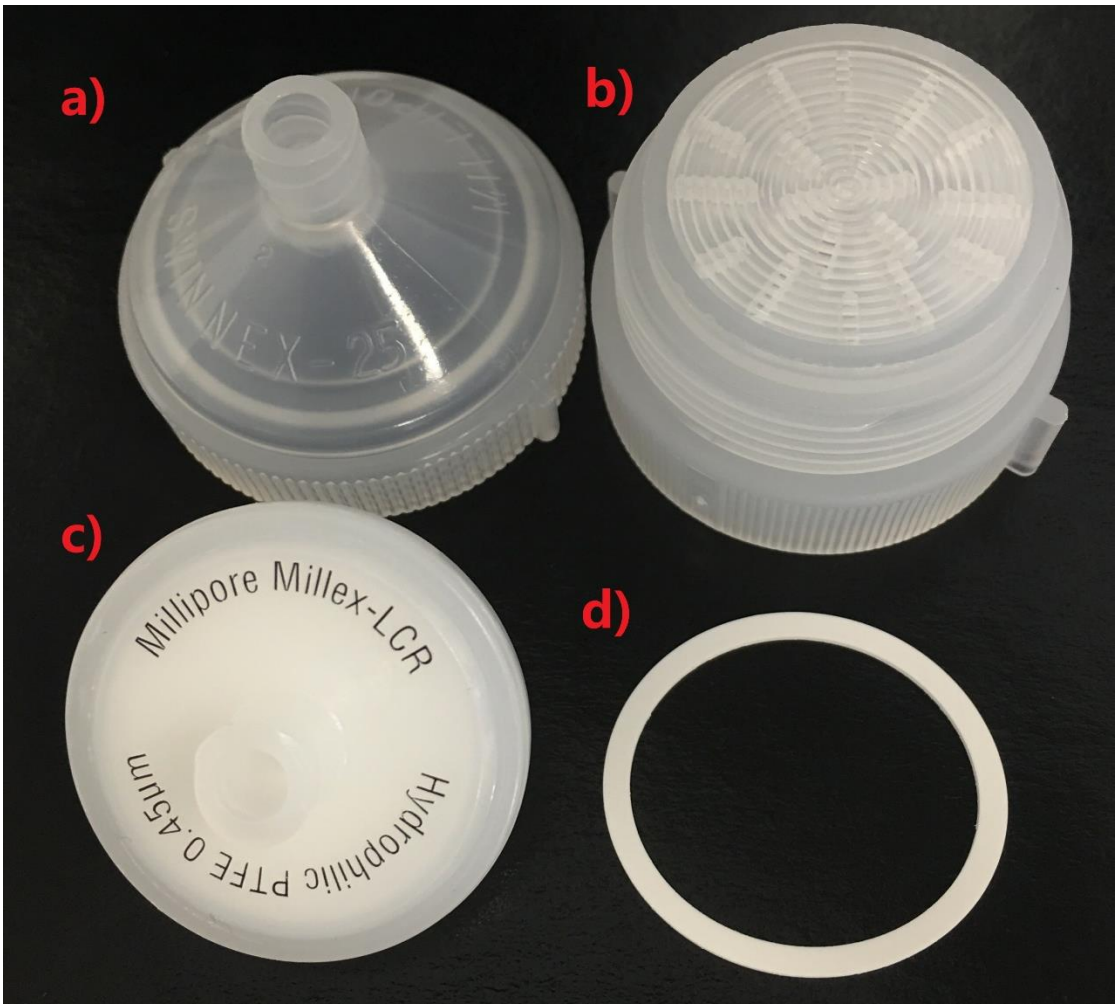

Fig. 1. a) & b) Filter holder assemblies, c) regular syringe filter, and d) silicon gasket.

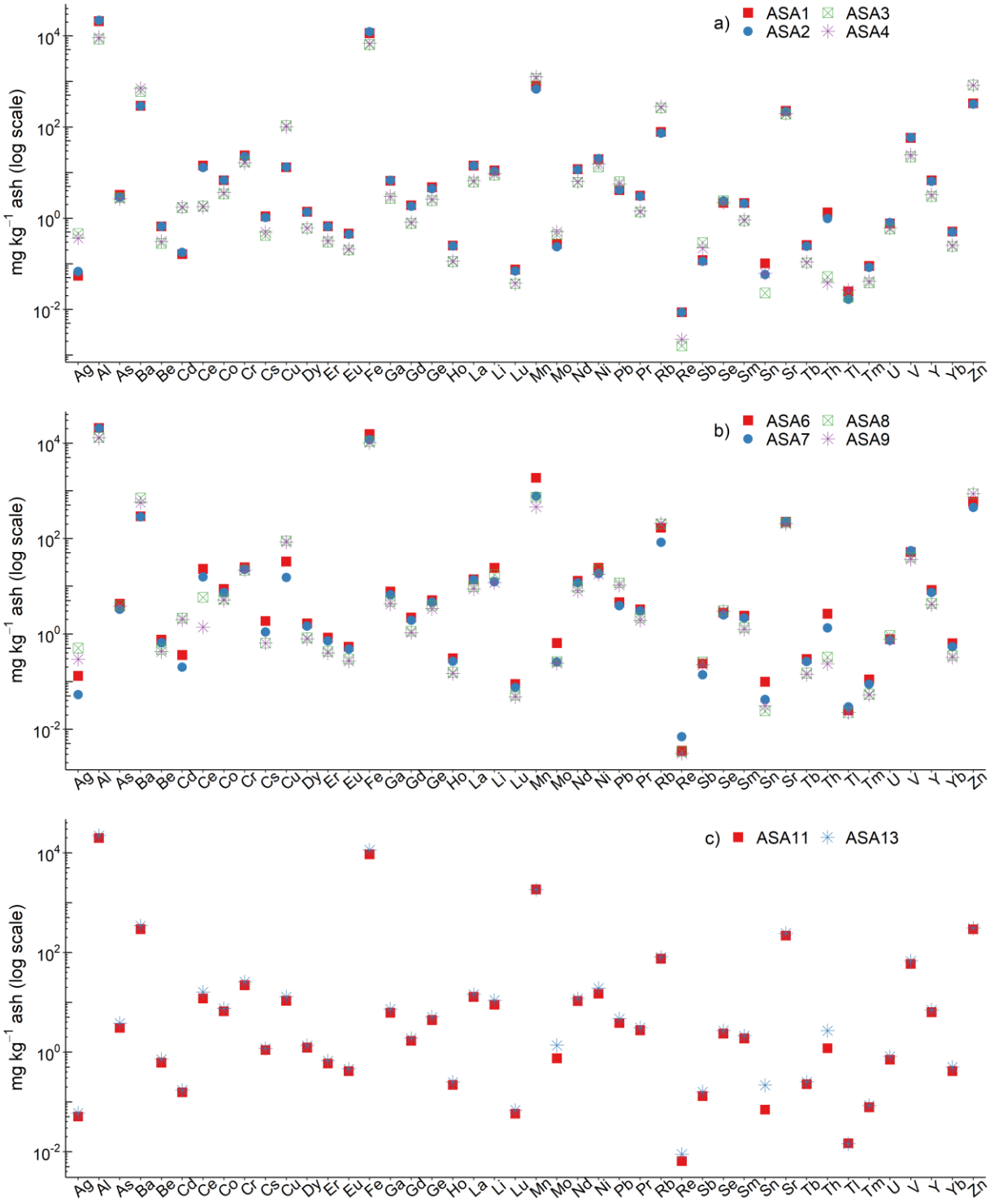

Fig. 2. Element concentrations (mg kg^{-1} ash) in a) ASA1–4, b) ASA6–9, c) ASA11 and 13 after leaching using different *Sphagnum* ash masses and filtration methods (see Table 2). *Sphagnum* mosses were collected from JPH4 and UTK bogs in October 2019. ASA = acid soluble ash. UTK = Utikuma.

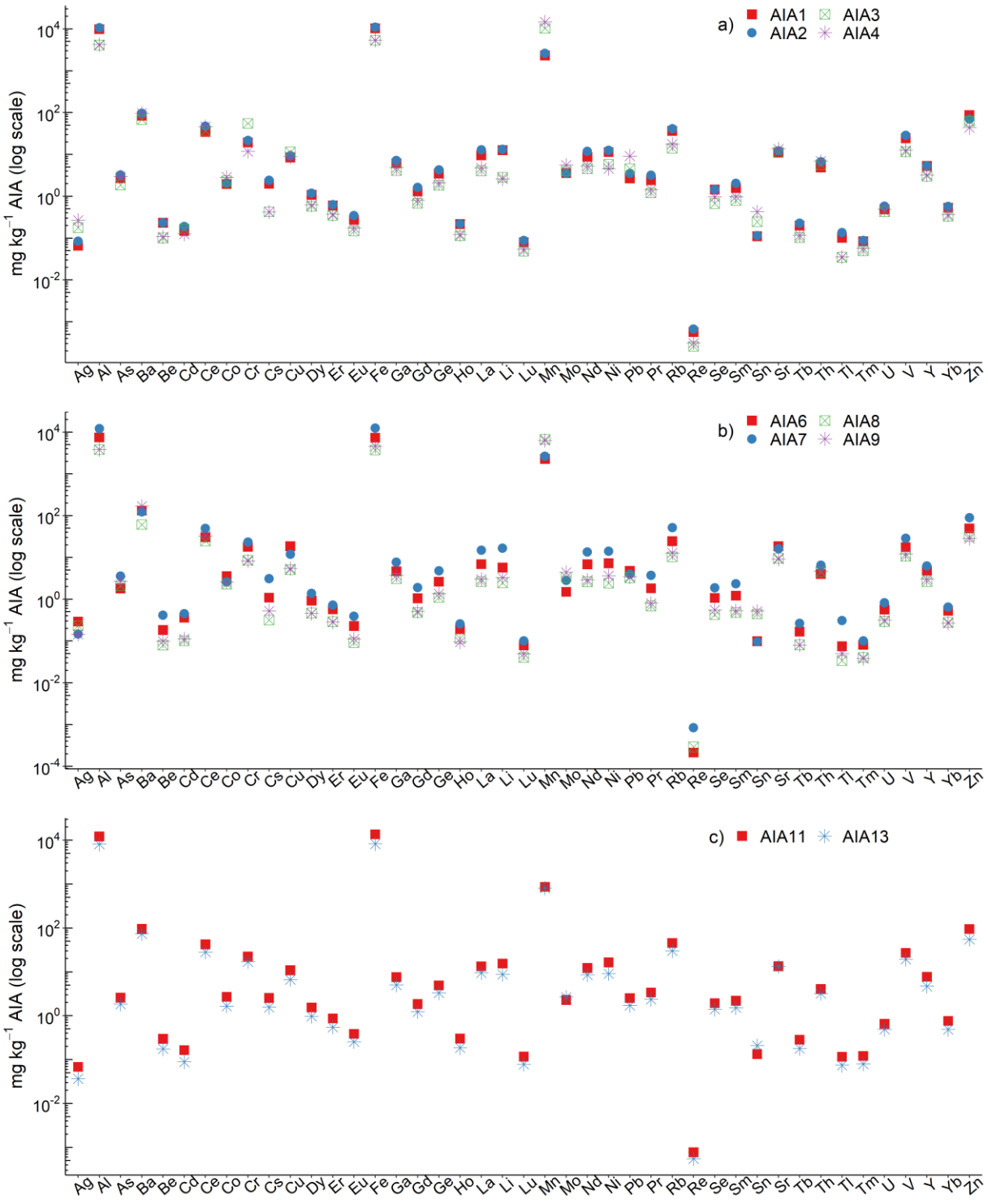

Fig. 3. Element concentrations (mg kg^{-1} AIA) in a) AIA1–4, b) AIA6–9, c) AIA11 and 13 after leaching using different *Sphagnum* ash masses and filtration methods (see Table 2). *Sphagnum* mosses were collected from JPH4 and UTK bogs in October 2019. AIA = acid insoluble ash. UTK = Utikuma.

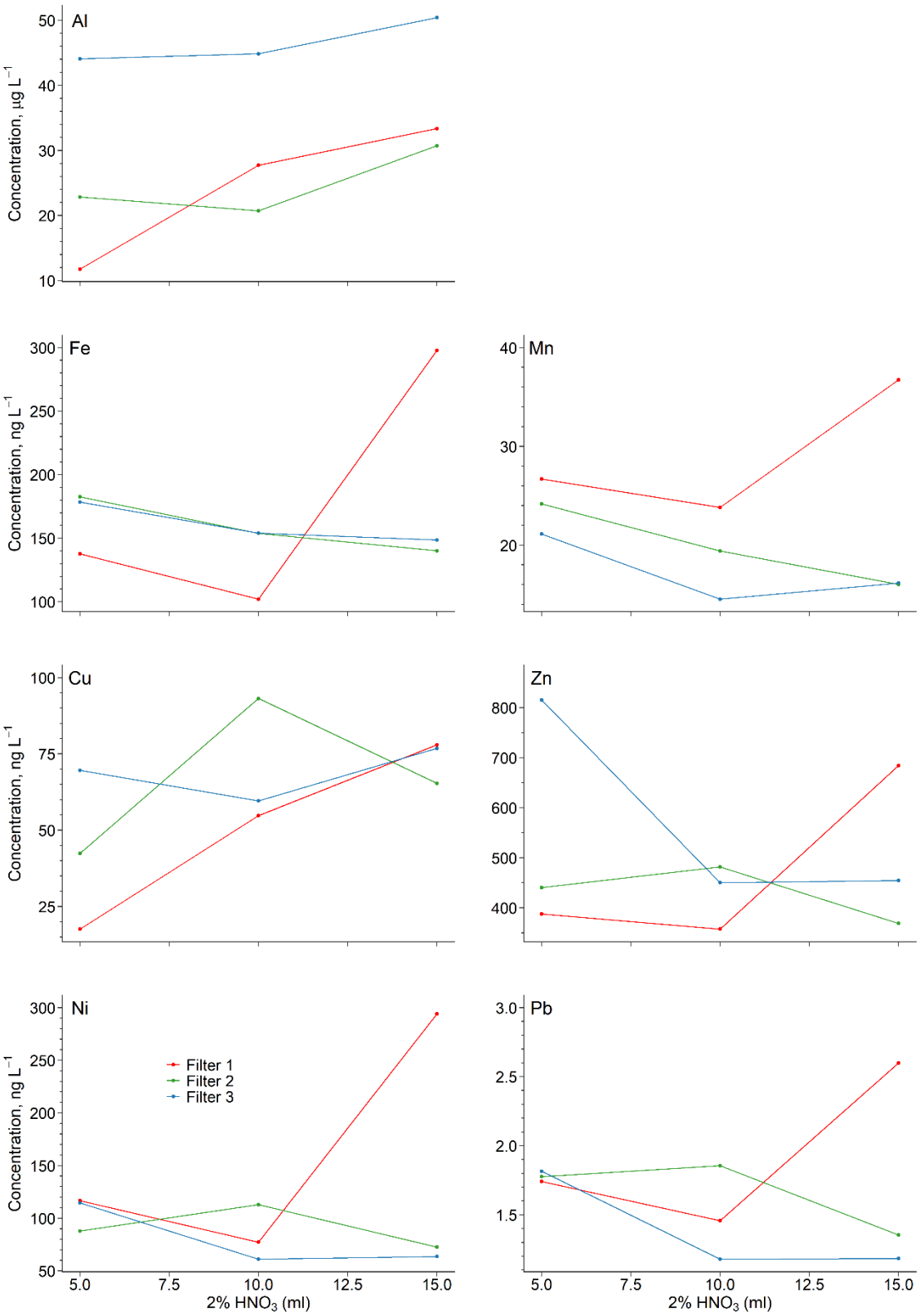

Fig. 4. Element concentrations (µg L^{-1} or ng L^{-1}) in filtrates when the filter membranes were cleaned with 5, 10, and 15 ml of 2% HNO_3.

APPENDIX II

Comparison of total concentrations of elements in *Sphagnum* moss digested with concentrated HNO_3 versus concentrated HNO_3 and HBF_4

1. Introduction

Various sample pre-treatment methods, such as evolving heating (e.g. electric heating plate, water bath, and microwave) and digestion systems (e.g. using hydrochloric acid (HCl), nitric acid (HNO_3), perchloric acid ($HClO_4$), hydrofluoric acid (HF), hydrogen peroxide (H_2O_2)), have been adopted to determine element concentrations in geological and biological materials.[1–4] Different sample preparation methods can lead to deviations in the detection of elements.[1] Closed-vessel microwave digestion was found to be the most efficient way for the rapid dissolution of both geological and biological samples, which minimizes the contamination from other samples and prevents the loss of volatile analytes.[5–9] Incomplete digestion sometimes occurs; silicate residues of plant samples, for example, would require digestion with HF to prevent elemental loss.[5] The addition of HF for digestion was found to be able to significantly increase element concentrations through decomposing samples bound to silicate minerals and other refractory oxides.[7] However, in addition to difficulties in handling acutely toxic HF and its associated health risks, the precipitation of metal fluorides would lead to the underestimation of some elements such as Al, Ba, Ca, Mg, and Se.[7,9,10] These metal fluorides, such as CaF_2, can also lead to the co-precipitation of rare earth elements by forming $(BF_4)^-$ complexes.[5] Boric acid (H_3BO_3) is often added for digestions containing HF to mask HF residues.[7,11] Nevertheless, complex digestion matrices can also result in problems during analysis, such as the heavy borate matrix introduced by the addition of H_3BO_3 and oxide interferences by digestion using HNO_3 and H_2O_2.[5,7,11] Not as extremely hazardous as HF, fluoroboric acid (HBF_4) as a fluoride source is an alternative to HF for dissolving silicates and refractory oxides, which could prevent the formation of fluoride precipitates.[7,11]

Optimized digestion with HNO_3 and HBF_4 has been proposed for soil, sediment, peat, and plant sample analysis.[3,11] Here, the differences in the digestion of *Sphagnum* mosses with concentrated HNO_3 versus concentrated HNO_3 and HBF_4 were compared, to evaluate if the addition of HBF_4 yields more satisfactory digestion results for *Sphagnum* moss.

2. Materials and methods

Sphagnum moss samples were collected in triplicate in October 2019 from JPH4 and Utikuma (UTK) bogs located 12 and 264 km away from the industrial centre, respectively. This centre is defined as the mid-point between two central upgraders. Moss samples were cleaned using tweezers to remove all foreign and dead materials, dried at 105°C in a drying oven, and milled using an agate mortar and pestle. To each milled sample, 3 ml of double-distilled concentrated HNO_3 was added with or without 0.1 ml of HBF_4 and digested in a microwave autoclave (Milestone, UltraCLAVE MA 033) under high temperature and pressure for 80 min. Quality control was ascertained by simultaneous digestion of water and solid standard reference materials (SRMs) of the National Institute of Standards and Technology (NIST), Spectrapure Standards AS (SPS), and Finnish Forest Research Institute (FFRI): NIST 1643f Freshwater, SPS-SW2 Surface Water, NIST 1515 Apple Leaves, and FFRI Moss-1343. The digested solutions were analyzed using inductively coupled plasma mass spectrometry (ICP-MS). SRMs of NIST 1643f and SPS-SW2 were also simultaneously analyzed.

Moss cleaning, drying, and grinding were done in the Prep Lab at the University of Alberta, which is of class 100,000, and is thus suitable for the preparation work (Details can be found on the SWAMP Lab website). The rest of the work was conducted in the metal-free, ultraclean SWAMP Lab at the University of Alberta.

3. Results and discussion

Most elements of NIST 1515 apple leaves showed great recoveries between 80 to 120%, except for Eu and Yb, which had recoveries above 120% and below 80%, respectively, regardless of the digestion acid used (Fig. 1). In terms of FFRI moss-1343, Al, Fe, and Ga exhibited recoveries higher than 120% for both digestion methods, whereas Mo, Tl, and U showed values lower than 80%. A clear increase in Mo recovery with an increasing amount of HBF_4 used for digestion, and a decrease in Tl and U concentrations as the addition of HBF_4 was increased from 0.05 to 0.1 ml have been reported.[3,11] Thus, an amount larger than 0.1 ml of HBF_4 might be required to obtain higher recoveries for Mo while a smaller amount may be needed for Tl and U. In addition, the element concentrations of FFRI moss-1343 are not certified but recommended by Steinnes et al.,[12] which might also have resulted in the recoveries being out of the range of 80–120%. The recovery of Sb in NIST 1515 and Th in FFRI moss-1343 digested with HNO_3 and HBF_4 exceeded 120%, while those digested solely with HNO_3 did not. An increase in the Sb recovery with an increasing amount of HBF_4 used was also reported.[3]

The element concentrations in *Sphagnum* moss generally showed minor variations when digested with or without HBF_4 (Figs. 2, 3). Conservative lithophile elements, such as Y, Th, La, and Ce, also did not show significant increases in concentration when HBF_4 was used. In general, the addition of HBF_4 for digestion did not exert a significant impact on the concentrations of elements in *Sphagnum* moss collected in this study.

References

(1) Pan, F.; Yu, Y.; Yu, L.; Lin, H.; Wang, Y.; Zhang, L.; Pan, D.; Zhu, R. Quantitative assessment on soil concentration of heavy metal-contaminated soil with various sample pretreatment techniques and detection methods. *Environ. Monit. Assess.* **2020**, *192* (12), 800. DOI: 10.1007/s10661-020-08775-4. Published Online: Dec. 1, 2020.

(2) Galindo-Riaño, M. D. Development and optimization of a digestion method for heavy metal determination in scleractinian corals by Atomic Absorption Spectrometry (AAS). *CiencMar* **2003**, *29* (4), 413–424. DOI: 10.7773/cm.v29i4.174.

(3) Javed, M. B.; Grant-Weaver, I.; Shotyk, W. An optimized HNO_3 and HBF_4 digestion method for multielemental soil and sediment analysis using inductively coupled plasma quadrupole mass spectrometry. *Can. J. Soil. Sci.* **2020**, *100* (4), 393–407. DOI: 10.1139/cjss-2020-0001.

(4) Rahfeld, A.; Wiehl, N.; Dressler, S.; Möckel, R.; Gutzmer, J. Major and trace element geochemistry of the European Kupferschiefer – an evaluation of analytical techniques. *Geochemistry: Exploration, Environment, Analysis* **2018**, *18* (2), 132–141. DOI: 10.1144/geochem2017-033.

(5) Prohaska, T.; Hann, S.; Latkoczy, C.; Stingeder, G. Determination of rare earth elements U and Th in environmental samples by inductively coupled plasma double focusing sectorfield mass spectrometry (ICP-SMS). *J. Anal. At. Spectrom.* **1999**, *14* (1), 1–8. DOI: 10.1039/A806720A.

(6) Alvarado, J. S. Microwave dissolution of plant tissue and the subsequent determination of trace lanthanide and actinide elements by inductively coupled plasma-mass spectrometry. *Anal. Chim. Acta* **1996**, *322* (1-2), 11–20. DOI: 10.1016/0003-2670(95)00586-2.

(7) Zimmermann, T.; Au, M. von der; Reese, A.; Klein, O.; Hildebrandt, L.; Pröfrock, D. Substituting HF by HBF_4^- an optimized digestion method for multi-elemental sediment analysis via ICP-MS/MS. *Anal. Methods* **2020**, *12* (30), 3778–3787. DOI: 10.1039/D0AY01049A. Published Online: Jul. 24, 2020.

(8) Amaral, C. D. B.; Fialho, L. L.; Camargo, F. P. R.; Pirola, C.; Nóbrega, J. A. Investigation of analyte losses using microwave-assisted sample digestion and closed vessels with venting. *Talanta* **2016**, *160*, 354–359. DOI: 10.1016/j.talanta.2016.07.041. Published Online: Jul. 22, 2016.

(9) Kuss, H.-M. Applications of microwave digestion technique for elemental analyses. *Fresenius J Anal Chem* **1992**, *343* (9-10), 788–793. DOI: 10.1007/BF00633568.

(10) Durand, A.; Chase, Z.; Townsend, A. T.; Noble, T.; Panietz, E.; Goemann, K. Improved methodology for the microwave digestion of carbonate-rich environmental samples. *International Journal of Environmental Analytical Chemistry* **2016**, *96* (2), 119–136. DOI: 10.1080/03067319.2015.1137904.

(11) Krachler, M.; Mohl, C.; Emons, H.; Shotyk, W. Analytical procedures for the determination of selected trace elements in peat and plant samples by inductively coupled plasma mass spectrometry. *Spectrochim. Acta B* **2002**, *57* (8), 1277–1289. DOI: 10.1016/S0584-8547(02)00068-X.

(12) Steinnes, E.; Rühling, Å.; Lippo, H.; Mäkinen, A. Reference materials for large-scale metal deposition surveys. *Accred Qual Assur* **1997**, *2* (5), 243–249. DOI: 10.1007/s007690050141.

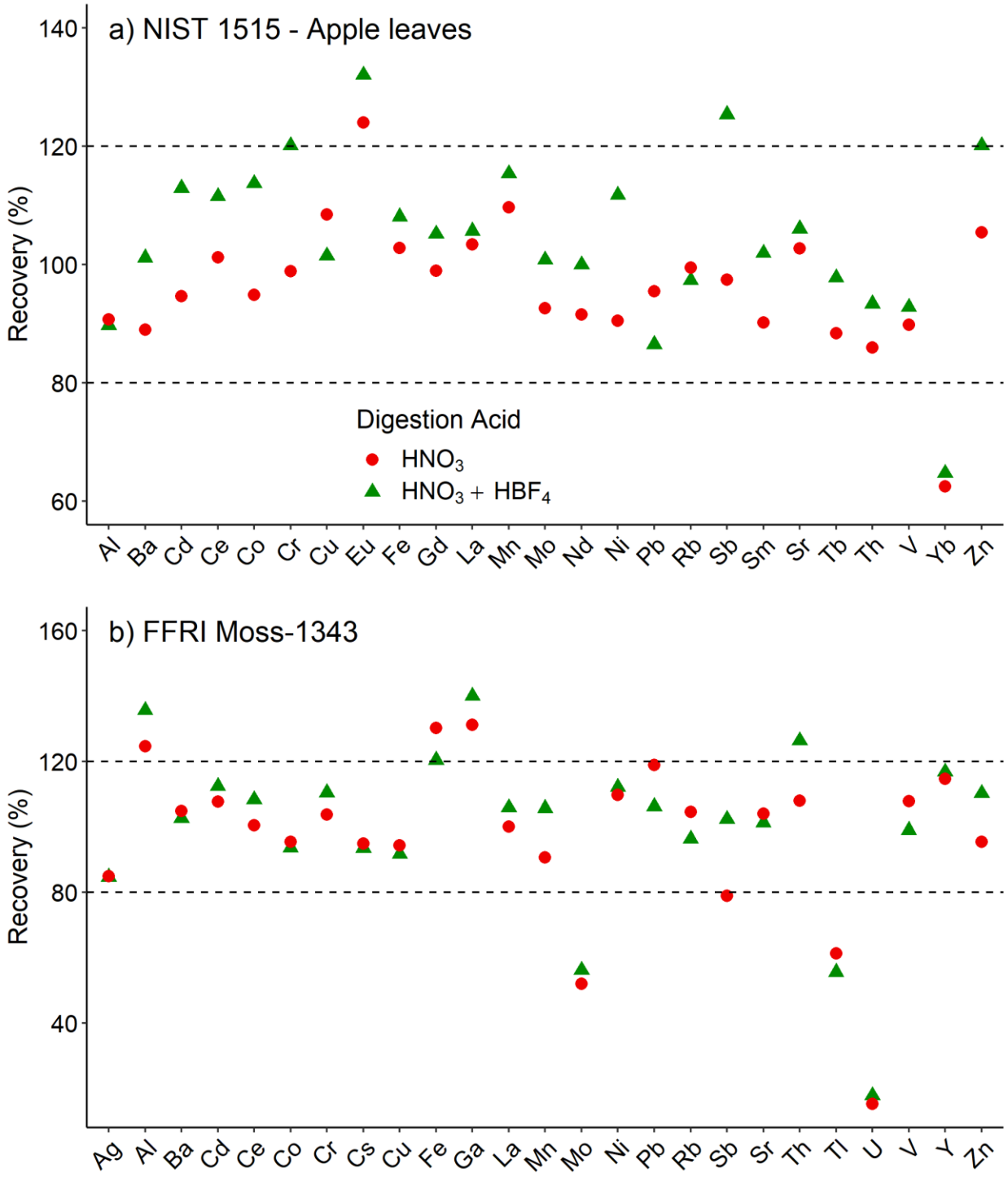

Fig. 1. Recoveries (%) of a) NIST 1515 Apple Leaves and b) FFRI Moss-1343 digested with HNO_3 or HNO_3 and HBF_4. NIST = National Institute of Standards and Technology. FFRI = Finnish Forest Research Institute.

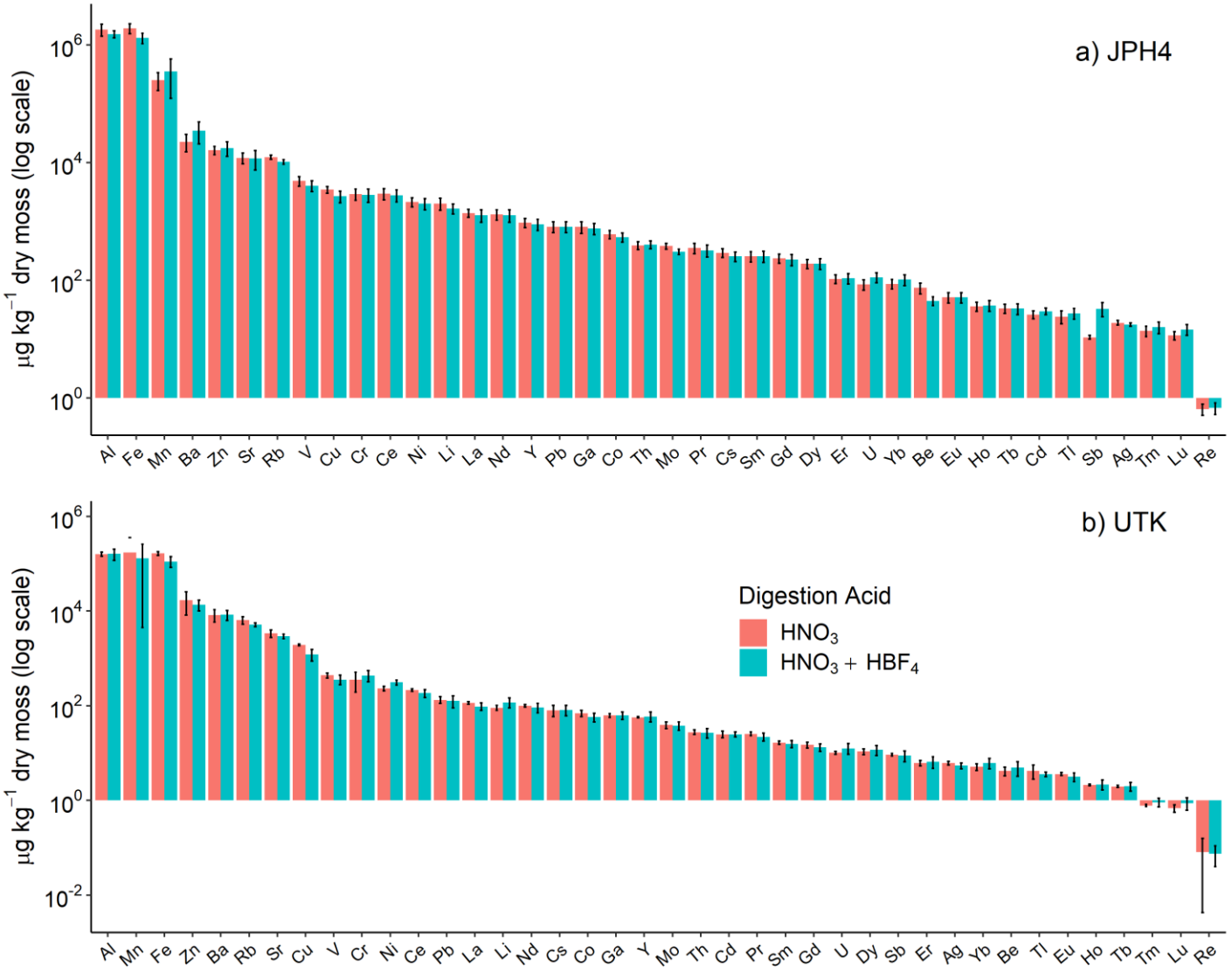

Fig. 2. Total concentrations (µg kg^{-1} dry moss) of trace elements in *Sphagnum* moss digested using concentrated HNO_3 with or without HBF_4. The moss samples were collected in a) JPH4 and b) Utikuma (UTK) bogs in October 2019.

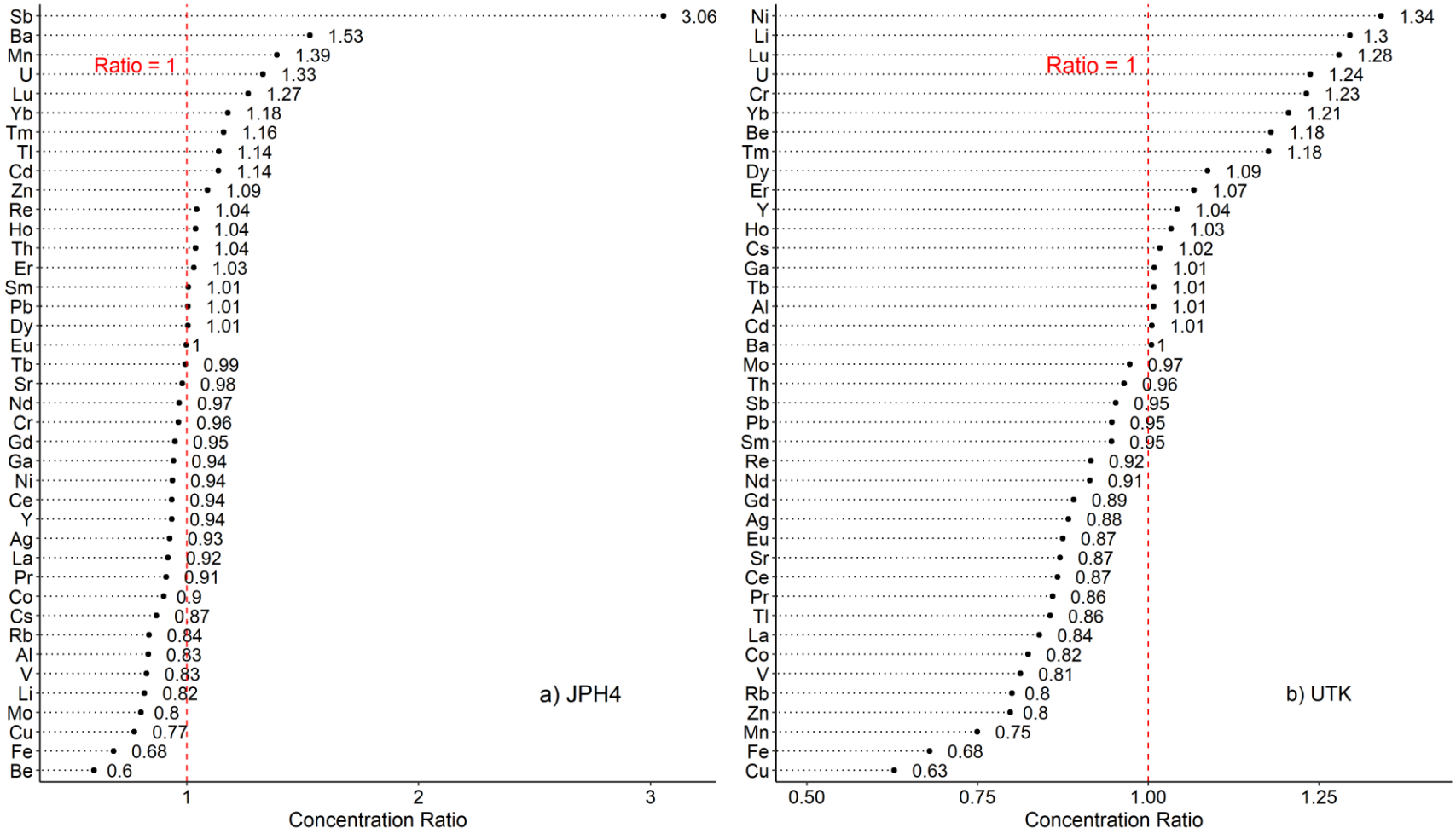

Fig. 3. Total concentration ratios of trace elements in *Sphagnum* moss digested using concentrated HNO_3 and HBF_4 to those digested solely with concentrated HNO_3. The moss samples were collected in a) JPH4 and b) Utikuma (UTK) bogs in October 2019.

APPENDIX III

Comparison of Al, Fe, Mn, and Zn concentrations obtained using inductively coupled plasma optical emission spectrometry (ICP-OES) and inductively coupled plasma mass spectrometry (ICP-MS)

1. Introduction

Inductively coupled plasma optical emission spectrometry (ICP-OES), which is also known as inductively coupled plasma atomic emission spectrometry (ICP-AES), and inductively coupled plasma mass spectrometry (ICP-MS) have been increasingly used for the determination of element concentrations.[1,2] They are preferentially selected over other techniques such as atomic absorption spectrometry (AAS), flame atomic emission spectrometry (FAES), instrumental neutron activation analysis (INAA), and X-ray fluorescence (XRF) spectrometry.[1,2] The mutual advantages of the two ICP-based techniques are their capability to analyze multiple elements simultaneously, a large analytical range, high sample throughput, low sample volume, and simple sample preparation.[3–5] In addition, ICP-MS has a low detection limit, high-resolution and tandem mass spectrometry, and a high level of inference control, but is not tolerant to samples with high total dissolved solids (TDS).[2–7] In contrast, ICP-OES has a higher tolerance for TDS, but has a relatively higher detection limit and some interferences persist.[3–5] Both instruments are expensive, and require a high level of staff expertise and high laboratory setup and operation cost (e.g. argon gas consumption).[2–5,8] Concentrations of Al, Fe, Mn, and Zn can be obtained from both ICP-OES and ICP-MS. Here, the differences in concentrations obtained using the two techniques are compared.

2. Materials and methods

The total (bulk *Sphagnum* moss) and acid soluble (acid soluble ash, ASA) concentrations of elements were analyzed using both ICP-OES and ICP-MS, as detailed in Chapter 2. Standard reference materials (SRMs) from the National Institute of Standards and Technology (NIST) and Finnish Forest Research Institute (FFRI), NIST 1515 apple leaves and FFRI moss-1343, were simultaneously digested and analyzed with the moss samples. Element recoveries of the SRMs are provided in Table 1.

All data analyses and visualizations were performed in R 4.1.1.[9] Concentration ratios of ICP-OES to ICP-MS were also calculated and visualized. With the data set being approximately normally distributed, paired one-sample t-tests were conducted on the concentration difference obtained using ICP-OES and ICP-MS. *p*-values and 95% confidence intervals (CI) were obtained.

3. Results and discussion

Both the total and acid soluble concentrations analyzed using ICP-OES yielded larger mean values for Al, and Fe, while smaller mean values for Mn and Zn (Table 2). The ranges of the concentrations were also generally larger in the ICP-OES data than those in the ICP-MS data, except for Mn and Zn in the ASA fraction (Table 2). Higher Zn concentrations measured using ICP-MS compared to using ICP-OES have also been reported.[10] The concentration ratios of ICP-OES to ICP-MS of Al and Fe were mostly greater than 1 for Al and Fe (Figs. 1, 2). In addition, the paired t-tests demonstrated the significantly larger concentrations of Al and Fe obtained using ICP-OES compared to ICP-MS ($p < 0.05$, 95% CI > 0; Table 3). Total Mn did not show significant differences between the two techniques and the ratio of the ICP-OES to ICP-MS concentrations varied among samples. However, it exhibited a significant difference in the ASA fraction ($p < 0.05$), but with a small 95% CI ([-0.54, -0.23] g kg^{-1} ash). The ratio of ICP-OES to ICP-MS of Zn

in ASA also varied among samples but still showed significant differences between the two methods with a small 95% CI (p = 0.01, 95% CI = [-0.080, -0.011] g kg^{-1} ash). This indicates that slightly higher Zn was obtained using ICP-MS than using ICP-OES. The concentration differences between the two methods could be attributed to the significantly higher concentrations of Al and Fe than those of Mn and Zn in the sample.[11] Although the dilution factors used for the final solutions analyzed using ICP-OES and ICP-MS were different, the ratios of element concentrations were the same. Thus, matrix effects, if present, should have been the same for both methods. Overall, ICP-OES generally yields larger values for Al and Fe and ICP-MS for Mn and Zn. More accurate results for B concentrations using ICP-MS compared to ICP-OES have been reported.[11] Using ICP-OES for major and minor element concentrations and ICP-MS for trace and rare earth element concentrations is being adopted in more and more studies.[2,12,13]

References

(1) Sapkota, A.; Krachler, M.; Scholz, C.; Cheburkin, A. K.; Shotyk, W. Analytical procedures for the determination of selected major (Al, Ca, Fe, K, Mg, Na, and Ti) and trace (Li, Mn, Sr, and Zn) elements in peat and plant samples using inductively coupled plasma-optical emission spectrometry. *Anal. Chim. Acta* **2005**, *540* (2), 247–256. DOI: 10.1016/j.aca.2005.03.008.
(2) Planeta, K.; Kubala-Kukus, A.; Drozdz, A.; Matusiak, K.; Setkowicz, Z.; Chwiej, J. The assessment of the usability of selected instrumental techniques for the elemental analysis of biomedical samples. *Sci. Rep.* **2021**, *11* (1), 3704. DOI: 10.1038/s41598-021-82179-3. Published Online: Feb. 12, 2021.
(3) Wilschefski, S. C.; Baxter, M. R. Inductively coupled plasma mass spectrometry: Introduction to analytical aspects. *Clin. Biochem. Rev.* **2019**, *40* (3), 115–133. DOI: 10.33176/AACB-19-00024.
(4) Thermo Elemental. *AAS, GFAAS, ICP or ICP-MS? Which technique should I use?*:*An elementary overview of elemental analysis*, 2001.
(5) Tyler, G. 1995. *ICP-OES, ICP-MS and AAS Techniques Compared*. ICP Optical Emission Spectroscopy Technical Note 05. Jobin Yvon Horiba. https://www.researchgate.net/profile/Olatunji-Sunday/post/Atomic-Absorption-Spectroscopy-vs-ICP-MS/attachment/59d654f379197b80779ac4c1/AS%3A523326150725632%401501782085752/download/ICP-OES__ICP-MS_and_AAS_Techniques_Compared.pdf.
(6) Prohaska, T.; Hann, S.; Latkoczy, C.; Stingeder, G. Determination of rare earth elements U and Th in environmental samples by inductively coupled plasma double focusing sectorfield mass spectrometry (ICP-SMS). *J. Anal. At. Spectrom.* **1999**, *14* (1), 1–8. DOI: 10.1039/A806720A.
(7) Alvarado, J. S. Microwave dissolution of plant tissue and the subsequent determination of trace lanthanide and actinide elements by inductively coupled plasma-mass spectrometry. *Anal. Chim. Acta* **1996**, *322* (1-2), 11–20. DOI: 10.1016/0003-2670(95)00586-2.
(8) Zeiner, M.; Pirkl, R.; Juranović Cindrić, I. Field-tests versus laboratory methods for determining metal pollutants in soil extracts. *Soil Sediment Contam.: Int. J.* **2020**, *29* (1), 53–68. DOI: 10.1080/15320383.2019.1670136.
(9) R Core Team. 2021. *R: A language and environment for statistical computing*; R Foundation for Statistical Computing. https://www.r-project.org/.
(10) Pan, F.; Yu, Y.; Yu, L.; Lin, H.; Wang, Y.; Zhang, L.; Pan, D.; Zhu, R. Quantitative assessment on soil concentration of heavy metal-contaminated soil with various sample pretreatment techniques and detection methods. *Environ. Monit. Assess.* **2020**, *192* (12), 800. DOI: 10.1007/s10661-020-08775-4. Published Online: Dec. 1, 2020.
(11) Kmiecik, E.; Tomaszewska, B.; Wątor, K.; Bodzek, M. Selected problems with boron determination in water treatment processes. Part I: Comparison of the reference methods for ICP-MS and ICP-OES determinations. *Environ. Sci. Pollut. Res.* **2016**, *23* (12), 11658–11667. DOI: 10.1007/s11356-016-6328-7. Published Online: Mar. 4, 2016.
(12) May, Z.; Rózsa, Z.; Kreiter, A. Message in a bottle: Analyses of 12–13th century vessels from an Ishmaelite settlement in Orosháza, Hungary. *J. Archaeol. Sci.: Rep.* **2021**, *38*, 103084. DOI: 10.1016/j.jasrep.2021.103084.
(13) Rosa, L. K.; Costa, F. S.; Hauagge, C. M.; Mobile, R. Z.; Lima, A. A. S. de; Amaral, C. D. B.; Machado, R. C.; Nogueira, A. R. A.; Brancher, J. A.; Araujo, M. R. de. Oral health, organic and inorganic saliva composition of men with Schizophrenia: Case-control study. *J. Trace Elem.*

Med. Biol. **2021**, *66*, 126743. DOI: 10.1016/j.jtemb.2021.126743. Published Online: Mar. 10, 2021.

(14) Steinnes, E.; Rühling, Å.; Lippo, H.; Mäkinen, A. Reference materials for large-scale metal deposition surveys. *Accred. Qual. Assur.* **1997**, *2* (5), 243–249. DOI: 10.1007/s007690050141.

Table 1. Element recoveries of standard reference materials analyzed using ICP-OES and ICP-MS.

		Al	Fe	Mn	Zn
ICP-OES	FFRI Moss-1343	132	109	87	84
	NIST 1515-Apple leaves	81	83	94	<LOD
ICP-MS	FFRI Moss-1343	136	120	106	110
	NIST 1515-Apple leaves	90	108	115	120

Note: FFRI = Finnish Forest Research Institute, NIST = National Institute of Standards and Technology. LOD = limit of detection. Element concentrations in FFRI moss-1343 were recommended values reported by Steinnes et al.[14]

Table 2. Concentrations of Al, Fe, Mn, and Zn in bulk moss (mg kg^{-1} dry moss) and acid soluble ash (ASA, g kg^{-1} ash) samples from 2015, 2019, and 2020 analyzed using ICP-OES and ICP-MS.

		ICP-OES				ICP-MS			
		Al	Fe	Mn	Zn	Al	Fe	Mn	Zn
Total	Mean	1033	850	322	<LOD	650	802	331	<LOD
	Min	93.3	70.0	51.4	<LOD	80.9	74.7	54.4	<LOD
	Max	2062	2425	912	<LOD	1283	2351	829	<LOD
	Range	1969	2355	861	<LOD	1202	2276	775	<LOD
ASA	Mean	17.1	11.1	1.23	0.450	14.3	9.39	1.65	0.490
	Min	3.37	2.20	0.431	0.118	4.98	4.23	0.451	0.0855
	Max	28.0	19.7	3.71	1.74	23.0	15.3	4.82	2.01
	Range	24.6	17.5	3.28	1.62	18.0	11.1	4.37	1.93

Note: Min = Minimum concentration. Max = Maximum concentration. Range = Maximum – minimum concentration. LOD = Limit of detection.

Table 3. p-values and 95% confidence intervals (CI) from paired t-tests of differences in concentrations (total and acid soluble concentrations in *Sphagnum* mosses collected in autumn 2015, 2019, and 2020) analyzed using ICP-OES and ICP-MS.

		p-value	95% CI
Total	Al	5.61E-09	[89.79, 166.88]
	Fe	1.35E-03	[19.45, 77.16]
	Mn	0.19	[-21.93, 4.40]
ASA	Al	< 2.2E-16	[2.98, 4.28]
	Fe	4.50E-11	[1.27, 2.13]
	Mn	5.82E-06	[-0.54, -0.23]
	Zn	0.01	[-0.080, -0.011]

Note: ASA = acid soluble ash.

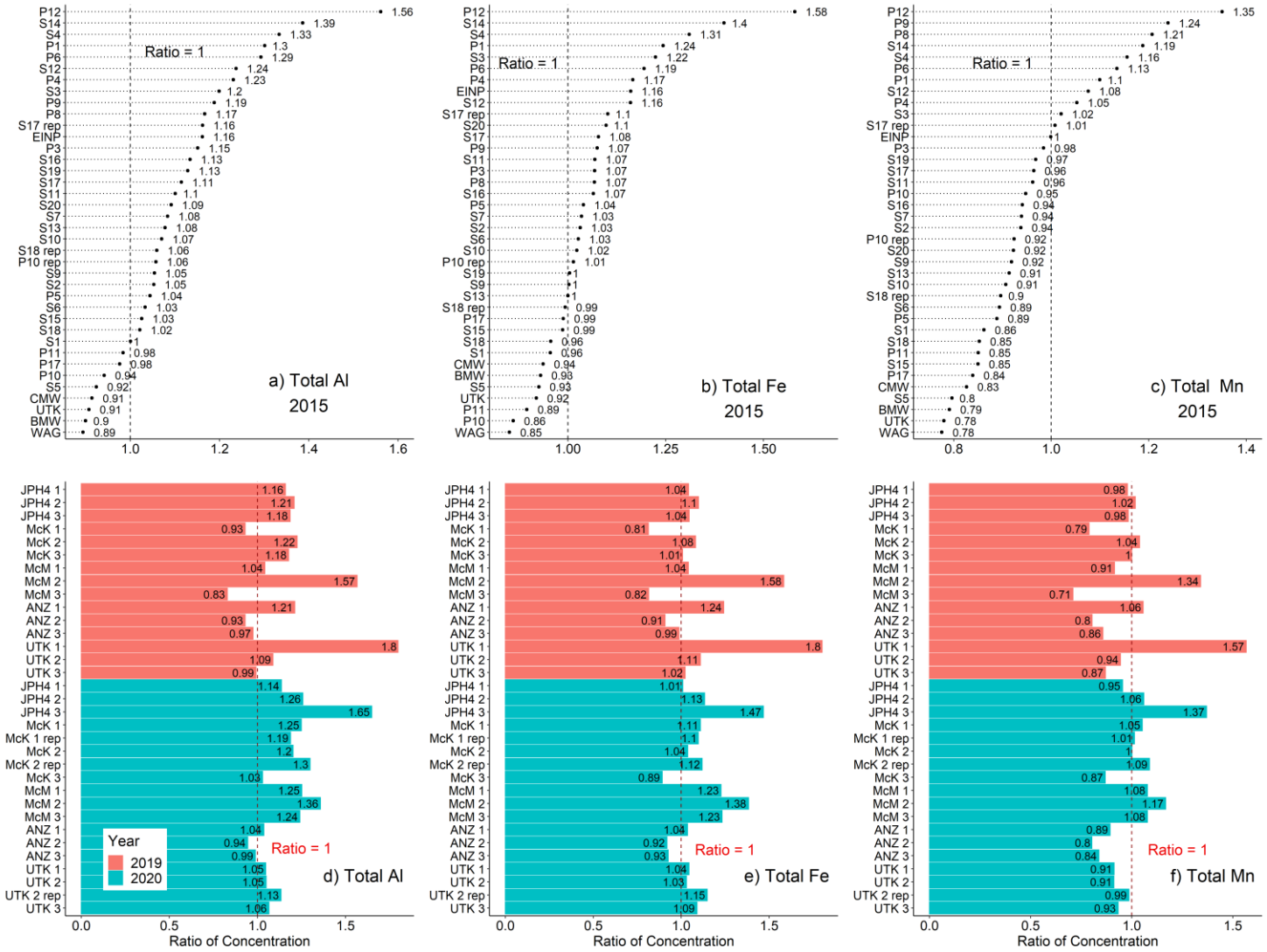

Fig. 1. Total concentration ratios of ICP-OES to ICP-MS of Al, Fe, and Mn in *Sphagnum* mosses collected in autumn 2015, 2019, and 2020. Rep = replicate. BMW = Birch Mountains Wildland, CMW = Caribou Mountains Wildland, EINP = Elk Island National Park, UTK = Utikuma, WAG = Wagner Natural Area, McK = Fort Mackay, McM = Fort McMurray, ANZ = Anzac.

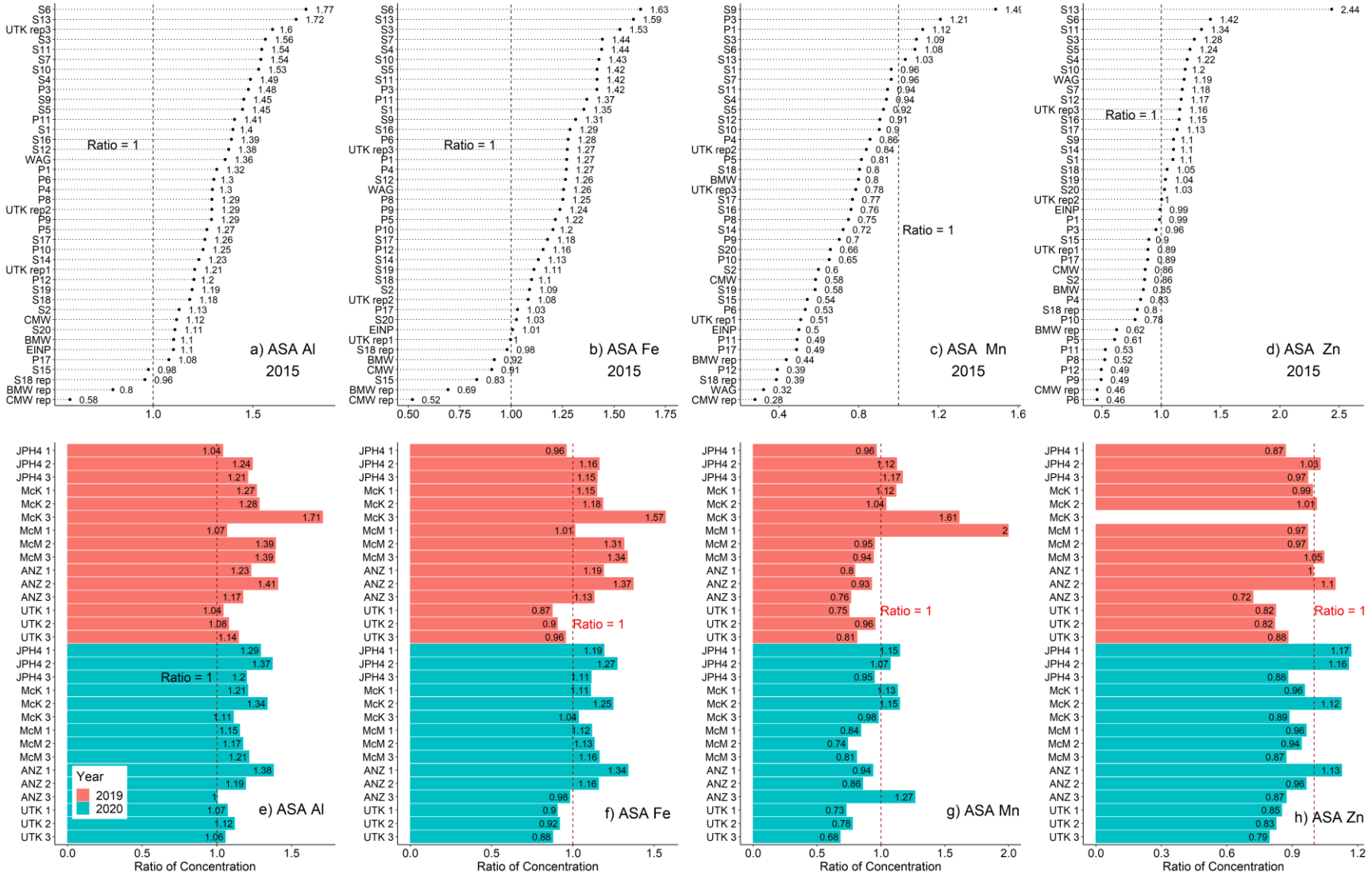

Fig. 2. Ratio of ICP-OES to ICP-MS concentrations in acid soluble ash (ASA) of Al, Fe, Mn, and Zn in *Sphagnum* mosses collected in autumn 2015, 2019, and 2020. Rep = replicate. BMW = Birch Mountains Wildland, CMW = Caribou Mountains Wildland, EINP = Elk Island National Park, UTK = Utikuma, WAG = Wagner Natural Area, McK = Fort Mackay, McM = Fort McMurray, ANZ = Anzac.

APPENDIX IV

Comparison of enrichment factors calculated using different reference elements

1. Introduction

Enrichment factors (EF) are usually calculated to determine whether there are additional sources of an element other than soil and wind-borne soil dust.[1] The EF is calculated as the ratio of the abundance of a given element to that of a conservative lithophile element in samples to the corresponding ratio in the earth's crust. [1] The element concentration in the earth's crust can be obtained from published articles, including those by Rudnick and Gao[2] and Wedepohl.[3] Here, the differences in EFs calculated using different conservative lithophile elements as the reference element are compared.

2. Materials and Methods

Moss samples were cleaned using tweezers to remove all foreign and dead materials, dried at 105°C in a drying oven, and milled using an agate mortar and pestle, as detailed in Chapter 2. To each milled sample, 3 ml of double-distilled concentrated HNO_3 was added with 0.1 ml of HBF_4 and digested in a microwave autoclave (Milestone, UltraCLAVE MA 033) under high temperature and pressure for 80 min. The digested solutions were analyzed using inductively coupled plasma mass spectrometry (ICP-MS). Enrichment factors were calculated with the obtained total concentration in moss using Y, Th, or Al as the reference element, as shown below:

$$EF = \frac{[TE/CLE]_{sample}}{[TE/CLE]_{UCC}}$$

where TE = trace element, CLE = conservative lithophile element, UCC = upper continental crust. Element concentrations in the UCC were obtained from Rudnick and Gao.[2]

3. Results and Discussion

When EFs were calculated using Y or Th as the reference element, the trends of the EFs of the sites were similar and the values calculated were close (Figs. 1, 2). When using Al as the reference element, the EFs of the sites generally exhibited the same trends as those using Y or Th, but the values were larger than those using Y and Th (Fig. 3). This could be attributed to the Al concentration being magnitudes higher than that of the other TEs in both UCC and moss, making the concentration ratios of TEs to Al very small for either UCC or moss. This could lead to larger errors and uncertainties when obtaining the EF. In contrast, the concentrations of Y or Th were in similar ranges as those of other TEs, so the uncertainties and errors could be smaller when obtaining the EF. In conclusion, the EF values calculated using Al were generally larger than those using Y and Th, but the trends of the EF for the sites were relatively consistent regardless of the reference element used. Using Y or Th as the reference element might be better than Al for calculating EFs of TEs considering the uncertainties.

References

(1) Rahn, K. A. 1976. *The Chemical Composition of the Atmospheric Aerosol*.
(2) Rudnick, R. L.; Gao, S. Composition of the continental crust. In *Treatise on Geochemistry,* 2nd ed.; Holland, H., Turekian, K., Eds.; Elsevier, 2014; pp 1–51. DOI: 10.1016/B978-0-08-095975-7.00301-6.
(3) Wedepohl, K. H. The composition of the continental crust. *Geochim. Cosmochim. Acta* **1995**, *59* (7), 1217–1232.

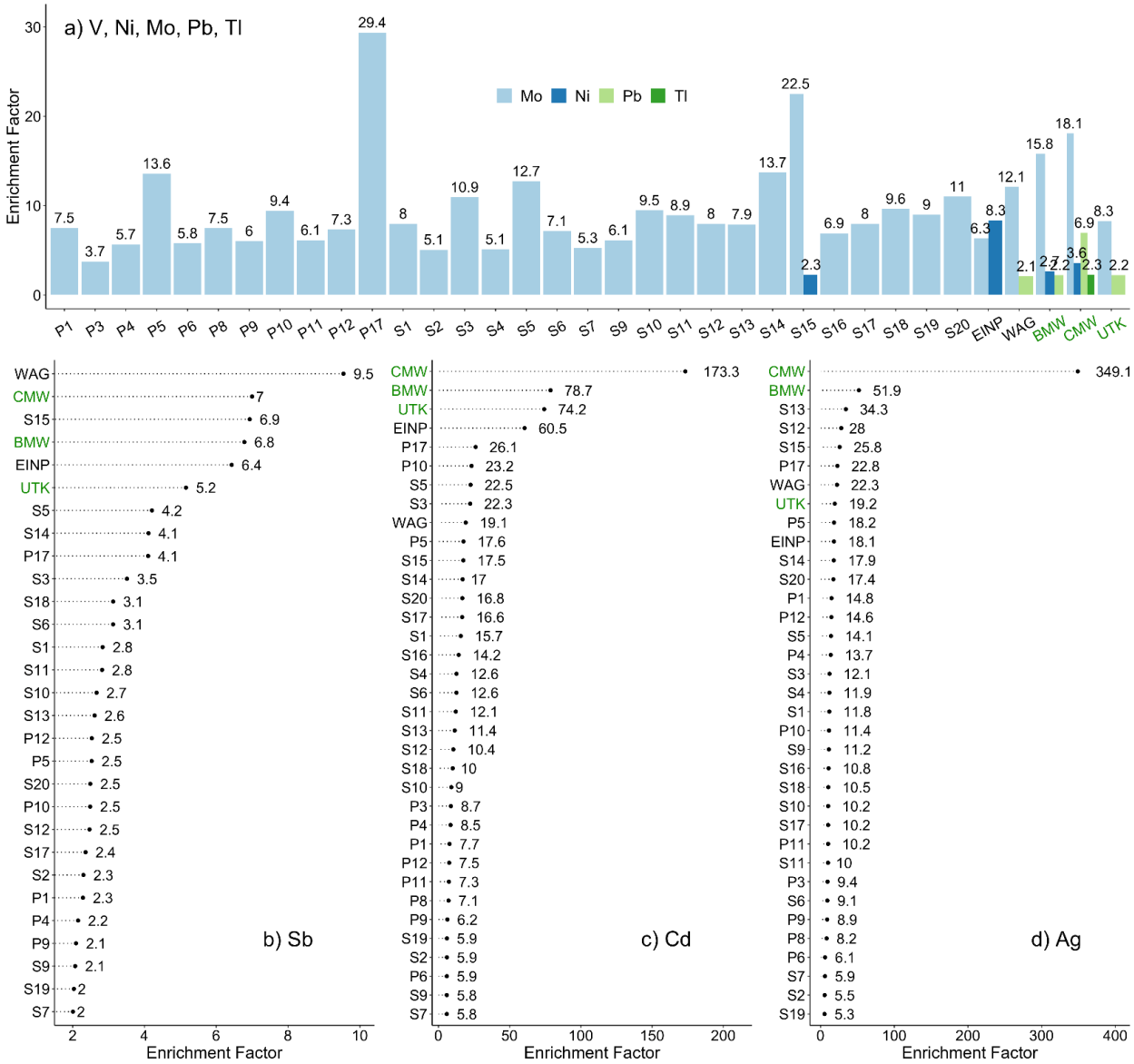

Fig. 1. Enrichment factors using **Y** as the reference element with values greater than 2 of a) V, Ni, Mo, Pb, Tl, b) Sb, c) Cd, and d) Ag of *Sphagnum* mosses collected from 2015. CMW = Caribou Mountains Wildland, BMW = Birch Mountains Wildland, UTK = Utikuma, WAG = Wagner Natural Area, EINP = Elk Island National Park.

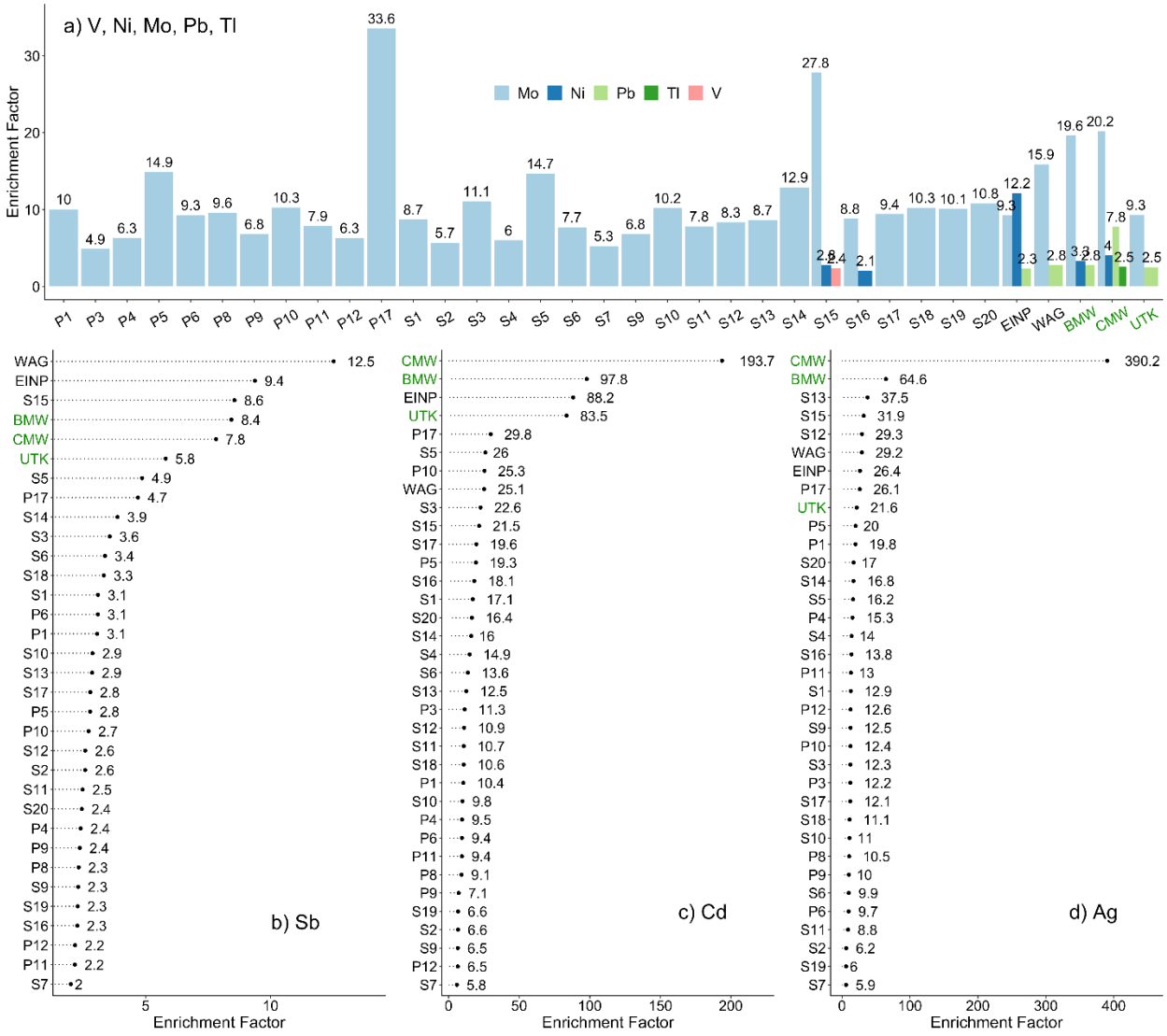

Fig. 2. Enrichment factors using **Th** as the reference element with values greater than 2 of a) V, Ni, Mo, Pb, Tl, b) Sb, c) Cd, and d) Ag of *Sphagnum* mosses collected from 2015. CMW = Caribou Mountains Wildland, BMW = Birch Mountains Wildland, UTK = Utikuma, WAG = Wagner Natural Area, EINP = Elk Island National Park.

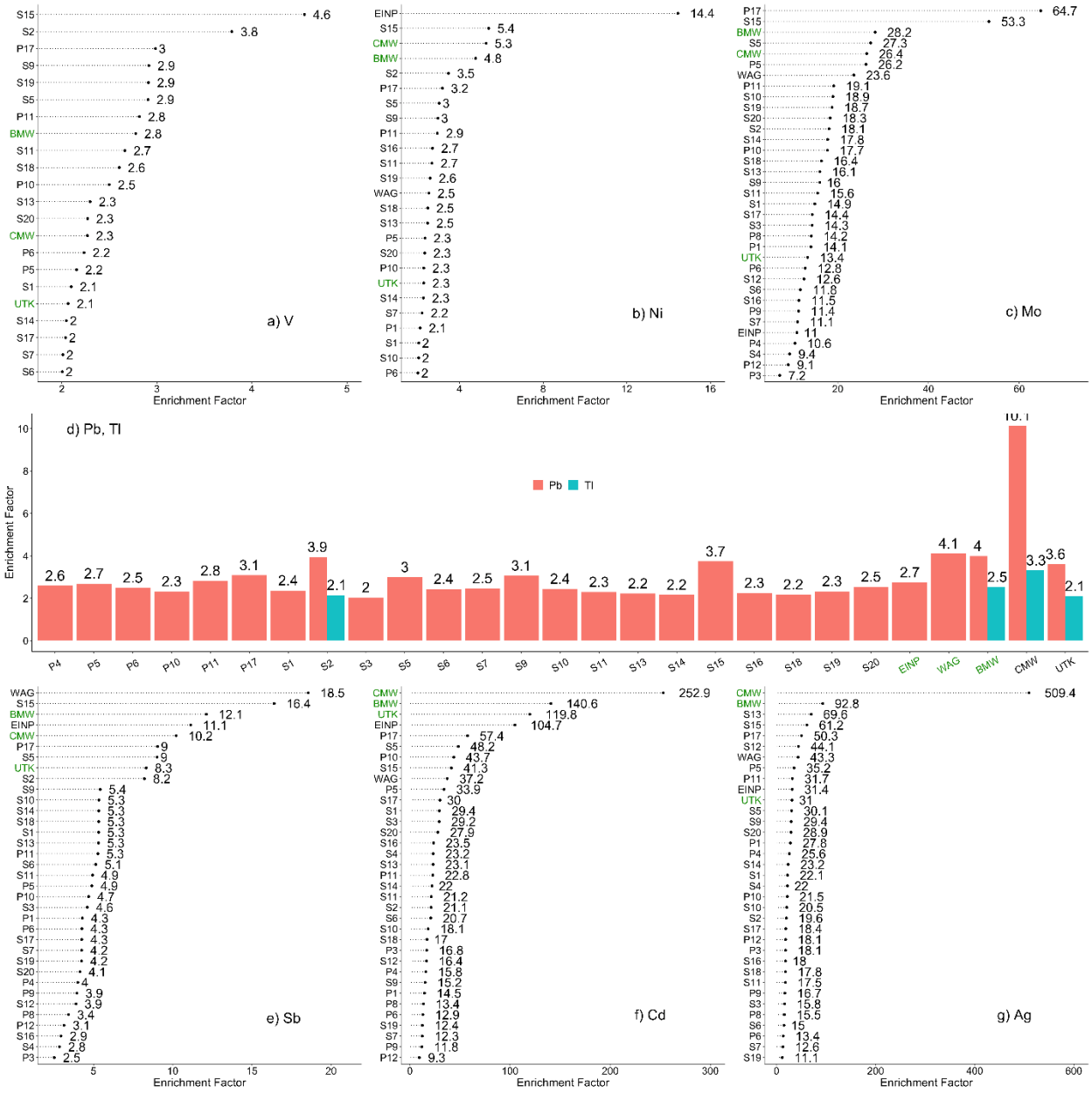

Fig. 3. Enrichment factors using **Al** as the reference element with values greater than 2 of V, Ni, Mo, Pb, Tl, Sb, Cd, and Ag of *Sphagnum* mosses collected from 2015. CMW = Caribou Mountains Wildland, BMW = Birch Mountains Wildland, UTK = Utikuma, WAG = Wagner Natural Area, EINP = Elk Island National Park.